ProQuest Number: 10290169

ProQuest 10290169

THE FORMATION AND MONITORING OF GASES ASSOCIATED

WITH THE SPONTANEOUS COMBUSTION OF COAL

presented by

MALCOLM COOPER

A thesis submitted in partial fulfilment of the

requirements of the Council for National Academic Awards

for the degree of Doctor of Philosophy

MAY 1991

Department of Chemistry and Physics
Faculty of Science
Nottingham Polytechnic
Clifton Lane
NOTTINGHAM
NG11 8NS

Collaborating establishment:
Technical Services and Research Executive
British Coal Corporation
Ashby Road
Bretby
BURTON-ON-TRENT
STAFFS
DE15 0QD

PS PHD 41

ABSTRACT

The analysis of gases associated with the spontaneous combustion of coal was investigated by developing gas chromatographic (GC) methods. This involved a detailed study of chromatographic columns in terms of optimising the selectivity and efficiency of component separation. Selectivity was controlled by modifying the stationary phase, whilst efficiency was varied by altering the physical dimensions of the column. Additionally the detection limits and sensitivity of a number of GC detectors were studied to provide equipment capable of analysing low levels of the gases. This work demonstrated the advantages of photoionisation detectors, which clearly have the potential for monitoring gases in a coal mine atmosphere.

An automated coal oxidation system was configured which allowed the gases formed during the spontaneous combustion of coal to be produced in the laboratory. This equipment automatically monitored temperature profiles and the production of permanent gases during the coal oxidation process. The system also had the capability of dynamically or isothermally oxidising coal samples. The frequent abstraction of gas samples from this system followed by GC analysis allowed the evolution profiles of these gases to be monitored. The evolution profiles of gases formed from the dynamic oxidation of coal provided information on the usefulness of these gases as indicators of spontaneous combustion. Carbon monoxide is currently used to indicate spontaneous combustion. This work suggested that ethene,

propene, acetaldehyde, acetone and carbonyl sulphide are also useful indicators of spontaneous combustion. A variety of other gases were demonstrated to be desorption products by repeating the experiments using nitrogen carrier gas.

The production rate of gases evolved from isothermal coal oxidation allowed kinetic constants, including the activation energy and reaction order of formation to be calculated. This information demonstrated that acetone, acetaldehyde and carbonyl sulphide were formed by similar reaction mechanisms to carbon monoxide. This work further validated the use of these gases as other indicators of spontaneous combustion.

ACKNOWLEDGEMENTS

CONTENTS

LIST OF PLATES

LIST OF FIGURES

LIST OF TABLES

CHAPTER 1

INTRODUCTION

1.1   Background to Coal

Coal is an important source of energy, with some eighty million tonnes per annum being burnt in this country alone. Although the use of coal as a supply of energy is presently diminishing, it will remain important for several reasons. Primarily, it is the only fossil fuel resource available in sufficient quantities to make up for the declining world reserves of petroleum and natural gas. Also, the expected future energy demands are so great that it will be necessary for coal to supply a significant fraction of those demands even when advanced nuclear and natural technologies have been developed. Coal has also been proposed as a useful feedstock for the organic chemical industry. Finally, it is anticipated that the use of coal in an environmentally acceptable manner will be achieved due to the present worldwide research being carried out.

Coal originated hundreds of millions of years ago, when vegetation grew much larger than today due to the warm and humid climate conditions. This vegetatation grew and died in swamp areas creating thick peat beds. In some cases these peat beds became submerged and covered with sedimentary deposits which later produced inorganic rocks. As time passed the actions of diagenesis and metamorphism eventually formed the coal found today. Due to the

differences in temperature and pressure during formation and differences in the original vegetation, coal is a term which includes a variety of substances covering a range of ranks. Rank is a term which describes the degree of coalification or geochemical maturity. Coal is formed by the process of coalification via the series shown below :-

LIVING MATERIAL -> PEAT -> LIGNITE ->

SUBBITUMINOUS COAL -> BITUMINOUS COAL -> ANTHRACITE.

The rank increases progressively from lignite (contains ca.65% carbon) through low rank and high rank coal to anthracite (contains ca.94% carbon). Other chemical changes across this series include a decrease in the volatile matter content and reactivity of the coal, as well as decreased percentage contents of oxygen and hydrogen. Physically, the series is characterised by a decreasing porosity and an increasing gelification and vitrification, and it can be seen that coal rank carries the same meaning as maturation and hence carbon content. Seyler introduced a rank classification system based on the elementary analysis of pure coal, which was extended and improved in 1931 and 1938 [1]. This method, considered a 'scientific masterpiece', essentially involved a coal 'band' in a carbon-hydrogen plot, but in practise has never been adopted due to difficulties in the procedures of elementary analysis [2]. The classification system used by British Coal involves the analysis of volatile matter content and caking property of the coal [3]. The latter of these two properties is determined by the Gray King assay, which

involves slowly heating the coal and visually examining the resulting coke [4]. Classification of a coal according to rank is then determined by plotting the volatile matter (absicca) versus the Gray-King coke type (y-ordinate). It is interesting to note that high rank coals (eg. anthracite) are classified in the 100 group, and this extends through the groups 200, 300 .... 800, the latter groups representing lower ranked coals.

1.2   Coal Composition

Coal is a heterogenous material which consists principally of carbon, hydrogen and oxygen, with lesser amounts of sulphur, chlorine and nitrogen, and a variety of trace elements.

Carbon is the major element present in coal, and as the organic backbone of the molecule accounts for between 65% and 94% of the total coal mass [5]. It is also present at much smaller concentrations in inorganic minerals such as carbonates.

Oxygen is present in coal at concentrations of 1 to 20%, principally as the organic form in alcoholic, phenolic, etheral, heteroaromatic etheral, carboxylic acid and quinone groups. There are problems with the quantitative measurement of oxygen since oxygen-bearing structures are affected by restricted accessibilty of coal to reagents, so the accuracy of these measurements is poor [6]. The concentration of oxygen is dependent on coal rank, increasing in lower ranked coals [5]. The sum of oxygen

present as -COOH, -OH, -OCH$_3$ and C=O represents 75 to 90% of the total organic oxygen, the remainder being referred to as 'unreactive oxygen', present in ether and heterocyclic structures. In lower ranked coals 50% is present in phenolic -OH and 25% is present in -COOH groups, with smaller amounts (2-3%) present in -OCH$_3$ groups [7]. Changes in oxygen functionality are rank dependent since in more highly ranked coals (C>82%), the majority of organic oxygen is evenly partitioned between -OH and C=O groups. Oxygen is inorganically bound in coal in minerals such as the oxides, carbonates and sulphates.

Hydrogen may exist in three forms in coal, in aliphatic and aromatic systems and in hydroxyl groups. The hydrogen content of coal varies from 3 to 10%, predominantly in the aliphatic and aromatic forms. By studying the thermal decomposition of coal, the rapid disappearance of hydroxyl and aliphatic hydrogen atoms suggests they are relatively unstable as compared to aromatic hydrogen atoms [7].

Sulphur can occur in coal in three main forms [8] :-

(i) **organic sulphur** - it is incorporated into the hydrocarbon backbone of the coal structure.

(ii) **sulphide minerals** - present in the coal inorganic fraction (eg. pyrites).

(iii) **sulphate minerals** - present in the coal inorganic fraction (eg. sulphate).

Typically, the total sulphur content of coal is of the order of 0.5 to 4.0%. The precise nature and bonding of organic sulphur in coal remains unresolved since there are

few methods of determining its functionality. The recent
work of Attar and Dupuis suggested that organic sulphur is
trapped in coal as thiolic sulphur, which condenses to
sulphidic and finally to thiophenic sulphur [9]. They
concluded that the majority of organic sulphur in high-
ranked coals is thiophenic, but in low-ranked coals it is
thiolic or sulphidic. In general, it has been suggested
that the organic sulphur content of coal varies from a
typical sulphur:carbon ratio of 1:100-300 to 1:50 in high
sulphur coal [10]. Since chloroform and pyridine extracts
and extraction residues have similar sulphur contents it
has been concluded that organic sulphur compounds are
distributed uniformly throughout the coal structure.

The dominant forms of inorganic sulphur are pyrite and
marcasite, which have the same chemical composition (FeS_2)
but different crystalline forms - pyrite is isometric, but
marcasite is orthorhombic. In fresh, unweathered coals the
sulphate minerals do not comprise of a significant portion
of sulphur in coal. However, the iron disulphide minerals
rapidly oxidise to form a number of hydrated sulphates,
specifically hydrated ferrous and ferric sulphate [11].

The early work of Francis and Wheeler produced the
conclusion that almost all nitrogen occurs in cyclic
systems in coal as pyrrole and pyridine derivatives [12].
More recently, a variety of investigations into the
nitrogen content of coal have revealed the presence of $N{\equiv}R_3$
and C-N=C groups [13]. These results have been confirmed by
the observed nitrogen:carbon ratios of 1:75 to 1:100. The

concentrations of nitrogen in coal are relatively constant at levels of 1 to 1.5%.

The mode of occurrence of chlorine in coal is debatable but it is believed to be present in the organic phase and as a mineral, the relative proportions being dependent upon the specific coal. In the mineral phase it is present as halite (NaCl) and sylvite (KCl). The original proof of the occurrence of chlorine in the organic phase was demonstrated by Edgecombe, who showed that chlorine could only be partially extracted with water [14]. Daybell et al have shown that on average 50% of chlorine is associated with organic matter, probably as hydrochlorides of pyridine bases [15]. However, the more recent studies of Pearce suggest that chlorine is entirely present in coal in one ionic form [16]. Chlorine is typically present at low levels of 0.05 to 0.3% in coal, but in some British coals it may be as high as 1%.

The heterogeneity of coal is such that it is not a mineral of constant composition but one whose chemical composition changes with coalification. It is an organic rock composed principally of macerals and subordinately of minerals which contains water and gases in submicroscopic pores. Macerals are organic substances derived from plant debris that have been subjected to decay, incorporated into sedimentary strata, and then altered physically and chemically by geological processes [17]. In concept a maceral is analogous with the minerals in inorganic rocks except that due to its complex organic composition the

physical and chemical properties of a coal maceral can vary widely. An overview of the properties of macerals has been given by Stach [18]. The study of macerals has historically involved the microscopic observations of transmitted light upon prepared sections of coal sufficiently thin to be translucent. More recently, coal samples are prepared according to British Standard specifications [19]. Essentially the coal is crushed, mounted in resin, and polished for microscopic examination by reflected light. The characterisation of the various members of the maceral groups and rules for their microscopic identification have been illustrated in the International Handbook of Coal Petrography [20,21]. The different petrographic groups have been listed below :-

   (i) **exinite** (also termed **liptinite**) - comprises mainly of spore cases, spore cuticles and resins and therefore has the lowest density of the group. This group has the highest volatility and contains more hydrogen than other macerals of comparable rank.

  (ii) **vitrinite** - originates from woody and cortical plant tissue, and contains more oxygen than other macerals of comparable rank.

 (iii) **inertinite** - closely resembles a woody charcoal being soft and friable in texture and has the highest density of the group. This group are relatively inert in carbonisation processes compared to the others having the lowest volatility, and they contain more carbon than other macerals of comparable rank.

This subdivision into three groups represents a useful simplification when attempting to correlate coal petrography with other properties. One particular example of this is that a measure of the coal rank may be obtained by petrography because the reflectance (specifically of vitrinite) increases progressively with coal rank.

The mineral matter of coal represents all forms of inorganic material associated with coal and includes optically identifiable mineral species as well as various complexed cations and anions [22]. The major constituents are listed below :-

  (i) **clay minerals** - these are the aluminosilicates and they commonly make up 50% of the total mineral matter content.

  (ii) **carbonate minerals** - these are composed of individual and mixed Ca, Mg, Mn and Fe carbonates.

 (iii) **sulphides** - mainly present as pyrite and marcasite (FeS_2) but also present as the lead and zinc sulphides.

  (iv) **silica** - this is present as quartz and usually accounts for up to 20% of mineral matter.

Perhaps the best definition of coal is that of Schopf - "Coal is defined as a readily combustible rock containing more than 50% by weight and 70% by volume of carbonaceous material" [23].

1.3   Coal Structure

A variety of physical and chemical approaches have been adopted to determine the structure of coal including oxidation, hydrogenation, hydrolysis, halogenation and instrumental methods such as X-ray crystallography, FTIR and NMR [24]. It is now generally agreed that coals have as their main building blocks aromatic and hydro-aromatic structures, with the basic unit an anthracene, phenanthrene or fluorene like structure. The presence of nitrogen and sulphur heterocycles in coal tars and other products of combustion suggests that occasionally one of these hetero-atoms is present in a 5- or 6-membered ring. These structures are also thought to be peripherally substituted by $-OH$, $-CH_3$ or $=O$ groups, and are sometimes held together with $-O-$ and $-CH_2-$ bridges. The presence of these links and of hydro-aromatic linkages between aromatic groups prevents good alignment of these building blocks causing buckling of the structure. This creates a fine three-dimensional struture, resulting in extensive coal microporosity. A variety of molecular configurations have been proposed for coal and the majority of these structures closely resemble each other. The model coal structure illustrated in figure 1, proposed by Wiser is a typical example which allows postulations of the chemistry of coal to be made [25].
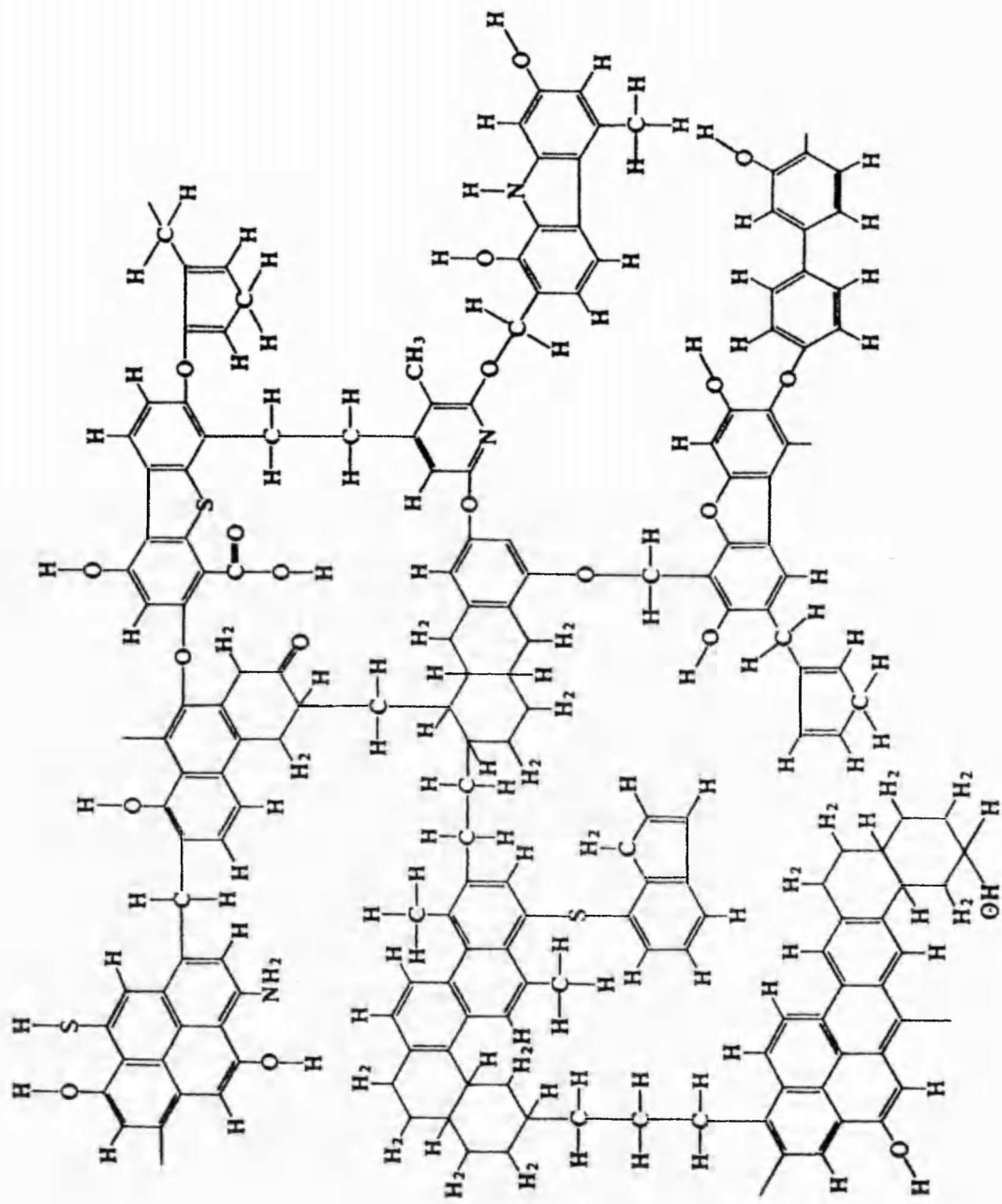
Figure 1   Proposed Structure of Bituminous Coal

Coal is a solid colloid and is therefore a highly porous material, with a significant portion of the total pore volume located in very small pores. Dubinin first suggested a classification for distinguishing between pores of different sizes [26], and this is now generally accepted as below :-

   (i) **macropores** - diameters greater than 20nm;

  (ii) **transitional pores** - diameters between 2 and 20nm;

 (iii) **micropores** - diameters less than 2nm.

Early workers concluded that the internal surface of coal consists of a macropore system in which pores are linked by 0.5-0.8nm passages, and a micropore system (also termed ultra-fine) which is similar to a molecular sieve structure [27]. More recently a bimodal pore model of coal has been proposed consisting of microporous regions surrounded by cleats and fissures as flow channels [28]. It is thought that the bag-like micropores become filled by diffusion and subsequently swell, this swelling then acting upon the macropore system by narrowing the flow channels. This effect was observed by studying the adsorption of methane using coal slices as test specimens in the work of Seewald et al [28].

When coals are heated, at low temperatures volatile matter is released from the carbon skeleton causing an opening up of the structure, creating additional porosity and surface area [29]. As the temperature is further raised and volatile release becomes small, the breakage of cross-links and better alignment of aromatic groups dominate,

resulting in a decrease of open pore volume and surface area. Thus the coal porosity is expected to go through a maximum over a certain temperature range, the size being dependent upon the parameters employed. Such changes in the porosity of coal during heat treatment have been studied by a number of workers. Generally the maximum porosity occurs at temperatures of 600°C [30,31].

1.4   Coal Oxidation

The aerial oxidation of coal is an exothermic reaction which occurs even at ambient temperatures. This reaction is so dominant that several workers have suggested that many investigations have been flawed by the oxidation of coal samples prior to the experiment [32,33,34]. The weathering and oxidation of coal alter its physical and chemical properties, including calorific value, pyrolysis, combustion, surface and carbonisation properties [35,36].

According to postulations by early workers the initial stages of coal oxidation are believed to involve the formation of a coal-oxygen complex typically termed 'oxy-coal' [37]. As early as 1916, Haldane recognised that the adsorption of oxygen by coal occurred by two different processes [38]. But it was not until the later work of Sevenster that the temperature dependence of the shift in equilibrium between physisorption and chemisorption was known [39]. The primary step of oxygen physisorption takes place readily at low temperatures (-80°C) since it requires a low activation energy. At increasing temperatures

physisorption diminishes rapidly and chemisorption ensues, which becomes appreciable at temperatures above -5°C. At temperatures above 50°C oxygen is totally chemisorbed by coal, and this produces a complex containing an active form of oxygen termed 'per-oxygen'. Jones and Townend have shown that the decomposition of the peroxy-complex occurs with the evolution of much heat between 70°C and 80°C, by measuring it from the oxidation of ferrous thiocyanate added to coal [40]. These authors termed the peroxy-complex in analogy with the similar oxidation processes of hydrocarbon oils, rubber and soybean oil. Chakravorty noted the similarity between activation energies of the thermal decomposition of the peroxy-complex (84-100 kJ/mol) and that of tetralin hydroperoxide (102 kJ/mol) [41]. From this he presumed the nature of the peroxy-complex to be of hydro-peroxide type. Also, he proposed that the breakdown of the peroxy-complex produced a free radical, which caused the overall oxidation reaction to proceed via a chain reaction mechanism. Chamberlain et al suggested that the formation and decomposition of peroxides occurs mainly in the aliphatic coal structure [42]. They postulated mechanisms to explain their observed production of alcohols, aldehydes and ketones during coal oxidation. This mechanism has been more recently investigated by Cole et al who reviewed data obtained by Dack et al who investigated the free radical concentration of Yallourn brown coal [43,44,45]. This work showed that the free radical decay obeyed second order kinetics. Cole et al proposed that this

could be accounted for by the reactions [43] :-

$$R\cdot + O_2 \longrightarrow ROO\cdot$$

$$ROO\cdot + R'H \longrightarrow ROOH + R'\cdot \quad \left.\begin{array}{l}\\\\\end{array}\right\} \text{chain breaking}$$

$$ROOH \longrightarrow RO\cdot + \cdot OH$$

$$RO\cdot + R'\cdot \longrightarrow ROR' - \text{second order radical termination}$$
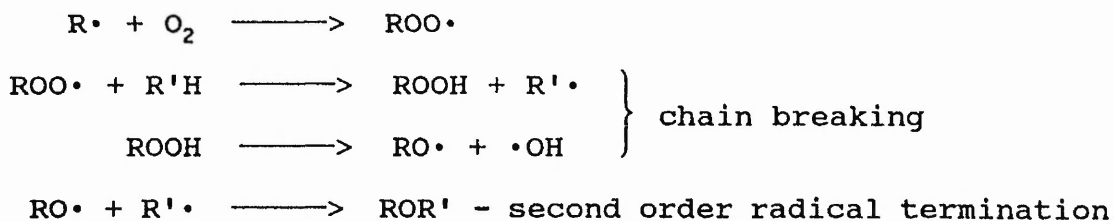
Petarca et al oxidised South African coals in the temperature range 80-180°C [46]. Their results agreed with Shanina et al and Polat and Harris, who found that the rate of oxidation decreased with increasing time of oxidation [47,48]. Some kinetic parameters were derived from the data obtained; activation energies were in the range of 35-38 kJ/mol; orders of the reaction varied from 0.83-0.95.

The behaviour of coal towards molecular oxygen has been studied by van Krevelen by microscopic examination [49]. In this work the appearance of 'oxidation edges' along the external surfaces of coal particles were noted as these edges showed a higher reflectivity than the coal matrix. They were most prominent in the vitrinite macerals, and this was suggested as a quantitative method for studying coal oxidation.

Since the oxidation of coal depends upon its' physical and chemical composition as well as the ambient reaction conditions, this process covers a wide spectrum of reactions. The carbon reactivity is expected to be influenced by the various interconnected aromatic and aliphatic moeities as well as the different substituents present in the coal structure. However, the initial chemisorption of oxygen by coal during air oxidation

-14-

results in the development of acidic functional groups within non-aromatic parts of the coal, specifically phenolic -OH, -COOH and C=O. The production of peroxide complexes which occur in the coal structure as discussed previously are accompanied by the oxidative abstraction of hydrogen to produce water according to Jones et al [50]. Further oxidation of coal leads to a more profound degradation of the structure, as illustrated in reactions postulated by Jensen et al that are shown in figure 2 [51]. This reaction scheme implies that the air oxidation of coal can degrade aromatic as well as non-aromatic structures. The humic acids are a chemically ill-defined complex mixture of dark brown or black solids which are similar to products formed by the action of fungal oxidases on plant debris to produce some soils (humus). The formation of these base-soluble products during coal oxidation is commonly accompanied by small amounts of formic, acetic and succinic acids, as well as CO, CO_2 and H_2O. Further oxidative degradation causes the breakdown of these structures to the sub-humic acids, and finally to simple benzenepolycarboxylic acids (BPCA). One example of these BPCA products is terephthalic acid, which is used commercially in the polymer industry. However, the ready availability of such acids produced by the oxidation of petroleum at a lower cost has meant that no commercial application has yet been made for the coal derived acids. Other uses suggested for the humic acids include the preparation of resins by reaction with epoxides, polyols

-15-
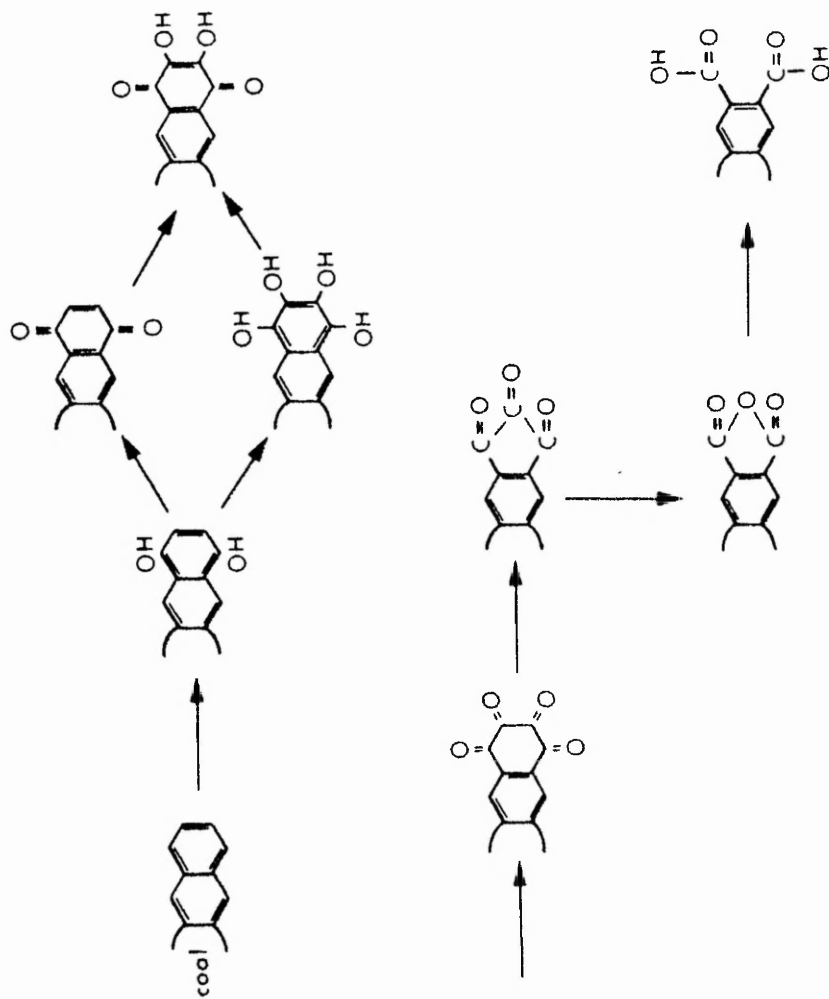
Figure 2   Postulated Reaction Path of Coal Oxidation

and ethanolamine. Although coal was not considered competitive as a source of these acids even after the world petroleum price increase of 1973, it is likely to become so in the future as the world reserves of oil diminish [52].

The continued oxidation of coal by it's exposure to air leads to autogenous heating which results in widely fluctuating 'spot' temperatures. A result of the exothermicity of coal oxidation and the incomplete dissipation of this heat is the development of coal hot-spots. Depending on the physical parameters present such as the localised air flow rate, this may result in spontaneous ignition and coal combustion. The heat associated with the active combustion of coal results in a rapid breakdown of the coal structure. This is perhaps best illustrated by referring to thermograms of coal carried out in air which show a large weight loss above a certain temperature. A critical temperature termed the decomposition temperature exists, which for non-anthracite coals increases with rank from 350°C to 400°C, above which substantial breakdown of the coal structure occurs and coal combustion ensues. An excellent discussion of the fundamentals of coal combustion has been produced by Essenhigh in which he reviewed 565 literature references [53]. Essentially the coal combustion mechanism involves a competition between pyrolysis (evolution of volatiles and charring of coal particle) and surface oxidation, which determines whether or not ignition takes place.

1.5   Kinetic Studies of Coal Oxidation

The exact mechanism of coal oxidation and the processes by which products are formed remain unknown to date. A substantial number of workers have identified the products of coal oxidation, but fewer have studied the rate change of their formation and the overall oxidation process. The important parameters that have been used to investigate the reaction kinetics include the evolution of gaseous reaction products, the consumption of oxygen and thermogravimetric methods of analysis.

1.5.1   Studies of Gases Evolved as Oxidation Products

Consideration of the model coal structure illustrated in figure 1 allows the initial coal oxidation reactions to be visualised. Since the principal components of coal are C, H and O, the products are expected to be CO, CO_2 and H_2O. It is apparent that by monitoring the concentrations of these gases the oxidation reaction may be followed. This approach has been adopted to study the coal oxidation process by many workers [42,54-58]. In these experiments a mass of coal is typically heated in a stream of combustion gas, and the products analysed as oxidation progresses. A review of the literature concerning the rate of production of gases evolved from heated coal reveals a variety of anomalies due to the different experimental conditions employed, producing a poor correlation between the results of different authors. Other critisicms of these studies are that the range of products studied was too restricted, the

upper temperature too excessive (ie. at temperatures >300°C coal decomposition products are formed) and the evolution rate of products have not generally been determined as a function of temperature. Chamberlain et al performed the most comprehensive study of this type when they carried out non-isothermal analyses of the rates of evolution of products of combustion from seventeen British coals [55]. The experiments involved heating 50g of 251-500μm coal at a programmed rate of 0.5°C/min in an air or nitrogen gas flow of 80ml/min. The effect of varying all of the experimental parameters were studied in this work, and it was found that the pattern or rate of evolution of gases was unaffected by :-

   (i) different heating rates.
  (ii) different coal particle sizes.
 (iii) the humidity of the air combustion gas.
  (iv) different flow rates of the carrier gas, provided
       sufficient oxygen remained available to satisfy the
       adsorption characteristics of the coal.

The large coal mass relative to the low gas flow rate was utilised to maximise the detection limits of the gaseous products. However, one problem derived from these experimental parameters was that the oxygen content of the air rapidly became totally consumed during the coal heating process providing only a relatively short period of time to study the rates of formation of oxidation products. Chamberlain studied the evolution of permanent gases and other higher hydrocarbons from heated coal and concluded

that the most sensitive indicator of the onset of coal oxidation was carbon monoxide but other useful indicators were hydrogen, ethene and propene. Since this work was carried out a number of advances in analytical technology have improved the limits of detection and sensitivity of gas sensors to such a degree that this conclusion needs to be re-assessed.

Tashiro et al have studied the evolution of a variety of gases similar to Chamberlain during heated coal experiments [56,55]. They have suggested that the oxidation of coal may be detected by observing the ratios of alkanes, since they claim that such measurements provide a sensitive indication of the coal temperature. Kim studied the low temperature evolution of hydrocarbon gases up to pentane [57]. Although she observed that the proportion of methane in the mixture decreases with temperature, the experimental apparatus was such that she could was unable to determine whether the gases were being desorbed or formed.

More recently Street et al used a similar experimental arrangement to Chamberlain to investigate the evolution of hydrogen from coal [58,55]. The experimental parameters involved a 140g mass of 211-104μm coal heated at a rate of 1.5°C/min with a flow rate of 250mls/min of air as the combustion gas. The large discrepencies between the results of these two workers are typical, illustrating the problems of obtaining consistent data from the literature.

Karsner and Perlmutter described oxidation in terms of 'chemical control' and 'diffusion control' by studying the

production of CO, CO_2 and H_2O [59]. They also described an oxidation model in terms of an effectiveness factor, and calculated activation energies to be 68-78kJ/mol [60].

Whiting and Langvardt used a thermogravimetry/capillary gas chromatography/mass spectrometry system to study the products evolved from a bituminous coal [61]. They observed a variety of products in the temperature range of 0-350°C, specifically CO_2, SO_2 and a variety of substituted benzenes and naphthalenes. They also proposed using TG/MS data to plot the intensity of specific mass/charge ratios versus coal temperature as a tool for monitoring the evolution of specific gases from the coal. Herod et al used this method of single ion monitoring MS to study the evolution of sulphur, oxygen and chlorine containing compounds from coals heated up to 300°C [62]. They concluded that small quantities of carboxylic acids, indanols, phenols, dibenzothiophenes and azo-dibenzothiophenes were evolved in the temperature range 130-300°C. They also showed that at temperatures up to 270°C the only chlorine containing compound produced was HCl. More recently Burchill et al used thermal analysis-MS to relate coal temperature changes to the evolution of a number of gases providing information on combustion performance [63].

The most recent work into the identification of the low temperature products of combustion of coal has been carried out by Gibson [64]. In this work, the author developed a range of techniques for the quantitative collection of gases evolved from heated coal using adsorption tubes. A

thorough investigation into these products was achieved by the desorption of the tubes followed by GC/MS and HPLC analysis. The combustion products of three coals were quantitatively analysed, and their effects on metal oxide semi-conductors studied. However, the prolonged analytical process meant that the evolved gases could only be determined at intervals of 50°C which limited the range of data obtained, and prevented an insight into the reaction kinetics and mechanism from being obtained.

By reviewing the data on previous work carried out into the gases evolved during coal combustion, it is possible to classify the gases evolved from heated coal into groups according to their chemical properties, as illustrated in table 1. This is a useful process since it aids future discussions of these gases.

1.5.2   Studies of Oxygen Consumption

The oxidation of coal results in the consumption of oxygen, and the observation of oxygen concentrations can therefore be used to follow this reaction. A study of the rate of oxygen consumption by coal in a flowing system was carried out by Carpenter and Giddings [65]. To summarise their conclusions, they observed that the rate of oxidation decreased with an increase in the rank of coal, and the oxidation rate increased with a rise in temperature.

Table 1   Classification of Evolved Gases According to Their Chemical Properties

CLASSIFIED GROUP	EVOLVED GAS	BOILING POINT(°C)	IONISATION POTENTIAL(eV)
Aliphatic Hydrocarbons	methane	-164.0	12.98
	ethane	-88.6	11.65
	propane	-42.1	11.07
	i-butane	-12.0	10.57
	n-butane	-0.5	10.63
	i-pentane	30.0	10.32
	n-pentane	36.1	10.35
Unsaturated Hydrocarbons	ethene	-102.0	10.52
	propene	-47.4	9.73
	ethyne	-75.0	11.40
	propyne	-23.2	10.36
Aromatics	benzene	80.0	9.25
	toluene	110.0	8.82
	p-xylene	138	8.45
	o-xylene	138-139	8.56
	o-xylene	143-145	8.56
Sulphur Gases	hydrogen sulphide	-60	10.46
	carbonyl sulphide	-50	11.17
	sulphur dioxide	-10	12.34
Oxygenated Gases	carbon monoxide	-191.5	14.01
	carbon dioxide	-78.5	13.77
	acetaldehyde	20.5	10.21
	methanol	64.6	10.85
	ethanol	78	10.48
	acetone	56	9.69
Miscellaneous Gases	hydrogen	-253	15.43
	water	100	12.60
	hydrogen chloride	-85	12.74

Note: i-butane has IUPAC nomenclature methylpropane.
       i-pentane has IUPAC nomenclature 2-methylbutane.

Banerjee et al studied the rate of oxygen consumption under isothermal conditions at different temperatures in the range 30 to 170°C [66]. They considered the oxidation process to be first order, and by using oxidation rate constant values and Arrhenius plots measured the activation energies of a number of Indian coals. They observed that the oxidation reaction shifts to continuously higher activation energies at higher temperatures, until a critical temperature was reached above which a steady reaction ensued producing similar activation energy values (46-54kJ/mol). This was termed the 'Threshold Temperature', and was found to vary between 85 and 120°C.

1.5.3   Thermogravimetric Studies

Oreshko carried out an investigation into the oxidation of coal in the 1950s utilising a thermobalance [67]. From the thermogravimetric data achieved by heating coal Oreshko was able to distinguish four distinct stages of the oxidation process :-

(i) From ambient to 70°C the coal undergoes a slight weight increase probably due to chemisorption (activation energy=14kJ/mol).

(ii) From 70 to 150°C a weight loss exceeding the earlier gain occurs, probably due to losses of intrinsic water from the coal structure (activation energy=25kJ/mol).

(iii) From 150 to 250°C a weight gain exceeding the earlier loss occurs, probably due to the formation of stable oxygen complexes and excessive heat production (activation

energy=67kJ/mol).

(iv) Above 250°C a sharp decrease in weight occurs which corresponds to incineration of the coal (activation energy=96-146kJ/mol).

Banerjee and Chakravorty used differential thermal analysis to study coal combustion in the temperature range 20-300°C [68]. Initially, up to 100-120°C an endothermic reaction ensued due to the release of water from the coal. After this an exothermic reaction of relatively low heat evolution continued up to 180-200°C. Finally, a highly exothermic reaction with great heat evolution occurred up to 230-300°C, and after a maximum the differential temperature began to diminish. The range of temperatures were quoted because they cover a number of coals, which allowed a categorisation of the susceptibility of an individual coal to oxidation. Basically, for poorly susceptible coals the second stage continues to a higher temperature and this delays the initiation of the final stage. This causes the final stage to occur at a much higher temperature than for more susceptible coals, even though once initiated, the exothermicity of the final stage is independent of the susceptibility of a coal to oxidation.

1.6   Spontaneous Combustion of Coal

Coal oxidation is an exothermic reaction which occurs upon its exposure to air producing a quantity of heat that is independent of the temperature. The rate of the

oxidation reaction is directly proportional to temperature, so that a higher temperature produces a faster oxidation rate. The spontaneous combustion of coal (also termed autogenous heating) refers to this self-heating oxidation process.

In an attempt to characterise spontaneous combustion by the application of petrography Falcon concluded that vitrinite was readily oxidisable, which 'may lead to spontaneous combustion'; exinite was described as 'having no particular tendency to spontaneous combustion'; and inertinite was 'not readily oxidisable' [69].

The conditions which determine whether or not low temperature oxidation will develop into spontaneous combustion in a coal mine are finely balanced. Two extremes exist - if the air flow rate is small then the rate of oxidation will be low and the heat will be dissipated at a rate faster than that at which it is generated. However, if the air flow rate is large this will have a cooling effect much greater than the heat produced by the coal oxidation process. If the rates of oxygen supply and heat dissipation lie between these limits it is possible for the oxidation to proceed at an increasing rate, termed a 'heating' (ie. a concealed outbreak of spontaneous combustion), and unless the process is arrested an open fire may result. Modern mining techniques involving retreating coal faces have reduced the risk of spontaneous combustion. However, when the coal face stops, which may occur for a variety of reasons, heatings continue to develop. Additionally, higher

ventilation rates have increased the risk of spontaneous combustion, and heatings have developed in coal seams which have previously been considered safe. A number of combative measures that may be used to remedy this process include digging, flooding, treatment with water or chemicals, infusion of inert gases and sealing off the fire [70].

Historically many areas have been abandoned, and as yet no solution to this problem has been discovered. Since modern coal mines require large amounts of capital investment (eg. Selby complex ca.£1500 million) the abandonment of a district underground is much more serious than in the past when it was hand worked. Also, the high cost of large quantities of machinery used underground has resulted in fewer working coal faces at each colliery producing higher tonnage outputs. Hence, even short interruptions in production give cause for concern, illustrating the need for the early warning of problems.

Spontaneous combustion also presents obvious dangers to the health and safety of miners, whose escape route to the surface may be several kilometres long. Not only are toxic gases, including smoke, released at an early stage, but an open fire could trigger methane and coal dust explosions. Such disasters are historically well known in most colliery villages, but the more recent explosion in the Stolzenbach lignite mine in Germany (1988) graphically illustrates the problem. Thus it can be seen that the spontaneous combustion of coal presents a serious problem to the mining industry, and it's early detection is extremely important.

1.6.1   Theories of Spontaneous Combustion

Historically a variety of theories have been proposed to explain the phenomenom of spontaneous combustion, the most important of which are reviewed below :-

(i) **Pyrites theory** - The first paper on spontaneous combustion was published by Dr. Plot, Professor of Chemistry, Oxford in his 'History of Staffordshire' in 1686 [71]. In this work he studied the occurrences of spontaneous combustion in coal heaps, and attributed them to the oxidation of pyrites (FeS_2). According to Schmidt the exothermic oxidation of pyrites associated with coal is described by equation (1) [72].

$$2FeS_2 + 7O_2 + 16H_2O \longrightarrow 2H_2SO_4 + 2FeSO_4.7H_2O + HEAT..(1)$$
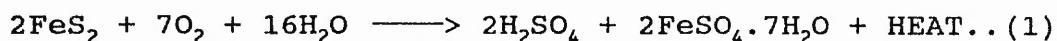
The heat of oxidation of pyrites was experimentally found by Lamplough and Hill to have a mean value of 13.8J/mol per ml of oxygen consumed [73]. However, it is now generally agreed that it is the fragmentation of coal, associated with the volume expansion of the oxidation of pyrites to ferrous sulphate, which has a greater contribution towards enhancing the combustion of coal by increasing its' surface area [74].

(ii) **Bacteria theory** - the role of bacteria in the spontaneous combustion of coal was studied by early workers since bacterial activity is known to be the cause of the spontaneous ignition of hay. This subject has been reviewed by Coward in which four of the six investigations studied provided evidence that bacteria could live on coal and were capable of causing a slight rise in temperature [75].

-28-

However, Graham found that a sterilised coal oxidised at the same rate as unsterilised coal, concluding that the mechanism of coal oxidation does not involve bacterial activity [76]. Scott quoted the committee on Spontaneous Combustion in Mines, 'The self-heating of coal is not in any way due to the presence of bacteria' [77].

(iii) **Humidity theory** - the hygroscopic nature of coal causes the generation of a large amount of heat when wetted with water. Graham stressed the importance of humidity in relation to spontaneous combustion, when he showed that the rate of oxidation of coal in water saturated air was increased by about 50% compared to the same reaction in dry air [76]. Later, Bhattacharya observed that when water is absorbed as a vapour the latent heat of vapourisation should be added to the heat of wetting, which will considerably increase the coal bed temperature [78]. It is therefore apparent that moisture aids coal oxidation whilst not being the primary cause for its' spontaneous combustion.

Mukherjee and Lahiri studied the mechanism of the reaction between water and coal at 100°C, and proposed the mechanism shown in equations (2a-2c), in which the brackets imply a chemisorbed species [79].

$$H_2O \longrightarrow (H) (OH) \longrightarrow (H_2) (O) \longrightarrow (H_2) + (O) \quad ...(2a)$$

$$C + (O) \longrightarrow (CO) \longrightarrow CO \quad ....(2b)$$

$$(CO) + (O) \longrightarrow (CO_2) + CO_2 \quad ....(2c)$$

It is interesting to note that this scheme could explain sources of CO and CO_2 other than from the low

-29-

temperature reaction between oxygen and coal, particularly since water is itself a product of this reaction.

(iv) **Coal-oxygen complex theory** - the interaction of coal with oxygen in the spontaneous combustion of coal is generally accepted to proceed via a coal-oxygen complex according to a variety of authors. This process has been described earlier in section 1.4 of this work, and it is believed that spontaneous combustion is primarily due to the increasing reaction between coal and oxygen. The reaction proceeds via the formation of peroxy complexes, and a model for the evaluation of spontaneous combustion using Western Canadian coals was recently studied by Bachelor et al [80]. It is generally well accepted that the susceptibilty of coal to spontaneous combustion is inversely related to coal rank, and they found that the peroxide and free radical contents also vary inversely with coal rank. They found that the reaction of coal samples with oxygen generated new peroxides, but the reaction of coal with oxygen-free nitrogen lead to peroxide decomposition creating new free radicals. Hence they concluded that the most important factor in the initiation of spontaneous combustion was the moisture-actuated decomposition of peroxides.

1.6.2 Detection and Assessment of Heatings in Coal Mines

There are a variety of physical indications which occur as a heating progresses. Initially traces of the smell known to coal miners as 'gob-stink' occur, and many

definitions of this have been given in the literature. Descriptions of gases (table 1) that could possibly cause the odour are listed [81] :-

(i) a close musty smell ------------- oxygenated species.

(ii) a petrolic or paraffin smell ---- aliphatic group.

(iii) an aromatic smell --------------- aromatic gases.

(iv) a mercaptan smell --------------- sulphur gases.

The next stage is the deposition of moisture, observed as sweating of the strata. This is caused by the high humidity of warm air from the heating area meeting the cooler ventilating air. At this stage creaking sounds may be heard which are due to the collapse or crack formation in the strata. Also, the temperature of the strata begins to rise, which may be detected by thermal imagers. British Coal uses commercial instruments such as the Probye and the Osprey for this purpose. Finally smoke is produced, which indicates that the incipient heating has reached the stage of active combustion.

Historically the British mining industry has relied upon CO measurement as the standard tool by which spontaneous heating activity is measured. Since a heating involves the consumption of oxygen as well as the formation of products such as CO, Graham devised a scheme whereby the ratio of CO produced to the O_2 consumed served as an indication of spontaneous combustion underground [76]. This value, termed the Graham ratio, has become the main method of chemical detection in most collieries which are susceptible to spontaneous combustion. Calculation of the Graham ratio,

which is dependent upon the fresh air constant proportions of oxygen and nitrogen being 20.93% and 79.04% respectively is shown below [82].

Laboratory Analysis :

CO_2=0.90%; CH_4=0.50%; O_2=19.50%; CO=0.0060%.

N_2=79.09% (N_2 calculated by difference).

O_2 associated with N_2 = 79.09 x $\dfrac{20.93}{79.04}$ = 20.94 ...(A)

O_2 present in sample = 19.50% ....(B)

O_2 deficiency = (A)-(B)

= 20.94-19.50 = 1.44%

CO present in sample = 0.0060% ....(C)

Graham Ratio = $\dfrac{CO}{O_2 \text{ deficiency}}$ = $\dfrac{(C)}{(A)-(B)}$ x 100 %

= $\dfrac{0.0060}{(20.94-19.50)}$ x 100 %

Graham ratio = 0.42%

Since this method relies upon the transportation of mine air samples taken in pressurised capsules underground to a laboratory for analysis, this passage of time represents a severe disadvantage of the system. However because this method is presently the most sensitive measure of the progress of a heating, the detection of an underground heating may result in the temporary installation of a mobile laboratory at a colliery to carry out this analysis.

The first continuous monitoring installations were based upon the German 'tube-bundle' system of sampling [83]. In this instance, each district had a tube through which air samples were drawn at intervals to an analysis point on the colliery surface, where the results were recorded on

-32-

charts. This system allowed the normal CO concentration for a district to be established, and slow rises in the CO levels indicative of the early stages of a heating could be observed. However, the main disadvantage with this system is the delay that can occur when the sample is some distance from the analysis point, which can be as long as 4 hours [84]. In order to overcome this problem, electrical transducers have been fitted in remote locations which transmit readings to a computer on the colliery surface. This system has the advantage of instantaneous indication, but the cross-sensitivity of the transducers to other gases results in false CO readings producing false alarms. As well as this lack of discrimination it is difficult to determine in the initial stages of a rise in CO whether this is a product of the early stages of a heating, or if it is some other factor such as barometric change, or a product of other legitimate mining activities such as diesel exhaust fumes or shotfiring. In order to deal with this problem of false alarms McCormick described an algorithm which resulted in the institution of a Multi-Discriminating Alarm (MDA) system [85]. This algorithm analyses historical CO data on a statistical basis, and calculates a geometric mean as the normal level. Five alarm points MDA1 to MDA5 are set at incremental levels of CO concentration above the norm, and a duration time is calculated that has to be exceeded before the alarm is triggered. The MDA system has not halted but merely limited the number of false alarms.

An interesting form of investigational work is presently being carried out at the U.S. Bureau of Mines concerning a sub-micrometer paticulate detector first suggested by Hertzburgh [86]. The operating principle is based upon the production of minute particles ($<0.1\mu$m size) that are invisible to the human eye during the combustion of wood, plastic and coal. Although the production of such particles from heated coal dust has been demonstrated, the applicability of this technique to the heating of coal strata as occurs underground remains to be seen.

A review of an internal Headquarters Technical Department report on 'Underground Mine Fires (1987-1988)' reveals a poor detection rate of such occurrences despite extensive automatic environmental monitoring systems [87]. From a total of 96 fire incidents only on 3 occasions was the alarm system triggered, and inspection of the data showed significantly increased levels of CO had occurred on a further 7 occasions.

An obvious method of overcoming these problems would be the identification and monitoring of indicator gases other than CO which show the early development of a heating. This would prevent the regular occurrence of false alarms which still occur, even with MDA, due to the actions of routine mining activities of diesel locomotives and shotfiring. The work of Gibson identified a number of pertinent indicator gases [64]. It is the purpose of this work to study the formation and monitoring of the gases which are associated with the spontaneous combustion of coal.

1.7 Gas Composition of a Coal Mine Atmosphere

The atmosphere in a coal mine differs from fresh air because coal mining operations always produce pollutant gases in quantities which vary widely from colliery to colliery. For this reason fresh air is continually drawn through the working areas to ensure a minimum oxygen concentration of 19% is maintained. This is also to dilute pollutant gases as required by legislation that has been reviewed in a handbook for colliery officials [88]. According to Jones these gases may be classified into three major groups as described [89]:-

(i) AIR - Assumed to consist of a ternary mixture of $O_2(20.93\%)$, $CO_2(0.03\%)$ and $N_2(79.04\%)$. The 0.93% quantity of argon known to be present in air is assumed to be nitrogen within British Coal in order to simplify calculations, since it is inert.

(ii) EXCESS INERTS - These gases are termed blackdamp, and consist of a mixture of excess nitrogen and carbon dioxide. They increase in concentration as the oxygen content of a mine air is consumed, and their quantities are measured by calculating the difference between the concentration determined by an analysis and that equivalent to the measured oxygen content.

(iii) COMBUSTIBLE GASES - These gases consist of firedamp (composed of 90-95% methane and smaller quantities of higher hydrocarbons), carbon monoxide, hydrogen and hydrogen sulphide. If a heating occurs the relatively small quantity of carbon monoxide present under normal mining

conditions increases significantly. If the heating progresses to a sufficiently high temperature, hydrogen may be formed. The major problem with these gases is the risk of explosion. The plotting of a Coward diagram determines whether or not an atmosphere is explosive due to a single component. If a mixture of explosive gases are present, the Hughes and Raybould method, which is similar to that of Coward is used, in which a plot of oxygen concentration versus total combustibles concentration reveals a triangle of explosibility. The constitution of the gas mixture allows a corresponding point to be plotted on this diagram, and if it is present in the triangle the mixture is explosive. A fuller explanation of these methods is provided by consulting the MSc thesis presented by Jones [89].

Firedamp is evolved from coal and other carbonaceous sediments such as shale, as well as porous strata, to which it has previously migrated from coal. It is a gaseous mixture which is desorbed from such matter as the mining process removes the burden of pressure of earth. However, the composition of initially evolving gas cannot be used to indicate relative amounts of the component gases in the seam because of differing desorption rates. Thus, coal commonly has a methane:ethane content of 10:1 even though mine air contaminated with firedamp from this coal would normally contain these gases in a ratio of about 30:1, due to the greater desorption rate of methane [90]. In order to overcome the large concentrations of firedamp that are

released when coal is mined the process of firedamp drainage is necessary. In this process firedamp from strata overlying or underlying the coal seam being worked is extracted before the gas has escaped into the ventilation current. The need for firedamp drainage is now greater because modern mining involves a more rapid rate of daily advance. The primary objective is one of safety, but there are presently a number of coal mines from which the drained firedamp is sold as a source of methane fuel. Typically the drained firedamp gas contains a minimum of 40% methane.

The presence of firedamp constituents in the ventilating air of a coal mine are dependent upon a number of variables including the ventilation conditions and the rate at which coal is being mined. The hydrocarbon components present in firedamp are methane, ethane, propane, methylpropane, n-butane, methylbutane and n-pentane [91]. The relative concentrations of these gases follow a logarithmic pattern in the ventilating air as the series is progressed from methane, as illustrated in the typical mine air analysis below (concentration units are ppm) :-

methane=8500;ethane=320;propane=95;butanes=20;pentanes=5.

A general conclusion derived by Gedenk is that the composition of saturated hydrocarbon gases evolved from coal seams depend upon the rank of the coal being mined, and the depth of the seam [92]. Deeper coal seams and higher ranked coals tend to contain higher proportions of lighter hydrocarbons. This is believed to be related to the fact that the stability of members of a homologous series

increases as the number of carbon atoms decreases. It also forms the basis for a technique in which the evolution of firedamp can be related to the coal seam from whence it originated, the ethane/methane ratio [93].

1.8   Chromatographic Analyses of a Coal Mine Atmosphere

The complex gaseous composition of a coal mine atmosphere necessitates the use of chromatographic methods to separate and analyse the low concentrations of trace components. The recent improvements in instrumentation have made possible the use of gas chromatographic (GC) systems in remote situations. It has therefore been proposed to develop and study such instrumental systems for eventual use in the underground environment of a coal mine. This required a detailed study to be made of the factors which affect the chromatography process [94-102]. Consideration must be given to the individual components of a GC system, which may be classified as shown below :-

(i) **Sample Introduction System** - In order to minimise the band broadening effects that lead to a poor separation the gas sample must be introduced onto the stationary phase as a non-dispersed band. Conventional methods involve mechanical devices or electronically activated systems that have large power requirements incompatible with underground use.

(ii) **Chromatographic Column** - This is the heart of a chromatograph since it is where the separation of the gaseous mixture takes place.

(iii) **Detector** - This measures some bulk property of the eluting components and produces an electrical signal that is amplified to quantify the separated components [103]. Selective detectors are not primarily required since the analytes would elute sequentially from the column. The detection limits of the gases of interest can be improved by using detectors with greater selectivity towards these gases.

1.9   Objectives of This Work

The detection of underground fires at the earliest possible stage is required because belated action may allow the fire to spread to adjacent areas. At present, systems based on the accurate monitoring of CO concentrations and the CO/O_2 deficiency ratio are primarily used to determine the presence and status of spontaneous combustion and underground fires. There are several problems with these techniques, particularly delayed analysis times and the production of false alarms due to routine mining activities such as the emissions from diesel locomotives and shotfiring. In order to improve on these systems the monitoring of other gases associated with the spontaneous combustion of coal is proposed. As an initial step a laboratory study of the low temperature combustion products of coal is necessary. The complex variety of gases evolved from heated coal necessitates the use of gas chromatographic methods of analysis. Since the eventual use of such equipment will be in a hazardous environment for

prolonged periods, constraints are placed on the GC parameters employed. This work therefore requires an investigation into these parameters, as well as the response characteristics of a number of suitable detectors.

The most recent investigation into gases evolved from the low temperature heating of coal was carried out by Gibson, who utilised a method of sample enrichment by collecting the analytes onto adsorbent tubes [64]. Although the use of thermal desorption analysis techniques allowed the detection of low levels of these gases, the analytical methods were so prolonged that the data obtained was limited. In order to improve on these methods this work will concentrate on reducing the analysis times and maximising the limits of detection by optimising the chromatographic parameters employed. This will allow the frequent collection of analytical data during the coal combustion process, thereby aiding the interpretation of the reaction kinetics and mechanisms of the formation of evolved gases. The collection of such detailed data will also allow an interpretation of the ratios of gases evolved during coal combustion to be carried out. This information could produce useful information on the different stages of low temperature coal combustion, providing an insight into the breakdown of the coal structure under these conditions. As a further guide to the combustion process there will be continuous studies of the coal temperature and major combustion products using equipment configured in this work.

CHAPTER 2

DEVELOPMENT OF SEPARATION METHODS

2.1   Introduction

It has been proposed to use GC in order to continuously monitor specific indicator gases evolved during the early stages of the spontaneous combustion of coal. An understanding of the chromatographic interactions leading to selective separations was therefore necessary in order to optimise the separation performance [94-102,104]. The principles of gas chromatography involve a distribution equilibrium of the sample between the stationary phase and mobile phase, which creates a partitioning process [95].

The specifications required for a stationary phase to be used in this work were :-

(a) a satisfactory separation of the components of interest in a minimum time.

(b) stable solid surface characterisitics for reproducible chromatography and an analytically robust system.

(c) isothermal operating conditions, since in a portable GC temperature programming would require additional instrumentation and could affect the robustness of the method.

(d) a minimum column operating temperature of 50°C, since some underground districts may attain temperatures of 35°C; a maximum temperature operating as low as practical to minimise power requirements.

These factors clearly placed constraints on the GC conditions that may be employed in this work.

Stationary phases have been classified in the literature by using retention indices in order to simplify their selection [105-108]. Also, Scott suggested a technique for determining the optimum conditions necessary to effect a separation by GC [109]. More recently the computerised Simplex method has been developed, which involves optimising a chromatographic response function [110-112]. The Simplex method was not considered appropriate for use in this work due to the external constraints placed on the GC conditions discussed earlier.

The approach to developing suitable separation methods in this work essentially involved a review of the literature for stationary phases capable of separating the gases of interest. This was followed by a study into improving the separation achieved by these stationary phases. The optimisation of this separation required a minimum analysis time with satisfactory resolution and peak separation. There are a number of mathematical definitions of peak resolution (see Appendix 1), but the simplification adopted by Perry is considered here [97]. In this approach the resolution may be considered to be a function of relative retention and the number of theoretical plates present on a column. Alternatively, the factors which may be controlled to improve peak resolution are selectivity and efficiency. In order to improve the separations in this work these factors were studied separately.

As recently as April 1989 it has been stated that "control of selectivity remains the essential key to further improving chromatographic performance" [113]. The concept of adjusting column selectivity in order to separate a group of compounds has been termed "selectivity tuning", and this has been reviewed in the literature [114, 115]. This has been extended to optimise the composition of a stationary phase for the analysis of complex mixtures by using "window diagrams" [116-119].

The efficiency of a column may be considered in terms of the number of theoretical plates (ie. equilibrium steps) present according to the plate theory. A theoretical plate is an imaginery length of the chromatographic column wherein complete equilibration of the solute between the mobile and stationary phases is attained [120]. This model has recently been reviewed by several workers [121,122]. The number of theoretical plates is determined by dynamics and the physical characteristics of the column. The van Deemter rate theory permits the efficiency of a column to be quantified in terms of the physical dimensions of the column, column packing and the thermodynamic retention processes [123,124]. This involves plotting a van Deemter graph, which may be expressed by equation 3.

$$h = A + B/u + C.u \ldots\ldots\ldots\ldots (3)$$

In this equation A, B and C are constants, u is the average linear carrier gas velocity and h is the height equivalent to a theoretical plate. An interpretation of this equation allows the pratical factors which affect the number of

theoretical plates to be studied and hence optimised.

A glossary of the definitions and calculations of chromatographic parameters used in this work have been listed in Appendix 1.

A survey of the different column packing materials that may be used for the separation of aliphatic and unsaturated hydrocarbons using gas-solid chromatography was carried out [125,126]. This indicated that the most suitable materials were porous polymers, porous silica beads or activated alumina. The chromatographic properties of porous polymers have been reviewed by Dave and by Hollis [127,128]. Commercially available materials include the Porapak series and the Chromosorb century series. The retention data obtained from the literature revealed Porapak Q and Porapak S to be the most suitable [129].

A number of reviews of the chromatographic use of porous silica beads have been published, and two materials are commercially available - Spherosil and Porasil [130-132]. The porous silica beads most suitable for this work are Porasil C, since this type has a lower surface area than type B (C=100m^2/g, B=185m^2/g), and would therefore require less surface modification.

Scott et al carried out much of the early work into the use of alumina as an adsorbent [133-135]. The surface modification of alumina has more recently been examined by Naito et al [136-138]. The effects that surface modification and a variety of physical processes have upon the adsorption properties of alumina are diverse. A

-44-

thorough understanding of these may allow the required selectivity to be achieved.

Stationary phases which may be used to separate sulphur gases in a GC system have been studied by several workers [139-141]. The most suitable technique to date has been described by de Souza et al, who used Porapak Q to separate low molecular weight sulphur gases [139].

Literature on the separation of the oxygenated gases studied in this work has been reviewed by workers in the brewing and dairy industries [142,143]. Polar stationary phases such as Carbowax are typically used for the separation of these gases [144].

In recent years physical column characterisitics have been studied in order to improve column efficiency [145]. This has resulted in the development of micropacked and open tubular columns. A comprehensive study of micropacked columns has been presented by Cramers and Rijks [146]. An excellent review of the development of open-tubular columns has been produced by Jennings [147].

2.2   Equipment

A Pye 104 gas chromatograph equipped with a single channel FID and fitted with a Pye-Unicam six-way gas sampling valve containing a 0.5ml sample loop was used.

An Intersmat 120 gas chromatograph was also used equipped with a single channel FID and a Valco 10-way solenoid gas sampling valve with a range of sample loops.

A Pye series 304 GC equipped with a FPD and fitted with

a PTFE gas sampling assembly containing a 2.5ml sample loop was used for the analysis of sulphur gases.

Hewlett-Packard 3396A and 3390A integrators were used to record solute retention times and peak areas.

The carrier gases and flame gases employed were passed through charcoal and molecular sieve purification traps (Phase Separations, Deeside Industrial Park, Deeside, Clwyd.) to remove trace organic contaminants and moisture.

PTFE tubing of internal diameter 1.59mm and 0.80mm was used as the column material (Phase Separations).

2.3   Chemicals and Reagents

The adsorbents used in this work as column packings have been listed below (Phase Separations) :-

Porasil C (WATERS) : particle size 80-100 mesh.

Porapak Q (WATERS) : particle size 80-100 mesh.

Porapak S (WATERS) : particle size 80-100 mesh.

Alumina F1 (ALCOA) : particle size 60-80 mesh.

A PoraPLOT Q open tubular column (10m long x 0.53mm i.d.) was obtained commercially from Chrompack UK Ltd. (Unit 4, Indescon Court, Millharbour, London).

A DB-Wax open tubular column (30m x 0.53mm i.d.) was obtained commercially from Fisons Scientific Equipment PLC (Bishop Meadow Road, Loughborough, Leics.).

All other reagents used were of analytical reagent grade (Analar), obtained commercially from BDH Chemicals Ltd. (Poole, Dorset), and the solutions were prepared with doubly distilled, deionised water.

B.O.C. primary gas standards were used in this work as listed below in ppm (V/V):-

Standard 1 : methane,195; ethane,160; ethene,255;

propane,165; propene,180;

methyl propane,160; n-butane,230.

Standard 2 : ethene,205; propene,210.

Standard 3 : methane,155; ethane,195; propane,165;

n-butane,170.

2.4   Experimental

The adsorbents were packed into columns and used to isothermally separate the standard gas mixtures at a variety of column temperatures and carrier gas flow rates. In order to optimise peak resolution the two separation parameters selectivity and efficiency were studied individually. A variety of different column dimensions and experimental conditions were used, and these are described separately in each section.

2.4.1   Procedure for Packing Columns

PTFE column material was used due to its' inertness to the gases of interest and ease of handling. Additionally the transparency of the PTFE allowed the quality of the column packing procedure to be monitored by visual inspection for anomalies such as voids. A silanised glass wool plug was inserted into one end of the column which was then connected to a vacuum pump. The packing material was drawn into the other end of the column via a small funnel

by the action of the pressure differential. During this process, the entire column assembly was vibrated to ensure an even distribution of the column packing. Attention was paid to the packing details described by Grob [99].

2.4.2 Preparation of Modified Alumina Adsorbents

10g of alumina F1 (60-80 mesh) was placed in an evapourating basin, and a solution containing a weighed amount of modifier in sufficient deionised water to produce a slurry was added. This was regularly mixed, and left to stand for several hours at room temperature when the water subsequently evaporated, leaving an even coating of the modifier over the entire alumina surface. This was then heated to 400°C in a muffle furnace for 4 hours, since this temperature represents the optimum adsorptivity of alumina [148]. Air was drawn over the modified adsorbent during the packing process. In order to prevent discrepencies in retention data caused by fluctuations in the time taken to pack a column, each packing material was exposed to the laboratory atmosphere for 24 hours to equilibrate. Then, before analysis was carried out on the column it was heated overnight (16 hours) to a temperature of 150°C with a helium purge of 40 mls/min in order to condition the column.

2.4.3 Study of Adsorbent Characteristics of Stationay Phases

The suitability of a variety of adsorbents (Porapak Q, Porapak S, alumina, porous silica beads) for the isothermal separation of a mixture of lower hydrocarbons was studied. Each adsorbent was packed into a column of dimensions 2m long x 1.59mm i.d., and used to separate a hydrocarbon gas mixture at a variety of different nitrogen carrier gas flow rates and column temperatures.

2.4.4 Study of Selectivity - Surface Modification of Alumina

Surface modification of alumina was carried out as described in section 2.4.2, and the modified adsorbent packed into a column 2m long x 1.59mm i.d. This was carried out to study increasing the selectivity of the adsorbent towards the separation of unsaturated components and their saturated analogues.

In order to study the effect of modifier concentration alumina was modified with sodium chloride in the range of 0, 1, 2, 4, 8 percent (w/w). Analyses of the hydrocarbon gas standard were carried out in duplicate at a variety of temperatures (53, 60, 70, 80°C) to ensure repeatability across this range. The lowest temperature was chosen because it represented the minimum at which the column oven would operate.

The effect of different heat treatments of modified alumina were investigated by heating alumina, which had previously been modified with 2%(w/w) NaCl, overnight

(16 hours) at a variety of different temperatures, termed the post-heating stage. Helium carrier gas was used to purge the column at a volumetric flow-rate of 40 mls/min during the heating process. The temperatures used were 20, 60, 100, 150, 200, 250°C. The resultant modified adsorbent was used to carry out the isothermal separation of a hydrocarbon mixture in duplicate.

In order to study the effect of the modifier cation upon the adsorbent retention properties, a variety of 2%(w/w) metal chloride modified aluminas were initially prepared. The alkali metals studied were lithium, sodium, potassium and caesium. The rubidium salt was not studied. The same modifiers were later prepared at a constant molar weight loading of 0.340mmol/g (modifier/alumina), since this represented an equivalent molar concentration of salt per unit surface area. This corresponded to a similar alumina surface coverage for each salt. Other cations studied at 0.340mmol/g salt weight loading included hydrogen, copper and silver. Since silver chloride is insoluble silver nitrate was used to study the effect of this cation. A sodium nitrate modifer was prepared at the same weight loading in order to ensure that the nitrate anion of the silver nitrate did not appreciably affect the adsorption properties. A typical calculation of the weight loading is shown on the next page.

LiCl   Mol.Wt.= 42.4   (ie. 1 mol = 42.4g)

0.340 mmol/g = 0.340 mmol LiCl / 1g alumina.

0.340 mmol/g = (0.340 x 42.4/1000)g LiCl/1g alumina.

0.340 mmol/g = 0.0144g LiCl / 1g alumina.

0.340 mmol/g = 0.144g LiCl / 10g alumina.

(ie. 1.44% w/w LiCl = 0.340 mmol/g).

The weight/weight proportion of modifier to alumina necessary to prepare a 0.340mmol/g loading for each of the salts studied in this section is listed in table 2. The preparation of a 0.340mmol/g HCl modified alumina was achieved by using a dilution of concentrated hydrochloric acid as shown below :-

conc. HCl = 11.5M = 11.5 mol/litre

50mls x (6mls conc.HCl ———> 1000mls) = 3.40 mmoles HCl

3.40 mmol HCl/10g alumina = 0.340 mmol/g

For each modified adsorbent a column was prepared and post-heated overnight (16 hours) at 150°C with helium carrier gas purging at a volumetric flow-rate of 40mls/min. An isothermal chromatographic separation of the hydrocarbon gas mixture was carried out in duplicate to ensure repeatable data was obtained for different column temperatures utilising the modified alumina adsorbents. The experiment was also repeated using a post-heating temperature of 200°C, when similar trends were observed.

An investigation into the effect that the anion of a modifier salt has upon the retention properties of alumina was carried out by preparing modifiers containing a common

**Table 2   Proportion of Modifier Necessary to Provide
a Loading of 0.340 mmol/g**

Modifier	M.W.	mmol/g	w/w (%)
LiCl	42.4	0.340	1.44
NaCl	58.5	0.340	2.00
KCl	74.6	0.340	2.54
CsCl	168.4	0.340	5.73
$CuCl_2$	134.5	0.340	4.57
$NaNO_3$	85.0	0.340	2.89
$AgNO_3$	169.9	0.340	5.78
$AgNO_3$	169.9	0.118	2.00
$AgNO_3$	169.9	0.029	0.50
KF	58.1	0.340	1.98
KCl	74.6	0.340	2.54
KBr	119.0	0.340	4.05
KI	166.0	0.340	5.64

M.W. - Molecular Weight.

potassium cation and the fluoride, chloride, bromide amd iodide anions. Calculation of the weight loadings necessary to produce a constant 0.340 mmol/g (modifier/alumina) loading are shown in table 2. An identical experimental method was adopted to that used to study the effect of the modifer cation in the previous paragraph.

In order to study the repeatability of retention times a column was packed with 0.340 mmol/g LiCl modified alumina adsorbent and was used to analyse the gaseous hydrocarbon mixture over a prolonged period of time.

2.4.5   Study of Selectivity - Surface Modification of Silica

The surface modification of porous silica beads (Porasil C) was studied using separate inorganic and organic modifiers. The inorganic modifier used was NaCl at a loading of 2%(w/w), and this was prepared as for alumina, described in section 2.4.2. The organic modifer used was phenylisocyanate. Phenylisocyanate modified Porasil C was obtained commercially as 'Durapak' (Phase Separations). These modified Porasils were studied as a technique of increasing the selectivity of the adsorbent towards the separation of unsaturated components and their saturated analogues. In order to study this effect, columns of similar dimensions (2m long x 1.59mm i.d.) were packed with the adsorbents and used to separate a gaseous hydrocarbon mixture at a variety of temperatures. Similar carrier gas flow rates were used for each column to ensure an adequate comparison was made. The maximum column temperature at

-53-

which phenylisocyante modified silica could be operated was 60°C.

2.4.6 Study of Efficiency - Study of Physical Column Characteristics

Columns 1m long x 1.59mm i.d.and 1m long x 0.80mm i.d were packed with untreated alumina F1, and similar columns were packed with Porapak Q according to the procedure in section 2.4.1. Care was taken with the narrower columns since they took a longer time to pack. A number of chromatographic separations of the hydrocarbon mixture were then made using these columns at a variety of different carrier gas flow rates and column temperatures. Typically hydrocarbon standard no.1 was used as the test mixture, but for columns with poor separation characteristics, separate analyses of hydrocarbon standards no.2 and no.3 (p.47) were carried out.

The size of the gas samples injected onto the column was dependent upon the physical column dimensions employed in order to reduce extra-column effects such as band broadening, for example :-

packed column i.d.=1.59mm : sample size = 500μl;

packed column i.d.=0.80mm : sample size = 100μl;

open tubular column i.d.=0.53mm : sample size = 10μl.

2.4.7 Study of Open Tubular Columns

The separation of several different gas mixtures were studied by using a variety of open tubular columns of internal diameter 0.53mm.

-54-

2.5   Results and Discussions

Comparison of the retention properties of different stationary phase systems required the determination of the column dead-time. Although the methane retention time is often used as an approximation of the dead-time, the use of the highly adsorbent stationary phase materials that were necessary to separate C1-C4 components caused the column dead-time to become significant. A novel and rapid method for the determination of column dead-time was therefore developed, and has been fully described in Appendix II. This method was used to calculate the column dead-time and partition ratios (k) for each solute from the retention data obtained from the work. This allowed the calculation of other chromatographic variables as illustrated in Appendix I, which have been used to interpret the different characteristics of the adsorbents.

2.5.1   Comparison of Different Stationary Phases

A comparison of the retention data obtained using the different adsorbents at an identical column temperature of 50°C is illustrated in table 3 (p.58). This clearly shows the elution order from each of the adsorbent columns, and demonstrates the better separation of unsaturated and saturated analogues achieved by the alumina and silica.

The Porapak Q and S column packings were found to be insufficiently selective to resolve the separation of propene and propane, which were co-eluted. Porapak Q was clearly the more selective of the two towards the

separation of propane and propene, producing a relative retention of 1.13 as opposed to 1.05 for Porapak S. Such systems would require 4500 or 28000 theoretical plates for a resolution of 1.0 for types Q and S respectively (N_{req} calculated as in Appendix 1). In order to achieve such a resolution between propene and propane a column length of 8m would be necessary since the 2m long Porapak Q column contained 1200 thoeretical plates (n calculated as in Appendix 1). The impracticalities of this system illustrate the need for an improvement in the factors which govern the resolution of a chromatographic separation - efficiency and selectivity. The latter of these factors cannot be altered for Porapak Q, a copolymeric cross-linked material, so factors affecting the efficiency of the separation were studied, as described in section 2.4.6.

Although alumina and silica produced better quality separations, the unsaturated components produced peaks that were severely tailed. In order to investigate methods of reducing this peak tailing, a study was carried out into the surface modification of these two materials as described in sections 2.4.4 and 2.4.5. This information was also used to study the factors which affect selectivity to be carried out, thereby indicating how the separations could be improved.

The retention data obtained using the three adsorbents - alumina, Porasil C, Porapak Q - were used to calculate the adsorption enthalpies of solutes in the hydrocarbon mixture. This calculation was achieved by utilising a

-56-

derivation of the van't Hoff isochore illustrated in Appendix I (equation 10). From this equation, a graph of ln(k) versus (1/T) produces a linear plot of slope ($\Delta H_{ads}/R$) and y-intercept c (a constant of integration). Hence, a number of chromatograms were obtained over a temperature range of 50°C to 90°C for each adsorbent, and the partition ratio (k) for each solute calculated as described in Appendix I.

The adsorption enthalpies have been illustrated in table 4, which clearly shows that the order of adsorption enthalpy for all of the adsorbates is,

Porapak Q > Alumina > Porasil C.

It is interesting to note that for alumina and Porasil the unsaturated components have adsorption enthalpies greater than their saturated analogues, but the reverse is true for Porapak Q. This fact is borne out in the retention data illustrated in table 3.

Table 3   Comparison of Retention Properties of Adsorbents

Solute	Porasil C		Alumina F1		Porapak Q		Porapak S	
	k	α	k	α	k	α	k	α
Methane	0.29		0.55		2.32		2.52	
Ethane	0.80		3.35		9.64		9.56	
		1.95		2.22		1.37		1.25
Ethene	1.56		7.44		7.05		7.65	
Propane	2.14		18.61		50.11		50.53	
		3.50		3.17		1.13		1.05
Propene	7.50		58.92		44.17		48.12	
Methyl-propane	5.01		92.01		202.2		220.2	
Butane	5.98		116.64		280.4		305.2	

k = solute partition ratio,
α = solute relative retention time.

Table 4   Adsorption Enthalpies Determined Experimentally

ADSORBATE	ADSORPTION ENTHALPY (kJ/mol)		
	PORASIL C	ALUMINA F1	PORAPAK Q
Methane	7.7	7.8	20.5
Ethane	15.1	18.6	30.5
Ethene	21.2	26.8	28.5
Propane	22.3	29.0	40.2
Propene	33.5	36.7	39.4
Methyl propane	28.2	38.3	48.6
Butane	29.8	40.1	50.4

2.5.2   Study of Surface Modification of Alumina

The chromatograms achieved using unmodified alumina indicated two important facts. Firstly, the unsaturated components ethene and propene were more strongly retained than expected, having a greater retention than their saturated analogues. This was surprising since the boiling point elution order typically achieved in gas solid chromatography had clearly been altered. Secondly, the chromatographic peaks for ethene and propene showed a significant degree of tailing preventing the use of this unmodified adsorbent material. This is illustrated in table 5 which lists the peak asymmetries (measured as in Appendix I) for the hydrocarbon compounds analysed. These two facts indicated that some interaction between the unsaturated components and the adsorbent occurs producing a stronger attraction than that between the saturated components and the adsorbent. This is assumed to be a permanent electrical effect related to the charge of the pi-electron system of the unsaturated components and electric dipole on the adsorbent surface. Some peak tailing of the unsaturated solutes was detectable with 1%(w/w) loading of sodium chloride, and this has been completely eliminated at 2%(w/w) loading or above. Hence the need for modification of the adsorbent surface.

Table 5   Peak Asymmetry Measurements of Solutes Using Alumina Adsorbents

SOLUTE	PEAK ASYMMETRY (A_s) OF ADSORBENT					
	Unmodified alumina	1% NaCl alumina	2% NaCl alumina	4% NaCl alumina	8% NaCl alumina	
ethane	1.10	1.07	1.08	1.08	1.07	
ethene	2.07	1.21	1.05	1.06	1.05	
propane	1.08	1.05	1.11	1.10	1.10	
propene	2.04	1.25	1.09	1.06	1.10	

-60-

Figure 3 shows the dependence of the partition ratio of n-butane upon the salt loading, and clearly the partition ratio was reduced as the proportion of salt modifier added to the free alumina was increased. This effect was observed for the unsaturated solutes as well as the n-alkanes analysed. However, the effect upon the partition ratio was reduced as a greater proportion of the salt was added. This occurred to such an extent that there was no noticable difference between the retention properties of the 4% or the 8% (w/w) sodium chloride modified alumina. In another experiment n-butane was found to have zero net retention on a column packed solely with sodium chloride crystals (ie k=0). This suggested that n-butane had no adsorptive interaction with pure sodium chloride. Since the partition ratio for butane was not zero even at 8%(w/w) loading (ie. k=25 at 60°C) this indicated that the surface modification of alumina was not simply a physical phenomenom of the salt blocking the alumina surface. Salt-modified alumina was post-heated at 400°C during preparation. It is suggested this step produced a reaction between sodium chloride and alumina which creates a surface layer less adsorptive than untreated alumina.

An SEM study of the surface of sodium chloride modified alumina adsorbents was carried out to ascertain the extent of the surface coverage. The samples were initially studied directly and later with a conductive gold coating. This was necessary to prevent the build-up
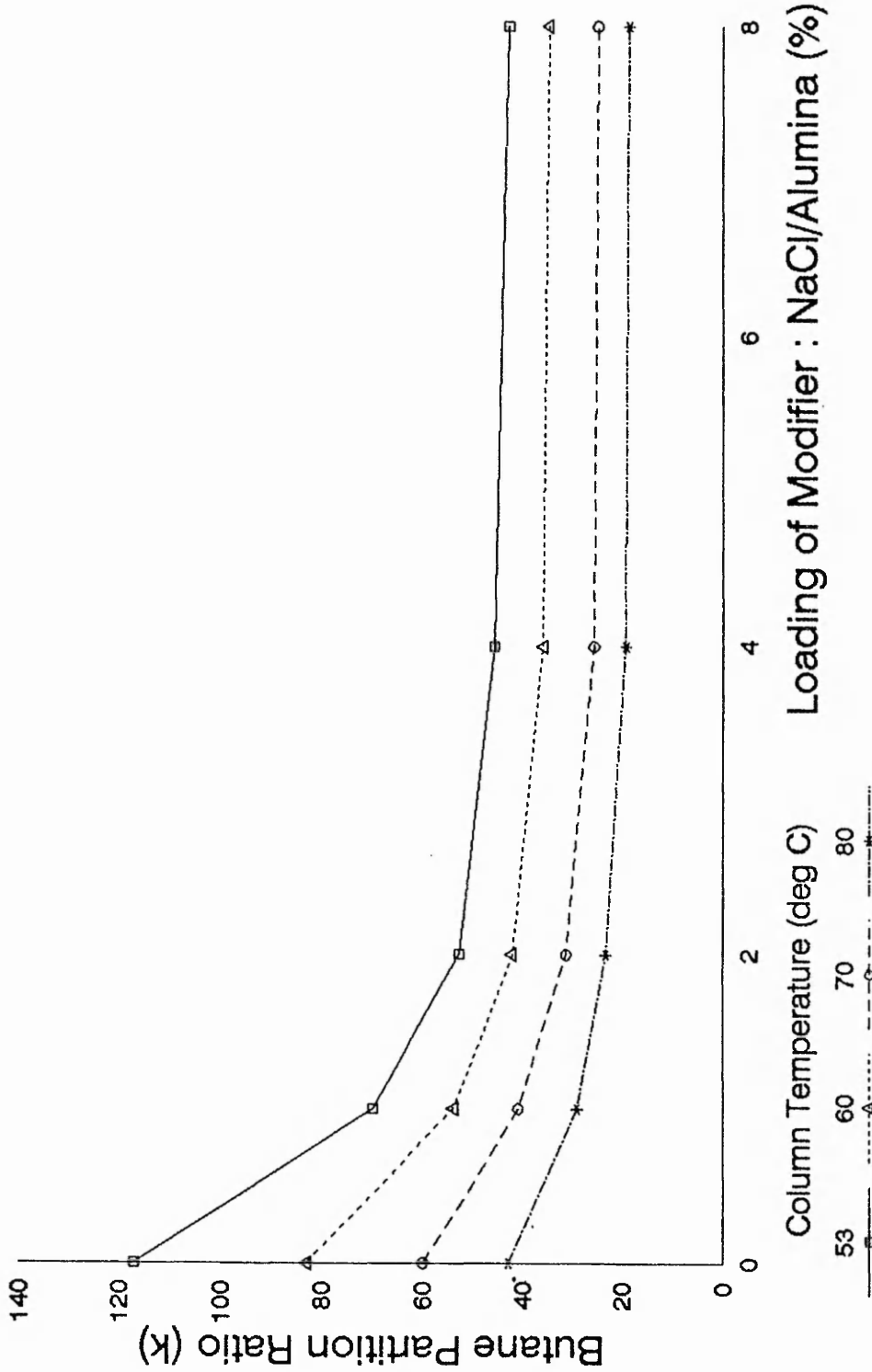
Figure 3   Dependence of Butane Partition Ratio on the Loading of Alumina Modifier

of electrostatic charge which occurred on the alumina surface due to its' non-conductivity. An even coverage of the sodium and chlorine atoms was clearly visible on all of these modified adsorbents with the exception of the 8%(w/w) NaCl/alumina. This adsorbent showed signs that the modifier had 'salted out' since crystals of sodium chloride were clearly visible, as shown in the SEM photomicrograph in plate 1. A possible explanation for the similar retention properties between the 4% and 8%(w/w) NaCl modified aluminas could therefore be that at concentrations above 4% growth of sodium chloride crystals occurs. As mentioned previously, there is no adsorptive interaction between the solutes and crystals of pure sodium chloride. It is therefore reasonable to assume that a 4%(w/w) sodium chloride loading represents the practical maximum of alumina modifier without crystal growth.

The effect of post-heating treatment upon the adsorptivity of modified alumina is illustrated in figure 4, which shows a plot of the partition ratio of n-butane against the temperature at which the column was post-heated. This demonstrates that at higher post-heating temperatures larger partition ratios are obtained, indicating a much greater adsorbate/absorbent interaction. Thus, across the temperature range 20-250°C the modified alumina becomes more activated as the temperature is increased, but the activity increases at a slower rate at higher temperatures. The relative

100μ
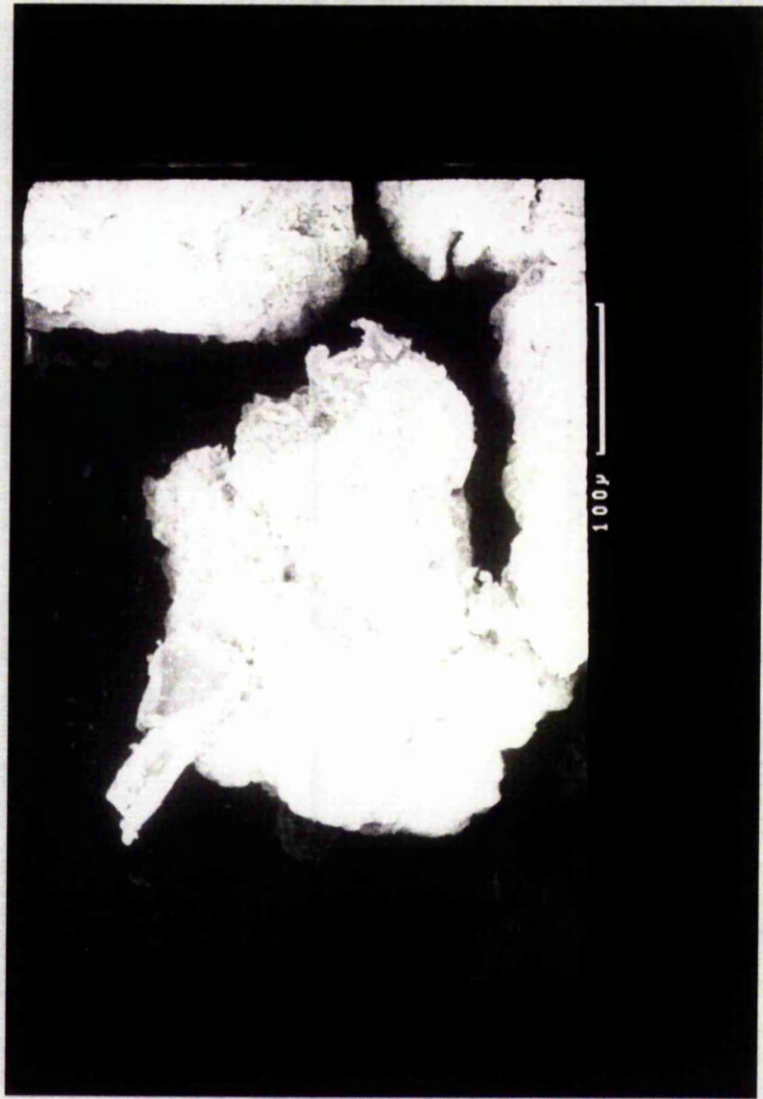
Plate 1   SEM Photomicrograph of NaCl Modified Alumina (8% w/w)
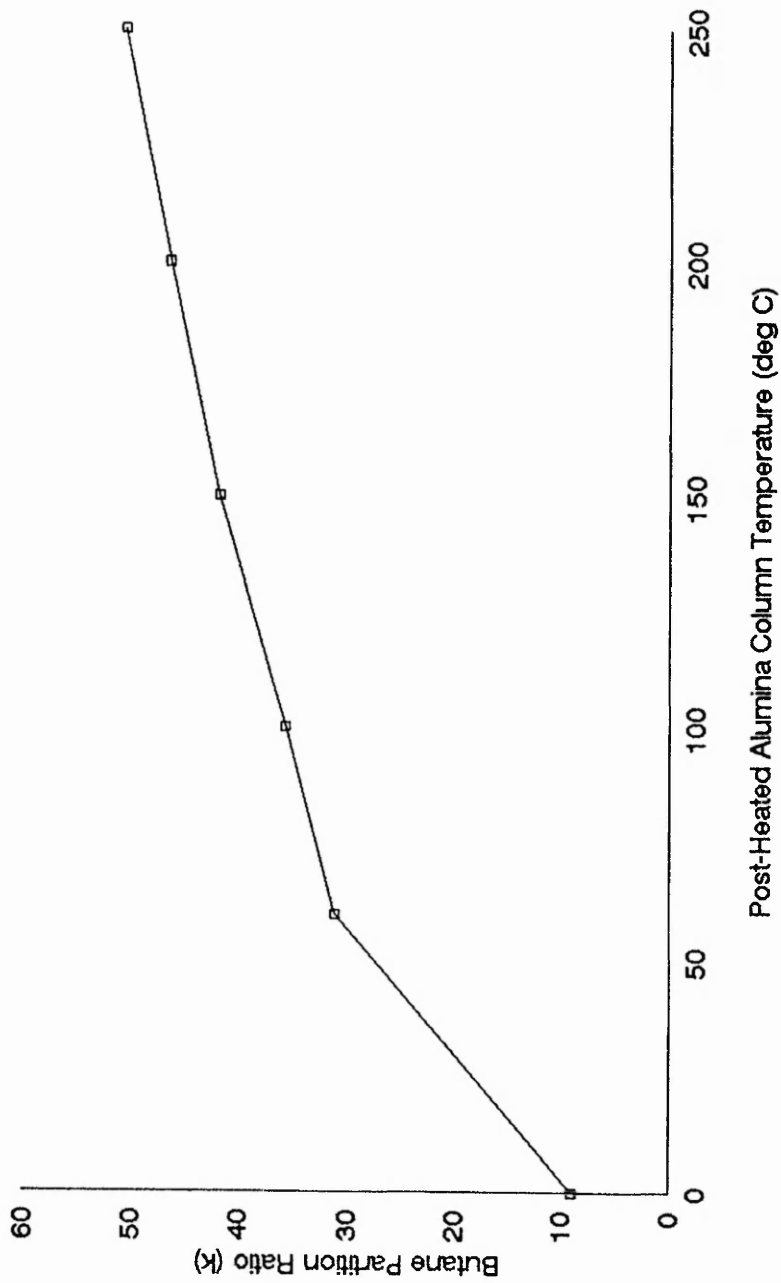
Figure 4 _Dependence of Butane Partition Ratio on the Post-Heated Alumina Temperature_

partition ratios for ethene/ethane, propene/propane and methyl propane/n-butane have been calculated, and these values have been plotted against the column post-heating temperature in figure 5. This allows an insight into the effect that the column post-heating temperature has upon the retentions of unsaturated components relative to their saturated analogues. The methyl propane/n-butane values were calculated to act as a reference, since neither of these components are unsaturated. Figure 5 shows that there is a direct relationship between the temperature at which the column is post-heated and the selectivity for an unsaturated compound relative to its' saturated analogue. An increased separation is achieved when the post-heating temperature is increased. This is practically illustrated in figure 6 which shows the chromatograms achieved under these experimental conditions, demonstrating the relative shifts in retention of ethene and propene. It is therefore apparent that some modification of the adsorbent surface takes place by post-heating at differing temperatures. This modification affects adsorbent interaction with solutes that contain pi-electrons to a greater degree than solutes which do not. Loss of water from the adsorbent surface could occur together with increasing formation of a modified surface structure at higher temperatures, which alter the pore structure of the adsorbent. This was investigated by using a Fourier Transform Infra-Red spectrometer to determine the IR spectra of the aluminas
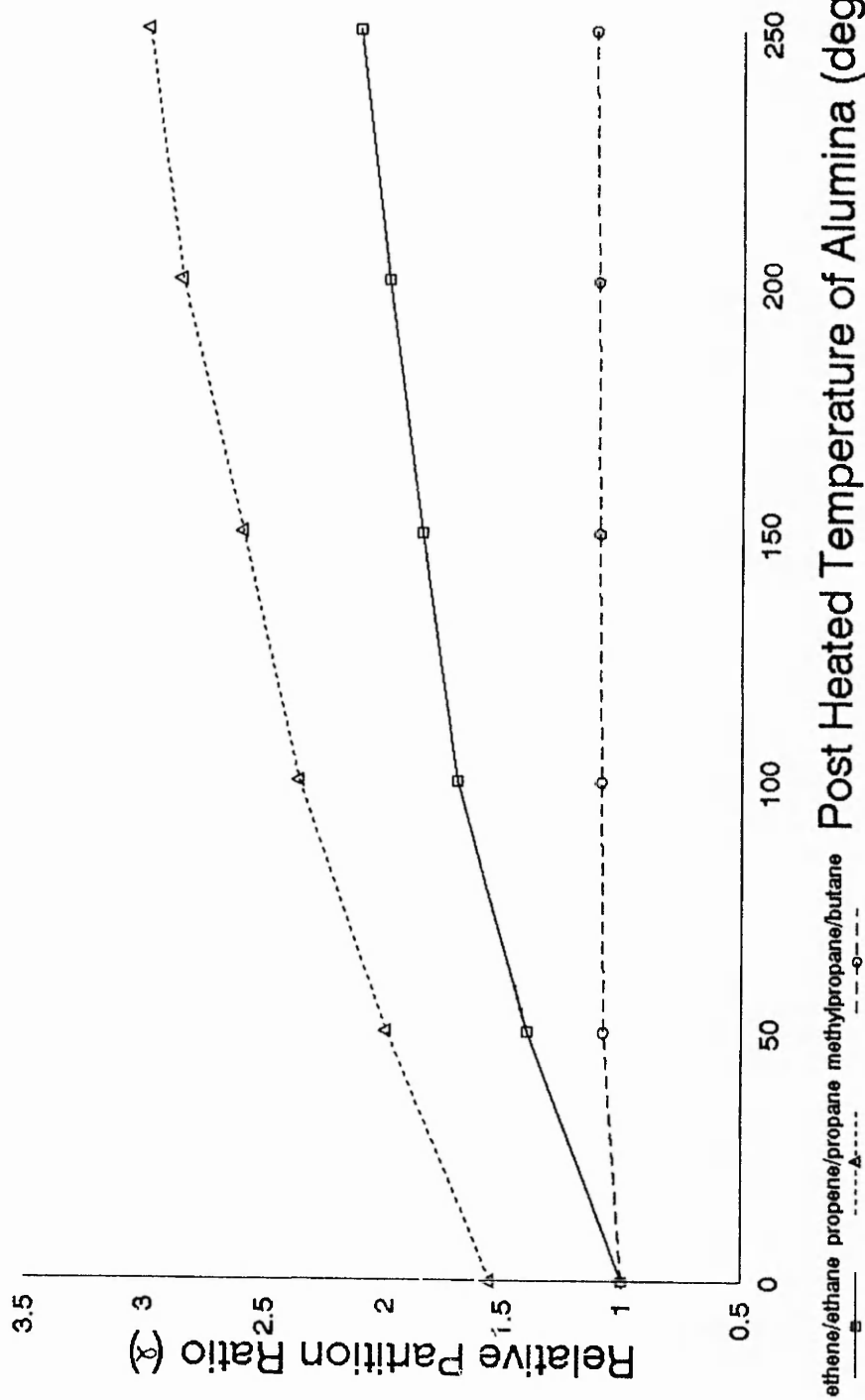
Figure 5   Dependence of Relative Partition Ratio on the Post-Heated Alumina Temperature

-67-

Figure 6 Chromatograms Illustrating Temperature Controlled Selectivity of NaCl (2%w/w) Modified Alumina

60°C: 0.239, 0.492, 0.638, 1.340, 2.587, 4.107, 4.665

100°C: 0.239, 0.515, 0.780, 1.414, 3.175, 4.571, 5.261

150°C: 0.244, 0.540, 0.900, 1.630, 4.075, 5.448, 6.353

200°C: 0.251, 0.570, 1.017, 1.781, 4.872, 6.174, 7.260

250°C: 0.252, 0.583, 1.036, 1.864, 5.408, 6.645, 7.893

Solute elution order :

methane, ethane, ethene, propane, propene, methyl propane, butane.
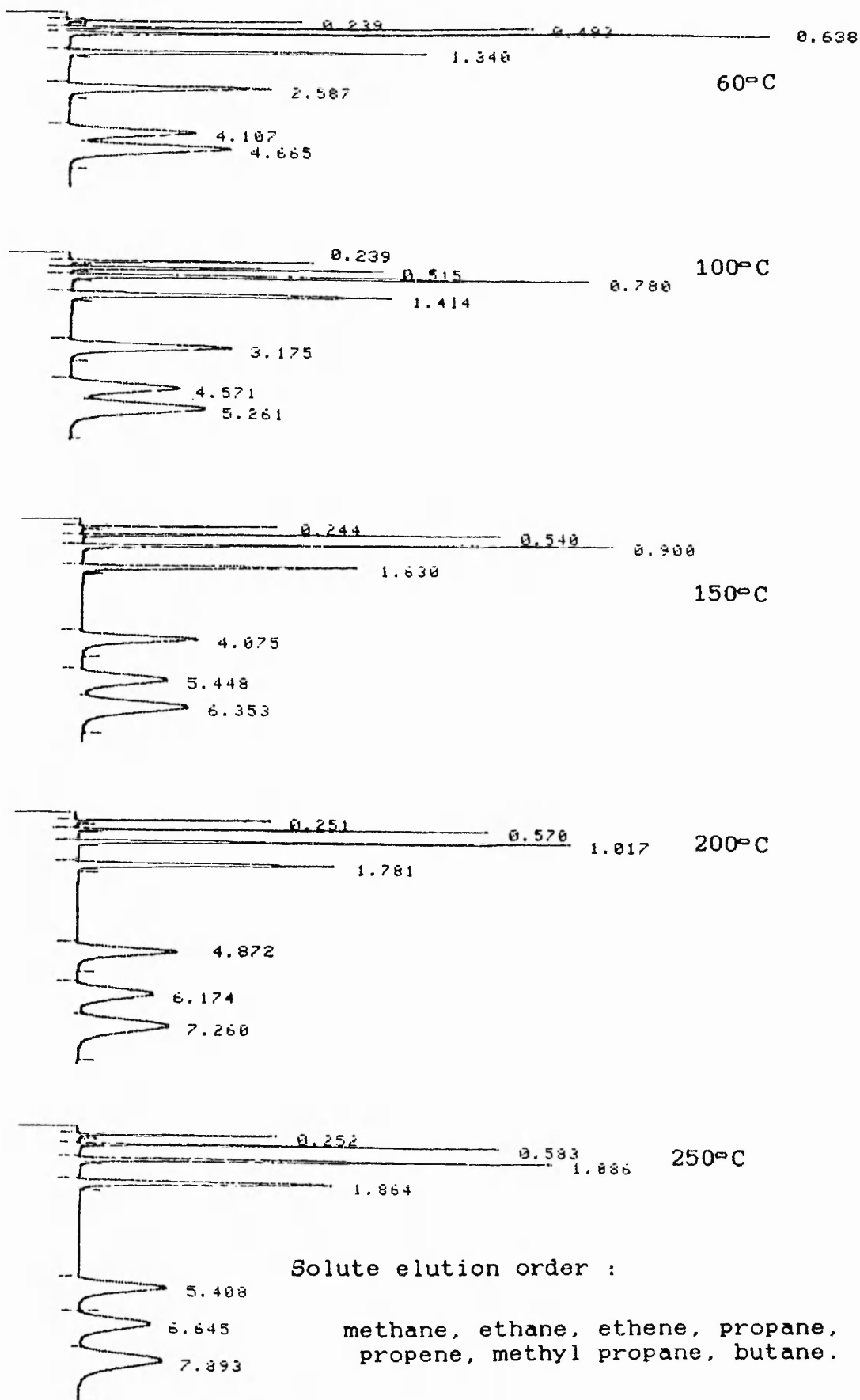
Analytical Conditions :
Temperature=60°C, He carrier gas=40mls/min.

-68-

by the KBr disc method and also using a diffuse
reflectance (DRIFT) cell accessory. Neither of these
techniques yielded useful information due to the low IR
energy throughput. Alumina physically blocked the IR
radiation in the KBr disc method, and in the DRIFT cell
accessory the alumina dispersion of IR energy proved the
limiting factor.

A study of the effect that the modifier cation has
upon the retention properties of alumina was carried out
using a column temperature of 60°C. Retention data
obtained were utilised to calculate the partition ratios
of ethene and propene relative to ethane and propane
respectively. In order to determine the effects of these
unsaturated components relative to their saturated
analogues, the partition ratios of n-butane were measured
relative to methyl propane to act as a reference. These
values were plotted versus the periodic group order of
the cation as illustrated in figures 7a, 7b and 7c. In
both diagrams an apparent periodic trend is noticable
across the cations Li, Na and K but this halts at Cs.
However, in this work comparison of the different alkali
halide modifiers was made by utilising a common weight
percentage of the modifer relative to alumina. Since one
possible mechanism of the modification process was by the
reaction and blocking of adsorption sites it was
considered to be more appropriate to compare the amount
of modifer in moles per gram of alumina. This would
correspond to an identical number of moles of the salt

Figure 7   Effect of Modifier Cation Upon Retention
Properties of Modified Alumina Adsorbent

Figure 7a

Figure 7b

Figure 7c
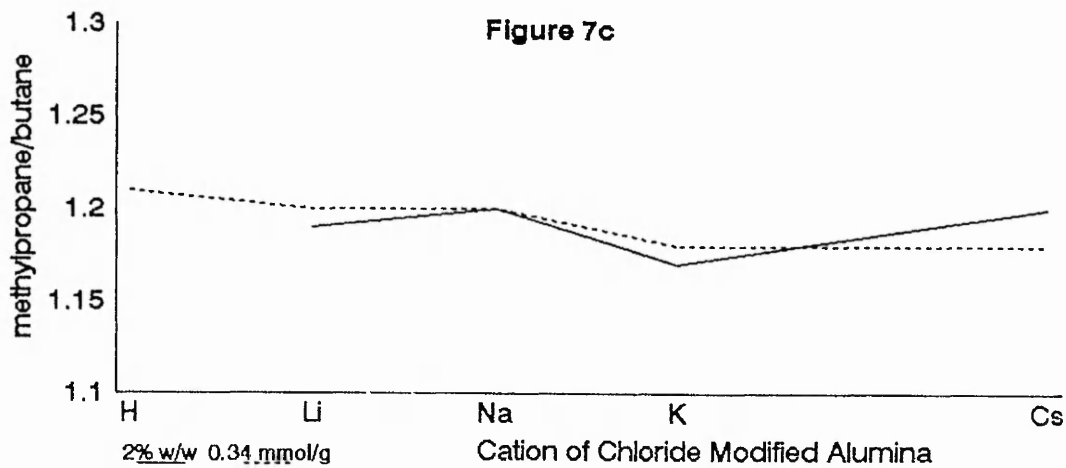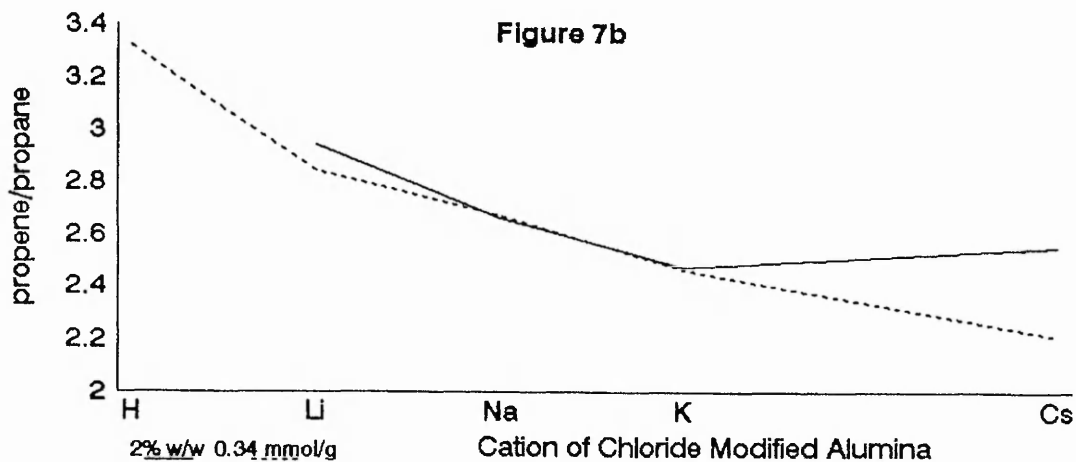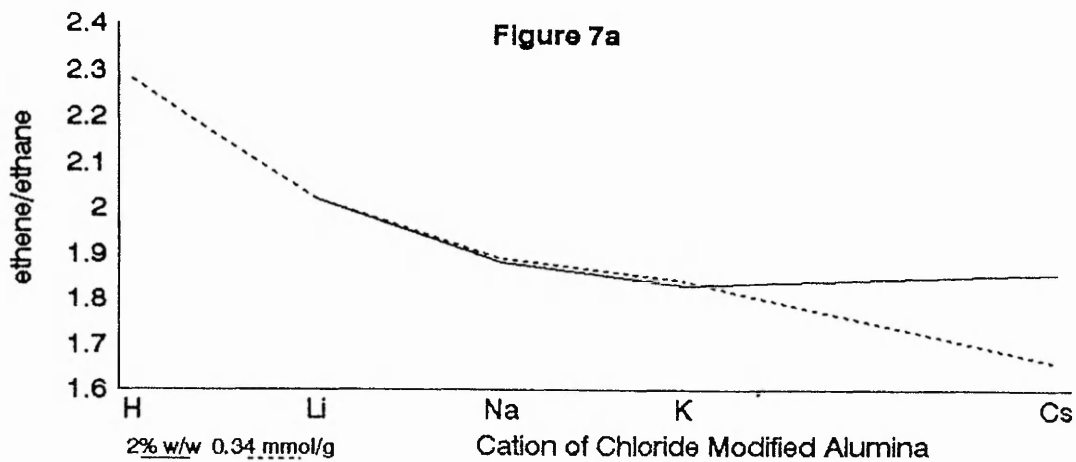
per unit surface area representing a similar alumina surface coverage for each modifier. Accordingly a variety of modified aluminas of similar mol/g loadings were prepared, the proportion of modifier being shown in table 2 (p.52). The 0.340 mmol/g modified alumina adsorbents were packed into columns and treated as the 2% modified alumina adsorbents discussed earlier in the experimental section. The resultant data for the former adsorbents are illustrated in figures 7a, 7b and 7c in comparison with the latter adsorbents. These diagrams show a group trend of increasing alkene/alkane separation with decreasing cation size. To further investigate this trend hydrochloric acid was used to modify the alumina at a concentration of 0.340 mmol/g and these values have been plotted in figures 7a, 7b and 7c. Clearly the hydrogen atom follows the same trend as the alkali metal cations. This trend is considered to be specifically related to the pi-electron system in an unsaturated solute since figure 7c clearly demonstrates no such trend exists for the saturated solute pair methylpropane/n-butane.

The retention data obtained at 60°C were used to calculate the partition ratios of ethene, propene and methylpropane relative to ethane, propane and n-butane respectively for $CuCl_2$, HCl, NaCl, $NaNO_3$ modifers. These values have been plotted in figures 8a, 8b and 8c. Clearly the divalent copper cation has a similar modification effect to the hydrogen cation. However, using a nitrate anion reduces considerably the partition

**Figure 8   Effect of Different Modifiers Upon Retention
Properties of Modified Alumina Adsorbent**

Figure 8a

Figure 8b

Figure 8c
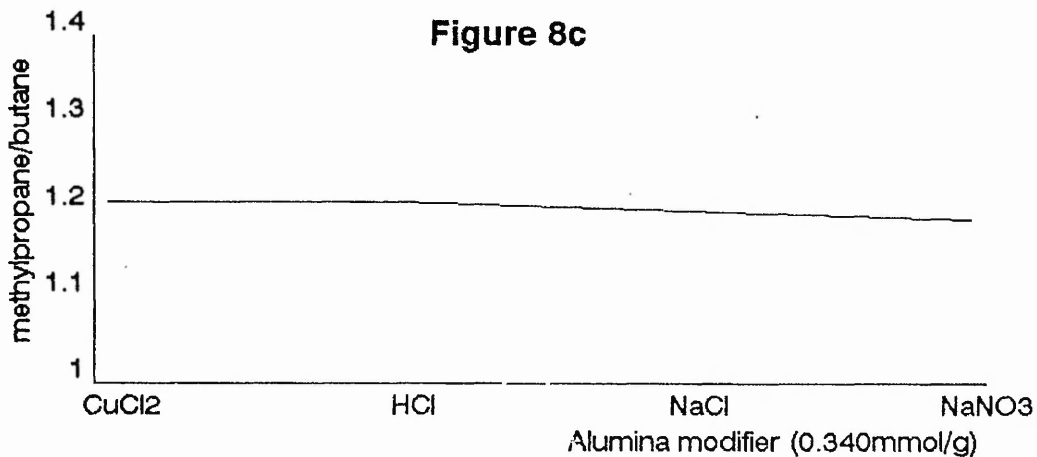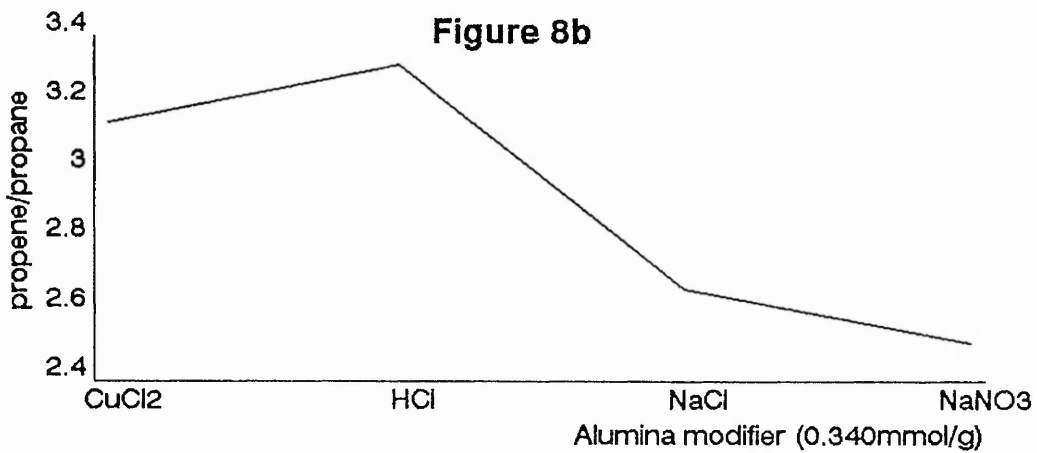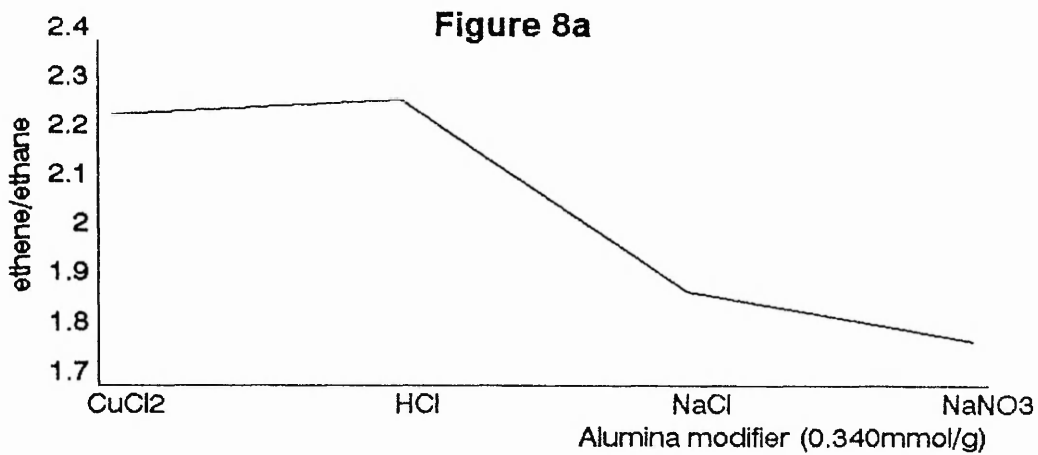
ratio of an unsaturated solute relative to a saturated one.

At 60°C the 0.340 mmol/g silver nitrate modified alumina adsorbed the unsaturated solutes in the hydrocarbon mixture to such an extent that they were effectively retained on the column. To reduce the adsorptivity of the adsorbent, two reduced modifier weight loadings were prepared, 0.118 and 0.029 mmol/g. However, using 2m lengths of column packed with these adsorbents produced a system that retained the ethene and propene components of the gaseous test mixture. In order to study the properties of these modified adsorbents, 10cm column lengths were packed and used to analyse the hydrocarbon mixture. Since these columns still exhibited high adsorptive retention characteristics towards unsaturated compounds, a gas mixture containing the homologous n-alkanes up to octane was used for analysis. The prolonged retentions of unsaturated compounds eliminated use of the partition ratios relative to saturated homologues. The retentions were therefore measured using retention indices as illustrated in Appendix I (equation 12). Measurements of the chromatograms obtained using these modified adsorbents have been illustrated in table 6. Clearly a significant degree of tailing was present using both of these modified adsorbents which may have resulted in the retention indices quoted in table 6 being erroneous. The peak tailing was such that these modified adsorbents

could not be used alone for quatitative purposes.
However, the ability of these modified adsorbents to
'shift' unsaturated chromatographic peaks was interesting
since ethene and propene peaks could be shifted to a
retention time greater than n-pentane. This could be
valuable for analysis of mine air which contains a
mixture of n-alkanes up to pentane (as described in the
introduction section).

Table 6   Chromatographic Measurements of Silver Nitrate
Modified Alumina Adsorbent

Alumina modifier	ETHENE		PROPENE	
	R I	A_s	R I	A_s
2.0% $AgNO_3$	542	3.9	616	4.0
0.5% $AgNO_3$	384	3.5	469	3.7

R I = Retention Index;
A_s = Peak Asymmetry.

The serial coupling of silver nitrate and sodium chloride modifed alumina adsorbent chromatographic columns was therefore investigated. In order to predict the retention order a diagram was plotted for the proposed column coupling illustrated in figure 9. This diagram involved a plot of the solute partition ratio versus the proportion NaCl to $AgNO_3$ modifier, and allowed optimisation of the combined stationary phases to be predicted. Clearly three optima occurred at ratios of 95:5, 75:25 and 35:65 of NaCl:$AgNO_3$ modified alumina stationary phases. Since $AgNO_3$ modified alumina produced an adsorbent that caused severe tailing of unsaturated solutes, the 95:5 ratio was selected which minimised the proportion of the $AgNO_3$ modifier. To study this adsorbent system two columns were serially coupled as follows :-

(1) 2m long 2% NaCl modified alumina.

(2) 10cm long 2% $AgNO_3$ modified alumina.

A gaseous hydrocarbon mixture was analysed, the column positions were reversed, and the hydrocarbon mixture re-analysed. The retention data for the saturated components in the mixture were as predicted from the diagram in figure 9. However, the unsaturated solutes were retained to a greater extent than predicted in figure 9, and produced peaks which tailed excessively (ethene A_s=3.14; propene A_s=3.27). Furthermore, a dramatic effect upon the ethene and propene partition ratios was noticable when the columns were reversed, which was unobserved for the saturated solutes. Essentially ethene and propene were
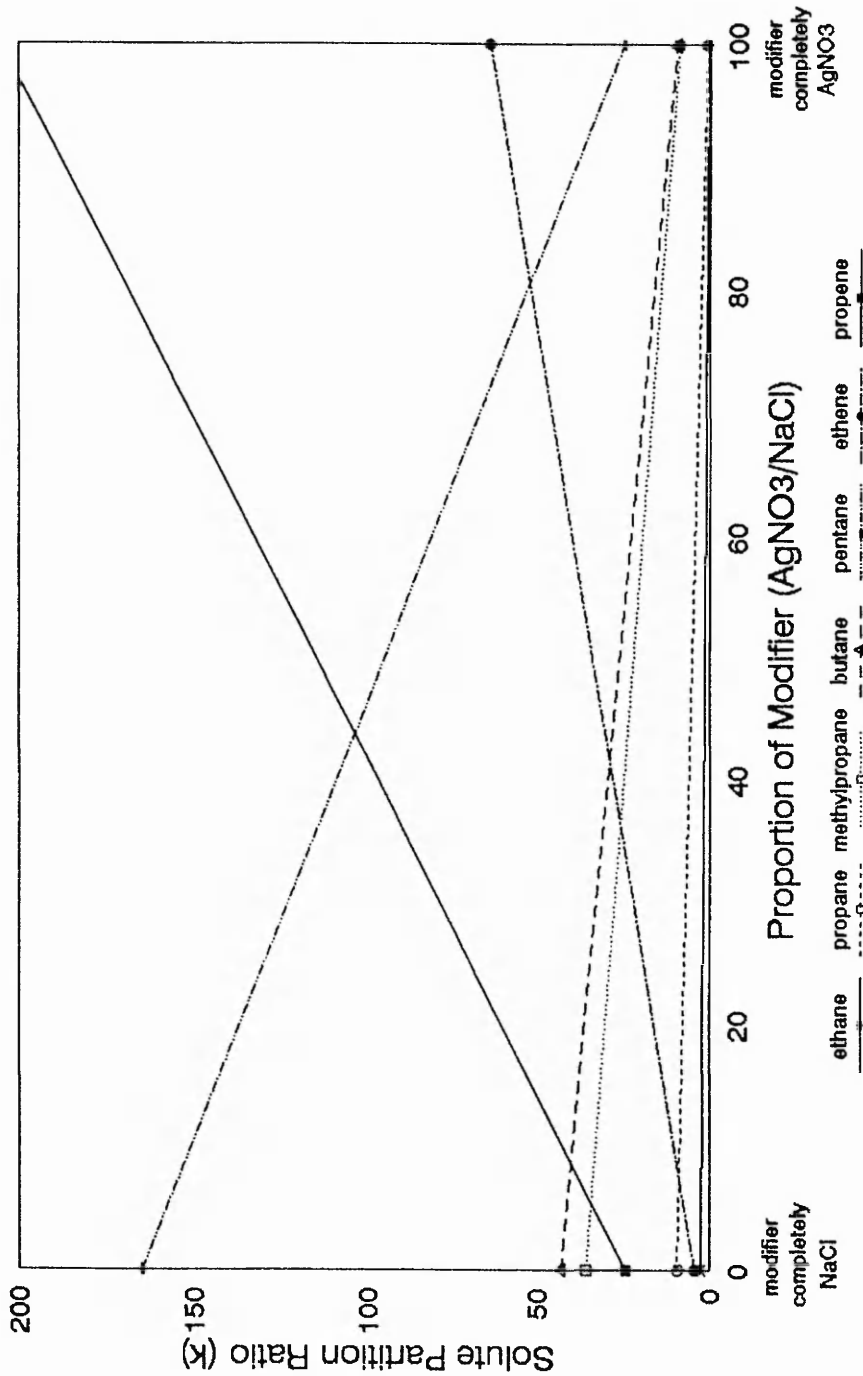
Figure 9 Plots of Solute Partition Ratios Against Proportion of Modified Alumina Adsorbent

more retained and more severely tailed when the primary column was the AgNO$_3$ modifier than when it was the NaCl modifier. Hence, the unsaturated solutes were more strongly adsorbed by the AgNO$_3$ modified alumina when this was the first column. However the reverse is usually observed, and is explained by greater adsorbent/adsorbate interactions that occur on the AgNO$_3$ column due to decreased pressure and a reduced compressibility factor when the column is placed last in a serially coupled system.

Alumina modified separately with potassium fluoride, chloride, bromide and iodide was used to obtain partition ratios for ethene, propene and methyl propane relative to ethane, propane and n-butane respectively as shown in figures 10a, 10b and 10c. This allowed the effect that the modifier anion had upon the adsorbent properties of alumina to be studied. No change in the relative partition ratios of methyl propane/n-butane as a function of the anion were recorded, so alterations in the other relative retention data could be attributed to the pi-electron system within the unsaturated components. Since no apparent group trend was observed it is considered that the effect of the anion in the alumina modifying process is secondary to the cation. Interaction between the pi-electron system and modified adsorbent was reduced in the order KF > KI > KBr = KCl. A similarity between the adsorption properties of the bromide and chloride modifier was noticable, these adsorbents having

Figure 10a

ethene/ethane vs. Anion of Potassium Halide Modified Alumina (0.340mmol/g)

Figure 10b

propene/propane vs. Anion of Potassium Halide Modified Alumina (0.340mmol/g)

Figure 10c

methylpropane/butane vs. Anion of Potassium Halide Modified Alumina (0.340mmol/g)
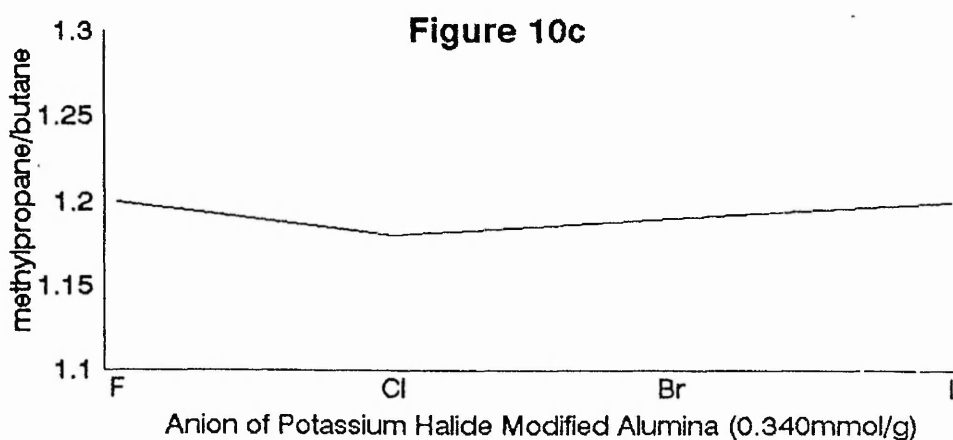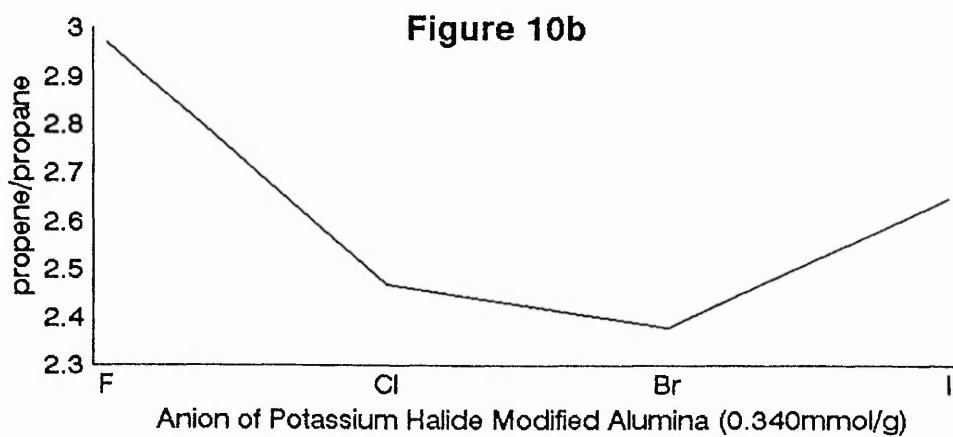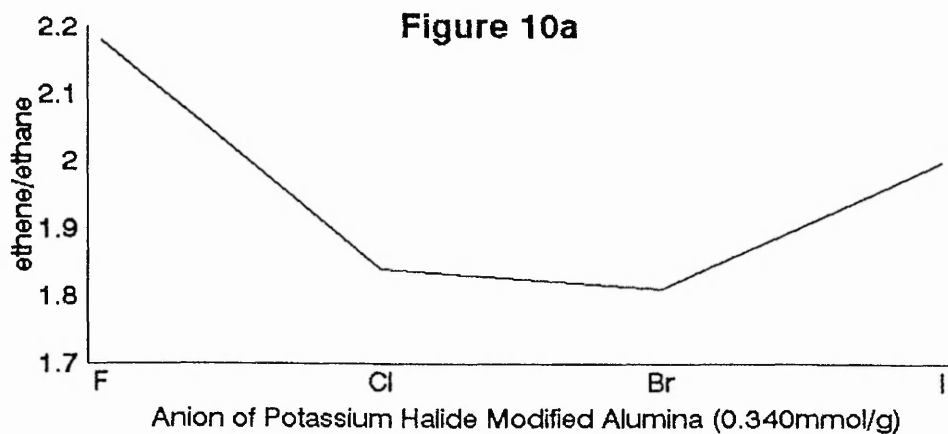
less retention for unsaturated relative to saturated systems than the iodide or fluoride modifier.

During the preparation of the potassium iodide modified alumina copious quantities of iodine vapour were given off as it was heated to 400°C. An attempt was therefore made to quantify the presence of the anion and cation of the modifier on the alumina. A surface study of these aluminas was therefore carried out using the SEM/EDXA (scanning electron microscope / energy dispersive X-ray analyser) to investigate the presence of inorganic modifier and details are shown in table 7.

Table 7   SEM/EDXA Analyses of Potassium Halide Aluminas

Alumina modifier	Atoms Detected by SEM/EDXA
KF	Al, K *
KCl	Al, K, Cl
KBr	Al, K, Br
KI	Al, K

* Fluoride is not detected by SEM, so this absence does not indicate the absence of fluoride from the alumina surface.

The most striking observation was the absence of
iodine atoms on the surface of the potassium iodide
modified alumina. To interpret these findings a quantity
of alumina was treated with 5.64% KI (w/w) as discussed
in the previous section, with the exception that this
modified adsorbent was not post-heated to 400°C. Analysis
of this sample on the SEM/EDXA revealed a large iodine
peak as shown in figure 11. It is therefore assumed that
heating the potassium modifed alumina to 400°C causes the
majority of iodine to be lost, presumably by
volatilisation. Hence the KI modified alumina is
effectively devoid of I anions, and this may be
considered a K modified alumina, with a greater abundance
of K cations avaliable for interaction with pi-electron
systems.

The presence or otherwise of fluorine atoms could not
be determined by SEM/EDXA. However, since the F anion
produced the greatest relative retention times for
unsaturated to saturated systems, the fate of the anion
was worth considering. The work of Moriguchi et al who
studied the modification of alumina with a variety of
metal fluorides proposed that a $KAlO_2$ species may be
produced by the surface reaction in equation 4 [136].

$$Al_2O_3 + KF \longrightarrow KAlO_2 + F^- \ldots\ldots\ldots (4)$$

It is suggested that the formation of some adsorbent
species (possibly KAl_2O) provides an adsorbent that has a
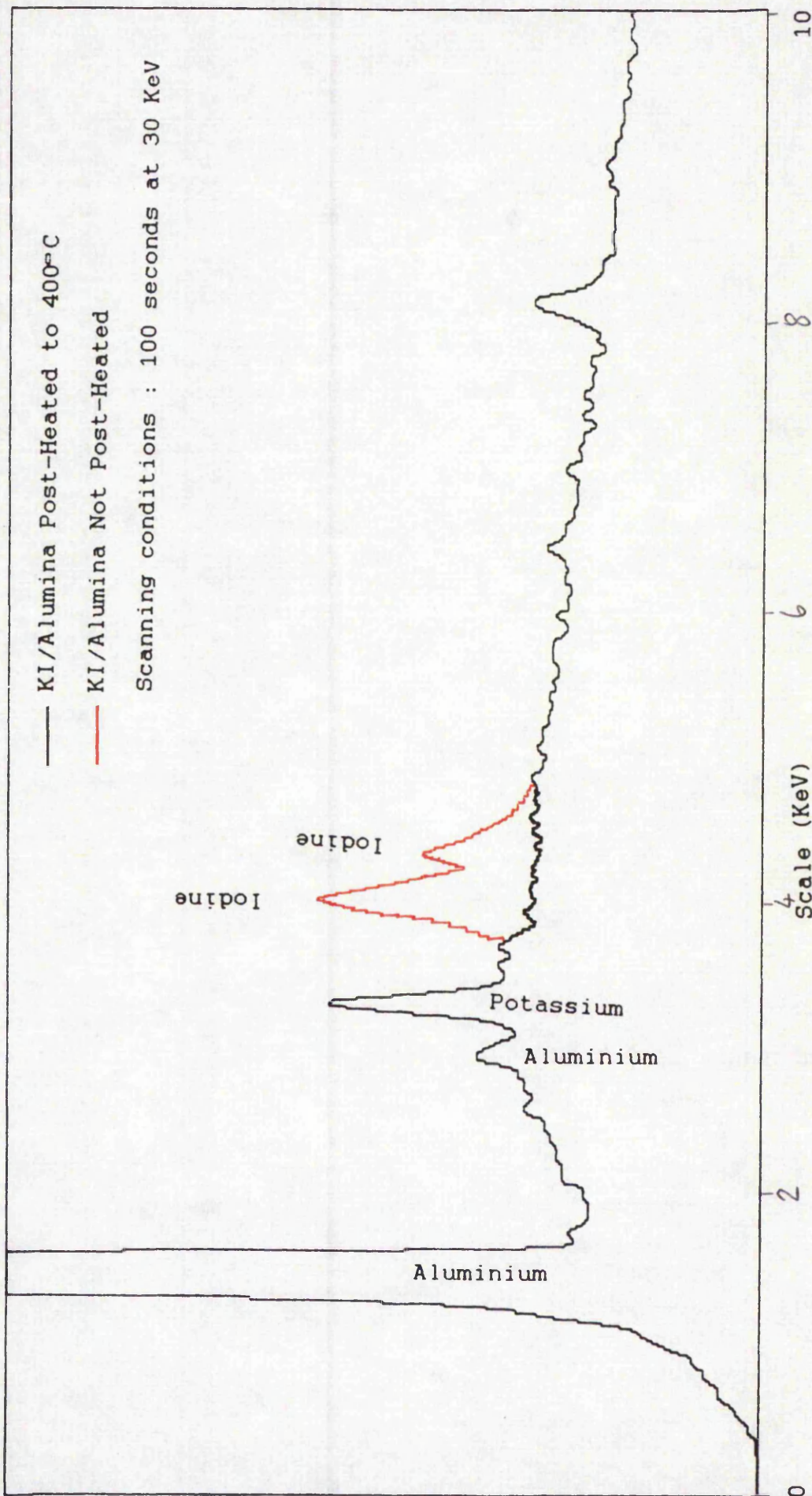
Figure 11   EDXA Spectra of Potassium Iodide Modified Alumina

greater attraction for the pi-electron system of unsaturated solutes than the other potassium halide modified alumina adsorbents.

The retention time stability of the LiCl modified alumina column over a 14 day period was studied, and has been illustrated in figures 12a, 12b and 12c. Clearly the relative retention of unsaturated to saturated systems becomes reduced over a period of time, presumably due to deactivation of the adsorbent by adsorption of water. This occurred even though the carrier gas employed in this work had been passed through a molecular sieve drying tube, and illustrates a disadvantage of using alumina as an adsorbent.

Figure 12   Study of Relative Retention Time Stability of a LiCl Modified Alumina Adsorbent (0.340mmol/g)

Figure 12a

Y-axis: ethene/ethane (1.88 to 2.04)
X-axis: Time Interval Between Analyses (days) — 0, 1, 5, 6, 11, 13, 14

Figure 12b

Y-axis: propene/propane (2.6 to 2.9)
X-axis: Time Interval Between Analyses (days) — 0, 1, 5, 6, 11, 13, 14

Figure 12c

Y-axis: methylpropane/butane (1.1 to 1.2)
X-axis: Time Interval Between Analyses (days) — 0, 1, 5, 6, 11, 13, 14
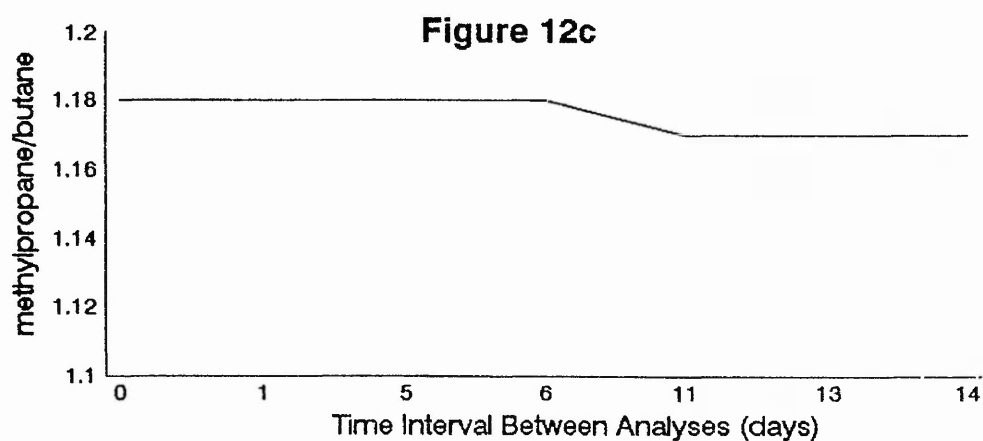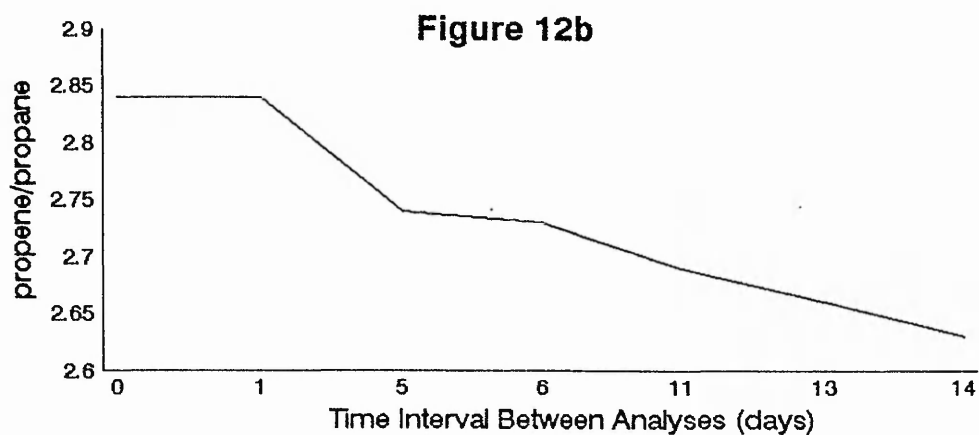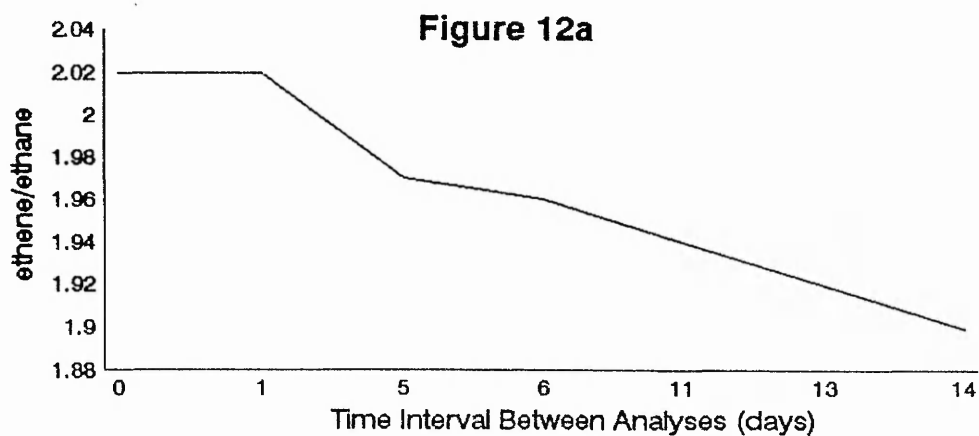
2.5.3 Study of Surface Modification of Silica

The chromatograms achieved using the unmodified porous silica beads Porasil C showed that this adsorbent had properties similar to those of unmodified alumina. The unsaturated components had a greater retention than their saturated analogues, and their chromatographic peaks showed a significant degree of tailing. This suggested interaction was occurring between the pi-electron system of the unsaturated components and the adsorbent, presumably related to charged dipoles within the adsorbent. The modification of the silica beads with an organic modifier (phenylisocynante) and an inorganic modifier (NaCl) reduced this tailing as illustrated by the peak asymmetries (measured as in Appendix 1) listed in table 8.

Table 8   Peak Asymmetry Measurements of Solutes
Using Modified Silica

SOLUTE	PEAK ASYMMETRY (A_s)		
	Unmodified Porasil C	2% NaCl Porasil C	Phenylisocyanate Porasil C
Ethane	1.10	1.10	1.05
Ethene	2.30	1.17	1.22
Propane	1.15	1.10	1.15
Propene	2.45	1.12	1.20

Both of these modifiers reduced the effectiveness of the relative positive character within the adsorbent. This suggested that the modification process does not involve an interaction between the chloride anion and the positive sites on the silica matrix. This process would not account for the effectiveness of phenylisocyanante, therefore modification of the surface dipole-dipole interactions most probably occurs. A comparison of the relative retentions of unsaturated to saturated systems on these adsorbents demonstrated similarities in the retention of solutes using NaCl and phenylisocyante modified porous silica beads. However the practical use of modified silica adsorbents for this work is limited due to the poor peak separation of propene from methyl propane and n-butane. This is illustrated in figures 13a-13c, which show that the retention indices of propene vary upon modification from 420-390 (calculated as in Appendix I, equation 12).

Figure 13a

Ethene Retention Index (RI) vs **Column Operating Temperature (deg C)**

Porasil C modifier
untreated   2% NaCl   phenylisocyanate

Figure 13b

Propene Retention Index (RI) vs **Column Operating Temperature (deg C)**

Porasil C modifier
untreated   2% NaCl   phenylisocyanate

Figure 13c

Methylpropane Retention Index (RI) vs **Column Operating Temperature (deg C)**

Porasil C modifier
untreated   2% NaCl   phenylisocyanate
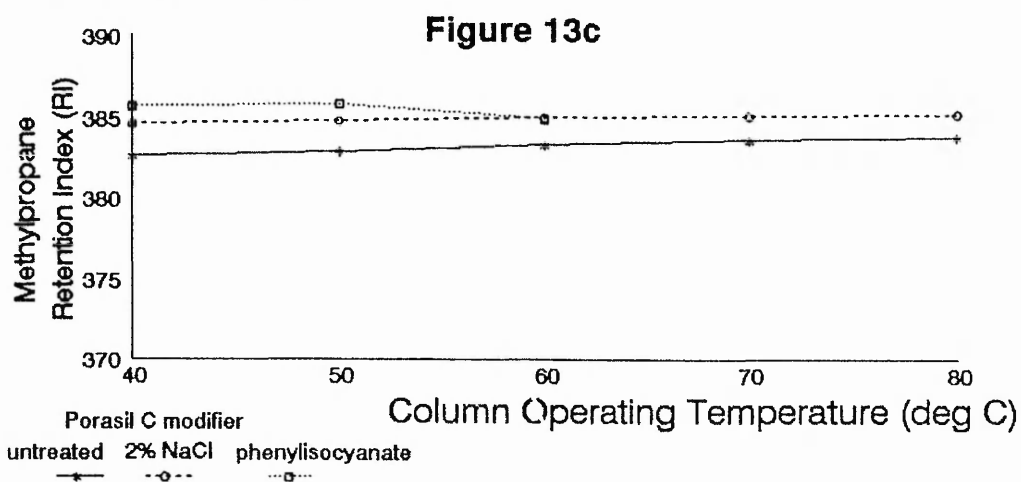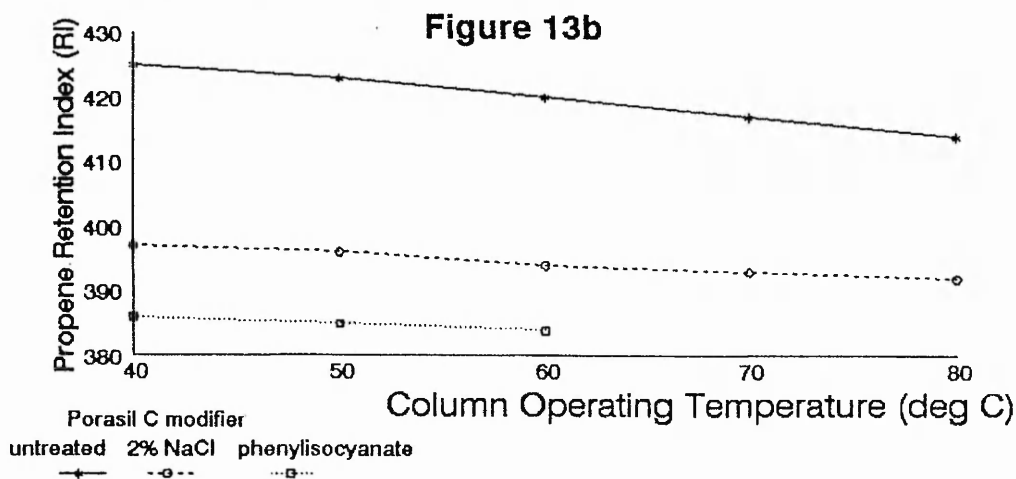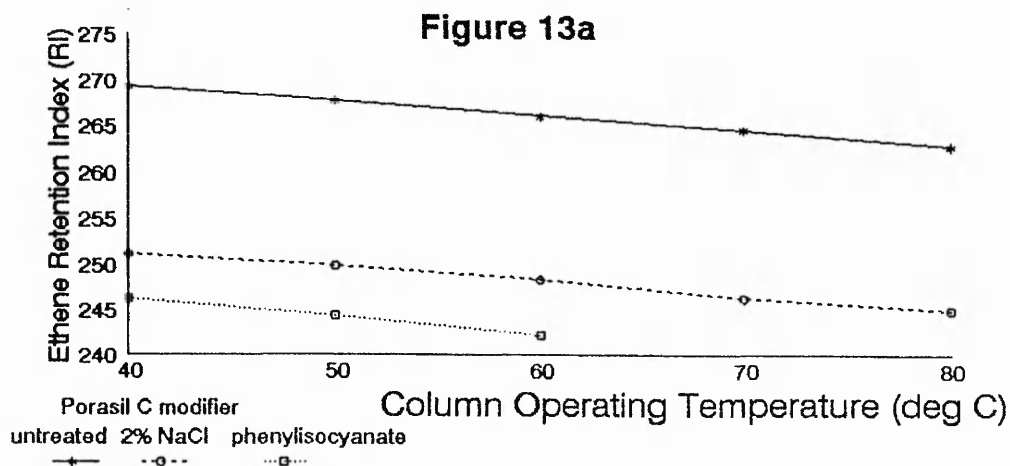
2.5.4 Study of Physical Column Characterisitics

The efficiency of a column is best studied by considering the number of theoretical plates present. This may be achieved by plotting a van Deemter graph of the mean linear carrier gas velocity (u_{lin}) versus the height equivalent to a theoretical plate (HETP). In order to plot a van Deemter graph a number of chromatographic separations must be made at a variety of carrier gas velocities maintained at a constant temperature. The number of theoretical plates is calculated by the physical measurement of peaks in the chromatogram as described in Appendix I.

This approach was adopted in order to study the effect that the column internal diameter has upon the efficiency. The chromatograms obtained at different flow rates for alumina and Porapak Q columns of differing i.d. (1.59mm and 0.80mm) were measured to calculate the HETP of a common solute. The analytical conditions used for each adsorbent were :-

Porapak Q : solute, propane; column temperature, 50°C.

Alumina : solute, butane; column temperature, 80°C.

A comparison of the van Deemter graphs for different column i.d.s was made for both alumina and Porapak Q, as illustrated in figures 14 and 15 respectively. In comparing the effects of column diameter, similar conclusions were reached using alumina and Porapak Q as the adsorbent. Essentially, a reduction in the column diameter caused a decrease in the HETP implying an
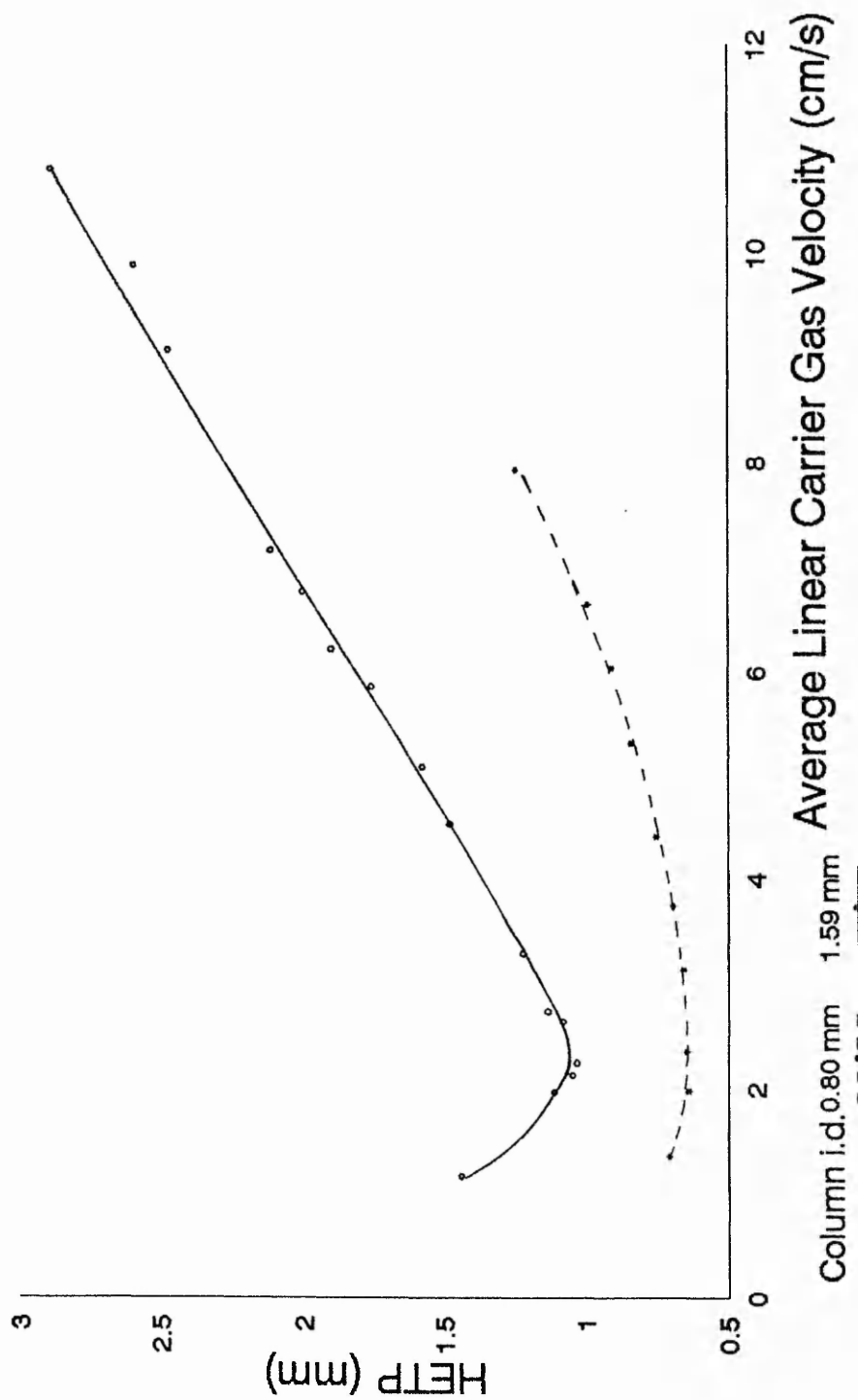
Figure 14 Comparison of van Deemter Graphs of Packed Alumina Columns of Different Internal Diameters

Column i.d. 0.80 mm   1.59 mm
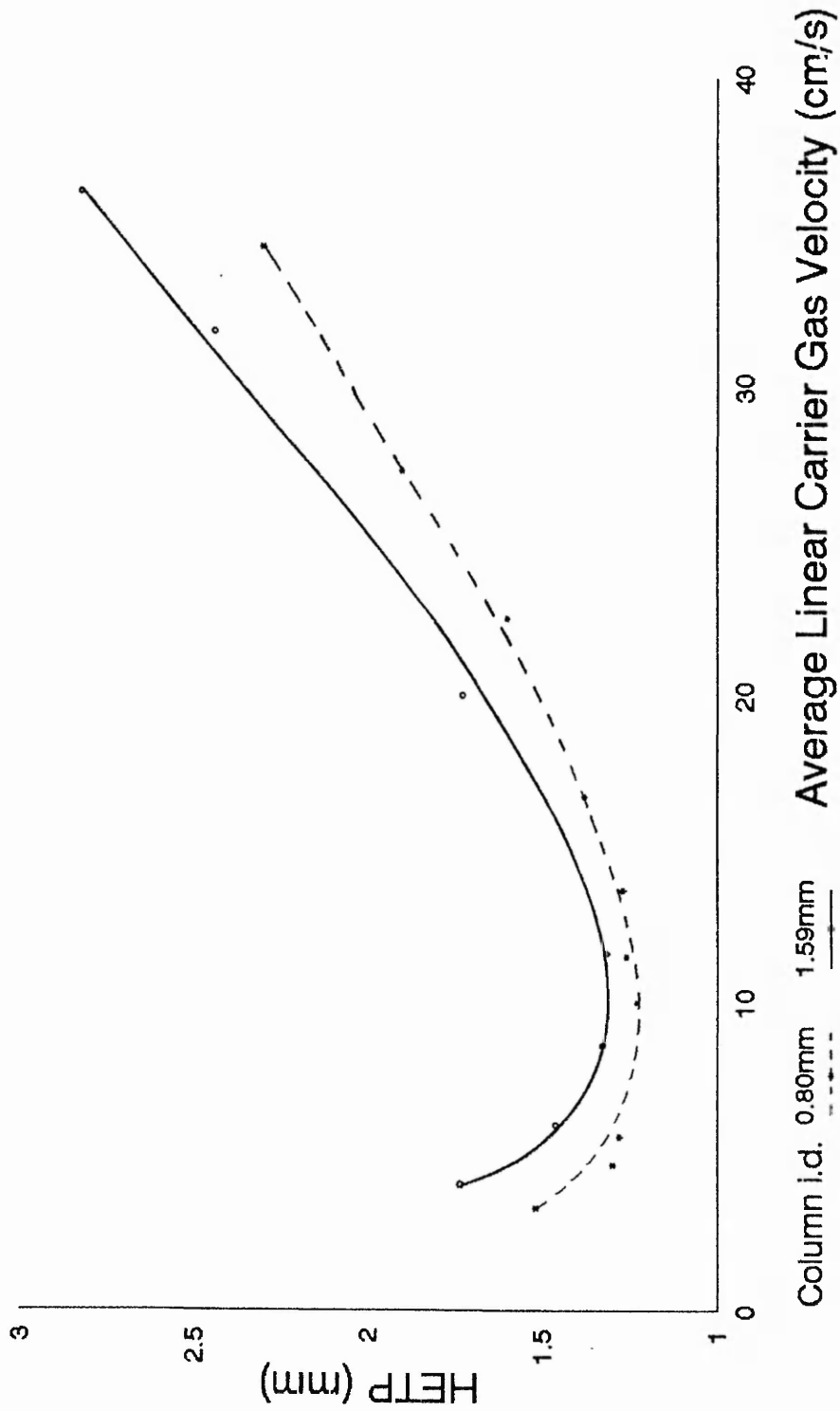
Figure 15   Comparison of van Deemter Graphs of Packed Porapak Q Columns
of Different Internal Diameters

Column i.d. 0.80mm   ┄┄┄   1.59mm   ────

increased column efficiency (ie. greater number of theoretical plates). However, the effect of a reduction in column diameter was greater for alumina than for Porapak Q as illustrated below, and this was attributed to the greater porous nature of the Porapak Q adsorbent.

Alumina particle size = 60-80mesh (0.251-0.191mm).

Alumina id=1.59mm: HETP=1.02mm at optimum u_{lin}, d_p/d_c=0.14

id=0.80mm: HETP=0.63mm at optimum u_{lin}, d_p/d_c=0.28

Porapak Q particle size = 80-100mesh(0.191-0.152mm).

Porapak Q id=1.59mm: HETP=1.31mm at optimum u_{lin}, d_p/d_c=0.11

id=0.80mm: HETP=1.20mm at optimum u_{lin}, d_p/d_c=0.21

d_p, mean particle diameter. d_c, column i.d.

Cramers and Rijks have proposed the term 'micropacked' for columns of i.d. below 1mm and d_p/d_c ratio below 0.3 [146]. Since d_p is the mean particle diameter and d_c is the column i.d. it can be seen that the columns of internal diameter 0.80mm may be termed micropacked. The lower HETP values obtained for a theoretical plate for alumina compared to Porapak are difficult to correlate since different column temperatures and solutes employed for each adsorbent.

Improvements in the column efficiency by altering the carrier gas were studied by comparing van Deemter graphs obtained for an alumina packed column of 0.80mm i.d. using helium and nitrogen carrier gases, as illustrated in figure 16. At linear carrier gas velocities approaching the optimum (ie. minimum HETP, h_{min}) nitrogen produced the lower HETP values and hence maximum
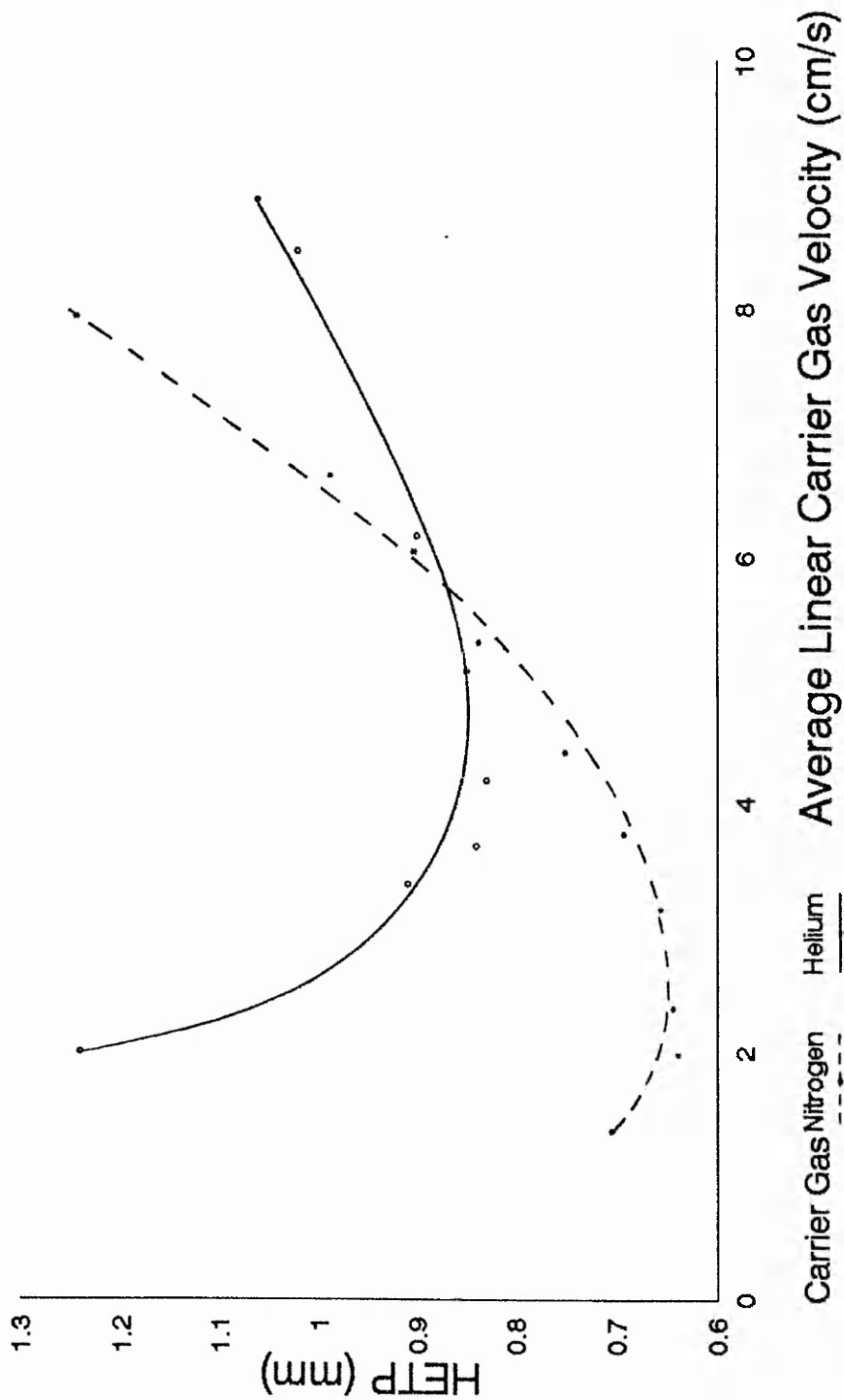
Figure 16 Comparison of van Deemter Graphs of Packed Alumina Columns
Using Different Carrier Gases

Carrier Gas Nitrogen ----   Helium ——

Average Linear Carrier Gas Velocity (cm/s)

HETP (mm)

efficiency in this diagram. h_{min} occurred at a higher velocity (3.9cm/s) using helium carrier gas than for nitrogen carrier gas (2.8cm/s) and at progressively higher carrier gas velocities helium became the more efficient carrier gas producing lower HETP values. In an attempt to interpret these results the A, B and C constants of the van Deemter equation were solved from the experimental data graphed in figure 16. These terms were calculated from experimental data by the least squares method using a Personal Computer. They showed B and C to be the dominant constants that differed. Values of $8.23mm^2/s$ and 0.015s for B and C respectively were obtained using nitrogen compared to values of $24.6mm^2/s$ and 0.011s using helium. The B values indicated that greater molecular diffusion of the solute occurred in helium as opposed to nitrogen, due to the helium molecules being lighter and smaller resulting in a greater degree of band broadening. Hence at low carrier gas velocities where the B term predominates nitrogen carrier gas produced a more efficient system and lower HETP values. But at high carrier gas velocities where the C term predominates the greater molecular diffusion of helium aided the separation process by improving the resistance to mass transfer. This resulted in a more efficient system and lower HETP values for helium at higher carrier gas velocities.

To facilitate further investigation into the physical column parameters a Porous Layer Open Tubular (PLOT)

column with a Porapak Q stationary phase was studied. The van Deemter graph illustrated in figure 17 shows the effect of different carrier gases for a propane solute at a column temperature of 50°C using the PoraPLOT Q column. Since open tubular columns contain no packing the A term of the van Deemter equation reduces to zero producing the Golay expression illustrated in equation (5) [149].

$$h = B/u + C.u \dots\dots\dots\dots\dots\dots\dots\dots\dots\dots\dots (5)$$

The constants of this expression were solved using experimentally obtained data, and the calculated values were :-

   nitrogen carrier gas : $B=28.7mm^2/s$. $C=0.0066s$.

   helium carrier gas : $B=90.0mm^2/s$. $C=0.0030s$.

These values verify those obtained using a packed alumina column, and the discussion of the different carrier gases used with the alumina column could be repeated using these results.

This data allowed a comparison to be made between the B and C values obtained for three columns of different physical dimensions and characteristics using the same solute (propane), mobile phase (helium) and stationary phase (Porapak Q) :-

Packed column i.d.=1.59mm : $B=60.9mm^2/s$; $C=0.0073s$.

Packed column i.d.=0.80mm : $B=35.5mm^2/s$; $C=0.0054s$.

Open tubular column i.d.=0.53mm : $B=90.0mm^2/s$; $C=0.0030s$.

The B values indicated that the greatest molecular diffusion of the solute occurred using an open tubular rather than a packed column. This was attributed to the
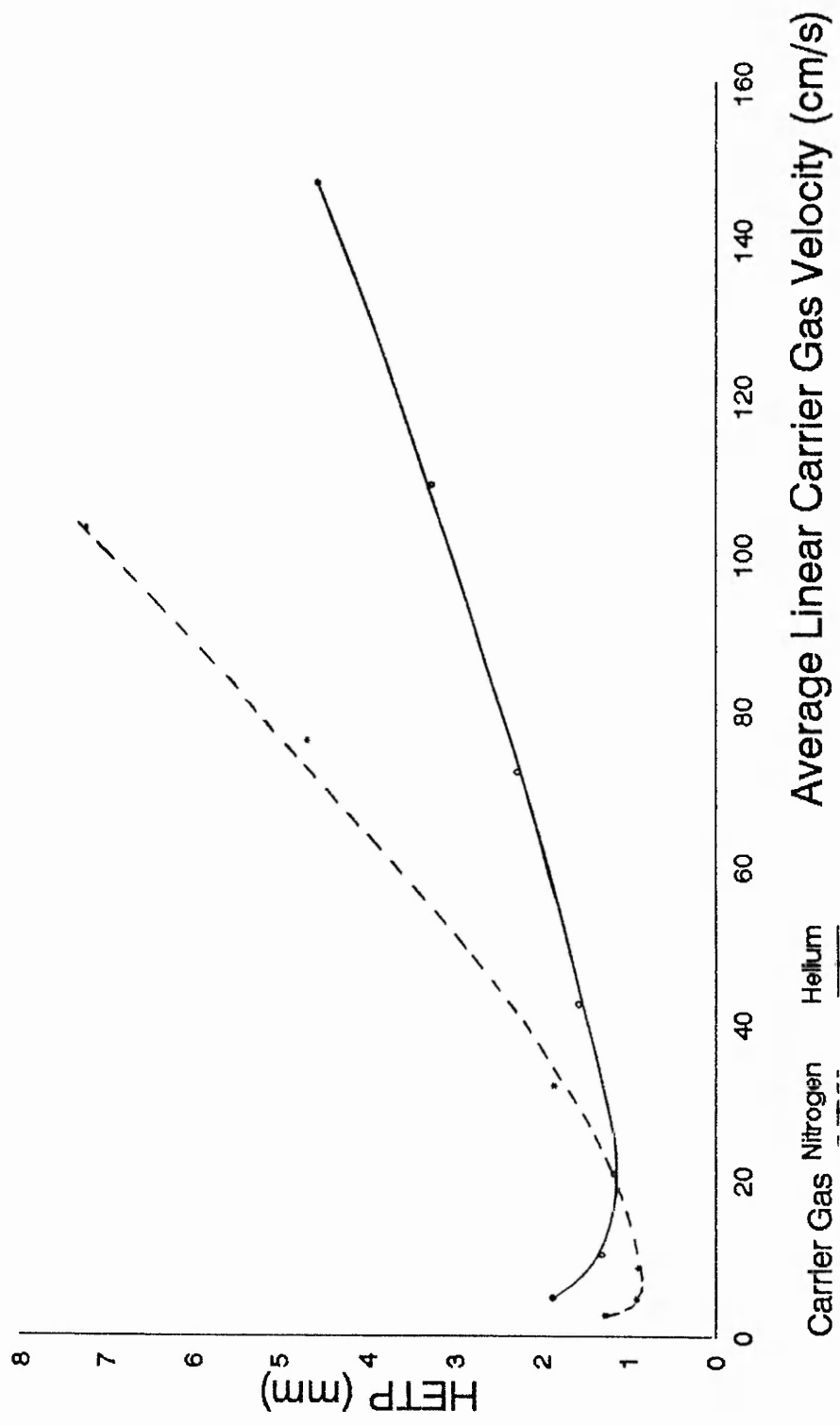
Figure 17 Comparison of van Deemter Graphs of a PoraPLOT Q Column Using Different Carrier Gases

presence of a greater mobile phase/stationary phase
interface using a packed column (due to the randomly
packed particles), rather than the continuous surface of
the internal column wall of an open tubular column. Hence
at lower carrier gas velocities the packed column would
be an equally efficient separating system.

The minimum C value was obtained using an open tubular
rather than a packed column, implying that the former has
a lower resistance to mass transfer than the latter.
Since the resistance to mass transfer involves two
processes -the solute adsorption onto the adsorbent and
its' subsequent desorption- it can be recognised that the
change from carrier gas multiple pathways through a
packed column to the single pathway through an open tube
results in a reduced mass transfer. Hence, at higher
carrier gas velocities greater efficiencies are achieved
using open tubular rather than packed columns.

A comparison of the retention data achieved using the
Porapak Q stationary phase in the variety of column
dimensions previously described is given in table 9.
These values were all calculated at a column temperature
of 50°C. The k and α values were used to calculate the
number of theoretical plates required to achieve a
propene/propane separation by using the formula for N_{req}
given in Appendix 1. The number of theoretical plates
required (for R=1) were 4400, 5150 and 3700 for the
respective column dimensions 1.59mm i.d., 0.80mm i.d. and
0.53mm i.d.

Table 9 Comparison of Different Columns Using Porapak O Stationary Phase

SOLUTE	PACKED i.d.=1.59mm		PACKED i.d.=0.80mm		OPEN TUBULAR i.d.=0.53mm	
	k	α	k	α	k	α
methane	2.32		1.15		0.19	
ethene	7.05	1.37	4.74	1.36	0.82	1.43
ethane	9.64		6.44		1.17	
propene	44.2	1.13	30.6	1.12	5.75	1.17
propane	50.1		34.2		6.72	
methyl- -propane	202		141		33.86	
butane	280		195		41.91	

The number of theoretical plates achieved at the optimum carrier gas velocity were determined from the van Deemter graphs previously plotted. These values were 760, 815 and 860 (plates per metre) for the respective column dimensions 1.59mm i.d., 0.80mm i.d. and 0.53mm i.d. Clearly a column length of 1m does not contain sufficient theoretical plates to resolve the propene/propane separation. Column lengths of at least 6m would be required for the packed columns (since $N_{eff} < N_{meas}$) to achieve the necessary number of theoretical plates, and such systems would require inlet pressures exceeding 8bars. However, an open tubular column length of 10m requires a pressure drop of less than 1bar, and this would produce 8600 plates. This illustrates the major advantage of open tubular columns - exceptionally small back-pressures allowing rapid flow rates producing fast analyses. A comparison of the separations achieved using each of the different physical types of column with Porapak Q adsorbent is illustrated in figure 18. The three chromatograms shown are each on a different attenuation since different sample sizes were employed for each column (as described in the experimental section) to prevent column overload.

The advantages of using the PLOT column proven, it was necessary to attempt optimisation of the carrier gas velocity. The optimum practical carrier gas velocity (OPGV) is generally accepted to be the point where the van Deemter graph becomes linear [150]. But the

Figure 18   Chromatograms Illustrating the Effects of
            Different Physical Column Dimensions
            Utilising a Common Porapak Q Adsorbent

Time
(mins)

Packed Column : 1m long x 1.59mm i.d.

Packed Column : 1m long x 0.80mm i.d.
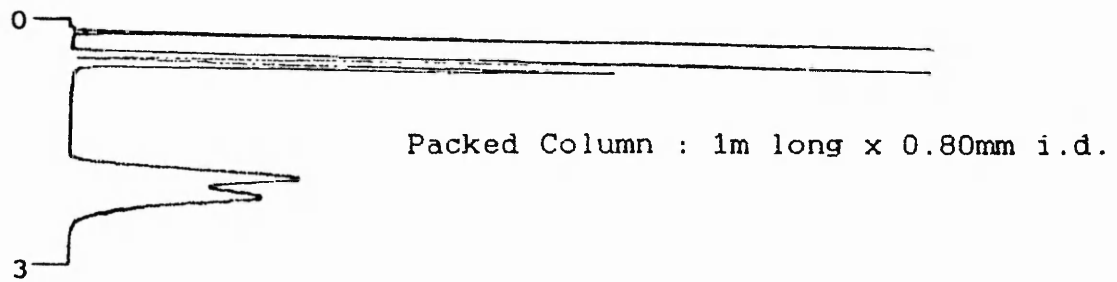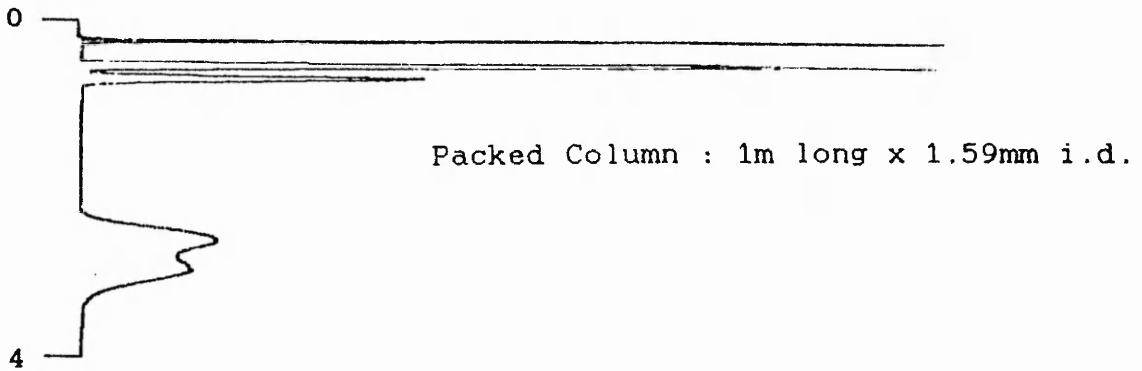
Column temperature = 50°C

Solute elution order:
        methane, ethene, ethane, propene, propane.

Open Tubular Column : 10m long x 0.53mm i.d.
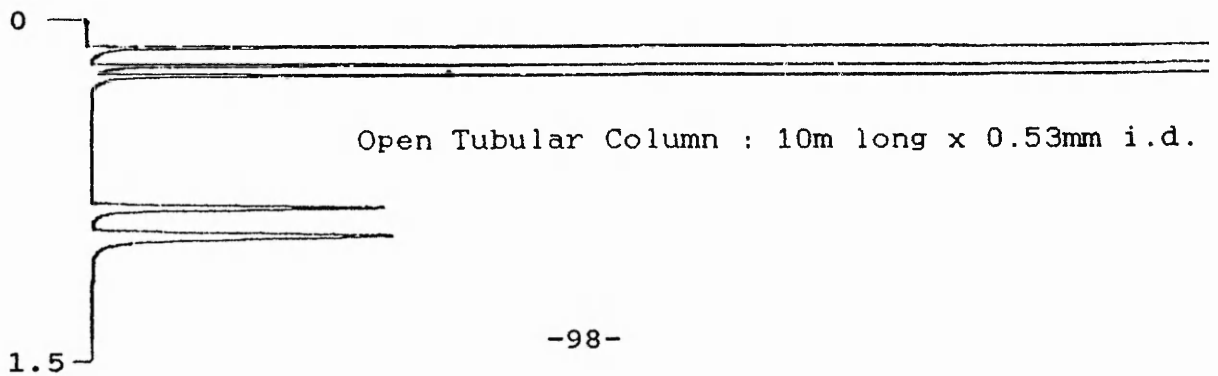
attainment of linearity in practise never occurs since the carrier gas velocity is affected by altering the column inlet pressure, and this alters diffusion effects within the column. However, the OPGV can be defined as the point at which the ratio of the number of theoretical plates to solute retention time (n/t_R) is maximised [100]. The OPGV can therefore be determined by plotting n/t_R versus u_{lin}, and measuring u_{lin} at the graph maximum. This has been plotted for PoraPLOT Q using helium and nitrogen carrier gases in figure 19, and reveals OPGV values of 50cm/s for nitrogen and 110cm/s for helium. It is also important to note that at increased gas velocities (greater than 15cm/s) there are significantly more plates per second using helium carrier gas compared with nitrogen. This indicates that helium is the carrier gas of choice for gas velocities greater than 15cm/s.

The number of theoretical plates required to achieve a separation is dependent only upon thermodynamic factors and therefore this does not vary with the mobile phase velocity. In order to achieve the required number of theoretical plates the velocity may be varied at a fixed temperature. Thus, a plot of mobile phase velocity versus the effective number of theoretical plates was recorded for each of the column temperatures studied as in figures 20a-20e. This data was obtained from a number of hydrocarbon gas analyses carried out at a variety of different carrier gas flow rates at column temperatures 40, 50, 60, 70 and 80°C.
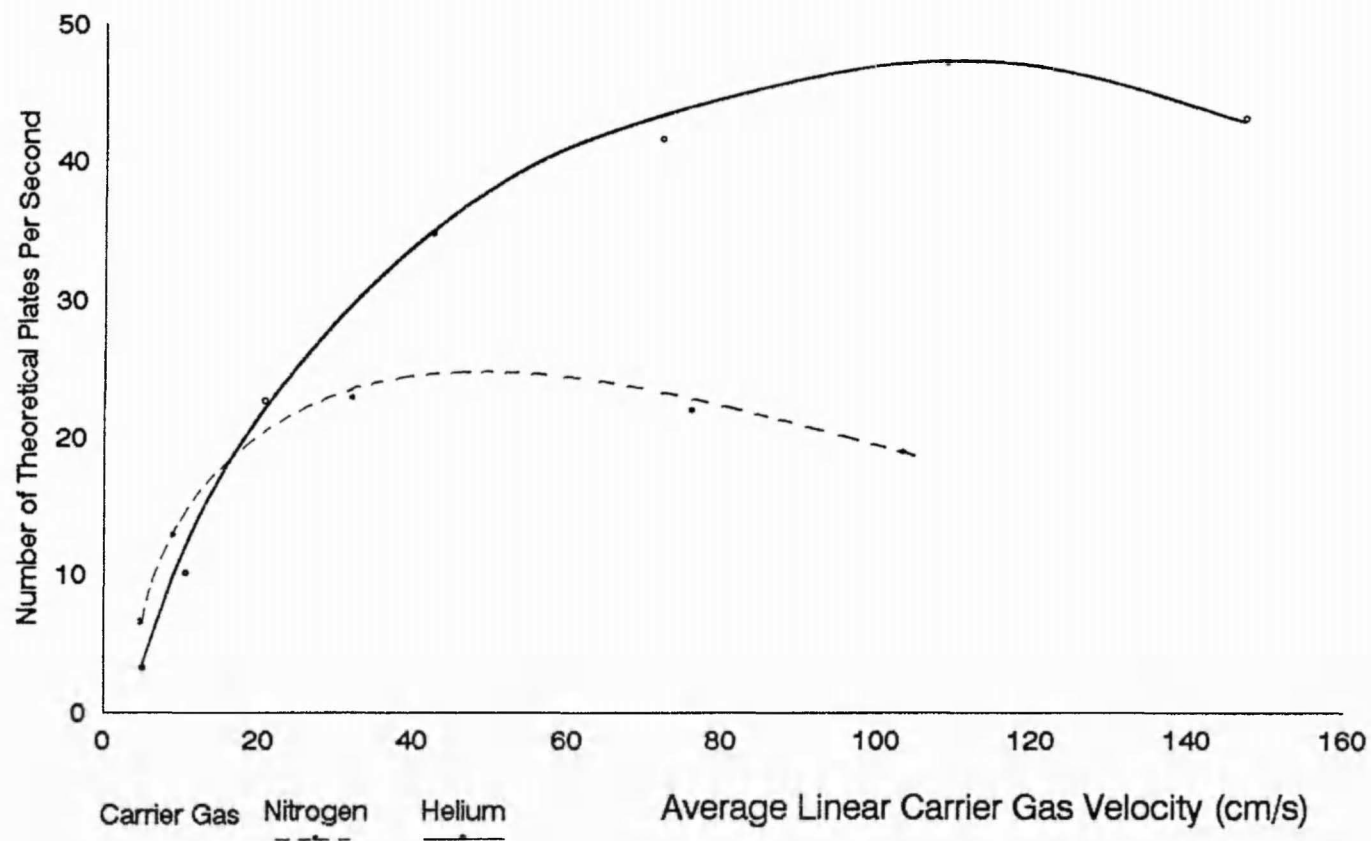
Figure 19   OPGV Graphs for the PoraPLOT Q Column Using Different Carrier Gases

Figure 20   Variation of Number of Theoretical Plates
With Carrier Gas Velocity for PoraPLOT O
at a Variety of Column Temperatures

Figure 20a   (40°C)

Figure 20b   (50°C)

Figure 20c   (60°C)
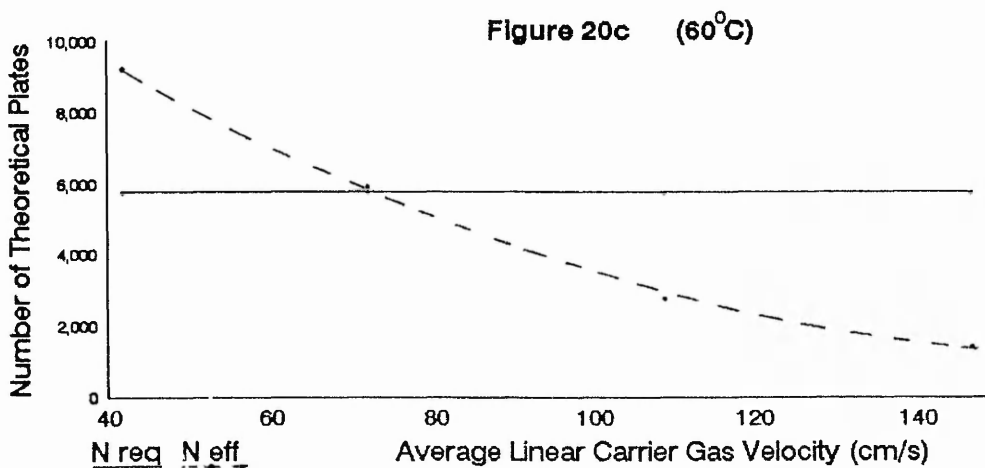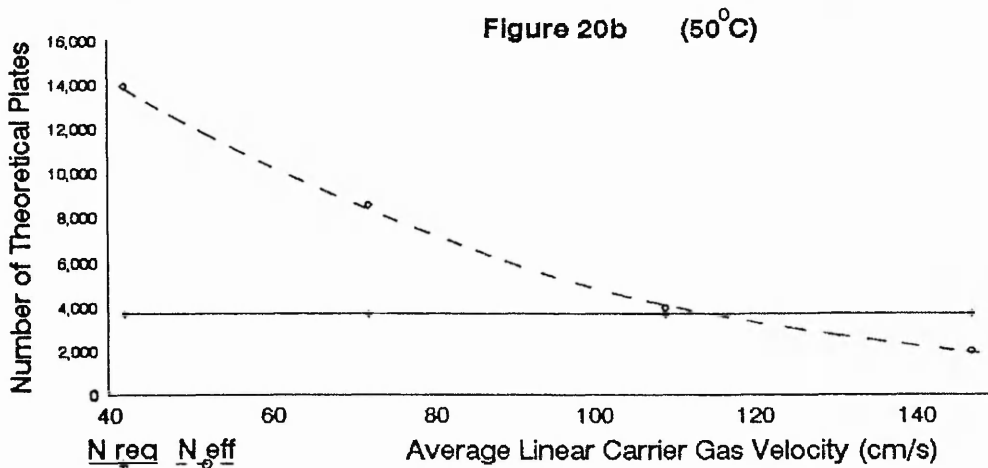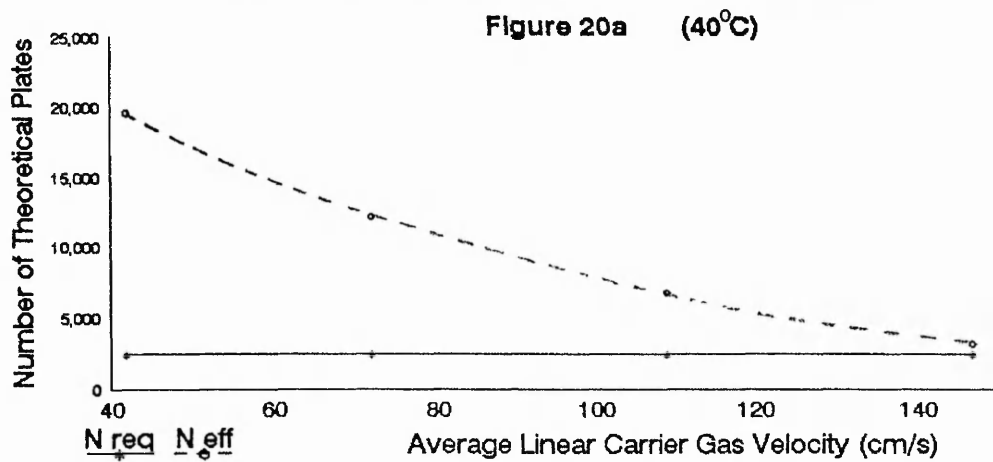
Figure 20   Variation of Number of Theoretical Plates With Carrier Gas Velocity for PoraPLOT O at a Variety of Column Temperatures

Figure 20d   (70^{0}C)
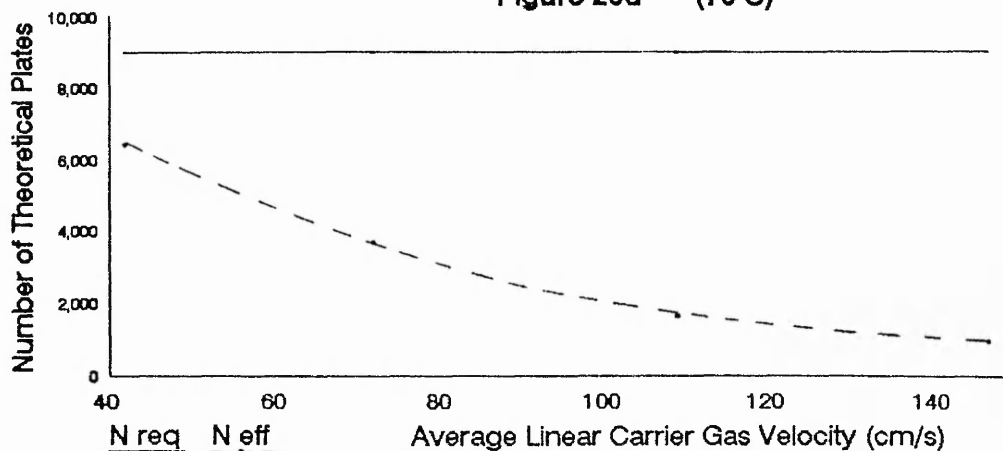
Figure 20e   (80^{0}C)
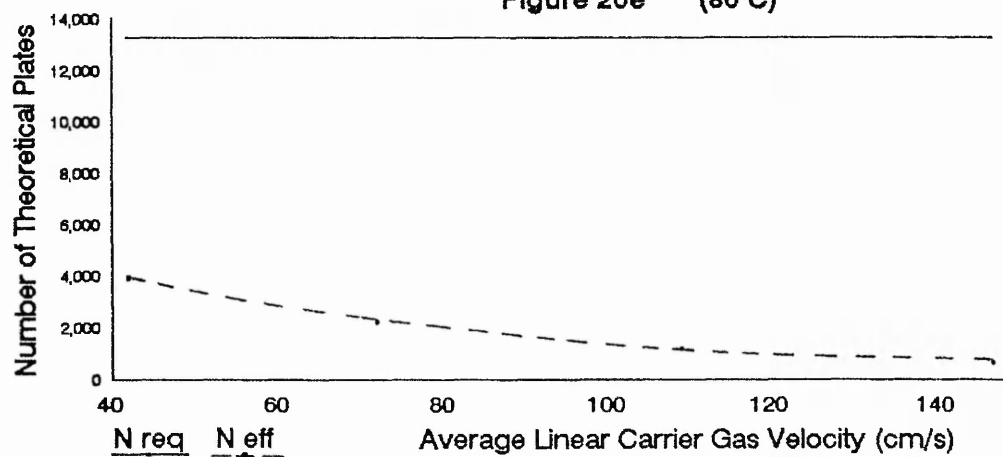
A plot of the number of theoretical plates required for R(resolution)=1 was then inserted into this diagram, and intersection of the two lines revealed the maximum carrier gas velocity for which there were sufficient effective theoretical plates to achieve the required separation. The optimum conditions for a rapid analysis time obtained from figures 20a-20e have been listed in table 10, which shows that these conditions involve a column temperature of 40°C and carrier gas velocity of 150cm/s. Since the final use of a chromatographic system employed to analyse gases present in a mine atmosphere is underground, a column temperature of 40°C was impractical since some parts of the underground mining environment may attain 35°C. Hence the optimum conditions for the most rapid analysis are a column temperature of 50°C and helium carrier gas velocity of 110cm/s, producing an analysis time of 80 seconds. A chromatogram of the lower hydrocarbons analysed under these optimum conditions is illustrated in figure 22. It is interesting to note that this method of determining the optimum analytical conditions has produced the same carrier gas flow rate as that described earlier (ie. OPGV = $2.u_{opt}$).

Table 10   Minimum Analysis Times Achieved

Temperature (°C)	u_{lin} (cm/s)	Analysis Time (secs) *
40	150	65
50	110	70
60	75	110
70 +	20	>110
80 +	<5	>110

* Time for propane peak to return to base-line
+ Results obtained by extrapolation

Figure 21 Chromatogram of Hydrocarbon Gas Mixture Using Optimum Analytical Conditions
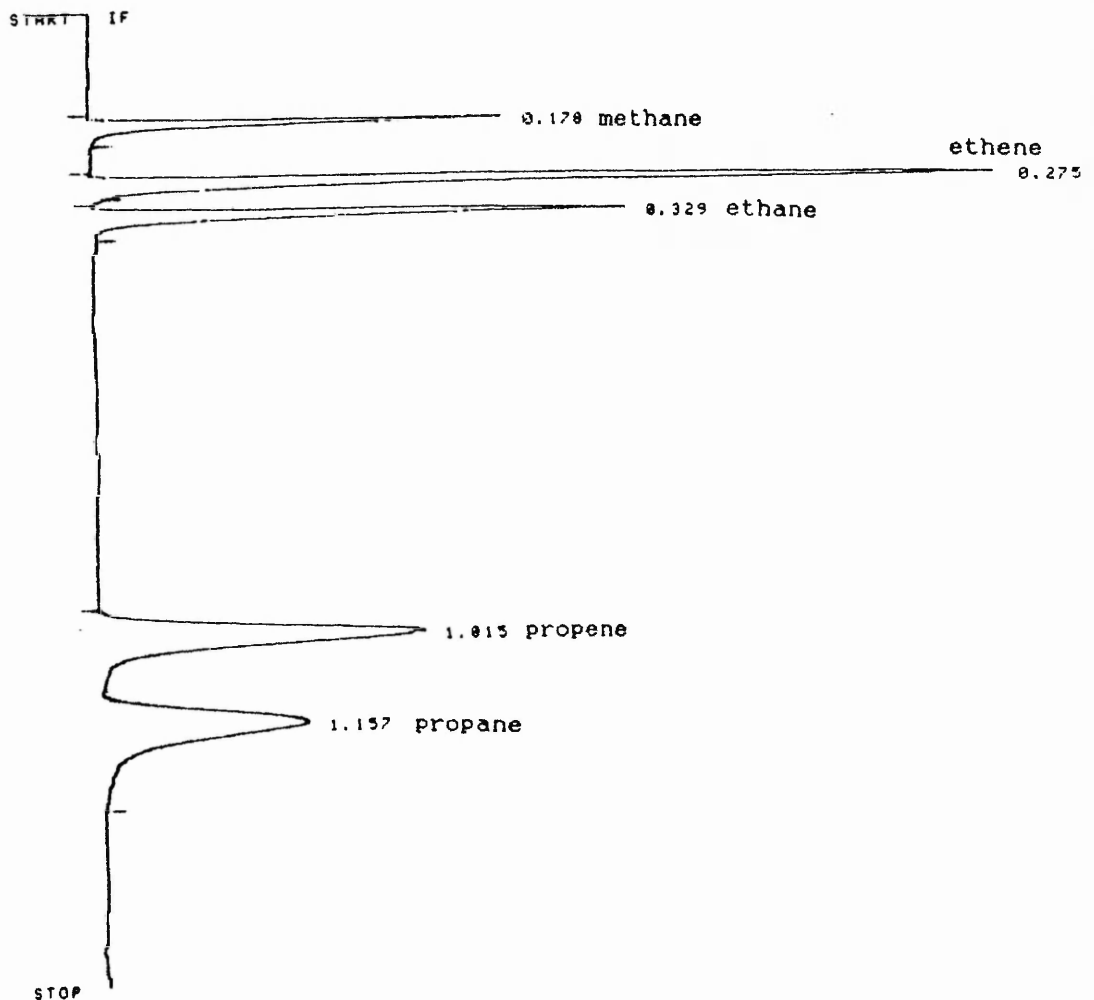
Analytical conditions:

  20µl sample size
  PoraPLOT Q column
  Column temperature = 50°C
  Helium carrier gas
  Linear flow-rate = 110cm/s
  Flame Ionisation Detector

-105-

2.5.5   Study of Open Tubular Columns

The large increase in column efficiency achieved by using an open tubular design was illustrated in section 2.5.4. This demonstrated that the most efficient method of separating the other analytes to be studied in this work would be to use additional open tubular columns. These were obtained commercially as described in section 2.3.

PoraPLOT Q was used to separate the range of sulphur gases to be analysed. A chromatogram of this separation has been illustrated in figure 22. A column temperature of 50°C was employed to allow use in a mine environment, and the carrier gas flow rate was such that adequate resolution of methane and ethane from hydrogen sulphide was achieved.

Separation of the range of oxygenated vapours was achieved by using a DB-Wax open tubular column. A chromatogram of this separation has been illustrated in figure 23, employing a column temperature of 50°C to allow use in a mine environment. It was also possible to separate the aromatic vapours using this column, as illustrated in figure 24.

Figure 22   Chromatogram of Sulphur Gas Mixture

START

1.10 H_2S

1.61 COS

2.75 SO_2

STOP
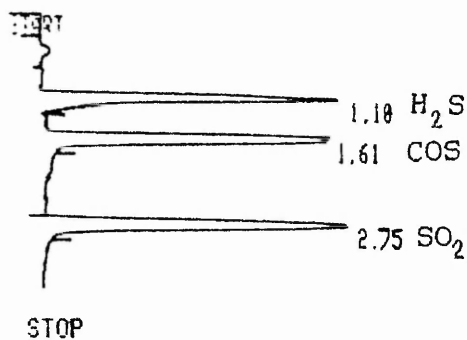
Analytical conditions:

    2.5ml sample size
    PoraPLOT Q column
    Column temperature = 50^0C
    Helium carrier gas
    Flow-rate = 6.7mls/min
    Flame Photometric Detector
    Detector temperature = 250^0C
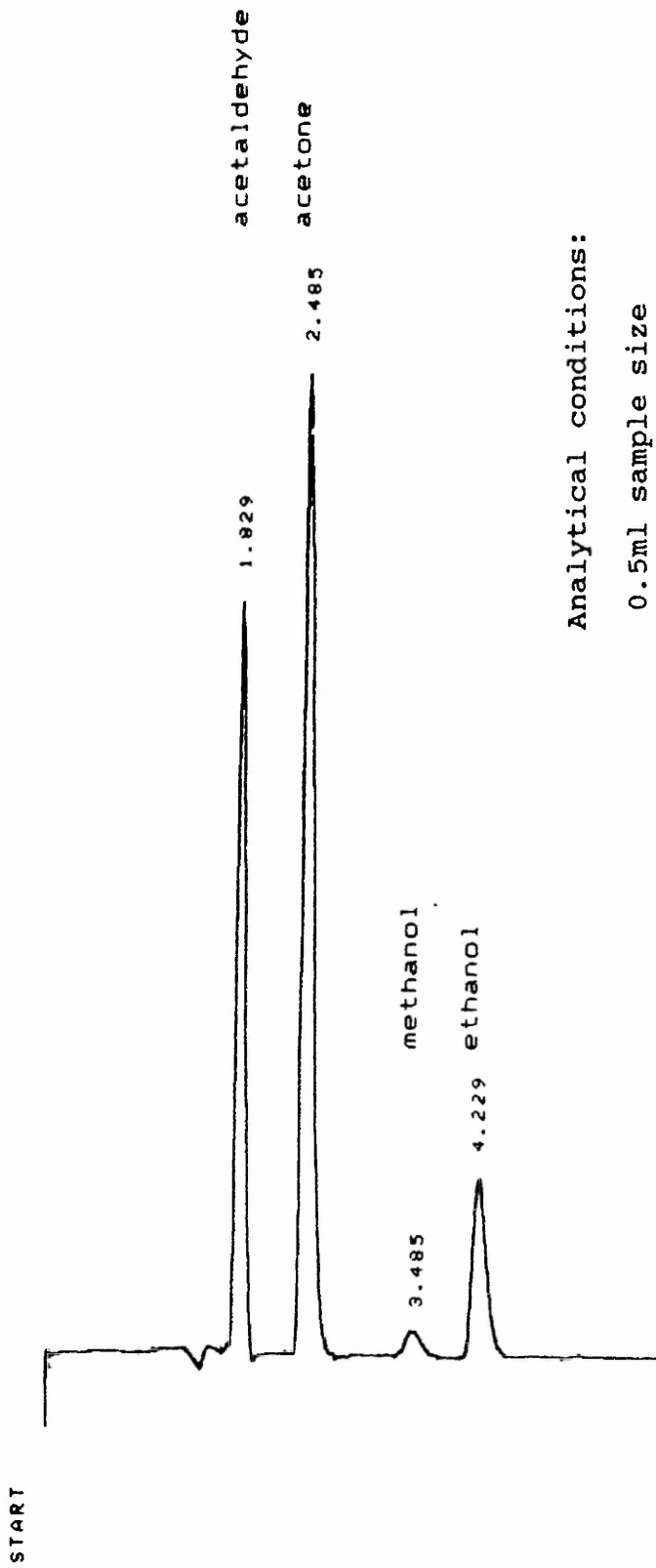
Figure 23 Chromatogram of Oxygenated Vapour Mixture

acetaldehyde

acetone

1.829

2.485

methanol

ethanol

3.485

4.229

START

Analytical conditions:

0.5ml sample size
DB-Wax column
Column temperature = 50°C
Helium carrier gas
PhotoIonisation Detector
(10.6eV)

Figure 24   Chromatogram of Aromatic Vapour Mixture
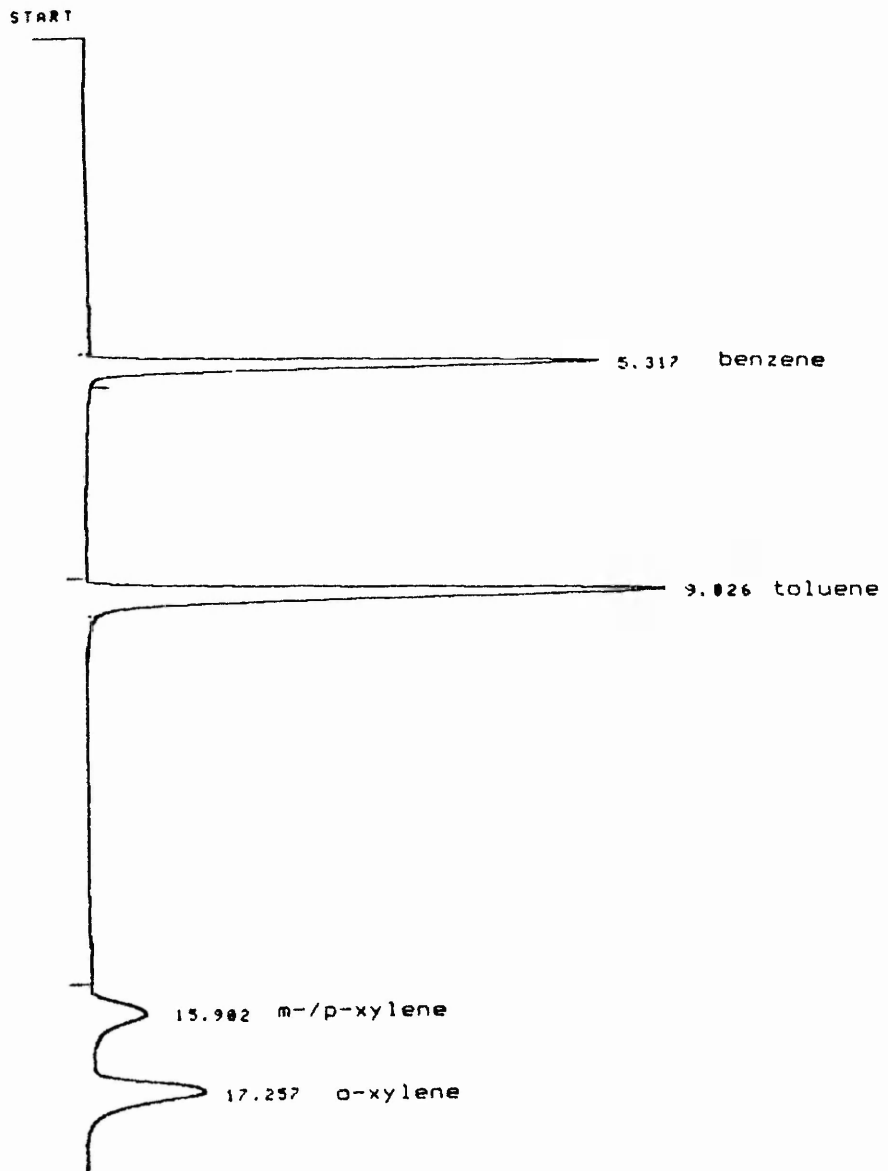
START

5.317   benzene

9.026   toluene

15.902   m-/p-xylene

17.257   o-xylene

Analytical conditions:

    0.5ml sample size
    DB-Wax column
    Column temperature = 50^{0}C
    Helium carrier gas
    PhotoIonisation Detector
    (10.6eV)

2.6   Summary of Conclusions

The surface modification of alumina produced a complex
adsorbent whose adsorption properties are altered, and
whose adsorptivity is reduced. This process has been
shown to be not a simple process of blocking available
adsorption sites, but is more likely to involve
production of complex $MAlO_2$ species (M is modifer cation).
The results obtained suggest that the alkali-metal ion is
the main factor responsible for the retention of
unsaturated solutes demonstrating that the anion plays a
secondary role in overall adsorbent retention
characteristics. The adsorption properties of modified
alumina are affected by the surface adsorption of water,
and can therefore be controlled by the temperature to
which the adsorbent is heated.

It is therefore apparent that alumina can be
specifically modified to produce a 'designer-like'
adsorbent with respect to the relative retentions of pi-
electron systems, by treating it with different
modifiers. The metal cation appears to dramatically
effect the retention properties of such a system, and
these properties are related to the physico-chemical
properties of the cation. Clearly the selectivity of
alumina may be controlled by suitable modification to
produce an adsorbent capable of separating components
without the need for extremely high column efficiencies.
However, the practical suitability of alumina as an
adsorbent in the continuous monitoring of a mine

atmosphere is limited since the retention properties are altered by ambient water.

Similarly, the surface modification of silica using organic or inorganic compounds produced adsorbents whose adsorption characteristics were markedly altered. The use of modified silica in the separation of the lower hydrocarbons was limited since these adsorbents produced the co-elution of propene with methyl propane or butane.

The use of Porapak Q was preferred for the analysis of mine atmospheres, since water was eluted as a peak therefore removing the problem of high humidity. The use of 'normal' (i.d.=1.59mm) Porapak Q packed columns was limited due to the poor selectivity between propane and propene for this adsorbent. However, by varying the physical column dimensions a dramatic improvement in the efficiency of the column was obtained, such that baseline separation of the solutes was easily attained using open tubular columns. Improvements in column efficiency were also noted by reducing the internal diameter of a packed column, although these improvements were less successful. Future work could be carried out into the detailed study of columns of still narrower i.d. in an attempt to optimise this parameter. This work would be complemented by an investigation into the effects of varying the particle size of column packing. A limiting factor of this work would be the excessive column backpressures produced, which would reduce the viability of developing a practical system.

The optimum arrangement for the hydrocarbon separation has been shown to be an open tubular column, the design of which aids fast analyses. Additionally, the optimum practical carrier gas velocity was demonstrated to be approximately equal to twice the optimum carrier gas velocity. This illustrated that optimisation of carrier gas velocities for the practical purposes envisaged in this work could be readily achieved by doubling the optimum carrier gas velocity, as determined from the van Deemter graph.

The optimum open tubular configuration of a column was reflected in the use of this design to analyse the other groups of gases in this work. It was possible to separate all of the gases of interest using PoraPLOT Q and DB-Wax open tubular columns.

CHAPTER 3

DEVELOPMENT OF ANALYTICAL METHODS

3.1   Introduction

The proposed monitoring of indicator gases required the development of GC methods for their analysis. The columns used to separate these gases have been developed in chapter 2. This chapter involves the complementry development of sampling systems and detectors necessary to complete the analytical methods.

The analysis of gases by GC requires introduction of the samples onto the stationary phase of a chromatogaphic system as a non-dispersed band. This is necessary to minimise the band broadening effects that lead to poor resolution of sample components. The use of GC systems in remote situations required the development of novel sampling systems since the use of conventional methods presented difficulties such as the requirement for manual control, or the use of relatively large quantities of power in electronically activated systems. In order to overcome these difficulties a 'home-made' sampling system was developed and studied. This system involved using a number of miniature solenoid valves interconnected with narrow bore PTFE tubing. The principal advantages of utilising these valves were :-

(a) inertness of the internal PTFE coating allowing the use of such a sampling system for reactive gases.

(b) small internal volumes of valves (15μl per valve) and tubing enable the production of a sampling system having a minimum dead volume.

(c) the characteristics of the valves (small, lightweight, low power consumption) identified their suitability for portable use.

(d) fast valve response time allowing accurate valve control.

(e) operation of the valves at pressures up to 60psi illustrated their robustness.

GC produces a separation of the analytes on a column prior to their detection, so the use of selective detectors was not a primary requirement. However an improvement in the detection limits of the gases of interest may be possible by employing detectors with a greater selectivity towards the gases of interest. A study of the response chracteristics of a variety of GC detectors would therefore be expected to improve the detection limits of the analyte gases. A review of the literature has revealed a number of detectors of interest [103], including :-

(a) **flame ionisation detector (FID)** - the operating principle involves the ionisation of eluting components in a hydrogen air flame, resulting in an electrical current passing between two electrodes across which a potential difference is applied. This detector only responds to organic compounds containing ionisable carbon atoms, and quantification is achieved by amplification of the ion current produced.

(b) flame photometric detector (FPD) - this detector uses a hydrogen-rich flame to decompose the eluting components generating an excited state of the analyte compounds, which subsequently emit radiation on returning to the ground state. A photomultiplier tube amplifies this emission after energy selection using a band pass filter. The resulting current is proportional to the quantity of analyte present, although this output signal is exponential. The detector is typically used to analyse sulphur and phosphorous containing compounds.

(c) photoionisation detector (PID) - the PID utilises a source of radiation in the vacuum ultra-violet region to excite the analyte molecules. Dissociation into a parent ion and an electron follows, the ions being collected in the ionisation chamber causing an electrical current to pass between a pair of electrodes across which a potential difference is applied. The selectivity of this detector can be modified by changing the energy of the ultra-violet radiation source, since different molecules have differing ionisation potentials (IP) (see table 1).

The analysis of hydrocarbons and oxygenated gases was to be investigated by using photionisation detectors (PID). An excellent discussion of photoionisation detection in GC in which 87 references are reviewed has been produced by Driscoll [151]. PIDs have typically been used to analyse hydrocarbons with greater than six carbon atoms possibly because these compounds represent greater hazards to health; hazard monitoring being the major analytical use

for PIDs [152, 153].

The analysis of sulphur gases was investigated by using a flame photometric detector (FPD). The detector response depends on the amount of sulphur compound present according to equation (6).

$$R = k.(S)^N \quad \ldots\ldots\ldots\ldots\ldots\ldots \quad (6)$$

R = detector response; k = constant;
S = sulphur analyte concentration; N = exponent.

Since S_2 species are responsible for the detector response, this response is proportional to the square of the concentration of sulphur analyte. However, Burnett et al have shown that the exponent value depends upon the structure of compounds, and the conclusions of other workers have shown agreement with this work [154,139].

The discussion of results in this chapter (section 3.5) involves reference to the 'limit of detection' of the analytical system. This refers to a signal to noise ratio of two (ie. the smallest amount of analyte that gives a peak height twice the noise level of the background signal) as described by Smith [155].

3.2   Equipment

Type LFYA 3-way inert solenoid valves, Minstac fittings, PTFE tubing of internal diameter 0.81mm (Lee Products Ltd., The Vale, Chalfont St.Peter, Gerrards Cross, Bucks).
Epson PC AX2 and a Thinklab ADC interface (3D Ltd., 4, Chase Side Works, Chelmsford Road, London).
10.2eV HNU PID (HNU Systems Ltd., 254 Europa Boulevard, Gemini Business Park, Warrington).

10.6eV and 11.7eV Photovac PIDs (Eden Scientific Ltd., Ham Common, Richmond, Surrey).

An Intersmat 120 GC fitted with a single channel FID with signal output to a Hewlett- Packard 3396A integrator, using a Valco 10-port solenoid gas sampling valve.

A Pye series 304 GC equipped with a Flame Photometric Detector (FPD) and fitted with a PTFE gas sampling assembly containing a 2.5ml sampling loop.

Dual detector output signals were monitored using a Perkin-Elmer/Nelson integrator system, which allowed post-run integration.

The carrier gases and flame gases employed were passed through charcoal and molecular sieve purification traps to remove trace organic contaminants and moisture (Phase Separations, Deeside Industrial Park, Deeside, Clwyd).

The equipment below was used to serially dilute gas mixtures on a volume/volume basis :-

1ml, 10ml, 100ml, 1000ml Hamilton gas tight syringes (Phase Separations).

1 litre, 5 litre tedlar sample bags (Chrompack UK, Ltd., Unit 4, Millharbour, London).

3.3   Chemicals and Reagents

A variety of BOC standard gas mixtures (in nitrogen) of Spectraseal grade were used, as listed below :-

1.   10ppm H_2S.

2.   2ppm, 20ppm, 100ppm COS.

3.   20ppm, 100ppm SO_2.

The gas mixtures contained gases at the following concentrations (ppm) :-

Standard 1 : methane,195; ethane,160; ethene,255

propane,165; propene,180;

methylpropane,160; n-butane,230.

n-pentane,205.

Standard 2 : ethene,205; propene,210.

Standard 3 : methane,920; ethane,1010; propane,900;

butane,950.

These gas mixtures were serially diluted as necessary using calibrated syringes and tedlar sample bags.

3.4   Experimental

3.4.1   Investigation of Sampling Systems

In order to investigate the usefulness of different valve arrangements as sampling systems for a GC a variety of configurations were designed, built and finally tested by connecting to a GC and used to carry out analyses. The valves were operated by using a series of relays incorporated in an interface controlled from programming instructions in a personal computer (PC) using RS-232 communications. The required accurate timing control of valve switching (±0.1sec) processes was achieved with the aid of the PC internal clock. Listings of the software used to control the valve sampling systems have been included in Appendix III.

The fundamental requirements for a sampling system were that both the chromatographic column and detector should be

continuously purged with carrier gas at a constant velocity. A variety of sample arrangements were studied, and the three which appeared to be the most interesting are illustrated in chronological order in figures 25a, 26a and 27a. A description of the operation of each system has been listed in the accompanying figures 25b, 26b and 27b.
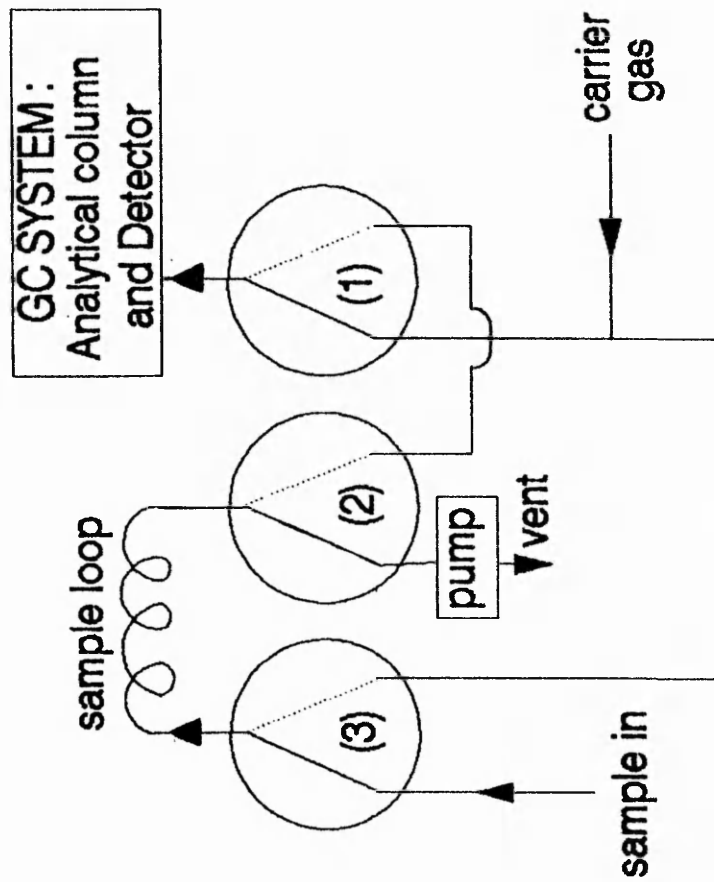
Figure 25a   Mark 1 Valve Sampling Arrangement

Figure 25b   Description of the Operation of Mark 1
              Valve Sampling System

STEP 1: The carrier gas passes through valve 1 via the
        column to the detector and is halted at valve 3.
        The sample is drawn through valve 3, the sample
        loop, then valve 2, by the action of the electical
        pump.

STEP 2: The electrical pump is stopped and all of the
        valves simultaneously switched on. The carrier gas
        passes through valve 3, flushes the sample loop and
        introduces the sample onto the column via valves 1
        and 2.

STEP 3: All of the valves are simultaneously switched off
        to return to the initial situation described in
        step 1.

              CRITICAL TIME INTERVAL

    SAMPLE INJECTION TIME PERIOD = (STEP3) - (STEP2).
       This is critical to prevent peak tailing.
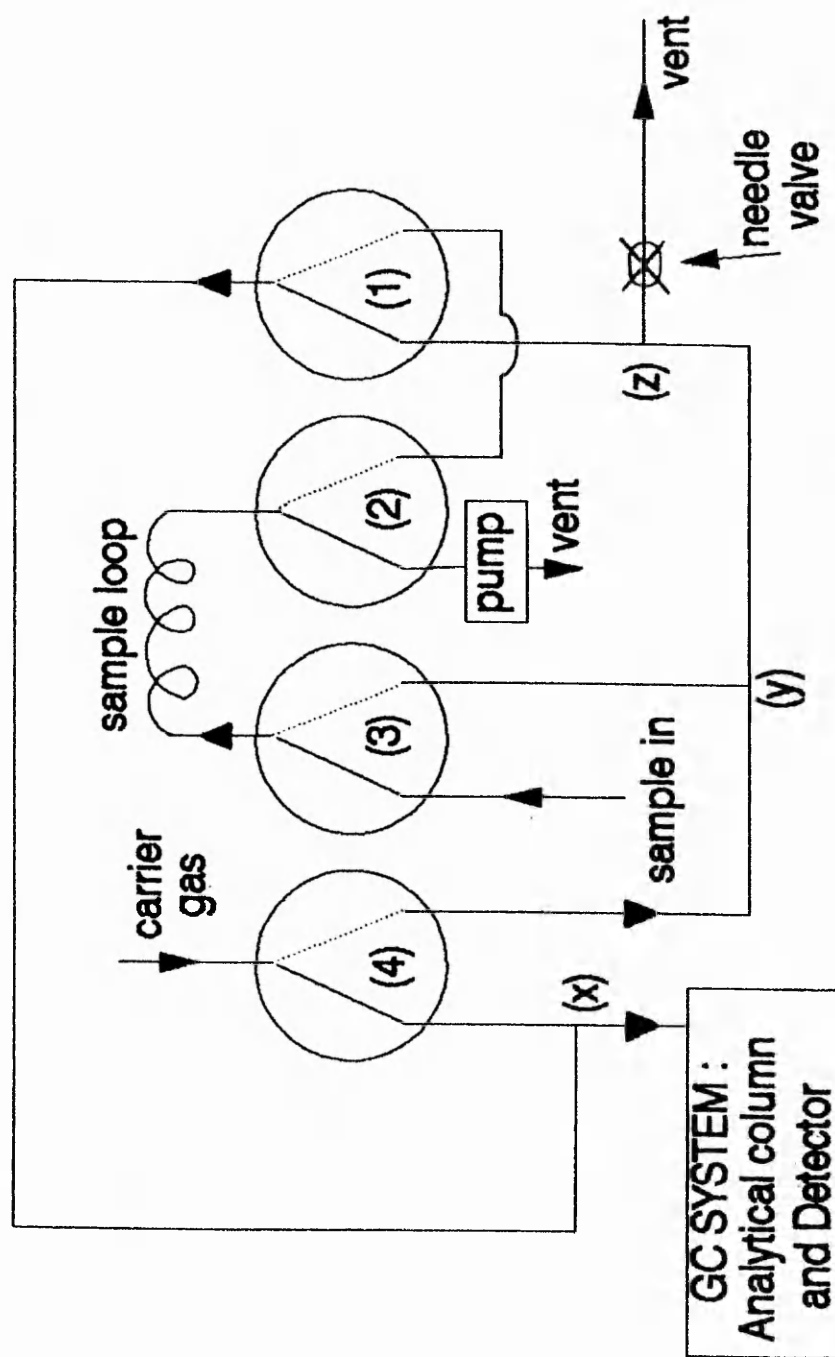
Figure 26a   Mark 2 Valve Sampling Arrangement

-122-

<u>Figure 26b</u>   <u>Description of the Operation of Mark 2</u>
<u>Valve Sampling System</u>

STEP 1: The needle valve is set to allow an even flow
through the vent and detector. The carrier gas
flows through valve 4 and T-piece x both to the
column and through valve 1, T-piece z and the
needle valve to vent. The action of the electrical
pump flushes the sample loop with the gas sample.

STEP 2: All four of the valves are simultaneously closed.
The carrier gas flows through valve 4 and T-piece
y through T-piece z to vent and also through valves
3, 2 and 1 onto the column.

STEP 3: Valves 3 and 4 are opened causing the carrier gas
to flush through T-piece x to the column, and
through valves 1, 2 and 3, the T-pieces y and z and
out to vent. This causes the sample loop to be
fully flushed during the analysis.

STEP 4: Valves 1 and 2 switch to return the valve system
to the original state shown in step 1.

CRITICAL TIME INTERVAL

SAMPLE INJECTION TIME PERIOD = (STEP3) - (STEP2).
This is critical to prevent peak tailing.
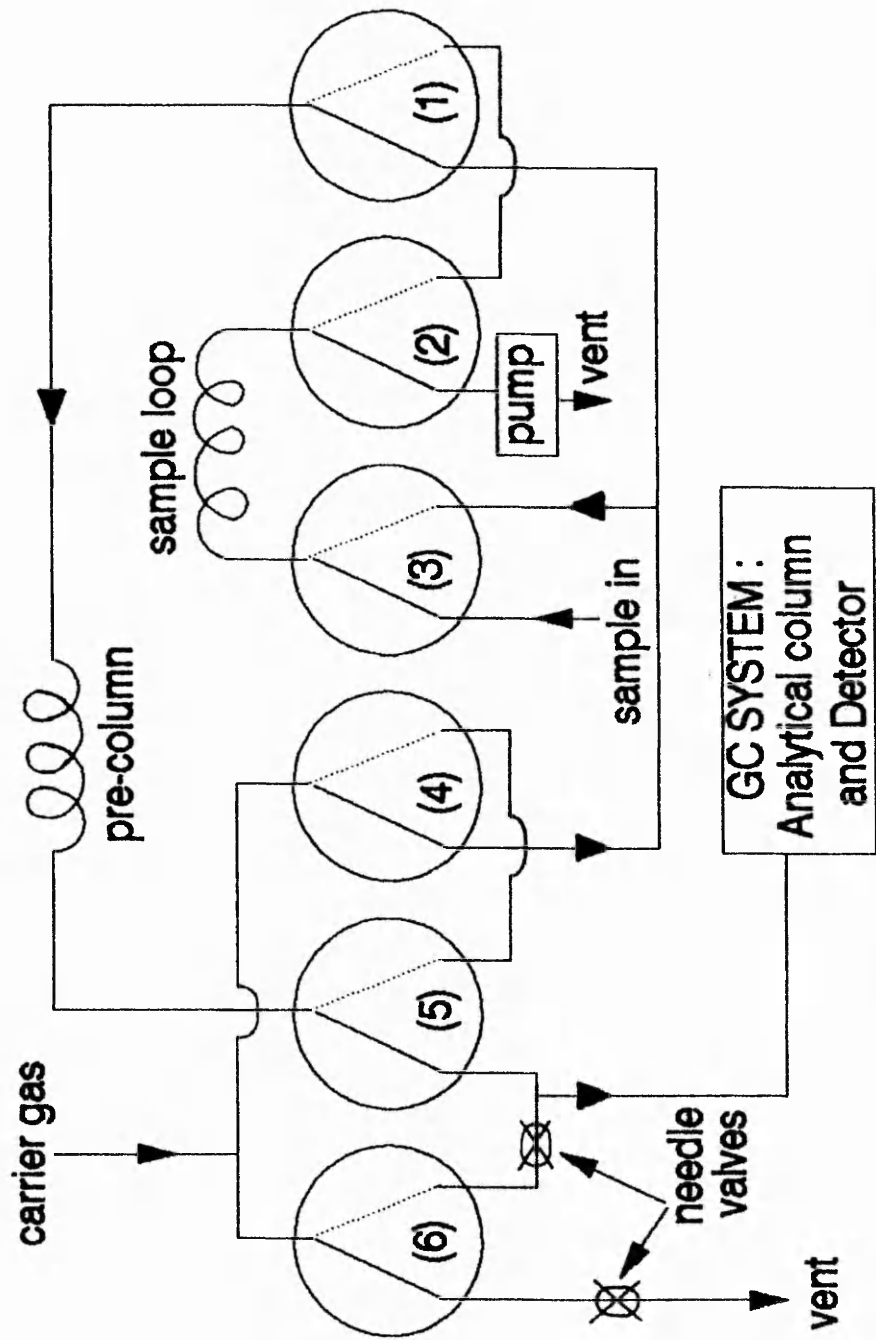
Figure 27a   Mark 3 Valve Sampling Arrangement

-124-

<u>Figure 27b</u>   <u>Description of the Operation of Mark 3</u>
            <u>Valve Sampling System</u>

STEP 1: The carrier gas passes through valve 6 to vent,
        and through valves 4 and 1, the pre-column, valve
        5, and the analytical column to the detector. The
        carrier gas flow is controlled by the needle valve
        positioned after valve 6. The action of an
        electrical pump draws a gas sample through the
        sample loop positioned between valves 2 and 3.

STEP 2: Valves 1, 2 and 3 close simultaneously causing the
        carrier gas flow to be diverted in order through
        valves 4, 3, 2 and 1, the pre-column and valve 5.
        The effect of this is to flush the sample from the
        sample loop onto the pre-column.

STEP 3: Valves 1, 2 and 3 simultaneously open producing a
        situation identical to that in step 1. Hence at
        this stage the sample resides on the pre-column,
        and elution of the components begins.

STEP 4: Valves 1, 2, 4, 5 and 6 simultaneously close. The
        carrier gas passes through valve 6, a needle valve,
        a second T-piece and the analytical column to a
        detector; and through valves 4 and 5, backflushing
        the pre-column, valves 1, 2 and 3 - this process
        flushing the sample loop. Control of the carrier
        gas flow rate was achieved by the needle valve
        situated between valves 5 and 6.

STEP 5: Valves 1, 2, 4, 5 and 6 simultaneously open to
        return the valve system to the original state in
        step 1.

                    CRITICAL TIME INTERVALS

    T1 = SAMPLE INJECTION TIME PERIOD = (STEP3) - (STEP2).
         This is critical to prevent peak tailing.

    T2 = SERIES TIME PERIOD = (STEP4) - (STEP3).
         Period during which the pre-column and
         analytical column are in series - This is
         critical to allow analyte gases to enter the
         analytical column.

    T3 = BACKFLUSH TIME PERIOD = (STEP5) - (STEP4).
         Period during which the pre-column is
         backflushed. This is critical to remove the
         interferent gases of relatively longer retention
         from the analyte gases.

3.4.2   Study of Suitable Detectors

(i) Study of Hydrocarbon Detectors

The 10.2eV HNU and 10.6eV Photovac PIDs were used in conjunction with a reference FID to study the response charateristics of PIDs to the aliphatic and unsaturated hydrocarbons. To evaluate these responses standard gas mixtures were analysed using each PID individually in series with the reference FID. The non-destructive nature of the PID required this detector to be positioned in series ahead of the FID.

The connection of the 10.2eV and 10.6eV PIDs in series was used to study the response of each PID to the individual hydrocarbon gases. This information was expanded by studying the effects of altering the relative positions of the PIDs. Accordingly a variety of gas mixtures were analysed using the two PIDs in series and re-analysed with the PID positions reversed.

(ii)   Study of Oxygenated and Aromatic Vapour Detectors

The 10.6eV Photovac PID was used in conjunction with a reference FID to study the response characteristics of the 10.6eV PID to the oxygenated vapours of interest. To evaluate these responses standard mixtures of the vapours were prepared using a static headspace technique, as described in Appendix IV. The PID was positioned ahead of the FID due to its non-destructive nature.

The response of the 10.6eV PID to the aromatic vapours of interest was studied by using the same conditions used

-126-

to analyse the oxygenated vapours. Standard vapour mixtures were prepared using a static headspace technique described in Appendix IV.

(iii)   Study of Sulphur Gas Detectors

The analytical conditions necessary to analyse the sulphur gases using a GC-FPD system were studied. The improvements obtained by using a PoraPLOT Q wide-bore column and helium carrier gas had previously been demonstrated in sections 2.5.4 and 2.5.5 and these conditions were therefore used.

A method of determining the exponent necessary to linearise the FPD output was studied which involved the analyses of a range of standard sulphur gas mixtures.

Since the ionisation potential of COS is high (11.17eV) this compound was also analysed using the same GC system with an 11.7eV Photovac PID. This work involved the analysis of a number of gas mixtures to study the usefulness of the 11.7eV PID.

3.5   Results and Discussions

3.5.1   Evaluation of Performance of Sampling Systems

The valve arrangement and a description of the operation of the mark 1 sampling system is shown in figures 25a and 25b. This was used to introduce a sample of 200ppm methane onto a GC, the resulting signal being recorded as illustrated in figure 28. Clearly peak tailing was observed during the early work, but this was decreased by reducing

RETENTION
TIME (MINS)

Time Interval
(seconds)

10.0

8.6

6.6

5.0

3.4

3.0

the time interval between steps 2 and 3 of the sampling operation. Complete elimination of the tailing was observed with the use of a 3 second time interval. However, there was a problem of sample carry-over since the sample loop was not completely flushed between analyses using this valve sampling arrangement. Hence the use of the mark 1 sampling system was limited.

A description of the operation and valve arrangements in the mark 2 sampling system has been given in figures 26a and 26b. When this system was used for the introduction of a 200ppm methane sample onto a GC peak tailing was noted and a secondary peak observed. To overcome these effects the time interval between steps 2 and 3 was varied, and the observed signal is illustrated in figure 29. Clearly the optimum time interval of 6 seconds prevented the appearance of a secondary peak, and a series of tests were performed using this configuration to study the repeatability of the sample introduction system. A statistical analysis of the results from a series of 11 injections of 1% methane sample produced a covariance of 1.3%, indicating an acceptable degree of analytical precision. The analysis of a 1% methane sample was carried out using two different sample loop volumes of $69\mu l$ and $155\mu l$ (calculated by measuring length and i.d. of sample tubing). The peaks obtained using each sample loop for the 1% methane sample showed that accurate quatitation was achieved, and confirmed the relative size of the sample loop internal volumes. Also, a study into sample carry-over revealed that less than 0.1%

RETENTION
TIME (MINS)

Time Interval
(seconds)

15.0

10.0

7.0

6.0
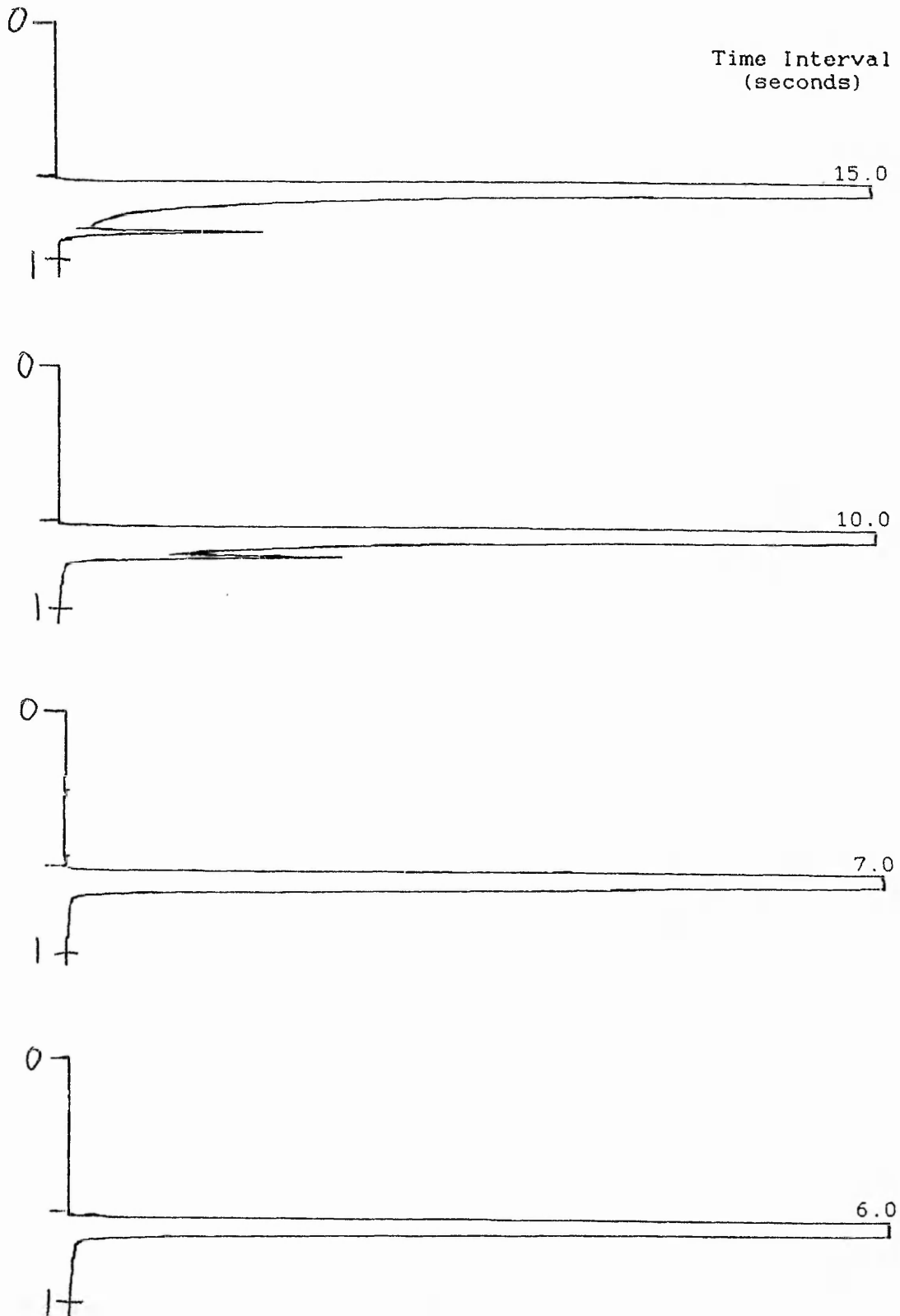
of a sample was carried over between analyses. This indicated that effective flushing of the system was being achieved between analyses. Thus the mark 2 system represented a viable method for the introduction of gaseous samples onto a chromatographic column. This has been demonstrated in figure 30, which shows a chromatogram of a gas mixture that was injected onto a GC-FID using the mark 2 sampling system.

Although the mark 2 system represented a viable technique for the simple introduction of gaseous samples onto a GC it did not allow for the multi-dimensional techniques necessary for the operation of a practical continuous monitoring GC. The application of a sampling system in the continuous monitoring of a mine atmosphere required a backflushing facility to prevent on-column accumulation of less volatile sample components and interference with subsequent chromatographic separations. In order to backflush samples during an analysis a variety of valve configurations were studied, and the mark 3 system illustrated in figures 27a and 27b proved the most appropriate. A constant carrier gas velocity was maintained throughout the analytical column to the detector by the control of two needle valves. These were strategically positioned so that the sample components at no time came into contact with them during an analysis. The concept of backflushing the precolumn was to ensure the removal of interferent components which were retained on the column longer than the analyte, preventing their carry-over

Figure 30   Chromatogram of Lower Hydrocarbon Gas
Mixture Using the Mark 2 Sampling System
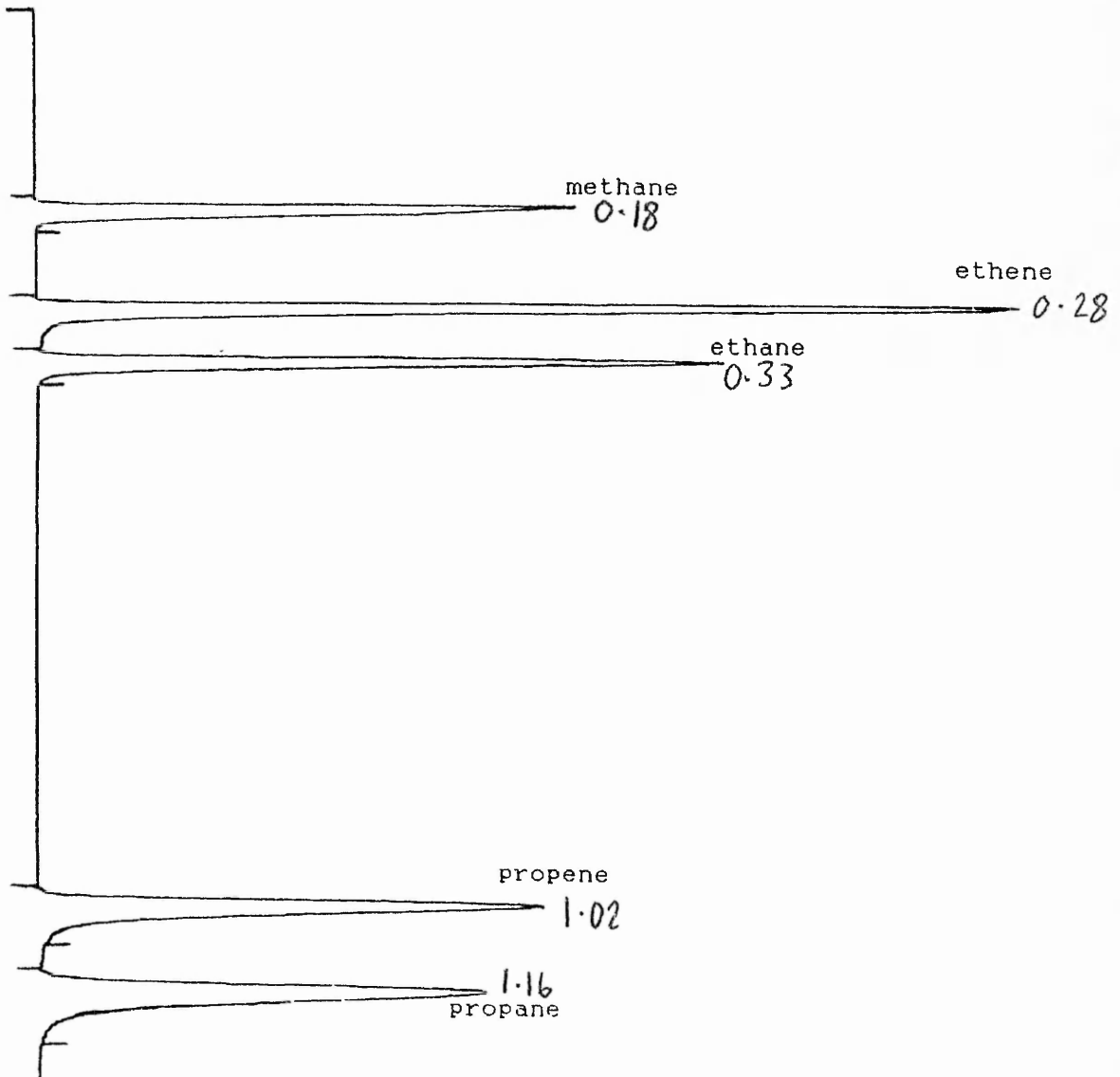
between analyses. Furthermore, this allowed the pre-column to be backflushed at a faster flow rate than the rate of forward flow thereby reducing the time taken for the backflushing process and increasing the scope of the system. The pre-column used in this work consisted of a 1m length of the PoraPLOT Q analytical column, which was accordingly reduced in size to a length of 9m. This system was successfully used to introduce samples onto a GC-PID system as shown by the chromatograms illustrating repeated analyses in figure 31.

3.5.2   Evaluation of Gas Detection Systems

(i)   Hydrocarbon Gas Detectors

Chromatograms illustrating comparisons of FID and PID responses have been demonstrated in figure 32. Since these detectors each employed different amplification circuitry it was not possible to make a direct comparison of the absolute responses. However the relative responses of each detector have been determined by normalising the response of each hydrocarbon to that of propane, and these have been listed in table 11. These results have been calculated by obtaining the peak areas noted from the integrator used for the analysis. It is clear that unsaturated compounds were detected more selectively using the PIDs rather than the FID. The FID showed typical behaviour of linearly increasing response with carbon number. Also, the 10.2eV PID had a greater unsaturated to saturated relative response than the 10.6ev PID.

Figure 31   Chromatograms Using the Mark 3 Sampling
             System

RETENTION
TIME
(MINS)
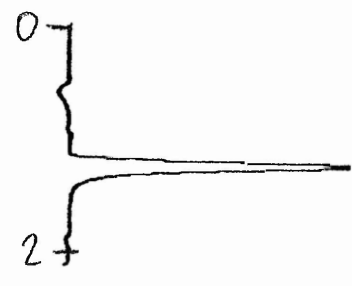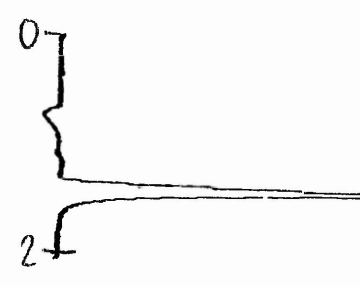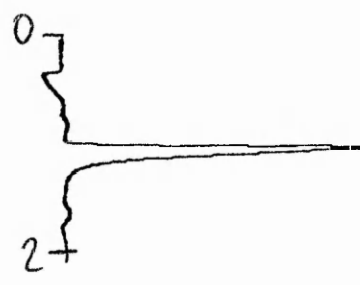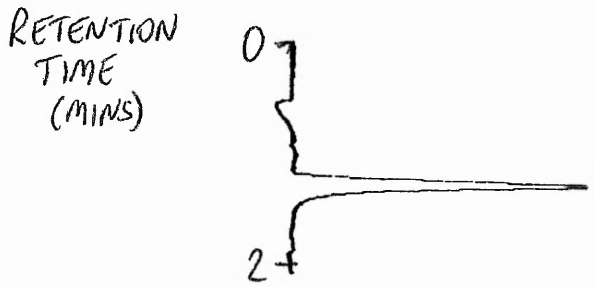
Sample = 1ppm COS

Detector = 11.7eV PID

Column = PoraPLOT Q

Column temperature = 50°C

    Same sample analysed
several times using Mark 3
   valve sampling system.

Conditions:

NaCl modified alumina (2%w/w) column packing
Column temperature = 60°C
Helium carrier gas
Flow rate = 40 mls/min

Solute elution order: methane, ethane, ethene, propane, propene, methylpropane, butane
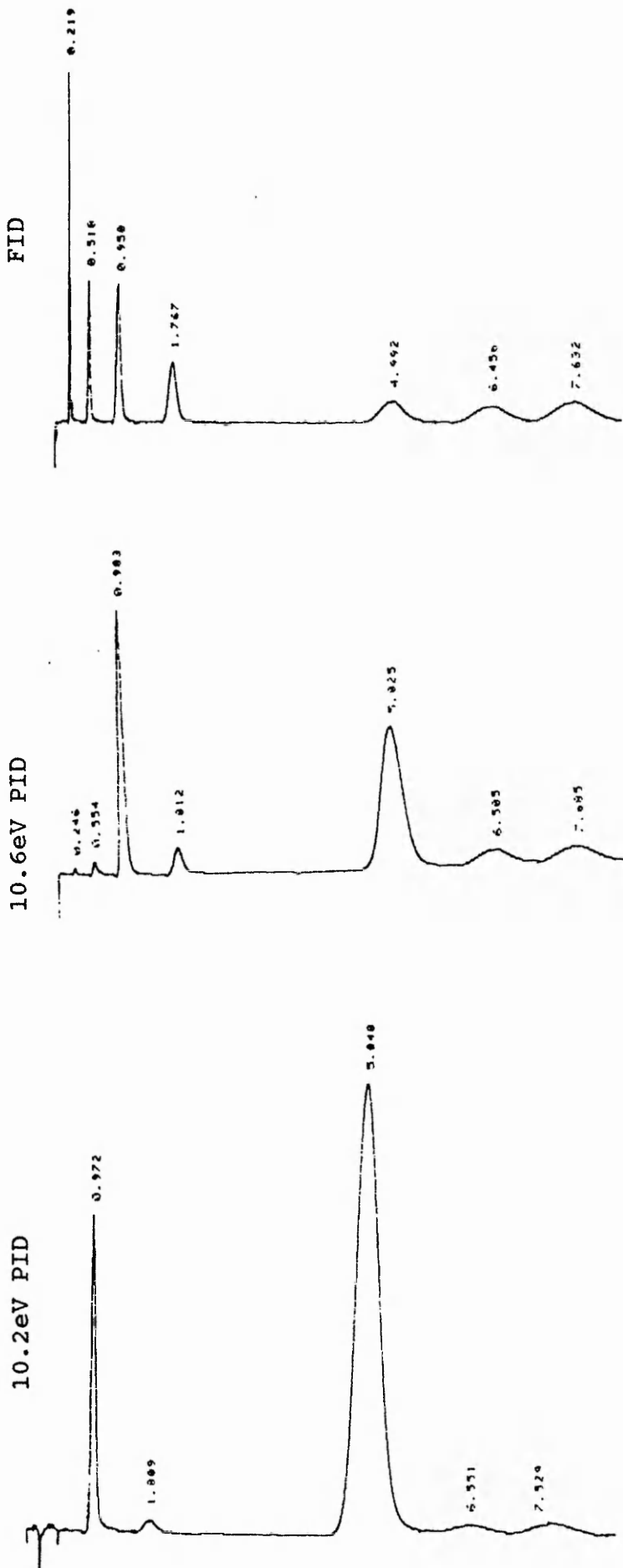
Figure 32 Chromatograms Demonstrating the Responses of a 10.2eV PID, 10.6eV PID and FID

-135-

Table 11   Comparison of Relative Responses of Detectors

ANALYTE	FID	10.2eV PID	10.6eV PID
Methane	0.30	-ve	0.04
Ethane	0.65	-ve	0.33
Propane *	1.00	1.00	1.00
Methylpropane	1.35	1.76	1.85
Butane	1.34	1.92	2.21
Ethene	0.62	5.11	2.73
Propene	0.98	46.39	7.69

* Responses calculated relative to propane.

The relationships between relative response and carbon number or ionisation potential (IP) of each hydrocarbon for each PID have been plotted in figures 33 and 34. They demonstrated that the IP of each compound predominantly determined it's relative response, and no such trend was observed for carbon number alone. When the compounds were divided into saturated and unsaturated systems, there was a clear trend for each homologous series of increasing detector response with increasing carbon number. However, this may have been due to the decrease in IP of compounds which accompanies the increasing carbon number of a homologous series.

In order to investigate the detection mechanisms of the PIDs they were placed in series for the detection of hydrocarbon mixtures, chromatograms showing these responses are shown in figures 35 and 36. Although the 10.6eV PID response was independent of the position of the detector, the 10.2eV PID response to certain compounds depended upon the postion of the detector. This variation in detector response has been highlighted in table 12, in which the results represent an average of 3 analyses.

Figure 33 Relative Responses of the 10.6eV PID to Hydrocarbons
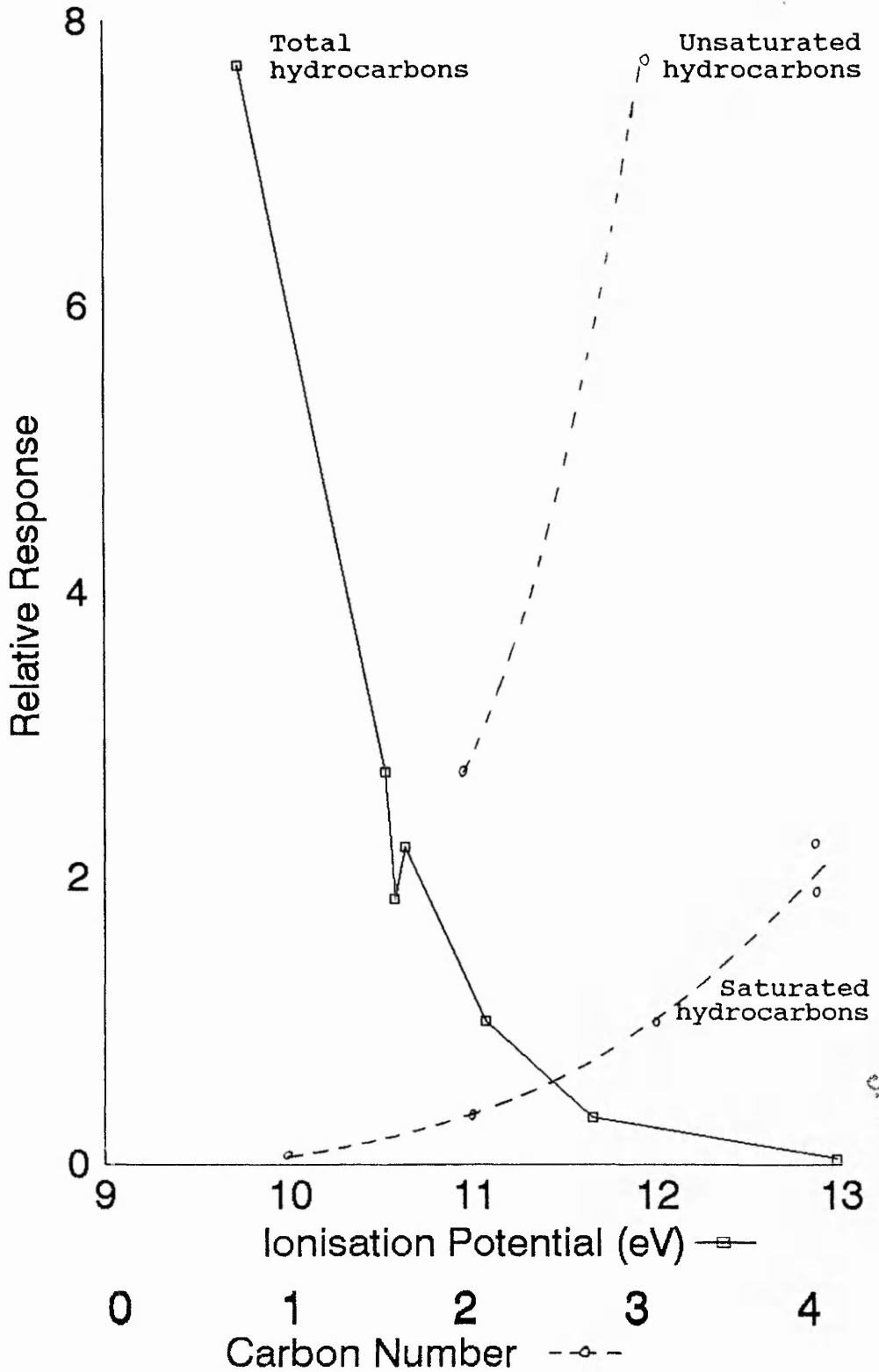
Figure 34   Relative Responses of the 10.2eV PID to Hydrocarbons
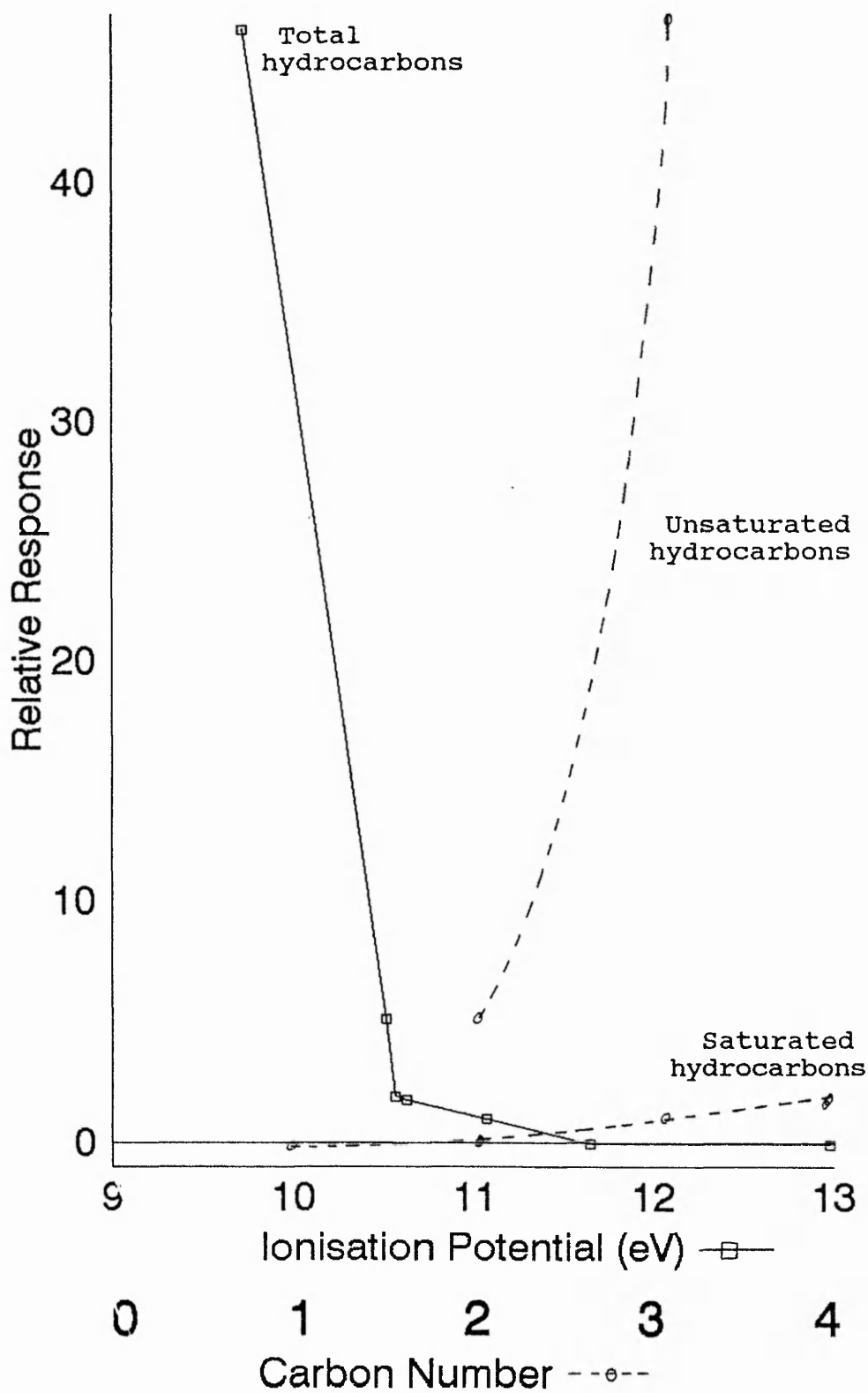
Figure 35   Chromatograms Illustrating the Effects of Serially Coupled PIDs for the Detection of Unsaturated Hydrocarbons

Detector order : 10.2eV to 10.6eV

ETHENE

PROPENE

10.2eV PID

10.6eV PID

Detector order : 10.6eV to 10.2eV

ETHENE

PROPENE
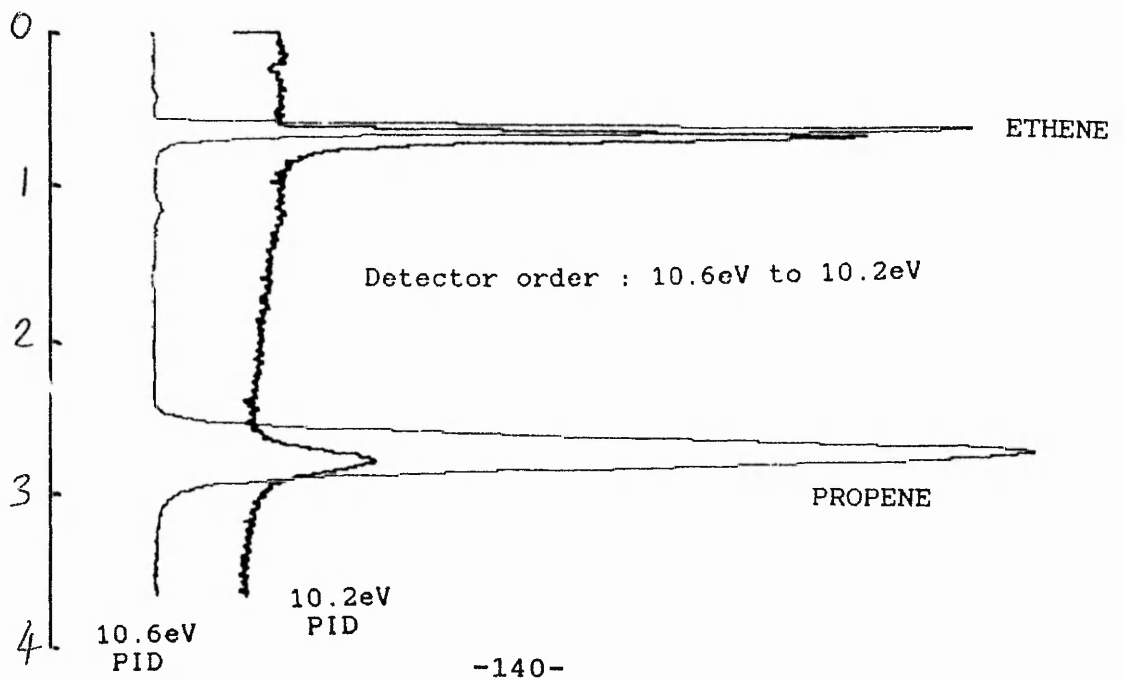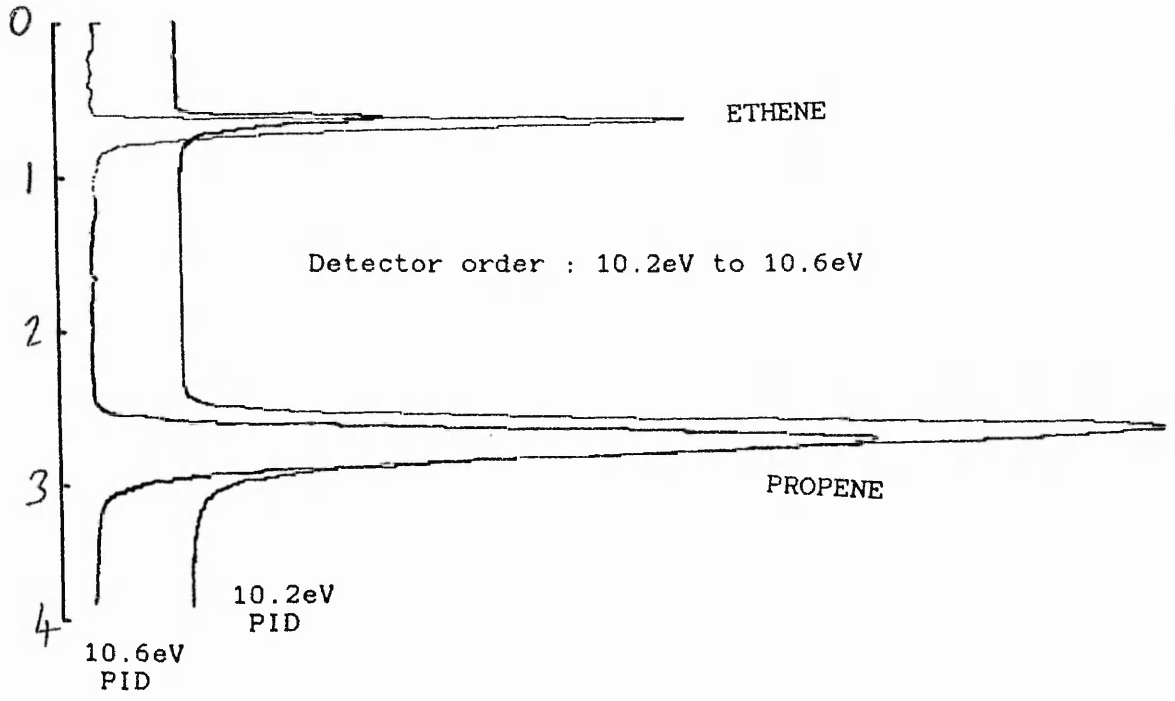
10.2eV PID

10.6eV PID

Figure 36   Chromatograms Illustrating the Effects of Serially Coupled PIDs for the Detection of Saturated Hydrocarbons

Detector order : 10.2eV to 10.6eV

10.2eV PID   10.6eV PID

Detector order : 10.6eV to 10.2eV
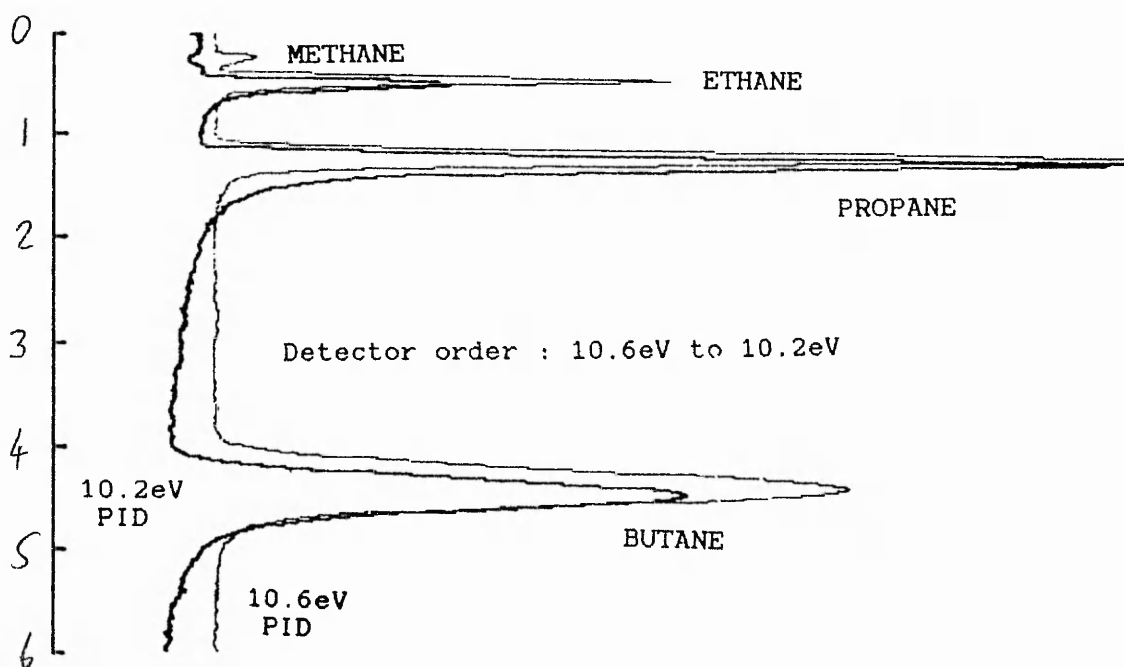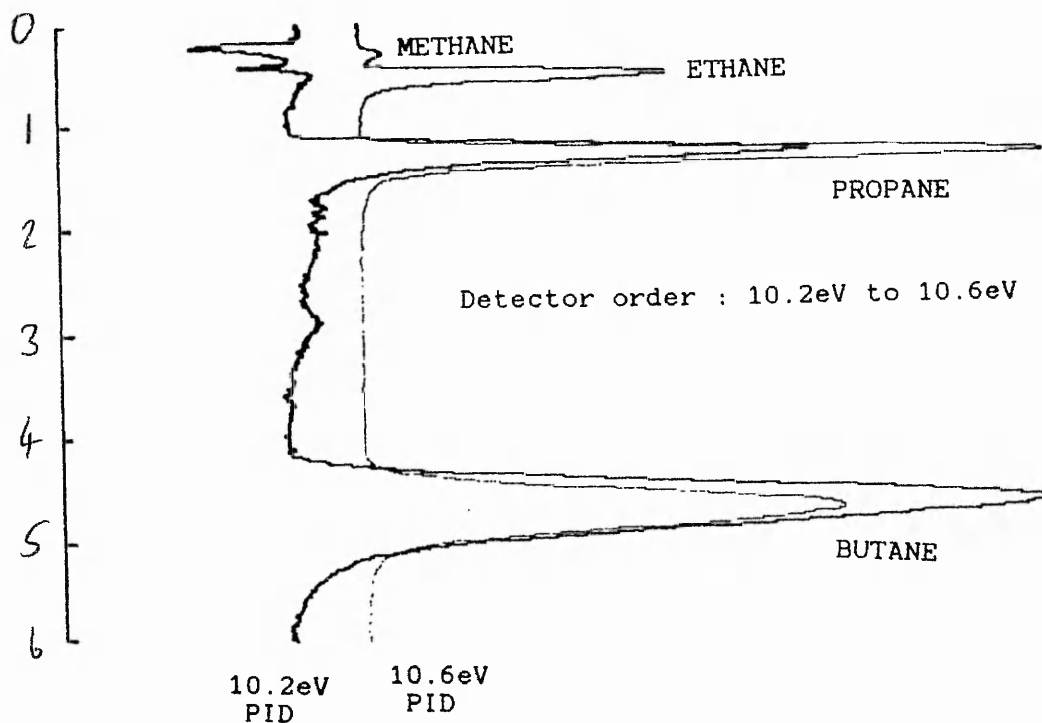
10.2eV PID

10.6eV PID

Table 12   Comparison of Normal 10.2eV PID Response to
10.2eV PID Reponse Using Analytes Previously
Subjected to a 10.6eV PID

| ANALYTES | RATIO OF 10.2eV PID RESPONSES | |
	(10.2eV PID)	(10.6eV PID——> 10.2eV PID)
methane	-ve	-ve
ethane	-ve	+ve
propane	1	2.27
butane	1	0.93
ethene	1	0.33
propene	1	0.01

The 10.2eV PID response to propane has been
significantly increased by prior analysis of these
compounds by the 10.6eV PID. However, the 10.2eV PID
responses to unsaturated hydrocarbons were diminished by
prior analysis of these compounds by the 10.6eV PID.
Clearly therefore the 10.6eV PID excites the analytes
reducing the parent molecular populations and excited
species thus reducing the apparent response of the 10.2eV
PID. Since the 10.6eV response was unaffected by prior
analysis of compounds using the 10.2eV PID it appeared
unlikely that the 10.2eV PID produced the same species as
those formed in the 10.6eV PID. A review of the available
literature on these detectors revealed that both the 10.6eV
and the 10.2eV PIDs produced similar ultraviolet energy.
(ie. 83% at 10.03eV and 17% at 10.64eV) [156,157]. The
designation of 10.2eV and 10.6eV as terms for these lamps
must therefore been assumed to be a commercial description.
Furthermore, since the photoionisation process is known to

-142-

be inefficient, (typically 0.001% to 0.1%) the different responses achieved by the 10.2eV PID are unlikely to be due to photoionisation processes from the previous 10.6eV PID [157].

The chief difference between these detectors was the method by which ultraviolet (UV) radiation was produced. The 10.2eV PID produces UV radiation by the application of a potential across a ring cathode and disc shaped anode which are housed in a lamp containing the gas. However, the 10.6eV PID produces UV radiation by the use of an inductance coil wrapped around a lamp connected to a radiofrequency circuit. This coil acted like an antenna by coupling electromagnetic radiation into the lamp to excite the gas by induction. The presence of this high frequency electromagnetic radiation could therefore have been the reason for the excitation of the analytes by the 10.6eV PID. An alternative explanation could involve the production of ozone by the 10.6eV PID, which was clearly distinguishable during use by its' odour. Since ozone is known to oxidatively cleave alkenes by the reaction shown in equation (7), this could explain the reduced alkene responses [158].

$$\begin{matrix} R1 \\ \quad \\ R2 \end{matrix} \!\!\! C\!\!=\!\!C \!\!\! \begin{matrix} R3 \\ \quad \\ R4 \end{matrix} \; + \; O_3 \; \longrightarrow \; \begin{matrix} R1 \\ \quad \\ R2 \end{matrix} \!\!\! C\!\!=\!\!O \; + \; \begin{matrix} R3 \\ \quad \\ R4 \end{matrix} \!\!\! C\!\!=\!\!O \ldots\ldots (7)$$
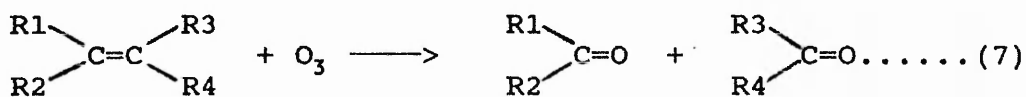
The lowest detection limits for unsaturated hydrocarbons were clearly achieved by using a PID. However, the operating conditions did not produce minimum detection limits since it was necessary to prevent peak overlap from

the saturated hydrocarbons present in a mine atmosphere. Typical detection limits were :-

ethene,1ppm; propene,0.3ppm.

Aliphatic hydrocarbons were best analysed by using a FID, producing the limits of detection :-

methane,0.5ppm; ethane,0.5ppm; propane,0.5ppm; methylpropane,1ppm; butane,1ppm; pentane,1ppm.

(ii)   Oxygenated and Aromatic Vapour Detectors

A comparison of the responses of a reference FID and a 10.6eV PID to the oxygenated vapours acetaldehyde, acetone, methanol and ethanol have been illustrated in figure 37. Clearly the PID represents an excellent method of detecting acetaldehyde and acetone, with detection limits considerably improved as compared to the FID.

The operating conditions did not produce the minimum detection limits since it was necessary to prevent peak overlap from the saturated hydrocarbons present in a mine atmosphere. Typical detection limits were :-

acetaldehyde,0.5ppm; acetone,0.1ppm; methanol,5ppm; ethanol,2ppm.

The operating conditions used to analyse the oxygenated vapours were also employed to analyse the aromatic vapours. A chromatogram demonstrating the separation and 10.6eV PID response to these vapours has been illustrated earlier in figure 24. The detection limits achieved were :-

benzene,0.1ppm; toluene,0.05ppm; m-/p-xylene,0.05ppm; o-xylene,0.05ppm.

10.6eV PID

FID

acetone
2.492 acetaldehyde
methanol
ethanol

1.499
1.842
3.608
4.398
2.532

1.833
2.492
3.526
4.300
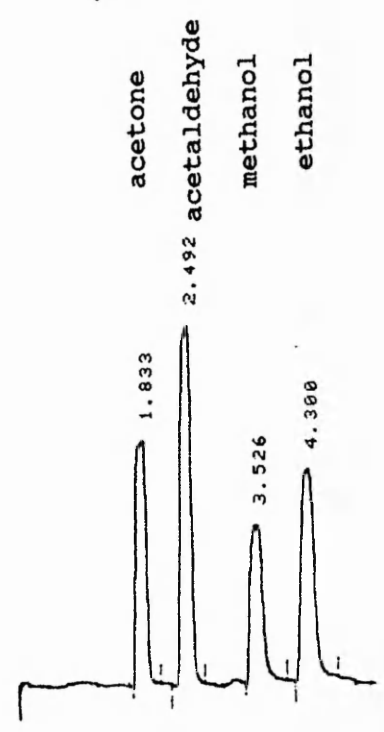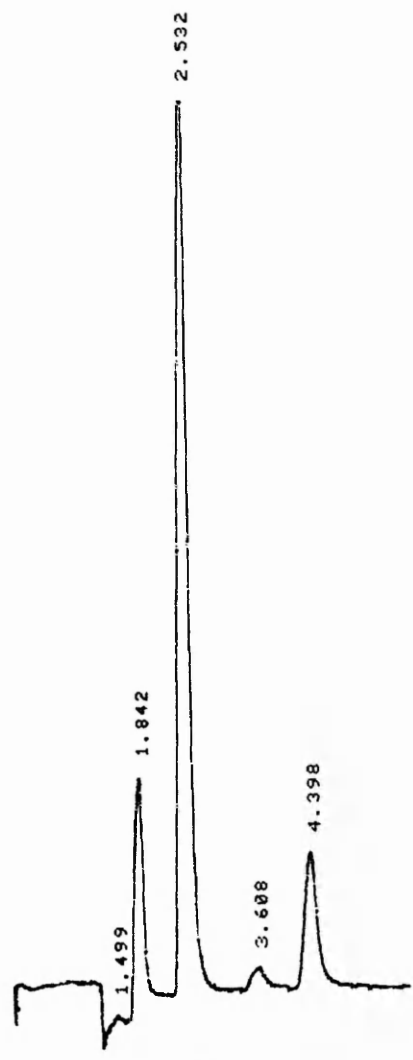
Figure 37   Comparison of the Responses of a FID and a 10.6eV PID to Oxygenated Vapours

(iii)   Sulphur Gas Detectors

The output from a FPD to sulphur compounds is exponential but this was linearised by the application of a suitable factor (the exponent) to the detector lineariation device. In order to determine the exponent value required for this linearisation, a number of gas standards of varying concentration were analysed using an exponent of 1.00. A graph of log analyte concentration was plotted as a function of log detector response. The slope represents the exponent value required to linearise the FPD output for the particular analyte, as illustrated in equation (8).

$$R = k.(S)^N$$

$$\log(R) = N.\log(S) + k.................(8)$$

$$(\text{ cf. } \quad y = m.x + c ..... \text{ for a straight line })$$

R, detector response; S, sulphur analyte concentration; N, exponent; k, constant.

Using this approach the exponents required to linearise the FPD output for the sulphur analytes of interest were determined and they have been listed in table 13.

Table 13   Exponents Required to Linearise FPD Output

ANALYTE	EXPONENT
H_2S	2.15
COS	1.80
SO_2	1.86

-146-

This technique of FPD linearisation was proven by re-analysing the COS gas standards using an exponent of 1.80. A graph of the detector response against gas concentration was found to have a correlation coefficient of 0.9995. This proved that the FPD output had been accurately linearised, as illustrated in figure 38.

The elution order of the sulphur compounds of interest using the PoraPLOT Q column was H_2S, COS, SO_2, as illustrated in the chromatogram in figure 22. H_2S was found to exhibit a slight degree of peak tailing, which was ascribed to the reactivity of the gas. It was necessary to treat the column with 10 injections of this compound prior to analysis in order to obtain reproducible peak measurements. Although other workers have described SO_2 as being particularly difficult to analyse fewer problems were encountered with this gas, which required 3 injections prior to analysis [140]. These problems were assumed to be due to the irreversible adsorption of these compounds onto surfaces within the analytical system. The effects of altering detector temperature and flame gas mixture were investigated by studying signals obtained for the sulphur compounds. They were optimised at a detector temperature of 250°C, and air and hydrogen flame gas flow rates of 30mls/min each.

The aliphatic hydrocarbons were analysed using these conditions since they were known to be present in a routine mine atmosphere. The FPD was slightly responsive to these compounds, producing a descrimination of about 2500:1 for
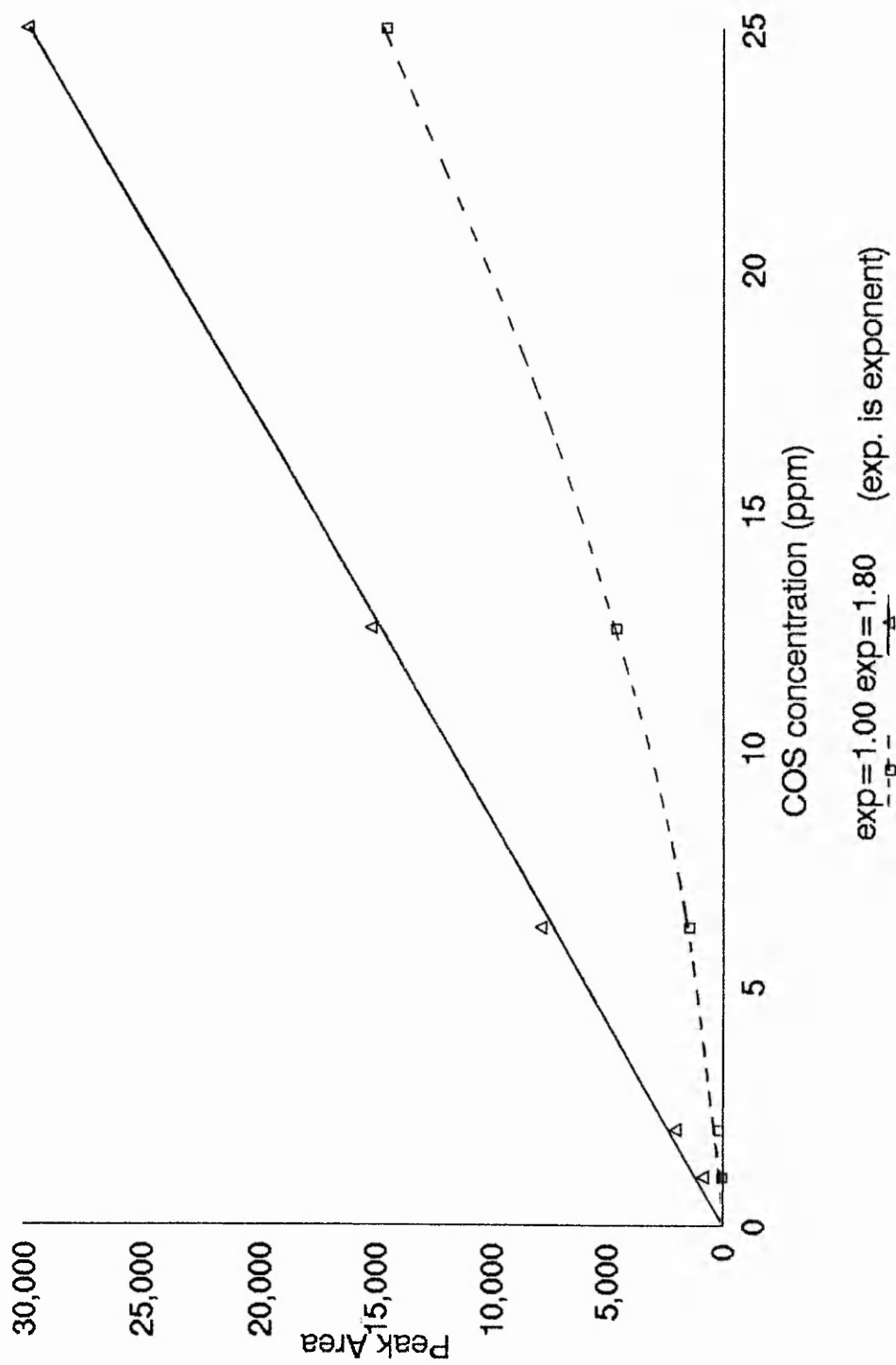
Figure 38 Effect of Linearisation Device Upon FPD Output Signal

(S compound per S atom):(alkane). The retention data obtained for these alkanes allowed Kovats Retention Indices for the sulphur compounds to be determined by calculating the column dead-time using the method described in Appendix II. The retention indices calculated for H_2S, COS and SO_2 were 237, 271 and 316 respectively. These values indicated that the presence of alkanes would not interfere with the analysis of the sulphur gases using this system.

The limits of detection of the sulphur gases were :- hydrogen sulphide,0.5ppm, carbonyl sulphide,0.1ppm; sulphur dioxide,0.5ppm.

The suitability of an 11.7eV PID for the analysis of COS was investigated by using a PoraPLOT Q column in the Pye 304 GC system that was used for the FPD. A comparison between the reponses of the 11.7eV PID and 10.6eV PID showed that the former detector exhibited a response to COS but relatively less response to the other components, whilst the latter showed no response to COS. This illustrates how some degree of selectivity may be achieved by altering the PID lamp.

The analysis of a COS standard that had been diluted with laboratory air produced an unknown peak that was eluted prior to the COS peak. The unknown solute was found by investigation to be water, which has an ionisation potential of 12.60eV. The close proximity of this peak to that of COS necessitated its' removal, in order to prevent problems of peak overlap. It was found by experimentation that the water could be removed by passing the sample

through $MgClO_4$ prior to injection onto the column, as illustrated by the chromatograms in figure 39. The $MgClO_4$ was experimentally proven not to adsorb any COS from the sample, and this was illustrated in figure 39 where the COS peak size remained constant regardless of it's passage through $MgClO_4$. The 11.7eV PID produced a negative response to air compared to zero response to nitrogen. This was shown experimentally to be due to oxygen, which has an ionisation potential of 12.06eV. The chromatograms shown in figure 39 illustrate that this response does not interfere with the COS peak.

The 11.7eV PID produced a detection limit of 0.1ppm COS using conditions which allowed the analysis of a mine atmosphere. However, the usefulness of this PID was demonstrated with only limited success due to the short lifetime of the lamp (ie. 20 days). This was assumed to be due to the hygroscopic nature of the LiF end window.

The use of an 11.7eV PID in an underground environment was therefore eliminated due to the limitations experienced in the laboratory.

Figure 39   The Response of a 11.7eV PID to a Variety of Gases

COS Standard in Nitrogen

H₂O

250ppb COS

Dried COS Standard in Nitrogen

Passed Through MgClO₄

250ppb COS

COS Standard in Nitrogen

1ppm COS

1.872

COS Standard in Air

OXYGEN

1.894 200ppb COS
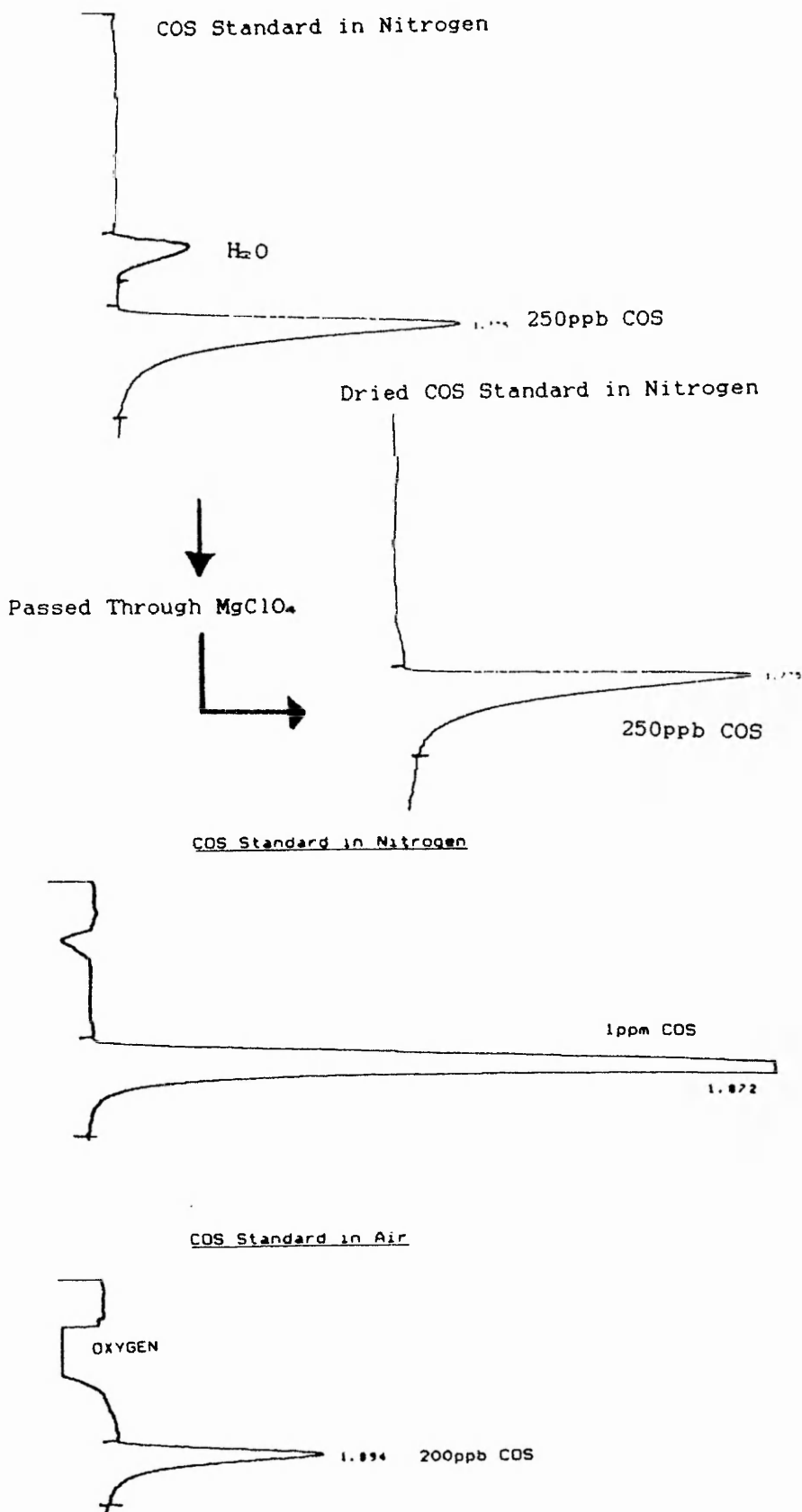
3.6   Summary of Conclusions

A number of different valve configurations were investigated and an arrangement representing a suitable gas sampling system for a GC was successfully demonstrated. This could represent the 'front end' of a GC analyser for use underground.

The response characteristics of 10.2eV and 10.6eV PIDs were investigated. They produced a greater response to unsaturated hydrocarbon systems relative to saturated hydrocarbons. Thus, their application in monitoring a mine atmosphere in which the former represent analytes and the latter the matrix is quite apparent. These detectors also produced excellent responses to the oxygenated and aromatic vapours of interest. They therefore represented detection systems capable of monitoring the gases and vapours to be studied in this work.

The use of an FPD and 11.7eV PID in the detection of sulphur gas analytes in the presence of other mine atmosphere gases was studied. The practical application of the 11.7eV PID was discounted due to the short lifetime of the detector lamp. However, the FPD represented a method of detecting the sulphur gases to be studied in this work.

The use of these detectors in conjunction with the columns described in chapter 2 therefore produced excellent analytical systems for the range of gases to be studied in this work. The detection limits of the proposed indicator gases using these analytical systems have been listed in table 14.

Table 14   GC Analyses of Proposed Indicator Gases

ANALYTE	DETECTION LIMIT (ppm)	GC COLUMN	GC DETECTOR
methane	0.5	PoraPLOT Q	FID
ethane	0.5	PoraPLOT Q	FID
propane	0.5	PoraPLOT Q	FID
methylpropane	1	PoraPLOT Q	FID
butane	1	PoraPLOT Q	FID
pentane	1	PoraPLOT Q	FID
ethene	1	PoraPLOT Q	10.6eV PID
propene	0.3	PoraPLOT Q	10.6eV PID
acetaldehyde	0.5	DB-Wax	10.6eV PID
acetone	0.1	DB-Wax	10.6eV PID
methanol	5	DB-Wax	10.6eV PID
ethanol	2	DB-Wax	10.6eV PID
benzene	0.1	DB-Wax	10.6eV PID
toluene	0.05	DB-Wax	10.6eV PID
m-/p-xylene	0.05	DB-Wax	10.6eV PID
o-xylene	0.05	DB-Wax	10.6eV PID
hydrogen sulphide	0.5	PoraPLOT Q	FPD
carbonyl sulphide	0.1	PoraPLOT Q	FPD
sulphur dioxide	0.5	PoraPLOT Q	FPD

CHAPTER 4

INVESTIGATION OF TECHNIQUES FOR STUDYING COAL OXIDATION

4.1   Introduction

An investigation of gases associated with the spontaneous combustion of coal required the development of a method by which these gases could be produced and monitored under carefully controlled conditions in the laboratory. The technique studied involved heating a known mass of coal at a programmed rate of temperature increase with air as the combustion gas. This produced a controlled coal oxidation process evolving products in a similar manner to those formed during the underground spontaneous combustion of coal.

It was necessary to observe the rate of coal oxidation during the heating process in order to relate this to the quantity of oxidation products formed. A number of workers have devised different methods of studying the rate of coal oxidation. Banerjee et al studied the oxygen consumption by measuring oxygen concentrations of the combustion gas at the exit of the coal bed chamber [66]. The success of this method depended upon the adsorption and reaction of oxygen during the coal oxidation process that occurred as the coal was heated. A measure of the coal oxidation process may also be produced by monitoring the evolution of CO and CO_2 in the combustion gas at the exit of the coal bed chamber [55]. A combination of these methods producing the

CO/O_2 deficiency ratio is recognised as one of the most sensitive measures of coal oxidation [76].

Thermal methods of analysis represent an alternative approach to monitoring the combustion characteristics of a coal sample. Thermogravimetric coal analyses have been carried out to study coal combustion characteristics [159,160]. However, differential thermal analysis is more applicable to monitoring coal oxidation since the process is exothermic. Briefly, this method involves plotting the temperature differential between a sample of coal and reference inert material as a function of the inert material temperature during a programmed rate of temperature increase. This method has been used by Banerjee et al to compare the spontaneous heating susceptibility of coals, and more recently by Wade et al [68,161]. Wade used the point at which the coal and reference temperatures crossed to denote the self-heating liability of coal. This technique formed the basis for the 'crossing-point method' in which a coal sample is heated in an oxidising atmosphere at a programmed rate of temperature increase [162]. The lowest temperature at which the exothermic coal oxidation reaction raised the coal temperature above that of the oven was termed the 'crossing point'. Coals which are more susceptible to spontaneous heating exhibit lower crossing point temperatures than the less susceptible coals.

4.2 Equipment

Pye 104 programmable GC oven.

Type T and type K thermocouples (RS Components Ltd., Corby, Northants).

100ml gas-tight syringe (Phase Separations, Deeside Industrial Park, Deeside, Clwyd).

Epson PC AX2, Star NL-10 Printer and a Thinklab ADC interface (3D Ltd., Interface House, Chelmsford Road, Southgate, London).

Icell Mark 2 - cold junction correction cell (Delristor Co. Ltd.).

Infra-red (IR) gas analysers - These are non-dispersive double beam IR analysers which measure absorption at wavelengths specific to the analyte :-

Carbon Monoxide : 4.7μm (2130cm^{-1}).

Carbon Dioxide : 4.3μm (2300cm^{-1}).

Methane : 3.3μm (3000cm^{-1}).

(Analytical Development Co. Ltd., Hoddesdon, England). Oxygen dedicated gas analyser - Dependent upon the paramagnetic susceptibility of oxygen. (Servomex Ltd., Crowborough, Sussex, England).

4.3 Chemicals and Reagents

B.O.C. gas standards for calibrating the dedicated gas analysers :-

Mixture 1 : 100% N_2.

Mixture 2 : 0.98% CO_2, 1.01% CH_4, 73ppm CO, in N_2.

Mixture 3 : 2.85% CO_2, 2.25% CH_4, 245ppm CO, in N_2.

Mixture 4 : 0.03% CO_2, 20.93% O_2, 79.04% N_2.

Mixture 5 : 2000ppm CO, in N_2.

Magnesium perchlorate 14-22 mesh (BDH Ltd, Poole, Dorset).

Soda-Lime 10-16 mesh (BDH Ltd, Poole, Dorset).

Silanised glass wool (Phase Separations Ltd, Deeside Industrial Pard, Deeside, Clwyd).

4.4   Experimental

4.4.1 Development of Automated Coal Combustion Generation Evolved Gas Analyser System (ACCG/EGA)

Apparatus was configured to generate and monitor coal oxidation products which has been termed the Automated Coal Combustion Generation Evolved Gas Analyser system (ACCG/EGA). A schematic diagram of this arrangement has been shown in figure 40. The working system as it was used is illustrated more graphically in the photograph in plate 2.

The coal sample was held in place in a pyrex glass tube (70cm long x 1.10cm i.d.) using silanised glass wool plugs. The glass tube was inserted into a Pye 104 temperature programmable GC oven, which increased the coal temperature. Temperatures of the coal bed and the GC oven were monitored by the use of three thermocouples as described in section (i). The carrier gas was passed through molecular sieve to remove gaseous impurities and a copper coil (200cm long x 0.16cm i.d.) inserted in the oven to preheat the carrier gas and avoid cooling effects. The resulting air was then directed through the coal bed. The fine detail of the

-157-
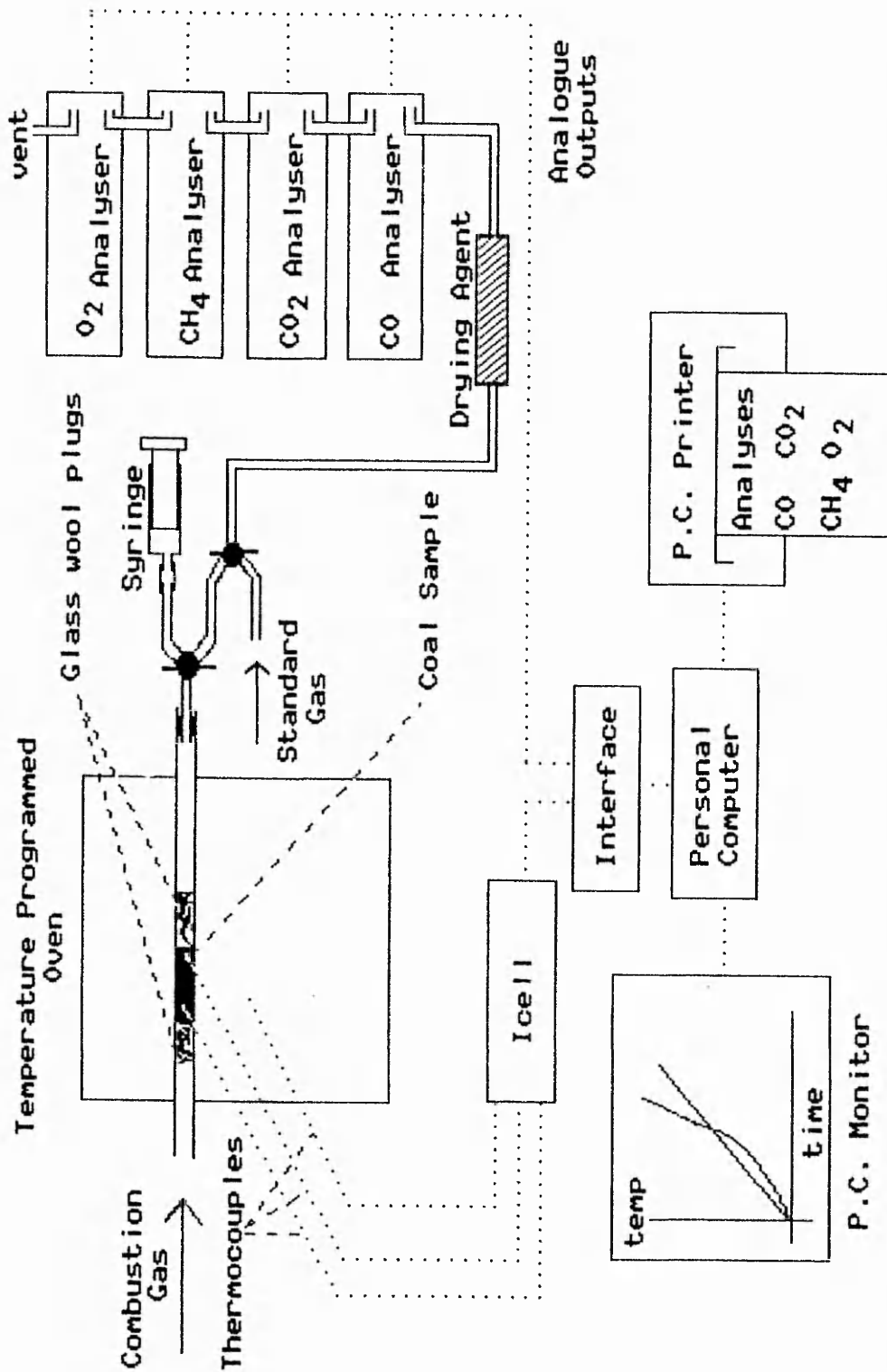
Figure 40   Schematic Diagram of Automated Coal Combustion Evolved Gas Analyser System
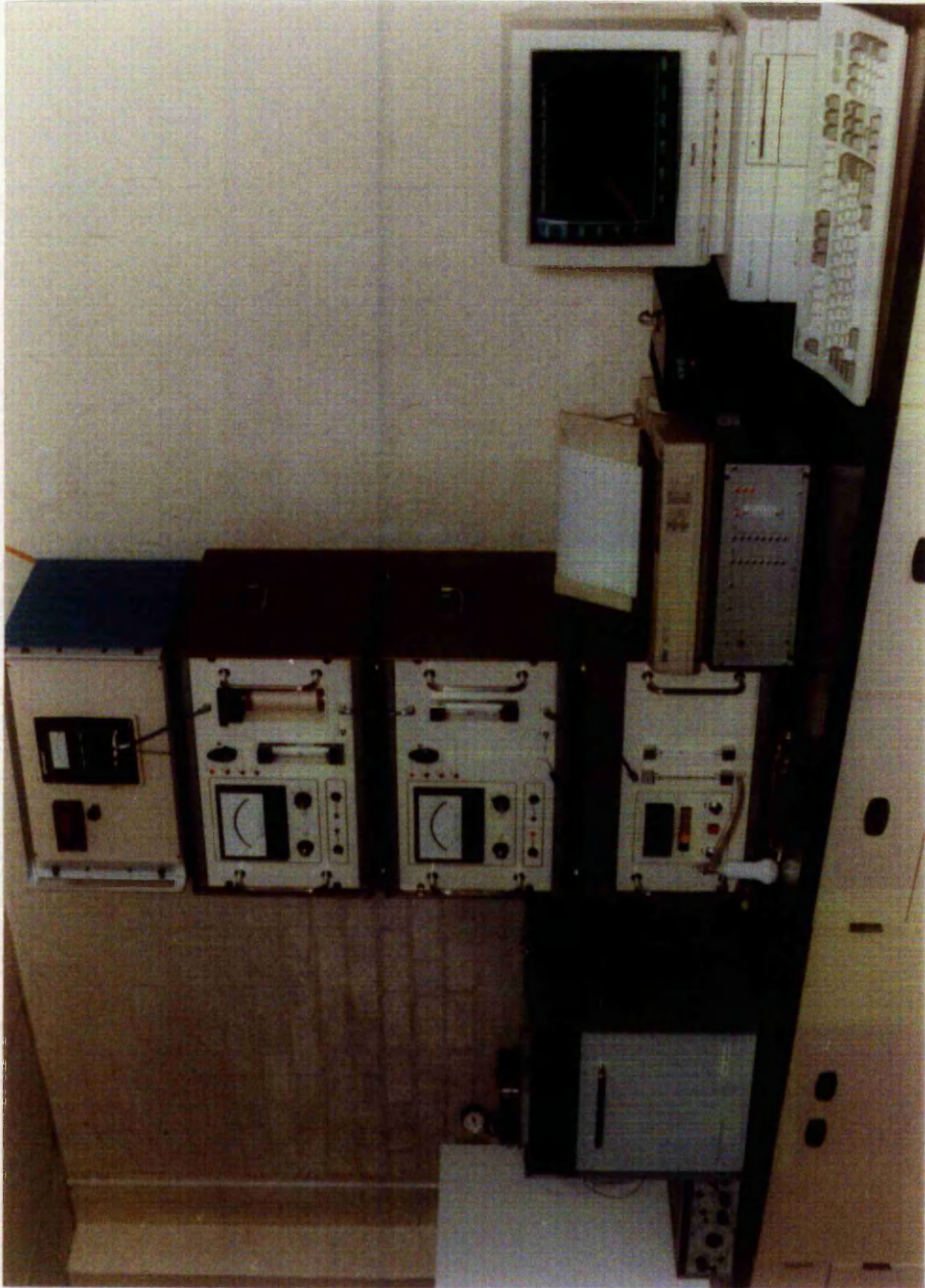
Plate 2 Photograph of Automated Coal Combustion Evolved Gas Analyser System

-159-

layout of apparatus within the oven is illustrated in figure 41. The carrier gas flow-rate was controlled by the fine needle valve and was monitored by the flowmeter. Flowmeters situated on the gas analysers illustrated in plate 2 were also monitored to ensure the integrity of the gas flow and to ensure that the system had no leaks.

The heated coal products were swept through an all glass system incorporating a drying agent (magnesium perchlorate) to four dedicated gas analysers. Specific gases evolved from the heated coal were continuously monitored using the analysers as described in section (ii).

Automation and data processing of the entire system was achieved using a PC as the controller and data logger running software developed by the researcher. A modular approach was adopted for the program which was developed in the C programming language. This software is listed in Appendix V. The analogue signals from the temperature and gas monitoring equipment were digitised by an ADC interface allowing the resultant data to be processed by the PC. This interface contained 8 channels which were multiplexed to a single 14-bit analogue to digital converter (ADC) chip. Thus the temperature measurements were displayed in real time on the PC monitor. Gas concentrations measured by the dedicated analysers were also listed in real time on the printer. All measurements made during heated coal experiments were written to files stored in non-volatile memory in ASCII format. This allowed subsequent retrieval of the information after completion of each experiment.
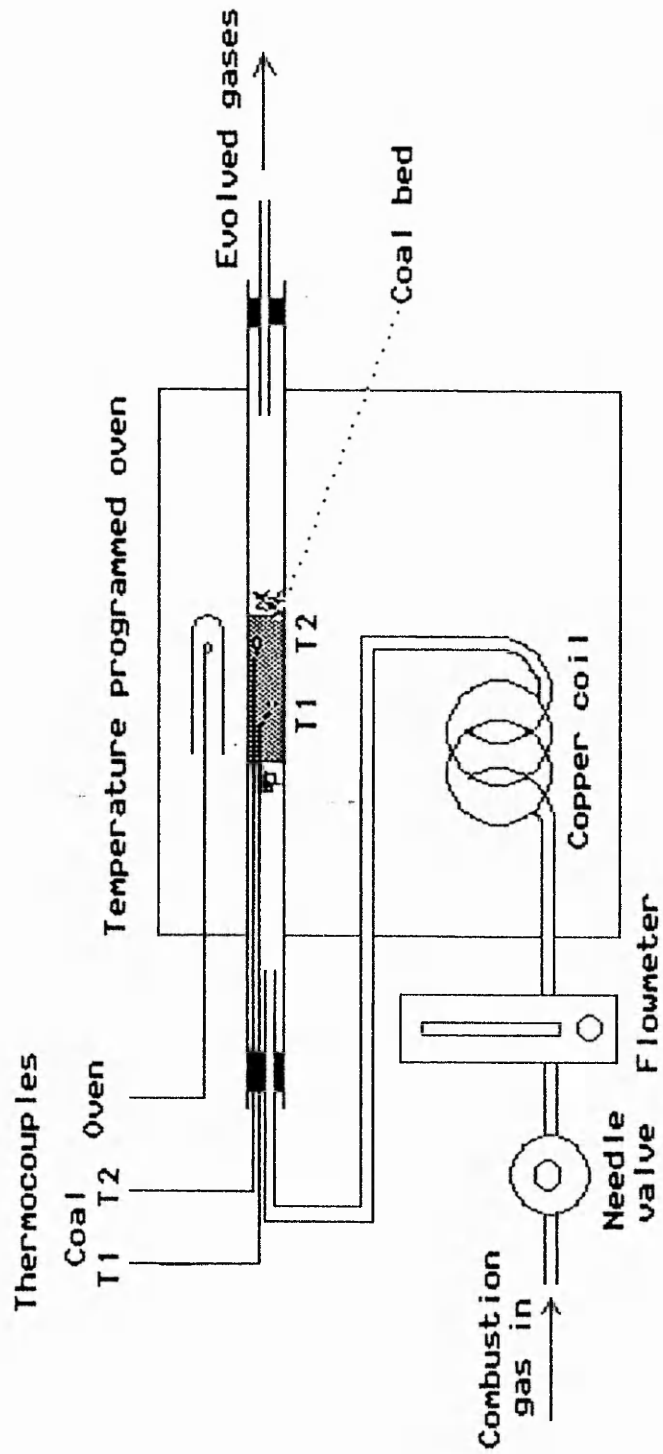
Figure 41   Design of Oven Apparatus in the Automated Coal Combustion System

4.4.1 (i) Measurement of Coal Bed Temperature

Measurement of the coal bed temperature relative to that of the temperature programmed oven was achieved by inserting two thermocouples into the coal bed and one in the oven. Type T thermocouples (Cu/Cu-Ni) were initially used since a temperature range of 0-300°C was to be monitored. However, problems were encountered with these due to their non-linear response. Type K thermocouples (Cr-Ni/Al-Ni) were therefore employed. Problems with the thermocouple tips inserted in the coal bed physically disintegrating were eliminated by using a stainless steel shielded design. Cold junction correction was maintained by the use of secondary thermocouples inserted into an 'ICELL' unit (temperature accurately controlled to 0.0±0.004°C) as illustrated in figure 42.

The thermocouple temperature was determined by measuring its e.m.f., which spanned approximately 0-12mV for the required temperature range (0-300°C). In order to automatically monitor these temperatures a PC was connected to the thermocouple output via an interface containing a 14-bit ADC having an accuracy of ±1 LSB. Hence a temperature range of 0-300°C was resolved to 4096 bits (ie. 2^{12}), giving a discrimination to approximately 0.1°C.

The monitoring system was calibrated by measuring the e.m.f. output from the thermocouples placed in a temperature controlled unit. The accurate temperature at which the thermocouples were calibrated was ensured by the utilisation of several probes calibrated to NAMAS
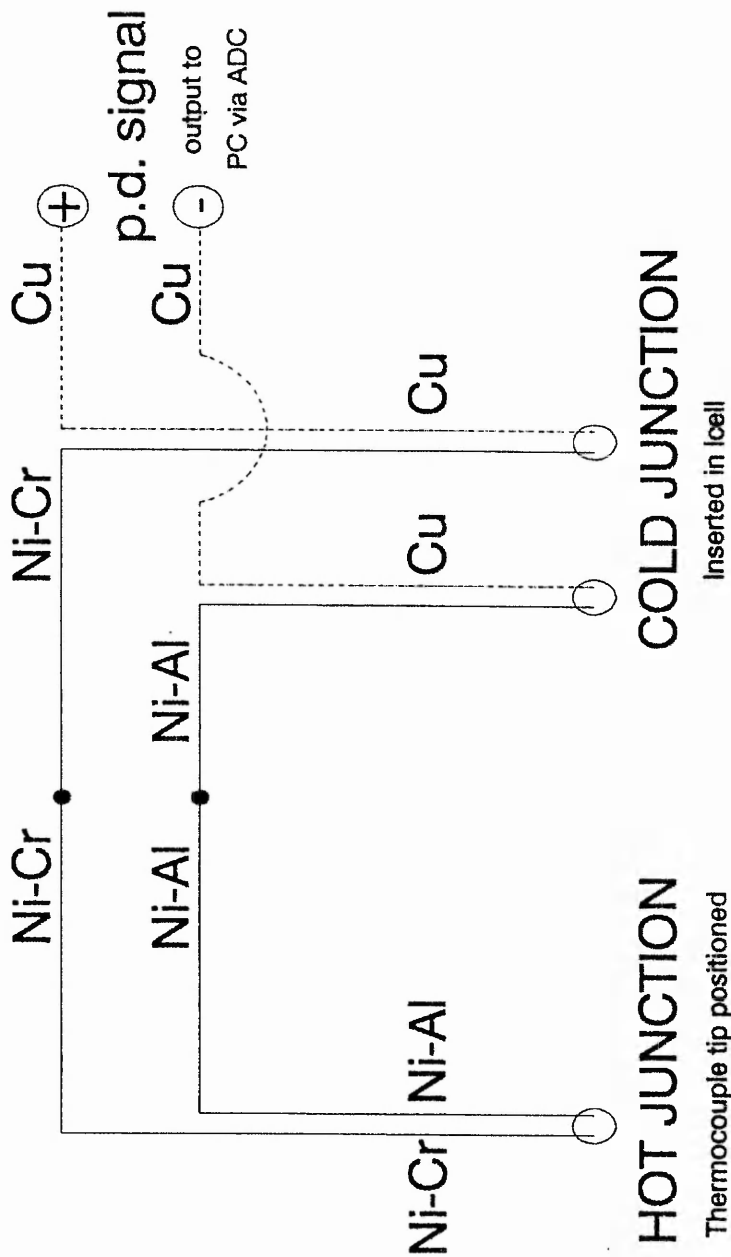
Figure 42 Diagram Demonstrating Thermocouple Cold Junction Correction

HOT JUNCTION
Thermocouple tip positioned
where temperature is to
be monitored

COLD JUNCTION
Inserted in Icell

p.d. signal
output to
PC via ADC

-163-

accreditation standards in British Coal laboratories. The application of standard voltages to the interface connected to the PC allowed a relationship between the analogue voltage and it's digital value to be obtained. This allowed direct determination of temperature from the thermocouples, as shown in the calibration chart listed in table 15. Since the thermocouples were clearly linear, formulae for each thermocouple relating the temperature to a digital value were determined using the linear expression 'y=mx+c'. These calibration formulae have been listed in table 15, and the incorporation of them into a computer program allowed the coal bed temperature to be monitored in real time. During an analysis this was measured once a minute and the complete data written to a stored file. Progress of the coal heating was observed in real time by displaying this data on a PC monitor. This process was achieved by a module of the program listed in Appendix V which plots each temperature value as a point on the graph shown on the monitor.

4.4.1 (ii) Monitoring Evolved Gas Analysers

The dedicated gas analysers were not absolute methods of analysis and required regular calibration with standard gas mixtures. These were introduced into the system by the control of taps shown in figure 40. Each of the analysers had an analogue voltage output as well as a mechanical or digital meter display. Accurate signal information was obtained by using the analogue output rather than the panel

Table 15   Calibration of K Type Thermocouples

Temperature (°C)	Digitised Thermocouple Output * CHANNEL No.			
	0	1	2	3
59.69	582	474	646	587
101.04	1060	903	1126	1059
150.30	1620	1407	1690	1612
202.28	2210	1938	2282	2193
252.55	2781	2453	2857	2757
Calibration data for y=mx+c :				
constant (c)	8.28	13.21	2.98	7.12
slope (m)	0.087782	0.097537	0.087310	0.088970
r^2	0.999989	0.999990	0.999990	0.999987

r = correlation coefficient.

* This value represents the thermocouple voltage ouput that has been digitised by the ADC.

meter. The calibration of these analysers showed that each voltage output was linear. In order to the automatically monitor the readings a PC was connected to the output of each analyser via a 14-bit ADC interface. The incorporation of formulae based on simple linear regressions into a computer program, as previously demonstrated for the thermocouples, allowed the gas concentrations to be monitored by the PC in real time.

During an analysis the gas concentrations were monitored once a minute and the complete data written to a stored file. Real time monitoring of these evolved gases was achieved by listing their concentrations on a printer.

4.4.2 Investigation of the Integrity of the Automated Gas Analyser System

The ACCG/EGA system was used to analyse a Bickershaw 'Blended Smalls' laboratory coal sample to obtain replicate sets of results. This was carried out to study different aspects of the coal oxidation process and relate coal temperatures to evolution profiles of different gases. Other objectives of this work were to ensure the equipment worked consistently and to study coal oxidation by empirically varying the reaction conditions. This work was important because a compromise in the conditions between two possible extremes had to be obtained. If insufficient coal sample was taken a reduction in the concentration of evolved gases at elevated temperatures may be due to exhaustion of the sample. Alternatively, if the flow-rate

of air carrier gas employed was insufficient a reduction in the concentration of evolved gases at elevated temperatures may be due to exhaustion of the oxygen. Some of the parameters of the oxidation process were constrained by external factors, as discussed in section 4.5.1.

The ACCG/EGA system was also used to analyse different particle sizes of the Bickershaw coal samples in triplicate to study the effect this had upon the coal oxidation process. The particle sizes studied were <211μm and 250-500μm, since equipment was readily available to obtain these particle size fractions ie. coal crushers and sieves.

4.5   Results and Discussions

4.5.1 Investigation of the Integrity of Automated Gas Analyser System

A plot of the oven and coal temperatures monitored during the analysis of the Bickershaw 'Blended Smalls' sample has been illustrated in figure 43. The plot of the oven temperature was linear due to the constant rate of temperature increase (ie. rate of 1°C/min). The coal temperature was monitored in two positions and the temperature profiles were observed to be similar. The temperature of the position nearest to the incoming air carrier gas increased up to 10°C greater than the other position at temperatures up to coal ignition. This was due to the coal oxidising more vigorously at the position of greatest oxygen concentration. This demonstrated that pre-heating the air carrier gas to eliminate cooling effects
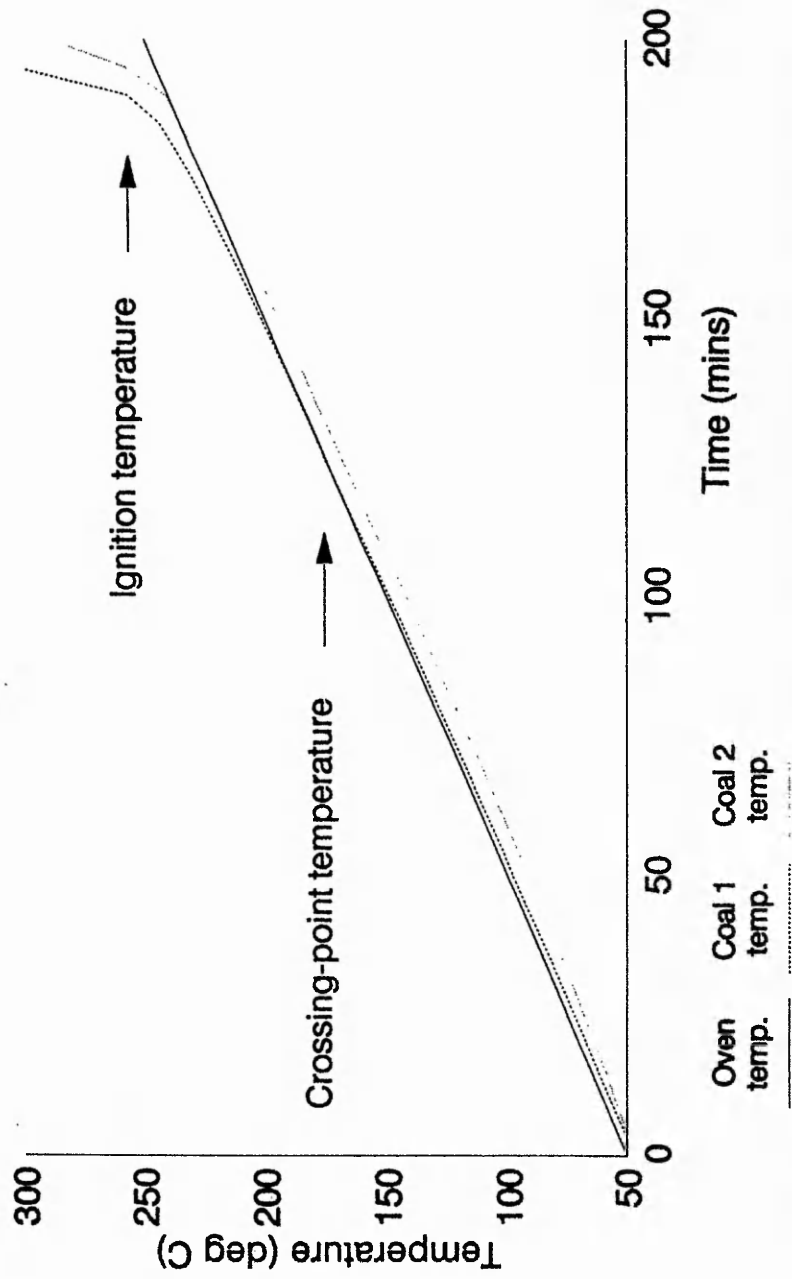
Figure 43 Graph of Temperature Profiles During Coal Oxidation

-168-

was successful. The temperature gradient across the coal body was minimised by limiting the coal sample size to 5g.

The increase of coal bed temperature with time showed a smaller rate of temperature increase relative to the oven up to approximately 90-110°C. This was assumed to be due to endothermic factors such as the specific heat capacity of the coal and the latent heat of vapourisation of water from the coal body. A separate investigation in which coal was dried and the experiment repeated demonstrated that the major factor was inherent moisture in the coal. At higher temperatures the coal bed temperature increased at a rate greater than the oven, which was presumed to be due to the exothermic coal oxidation process. This temperature difference decreased until at a critical point the oven and coal temperature became the same, which has been termed the 'crossing-point' temperature. The coal temperature then increased at an elevating rate until the 'ignition temperature' was attained. At this temperature the coal bed could be seen to glow, and the temperature increased at a faster rate. An upper coal temperature limit of 300°C was placed on the experiment to avoid danger.

The variation of permanent gas concentrations during the oxidation of the Bickershaw 'Blended Smalls' coal sample have been plotted in figure 44. Clearly oxygen was consumed as carbon monoxide and carbon dioxide were produced. It is interesting to relate the crossing-point and ignition temperatures to the gas concentrations in this diagram. These temperatures indicated two distinct stages of the
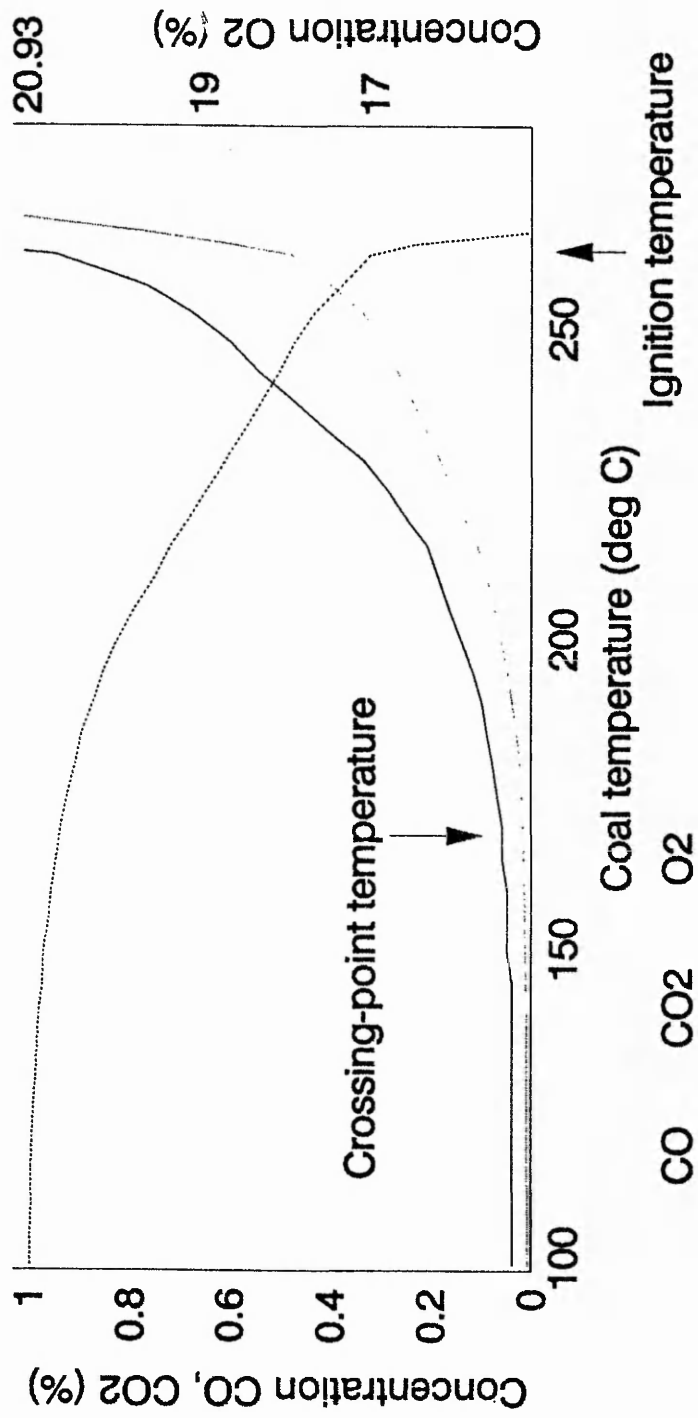
Figure 44 Graph of Permanent Gas Profiles Verse Coal Temperature

coal oxidation process. The onset of an advanced stage of coal oxidation accompanied the crossing point temperature, with an increasingly vigorous evolution of the carbon oxides and an increasing sorption of oxygen as the temperature increased. At the coal ignition temperature the coal oxidation process gave way to combustion, with a subsequent massive increase in reaction rate. Indeed, 5°C after this temperature was attained the concentration of O_2 was reduced to 0.5%, with CO and CO_2 concentrations increased to 5% and 10% respectively.

The Graham ratio (CO/O_2def.) was calculated as described in Chapter 1 (p.32), and its variation with coal temperature was studied. A comparison between the Graham ratio and the evolution of carbon monoxide versus coal temperature has been plotted in figure 45. Both of these functions were clearly exponential, but the ratio increased at a slower rate. It was interesting to note that the ratio increased at lower coal temperatures than the CO concentration. Although this was due to the limited CO concentration scale the Graham ratio clearly provides an excellent indication of the coal oxidation process.

The effects of varying coal oxidation conditions were investigated. A minimum carrier gas flow rate was required to reduce dilution effects upon the gases evolved from the coal oxidation process. However, the evolved gas analysers required a minimum flow rate of 500mls/min to operate successfully. The carrier gas flow rate was thus determined to be 500mls/min.
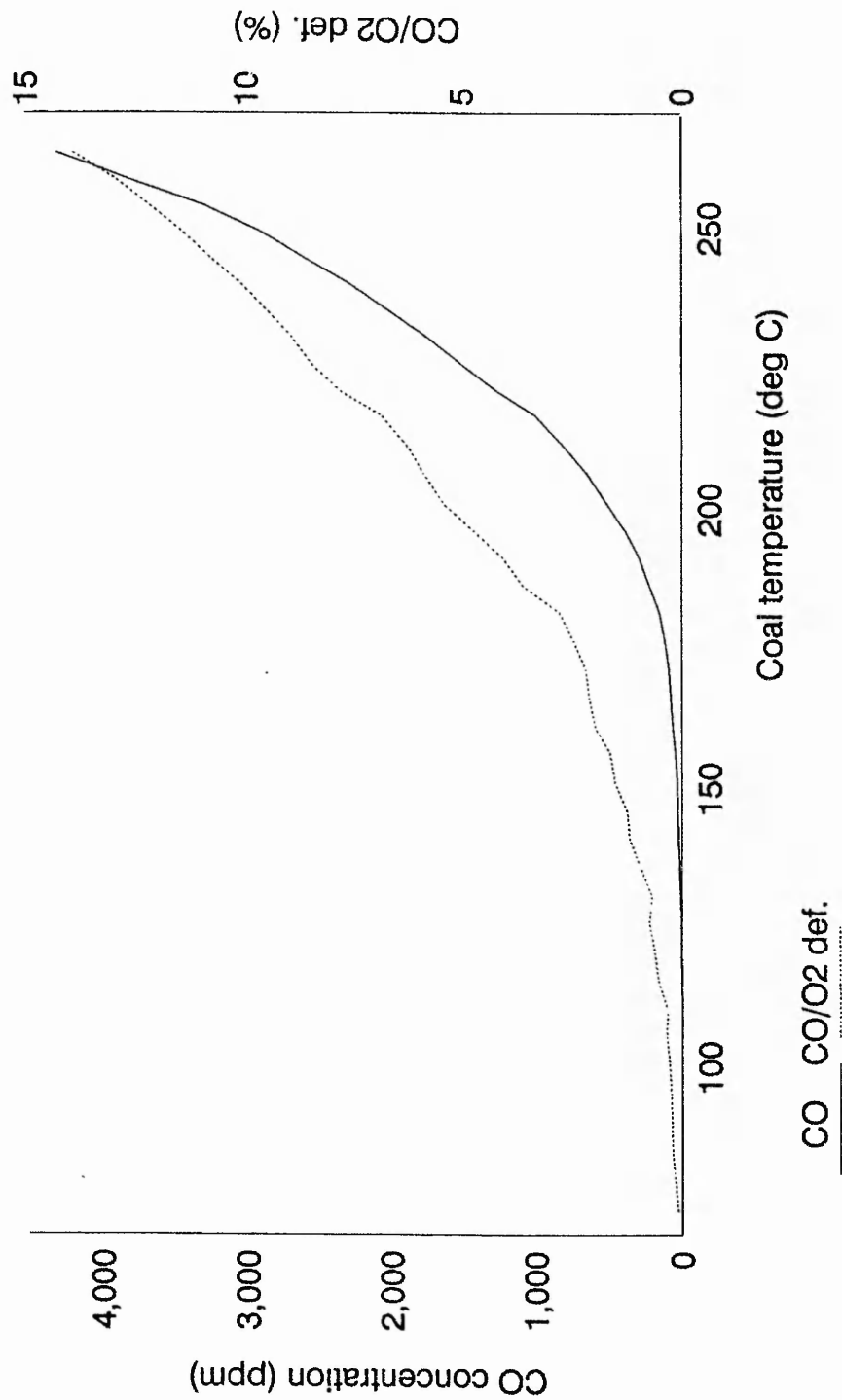
Figure 45   Comparison of CO Production with the CO/O2 def. ratio During Coal Oxidation

The minimum possible rate of coal heating was required to allow a thorough investigation of the oxidation process. This was limited to a rate of 1°C/min by the temperature programming capability of the oven employed.

The coal heating temperature range was determined experimentally. The minimum coal temperature studied was limited by the lowest operating temperature of the oven, which was 50°C. The maximum coal sample temperatures that might typically be expected to be studied were determined by observing figure 43 obtained for the Bickershaw coal sample, and were considered to be 300°C.

The size of the coal sample employed in this work was limited to 5g to minimise the temperature gradient across the coal mass, as discussed earlier in this section.

The analysis of coal samples of different particle size using the ACCG/EGA system were carried out to investigate the effect this had upon coal oxidation. A comparison of the evolution of carbon monoxide from coals of different particle size has been illustrated in figure 46. Clearly the evolution profiles were similar, with the coal sample of smaller particle size reacting at a faster rate. The rate increased relative to the coal of larger particle size at higher temperatures. This was considered to be due to the greater surface area of the smaller particles providing a larger area for the coal to oxidise. The slower oxidation rate of the larger coal particles was to be preferred for this work since it gave a longer time period to study the oxidation process. However, since the specification for
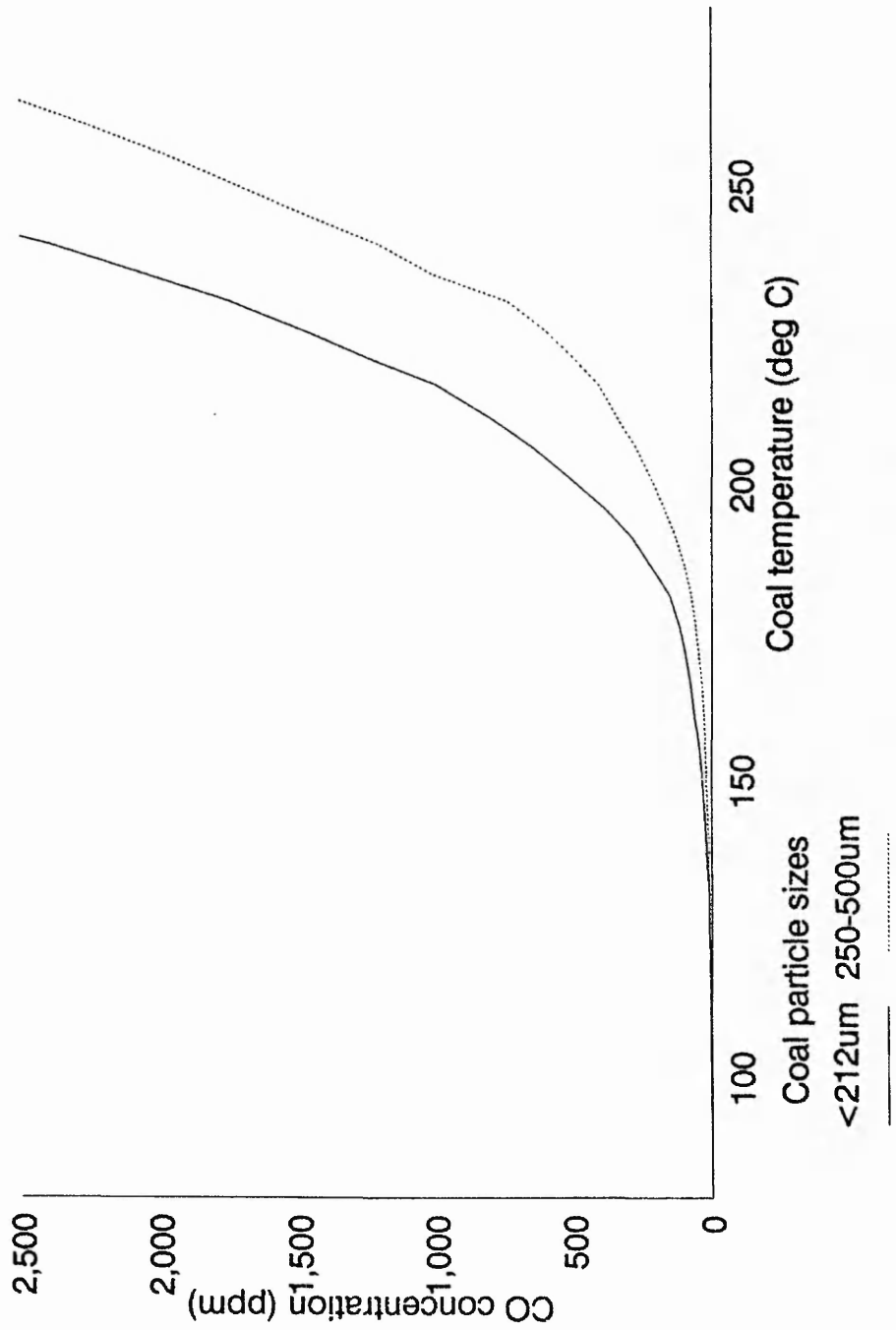
Figure 46   Effect of Particle Size Upon Coal Oxidation

coal analysis according to B.S. 1016 requires coal to be of particle size <212μm (<72mesh) this determined the coal particle size. The use of this size would allow coal samples studied by the ACCG/EGA to undergo full chemical analysis. Additionally, the use of a 250-500μm particle size range would produce a misrepresentative coal sample since excessively small or large particles would not be included.

4.6 Summary of Conclusions

An automated coal oxidation system was constructed which was capable of continuously monitoring specific gas concentrations. The successful development of this equipment was demonstrated by analysing a laboratory coal sample in replicate. These samples allowed coal oxidation conditions to be studied whilst a number of physical parameters were varied. This permitted the optimum analytical conditions used for coal oxidation to be empirically determined and these have been listed in table 16.

**Table 16   Analytical Conditions Used for
Coal Oxidation Work**

Coal particle size < 212μm
Coal sample size = 5±0.001g
Carrier gas flow rate = 500mls/min
Temperature range = 50-300°C
Programmed temperature rate = 1°C/min

CHAPTER 5

PRODUCTS OF DYNAMIC COAL OXIDATION PROCESSES

5.1   Introduction

Equipment for studying the oxidation of coal in a controlled manner was described in Chapter 4. The coal oxidation process includes initiation and propagation of evolved gases similar to those formed during the spontaneous combustion of coal. These gases were analysed for proposed indicators of spontaneous combustion using the GC instrumentation developed in Chapters 2 and 3. This enabled the monitoring of gases associated with the spontaneous combustion of coal to be studied.

The work of Chamberlain et al involved a comprehensive analysis of the gases evolved during the low temperature coal combustion process [55]. These gases were produced in a similar manner but using different conditions to the experimental work described in this chapter. Chamberlain more recently investigated the reactions which possibly occur during this oxidation process [42]. This work has been updated by Gibson, providing information on the evolution of gases formed during coal oxidation [64].

LaCount et al recently investigated sulphur in coal by a programmed temperature oxidation process [163]. They concluded that three distinct SO_2 evolution maxima occurred at 320, 430 and 480°C. These were correlated with the oxidation of sulphur in non-aromatic organic structures,

pyrites and aromatic structures respectively.

Gorbaty et al used X-ray absorption near edge structure (XANES) spectroscopy and X-ray photoelectron spectroscopy (XPS) to study the chemistry of organically bound sulphur in coal during mild oxidation [164]. These techniques indicated that organically bound sulphide sulphur becomes oxidised more readily than thiophenic sulphur, in agreement with LaCount et al. It would therefore be interesting to relate the evolution profiles of sulphur gases produced in this work to the forms of sulphur which exist in the coal samples studied.

The different combustion characteristics of macerals suggest that the petrographic composition of coal may be used as an indication of its ease of combustion [165,166]. It has been suggested that vitrinite and exinite promote ignition, with exinite producing an especially low ignition temperature [167]. A comparison of the crossing point temperature and petrographic composition of the coal samples studied in this work would therefore be interesting.

5.2 Equipment

Equipment as described in chapters 2,3 and 4.

Raymond laboratory grinding mill (Christison Scientific Equipment Ltd., East Gateshead Ind. Est., Gateshead.)

Endicotts brass analytical sieves to B.S.410; sizes 212, 250, 500μm. (Christison Scientific Equipment)

5.3   Chemicals and Reagents

Gas standards as described in chapters 2 and 3 were employed for the calibration of gas analysers and GC equipment.

5.4   Experimental

5.4.1 Preparation of Coal Samples

Samples of virgin coal strata were taken from a number of collieries and transported to the laboratory in the form of large sections (typical volume ca. 20cm x 20cm x 20cm). These samples were prepared and analysed in a matter of days to reduce the oxidation effects of ambient air. They were transported in the form of large sections and prepared by crushing on the day of analysis to minimise the desorption of gases from the coal. Samples were taken from the following seams of six collieries :-

   (i) Haigh Yard seam, Bickershaw colliery.

  (ii) YardRagman seam, Hem Heath colliery.

 (iii) YardRagman seam, Florence colliery.

  (iv) Barnsley seam, Rossington colliery.

   (v) Barnsley seam, Whitemoor colliery.

  (vi) Parkgate seam, Asfordby colliery.

The preparation of each sample involved manually breaking the coal into pieces and removing the external areas of relatively aged coal. This was followed by grinding the coal in a Raymond mill, then passing it through a $212\mu m$ (B.S. 72 mesh) sieve. A quantity of the sample was then removed by the method of coning and

quartering for chemical analysis, which was carried out according to the specifications of method B.S.1016 [168]. Additionally, some of the coal sample was passed through a 500μm sieve and collected on a 250μm sieve. This provided a quantity of coal for petrographic analysis, of size range 250-500μm [19].

A number of coal samples required a different sample preparation process in order to allow the desorption of gases to be studied. This involved subsampling a 40g coal lump from within the body of the large section of coal as described by Creedy [169].

5.4.2 Study of Coal Desorption Products

The method of Creedy was used to grind a coal sample under an atmosphere of nitrogen in a gas-tight container [169]. This involved placing a 40g coal lump in a brass mill barrel which contained several grinding rings. The gas-tight brass vessel was then pressurised to 0.5 bar above atmospheric pressure using nitrogen. The container was then placed in a grinding apparatus for 30 minutes to achieve a reduction in coal particle size to 50μm. This grinding action caused the release of gases desorbed within the coal structure. A gas-tight syringe was used to extract a sample of the gas mixture desorbed from the coal by opening a valve on the brass vessel. Although this method was developed by Creedy to evaluate methane gas emissions, a comprehensive analysis of the desorbed gases was achieved in this work by GC.

Coal samples taken from Hem Heath and Rossington were prepared in the manner described and the desorption products analysed.

5.4.3 Study of Dynamically Heated Coal Products

Initially each coal sample was prepared according to section 5.4.1, after which it was placed in the oven of the ACCG/EGA system described in chapter 4. This was then maintained at 50°C for 20 minutes to allow the gases produced in the range ambient to 50°C to dissipate. The oven temperature was then increased at 1°C/min up to the temperature at which ignition of the coal bed occurred. The conditions under which the ACCG/EGA system was operated have been listed in table 16.

During the coal heating experiment samples of evolved gases were regularly extracted using a gas-tight syringe by controlling the taps illustrated in figure 40. These gas samples were then analysed using the GC techniques described in chapter 2. The frequency of sampling was determined by the length of time taken by a GC analysis. Automation of the ACCG/EGA system enabled the researcher to carry out the GC analyses simultaneously.

The six coal samples listed in section 5.4.1 taken from different collieries were individually studied to ensure adequate repeatability of the experiment. Each coal sample was investigated three times using air as the carrier gas. The experiment was also repeated using nitrogen carrier gas in the ACCG/EGA system in order to study the coal

desorption products.

5.5   Results and Discussions

5.5.1 Analysis of Coal Samples

Chemical analysis and maceral composition of the coal samples have been listed in table 17. The chemical analysis was carried out according to method B.S. 1016 and the maceral composition was determined according to method B.S. 6127 [168,19]. These coal samples clearly provided a good cross-sectional representation since their compositions varied considerably. However, the results only apply to the specific coal samples transported to the laboratory for this work. They do not necessarily correspond to typical commercial data, since the sampling protocol for that work could not be followed. The reason was the relatively small sample size of the block of coal used in this work as compared to the 350kg sample which may be taken for routine coal analysis, according to B.S.1017 [170].

Table 17   The Chemical and Petrographic Analysis of Coal Samples Used for Coal Oxidation Work

SAMPLE DETAILS	Colliery Seam	Bickershaw Haigh Yard	Hem Heath YardRagman	Florence YardRagman	Rossington Barnsley	Whitemoor Barnsley	Asfordby Parkgate
CHEMICAL ANALYSIS	Moisture (%)	1.9	2.1	4.6	8.5	3.9	11.5
	Ash (%)	2.6	4.6	3.8	2.8	3.3	8.2
	Volatile (%)	30.8	34.3	32.3	29.6	32.0	31.2
	Calorific Value (kJ/kg)	30,910	32,100	31,340	30,450	32,120	26,220
	Chlorine (%)	0.51	0.63	1.06	0.81	0.46	0.32
	Total Sulphur (%)	2.12	1.16	0.51	0.48	1.18	1.10
FORMS OF SULPHUR	Pyritic Sulphur (%)	1.64	0.10	0.07	<0.01	0.11	0.65
	Sulphate Sulphur (%)	0.01	<0.01	<0.01	<0.01	0.01	0.01
	Organic Sulphur (%)	0.45	1.06	0.44	0.48	1.06	0.44
PETROGRAPHIC ANALYSIS	Vitrinite (%)	83.0	82.3	80.2	19.6	83.6	67.4
	Exinite (%)	5.6	4.4	4.0	24.2	5.4	7.0
	Inertinite (%)	8.6	11.0	13.4	56.2	10.2	20.4

5.5.2 Analysis of Coal Desorption Products

Analyses of gases desorbed from the Rossington and Hem Heath coal samples have been illustrated in table 18. The mixture of desorbed gases was also analysed for the species listed below :-

ethene, propene, benzene, toluene, xylenes,

carbonyl sulphide, hydrogen sulphide, sulphur dioxide, acetone, acetaldehyde, methanol and ethanol.

These gases were found to be below the limits of detection of the GC equipment used.

The aliphatic hydrocarbons listed in table 18 illustrate that after 2 hours the gas desorbed from coal was predominantly methane (90-95%). The large proportion of this gas was due to the relatively rapid desorption rate of methane as compared to the other aliphatic hydrocarbons. It has been accepted that methane equilibration is reached within two hours [210].

It is interesting to compare the composition of the gas desorbed from the Hem Heath coal 2 hours after grinding with the composition 12 hours after grinding, as illustrated in table 18. During this period composition of the desorbed gas changed from being predominantly methane to being a mixture of methane and ethane. This can be explained in terms of the methane being totally desorbed after equilibration (2 hours). The equilibration period for the other hydrocarbons is related to their desorption rates and would therefore be expected to be proportional to the geometry of the molecule. Hence, the concentration of

-184-

Table 18   Analysis of Gases Desorbed from Coal Samples

Coal Samples / Analyte	Rossington Barnsley seam (A)		Hem Heath YardRagman seam (A)		(B)	
	Conc. (ppm)	Composition (%)	Conc. (ppm)	Composition (%)	Conc. (ppm)	Composition (%)
methane	168,900	94.4	217,800	92.8	69,600	84.9
ethane	7,820	4.4	14,570	6.2	10,200	12.4
propane	1,850	1.0	2,240	1.0	1,950	2.4
i-butane	160	<0.1	90	<0.1	75	0.1
n-butane	90	<0.1	65	<0.1	85	0.1
i-pentane	<5	<0.1	<5	<0.1	25	<0.1
n-pentane	<5	<0.1	<5	<0.1	15	<0.1

(A) – Sample analysed after 2 hours.
(B) – Sample analysed after 12 hours.

Note: i-butane has IUPAC nomenclature methylpropane.
      i-pentane has IUPAC nomenclature 2-methylbutane.

ethane decreases between 2 and 12 hours since a proportion of it will have been desorbed. From 2 to 12 hours the concentrations of other hydrocarbons decreased relatively less than the other hydrocarbons because they have longer equilibration periods.

This study of desorption of gases from coal allows a perspective of mine air composition to be taken. Typically the ratio of methane:ethane is approximately 25:1 in a mine air, but 10:1 in the coal body. These differences may be explained in terms of renewable hydrocarbon sources coming from coal surfaces being freshly exposed as the coal face progresses. Since methane has a faster desorption rate than the other hydrocarbons it preferentially enriches the mine atmosphere. Clearly if the coal mining process was halted for a significant time this would allow the relative concentrations of other hydrocarbons to increase up to the proportions present in the coal.

The absence of gases other than aliphatic hydrocarbons from the desorbed gas mixture during this work does not necessarily imply that other desorption products do not occur. It is clear that these gases may require prolonged equilibration periods compared with the time intervals monitored in this work. Additional information on desorption products is discussed in section 5.5.4.

5.5.3 Studies of Temperature Profiles During Coal Heating

The work carried out in chapter 4 demonstrated that the crossing-point temperature of each coal may be determined

by monitoring coal and oven temperatures during the coal oxidation process. The relative reactivity of each of the coal samples studied was therefore determined by measuring the crossing-point temperature. These measurements were carried out during the studies of gases evolved from heated coal samples and have been listed in table 19. Clearly the most reactive coal studied was the sample from Rossington, with the Whitemoor and Hem Heath samples being relatively inert. However, these samples all represent a group of British coals which are particularly reactive.

Chapter 4 discussed the effect that high coal moisture contents had upon the crossing-point temperature measurement. Table 17 illustrates that the two most reactive coals, Rossington and Asfordby, have a relatively high moisture content which has the effect of artificially increasing the crossing-point temperatures. These two coals are therefore relatively more reactive than the results indicated in table 19.

An interesting relationship was observed between the exinite composition of the coal (table 17), and its crossing-point temperature. This has been illustrated in figure 47, which plots these two variables on the x and y axes. It is therefore clearly apparent that a measure of the reactivity of coal is given by its exinite composition.

These results provide an indication of the liability of a coal to spontaneously combust. They correlate well with the historical events at 5 of the collieries (ie. the reactivity of the Barnsley seam at Rossington is well
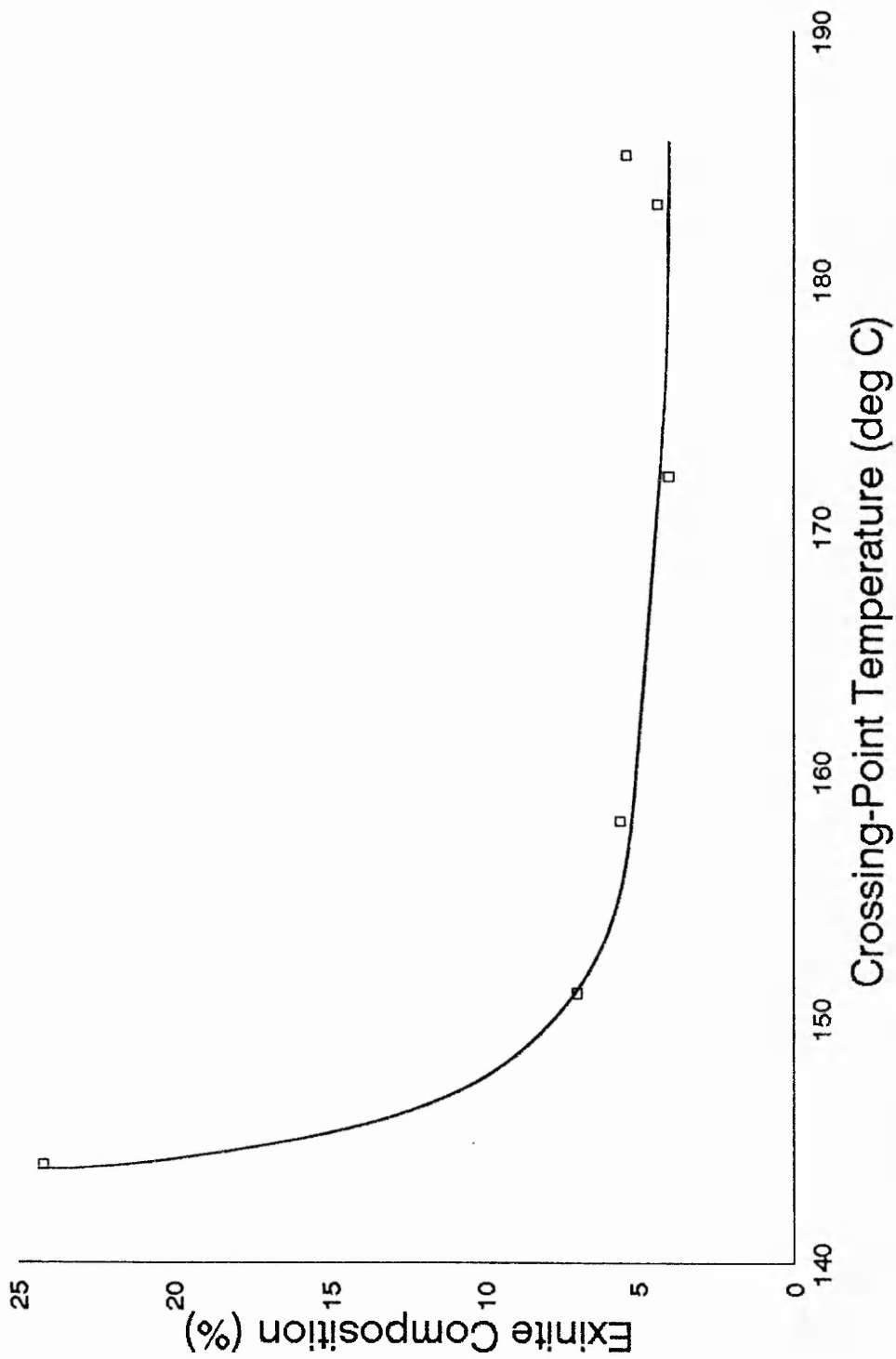
Figure 47 Graph of Crossing-Point Temperature Versus Exinite Composition of Coal Samples

known). A productive coal face has not yet been opened at Asfordby colliery, but the results obtained from coal samples taken from the seam to be mined indicate that the colliery could have problems with spontaneous combustion. Therefore the colliery has been fitted with extensive monitoring equipment.

Table 19   Crossing-Point Temperatures of Coal Samples

Colliery	Seam	Crossing-Point Temperature (°C)
Bickershaw	Haigh Yard	158
Hem Heath	YardRagman	183
Florence	YardRagman	172
Rossington	Barnsley	144
Whitemoor	Barnsley	185
Asfordby	Parkgate	151

5.5.4 Gases Evolved From Dynamically Heated Coals

The monitoring of evolved gas concentrations during the coal heating process resulted in the accumulation of large quantities of data. Typical evolution profiles of these gases are illustrated in a graphical format :-

BICKERSHAW (Haigh Yard)...figures 48.1-48.3, p198-200.

HEM HEATH (YardRagman)....figures 49.1-49.3, p201-203.

FLORENCE (YardRagman).....figures 50.1-50.3, p204-206.

ROSSINGTON (Barnsley).....figures 51.1-51.3, p207-209.

WHITEMOOR (Barnsley)......figures 52.1-52.3, p210-212.

ASFORDBY (Parkgate).......figures 53.1-53.3, p213-215.

The evolution profiles of gases formed from heated coal using oxygen free nitrogen carrier gas have also been plotted in these diagrams. These profiles correspond to coal desorption products due to the absence of oxygen.

The experimental data shows that the oxidation process in some coals did not produce the full range of evolved gases. The upper temperature studied was limited by ignition of the specific coal sample in the ACCG/EGA apparatus.

The profiles of gases evolved from each of the coals were reasonably similar, allowing for the different ranges plotted for each coal. However, the time between the sampling and analysis of the Asfordby sample may account for the lower results obtained for this coal sample.

Although the profiles of the aliphatic hydrocarbons were similar, the specific concentrations varied for different coal samples. These gases were clearly desorption products

as indicated by their production when coal samples were heated using nitrogen carrier gas. Furthermore, similar gas concentrations were produced using air or nitrogen carrier gas, indicating that coal oxidation does not itself produce aliphatic hydrocarbons.

The concentration differences for individual coals were considered to be due to different quantities of gas being desorbed from the coals prior to analysis. The work carried out in section 5.5.2 demonstrated that different coals desorb differing concentrations of aliphatic hydrocarbons within a few hours at room temperatures. Although this work involved dynamically heating the coal samples, it is clear that the evolution of gases would be affected by time delays of hours duration.

A relationship appears to exist between the maximum evolution temperature and the geometry of the hydrocarbon gas molecule evolved. This is in keeping with the observation that these evolved gases are desorption products.

The profiles of aromatic compounds evolved from heated coals were dependent upon the carrier gas employed in the experiment.

The evolution profiles of benzene using air carrier gas increased with increasing coal temperature. This suggested that benzene may represent a useful indicator of the coal oxidation process. However, for some other coals the evolution profile peaked at a certain temperature and decreased thereafter. Also, a reduced concentration of

benzene was produced when coal samples were heated using nitrogen carrier gas. This suggested that benzene is both a desorption and oxidation product of heated coal.

Toluene was the most abundant aromatic compound evolved. The gas profile increased, reached a maximum and decreased as the temperature increased using air or nitrogen as the carrier gas. The concentrations of toluene produced using both carrier gases was similar, indicating that it was a desorption product.

The evolution profiles of o-xylene and m-/p-xylene were similar. However, concentrations were significantly lower than toluene indicating that the xylenes were also desorption products.

The unsaturated hydrocarbons studied could be divided into alkenes and alkynes in terms of their evolution profiles. Ethene and propene demonstrated an increasing concentration with coal temperature using air carrier gas. The use of nitrogen carrier gas produced neither of these gases. This demonstrated that ethene and propene were products of coal oxidation, and represent useful indicators of spontaneous combustion.

Ethyne and propyne were not detected using either air or nitrogen carrier gas during the coal oxidation experiments. Therefore they could clearly not be considered as useful spontaneous combustion indicators. However, during the course of this work these gases were detected at coal temepratures in excess of the ignition temperature. This suggests that studying these gases may represent a useful

technique of monitoring a mine fire situation which has reached an advanced stage.

Discussion of the evolution of oxygenated gases requires consideration of the analyte detection limits by GC, as shown earlier in table 14 (p.153). The use of nitrogen carrier gas produced no oxygenated gases from heated coal, indicating that these gases were not desorption products.

The concentrations of acetaldehyde and acetone increased at increasing coal temperatures using air carrier gas. These gases therefore represent useful indicators of spontaneous combustion, since they are clearly products of coal oxidation. Both gases are equally useful because acetaldehyde is produced in concentrations four times greater than acetone, but the analytical limits of detection for acetone are five times better than acetaldehyde. Methanol and ethanol could not be detected during these experiments due to the poor detection limits listed in table 14.

No general trend in the evolution of sulphur gases during the coal heating process was observed, since each sulphur compound was produced in a different manner. Carbonyl sulphide was not evolved during the heating of coal using nitrogen as the carrier gas. However, when air was employed coal temperature increases were accompanied by increases in the evolution of carbonyl sulphide. This suggested that carbonyl sulphide represents a useful indicator of spontaneous combustion since it is clearly a coal oxidation product.

Sulphur dioxide was evolved from all heated coals when air was used as the carrier gas, and it was evolved from some of the coals when nitrogen was used. Sulphur dioxide is therefore an oxidation and desorption product and would not represent a useful indicator of spontaneous combustion. Hydrogen sulphide was only evolved from the heated Bickershaw coal sample when using nitrogen carrier gas.

The evolution of sulphur gases observed has been correlated with the forms of sulphur that exist in the coal samples studied. A complete analysis of the forms of sulphur in the coal samples studied is listed in table 17. Clearly the evolution of carbonyl sulphide was not affected by the sulphur content of the coals studied. However, a good correlation exists between the quantity of pyritic sulphur and the evolution of sulphur dioxide when the coal was heated using nitrogen as the carrier gas. This may be further extended to the evolution of hydrogen sulphide since the Bickershaw coal sample contains a greater concentration of pyritic sulphur than the other coals studied. The evolution of sulphur dioxide using air as the carrier gas appeared to be related to the organic sulphur content of the coal, with the exception of the Hem Heath and Asfordby samples. Other work carried out by LaCount et al could not be studied here since the speciation of organic sulphur into aromatic and non-aromatic forms was not carried out in this work [163].

Sulphur dioxide and hydrogen sulphide were evolved at much greater concentrations after the coal samples exceeded

-194-

their ignition temperatures. A detailed study of this was not carried out because it involved temperatures in excess of those studied in this work.

The evolved gases may be classified into groups according to the mechanism of their formation processes, (ie. oxidation or desorption) depending whether they were produced using air or nitrogen carrier gas respectively. A summary of the results and usefulness of the gases as indicators of spontaneous combustion are shown in table 20.

Other gases were also observed during these studies. Hydrogen was typically detected at low ppm levels when CO concentrations exceeded 400ppm, approaching levels of 20-30ppm when CO attained concentrations of 5000ppm. However, when the coal ignited during this work the levels of hydrogen increased significantly (ca. 200ppm).

Table 20   Classification of Evolved Gases Studied

CLASSIFIED GROUP	EVOLVED GAS	DESORPTION PRODUCT	OXIDATION PRODUCT	USE AS AN INDICATOR
Aliphatic Hydrocarbons	methane	YES	YES	NO
	ethane	YES	NO	NO
	propane	YES	NO	NO
	i-butane	YES	NO	NO
	n-butane	YES	NO	NO
	n-pentane	YES	NO	NO
Unsaturated Hydrocarbons	ethene	NO	YES	YES
	propene	NO	YES	YES
	ethyne	NO	NO	NO
	propyne	NO	NO	NO
Aromatics	benzene	YES	YES	NO
	toluene	YES	NO	NO
	xylenes	YES	NO	NO
Sulphur Gases	hydrogen sulphide	YES	YES	NO
	carbonyl sulphide	NO	YES	YES
	sulphur dioxide	YES	YES	NO
Oxygenated Gases	carbon monoxide	NO *	YES	YES
	carbon dioxide	NO	YES	YES
	acetaldehyde	NO	YES	YES
	methanol	NO	NO	NO
	ethanol	NO	NO	NO
	acetone	NO	YES	YES

* Carbon monoxide is desorbed from heated coal using nitrogen
  carrier gas if the coal is aged, due to the oxidation of the
  carbon and its subsequent adsorption onto the surface structure.

Note: i-butane has IUPAC nomenclature methylpropane.

5.6   Summary of Conclusions

The production of a range of gases was studied during the heating of several coal samples under carefully controlled conditions. The evolution profiles of these gases allowed their use as indicators of spontaneous combustion to be determined. These results demonstrated that ethene, propene, carbonyl sulphide, carbon monoxide, carbon dioxide, acetaldehyde and acetone represent useful indicators of spontaneous combustion.
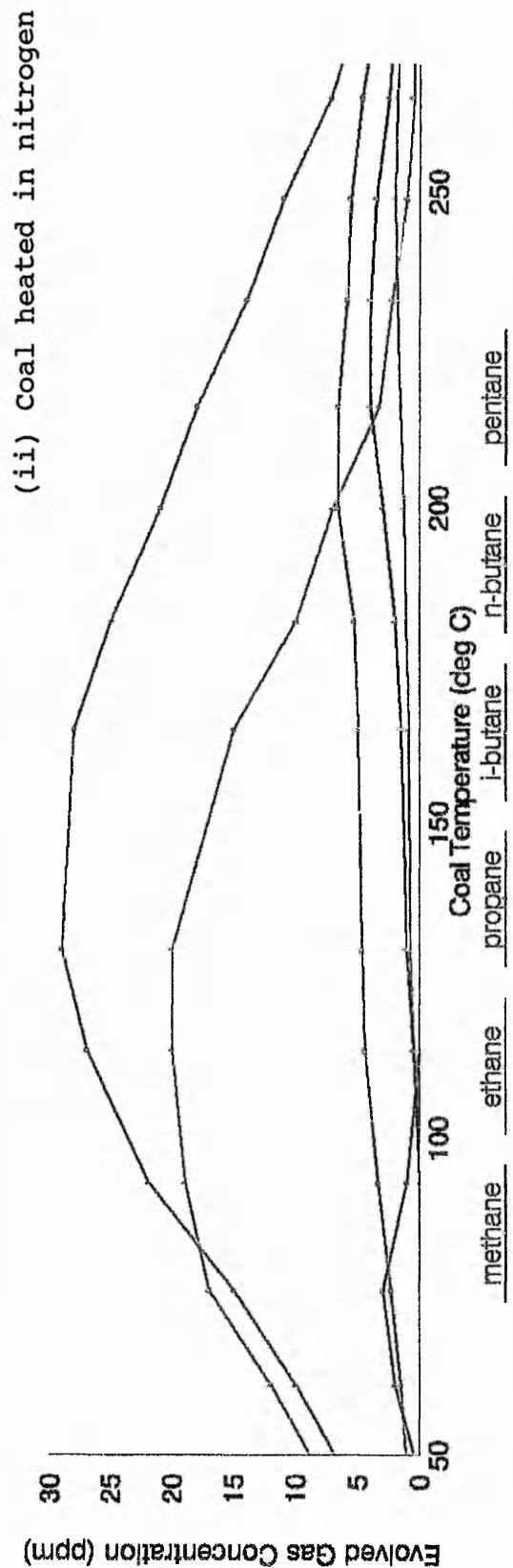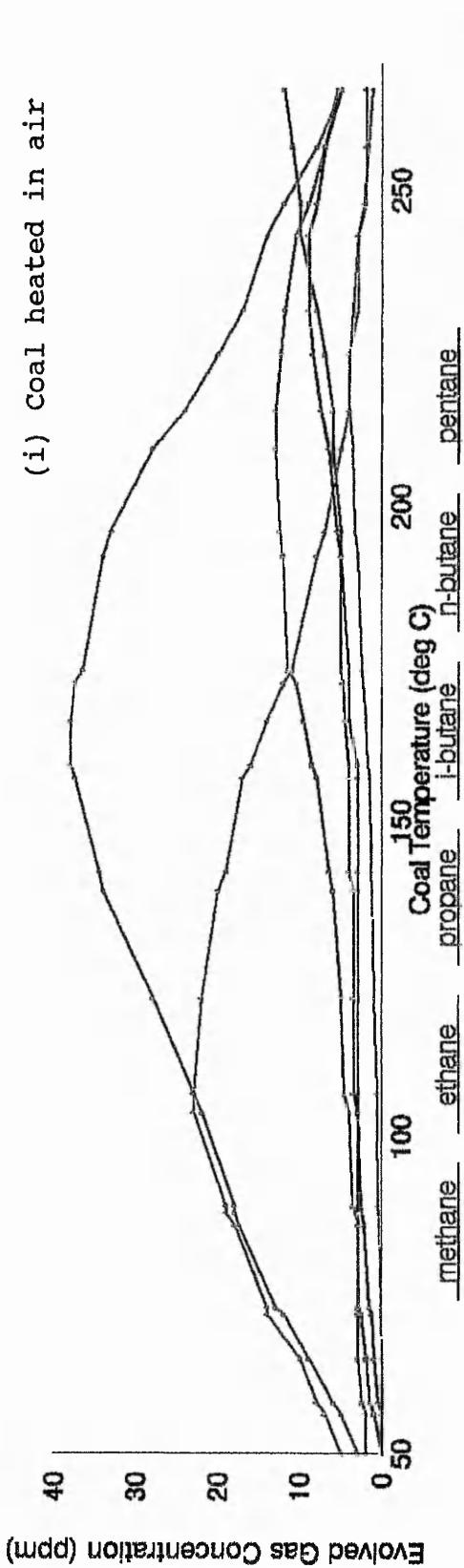
Figure 48.1 Gas Evolution Profiles from Heated Coal - Bickershaw (Haigh Yard)
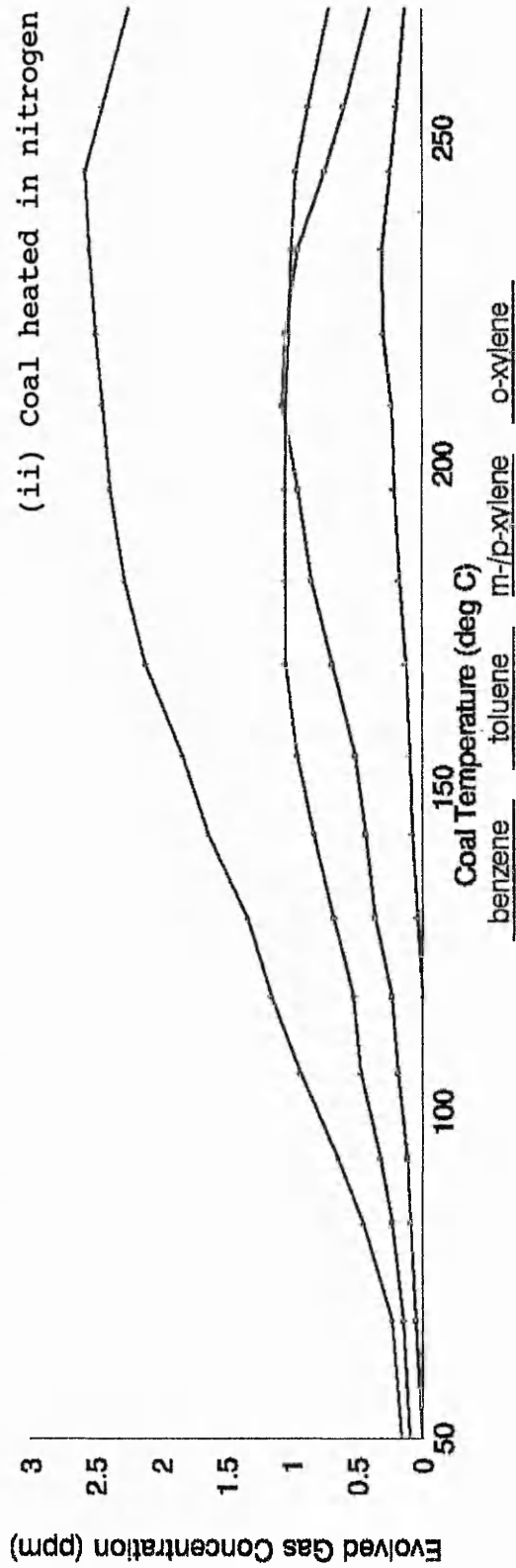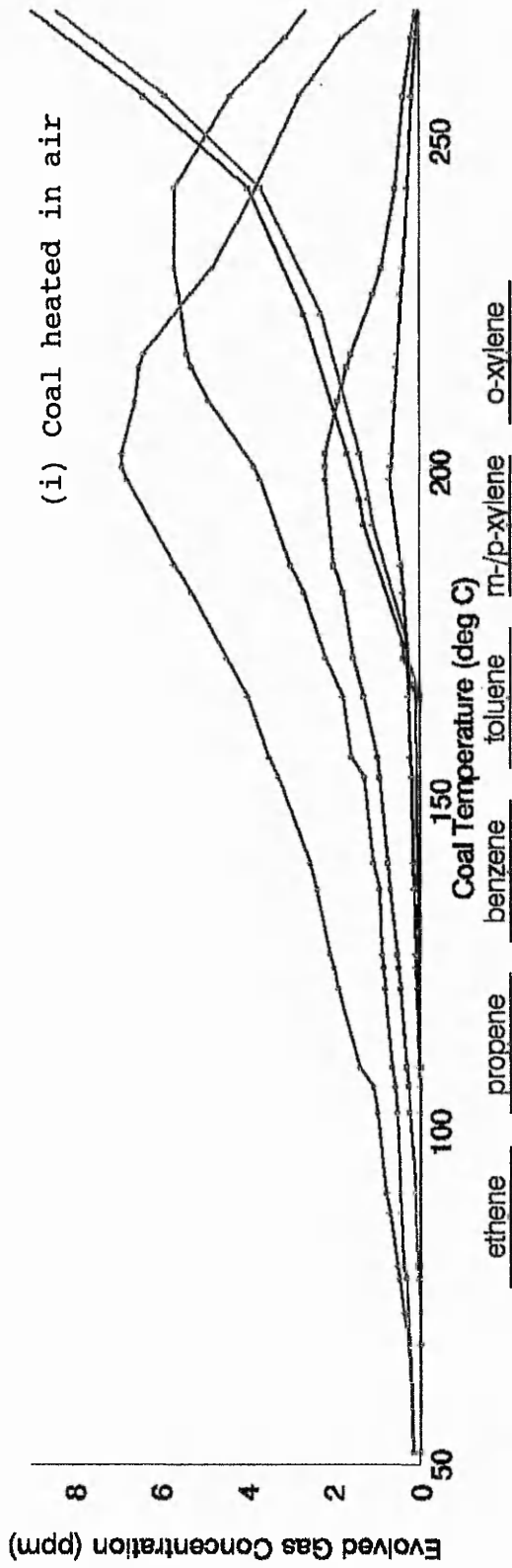
Figure 48.2 Gas Evolution Profiles from Heated Coal - Bickershaw (Haigh Yard)
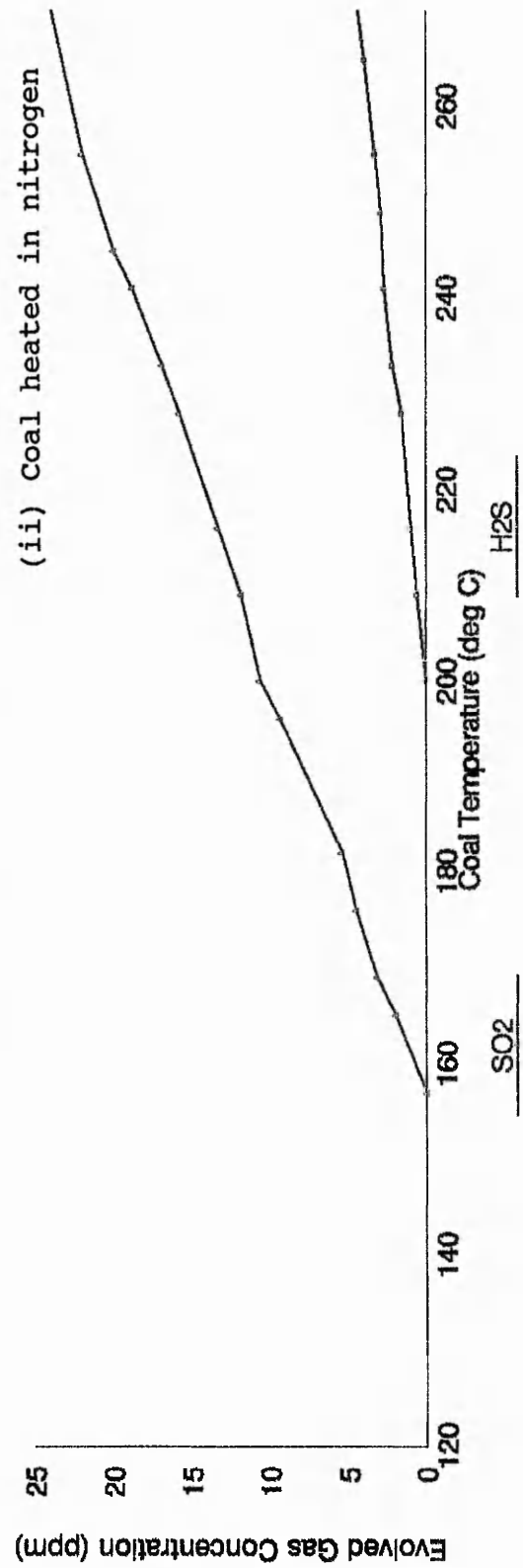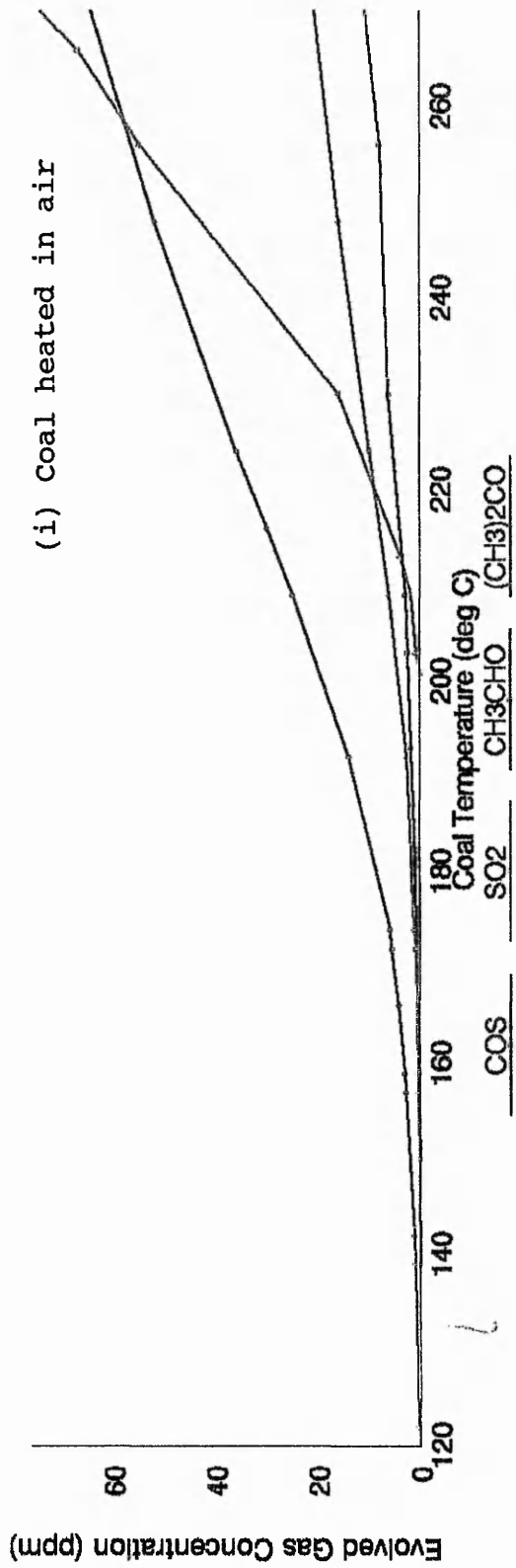
Figure 48.3 Gas Evolution Profiles from Heated Coal - Bickershaw (Haigh Yard)
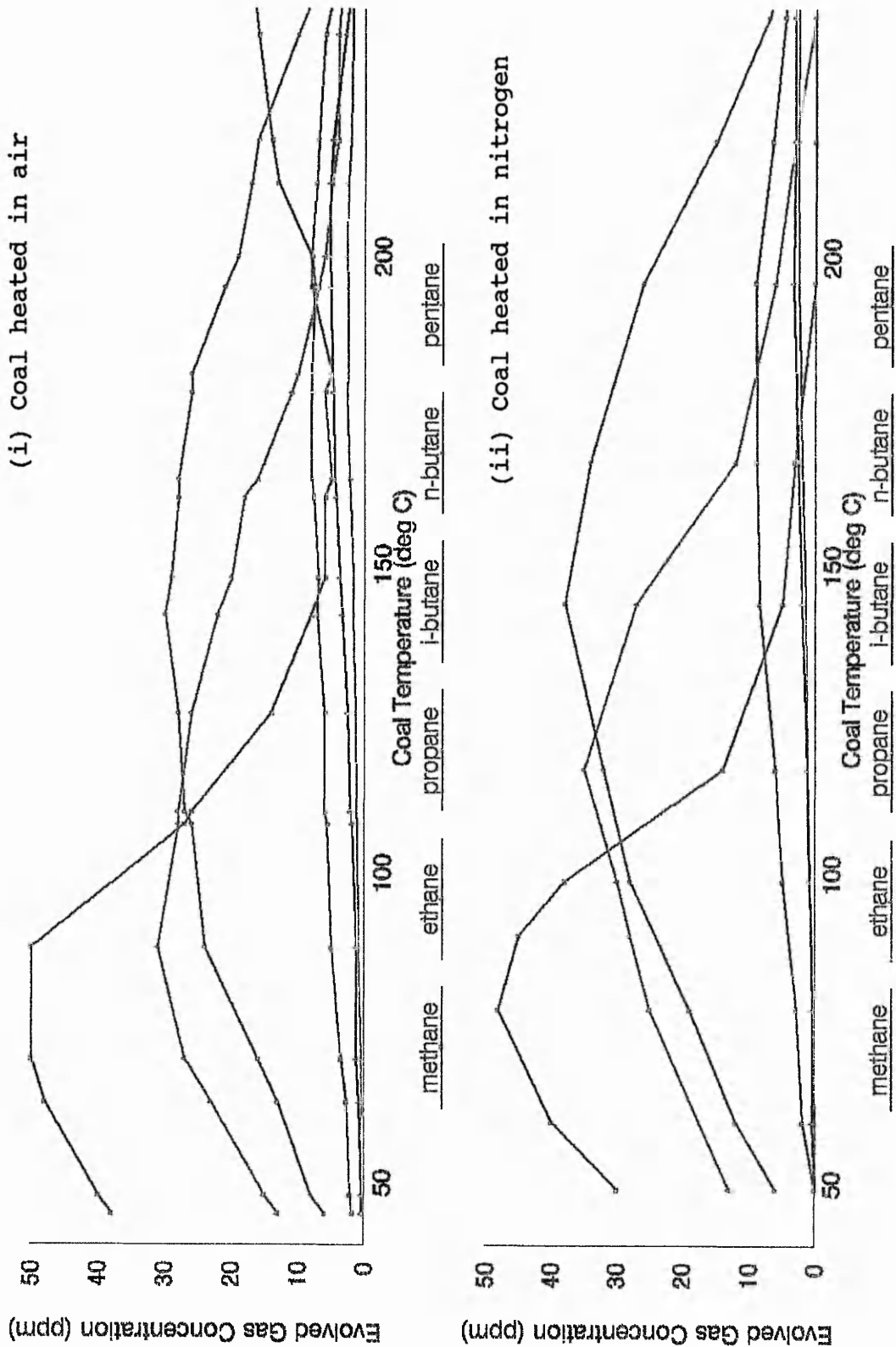
Figure 49.1 Gas Evolution Profiles from Heated Coal - Hem Heath (YardRagman)

(i) Coal heated in air

(ii) Coal heated in nitrogen

ethene   propene   benzene   toluene   m-/p-xylene   o-xylene
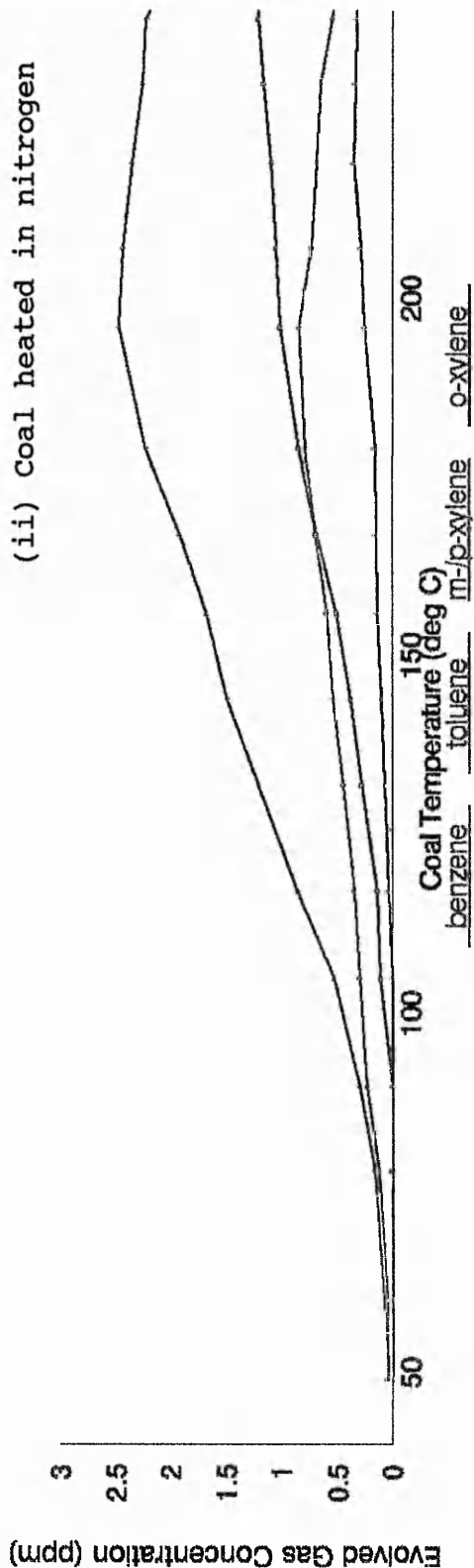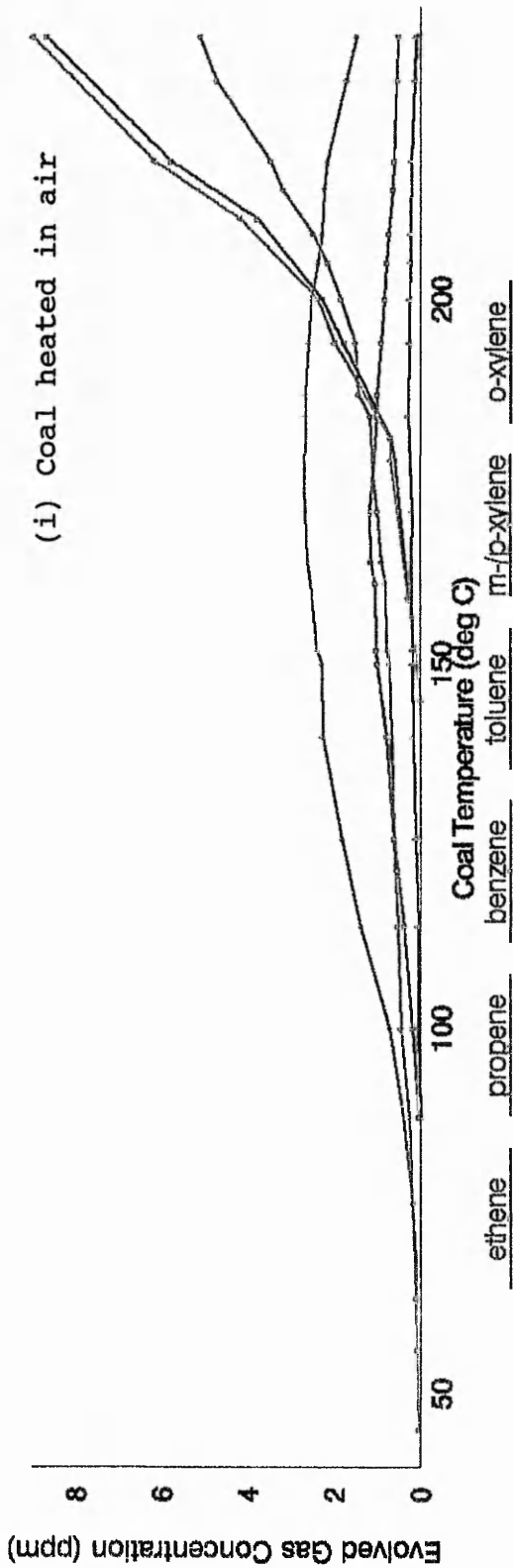
Figure 49.2   Gas Evolution Profiles from Heated Coal – Hem Heath (YardRagman)

(i) Coal heated in air

Evolved Gas Concentration (ppm)

Coal Temperature (deg C)

COS   SO2   CH3CHO   (CH3)2CO
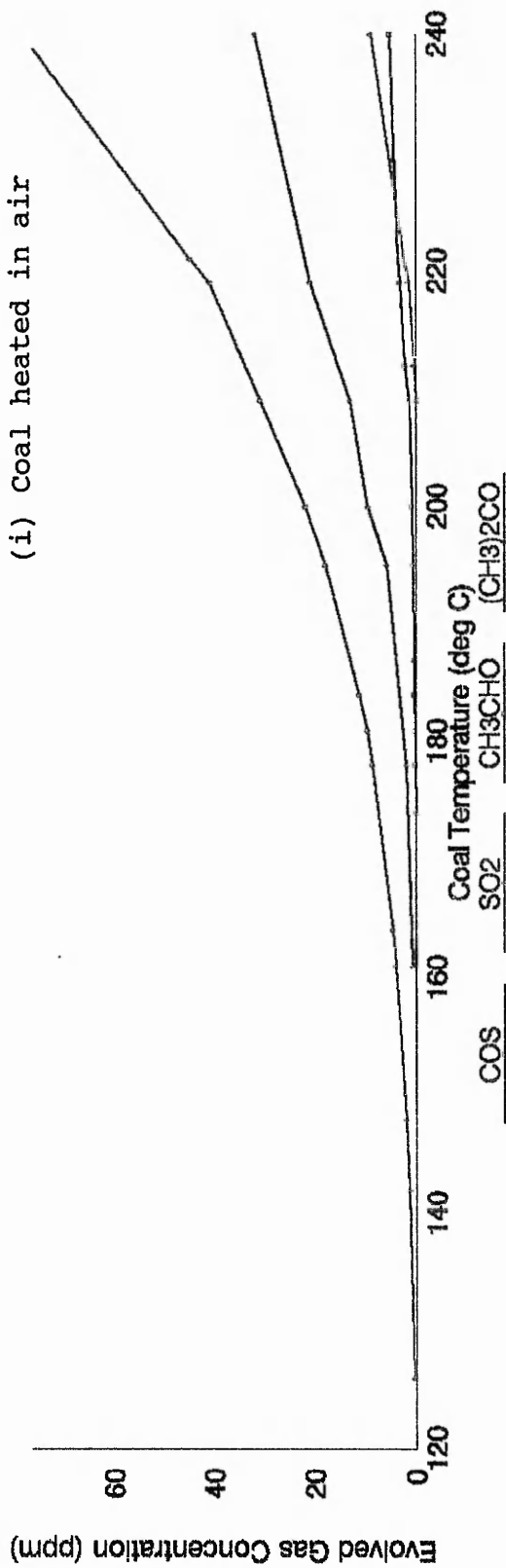
Figure 49.3   Gas Evolution Profiles from Heated Coal - Hem Heath (YardRagman)

(i) Coal heated in air

(ii) Coal heated in nitrogen
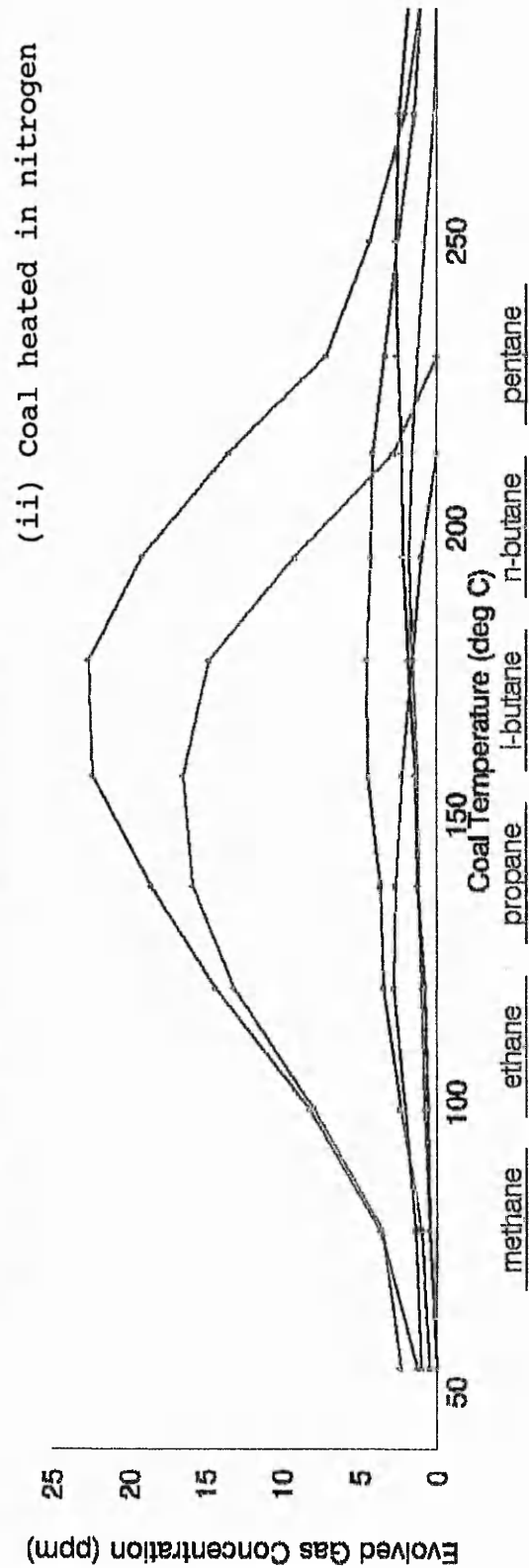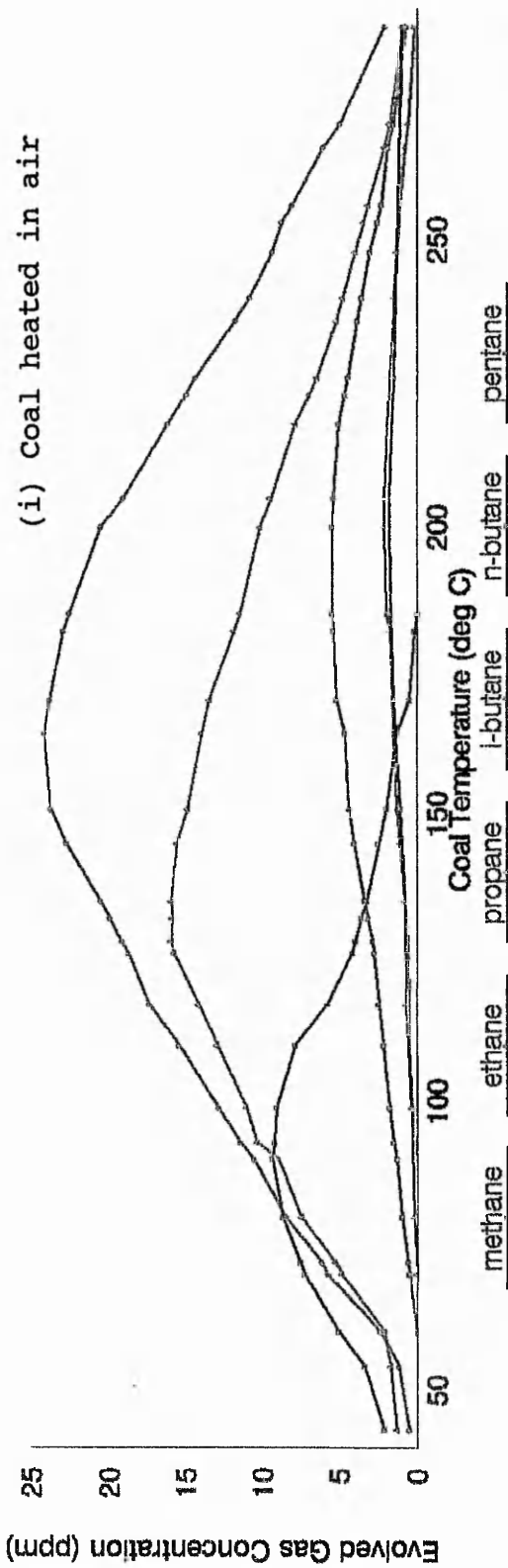
Figure 50.1 Gas Evolution Profiles from Heated Coal - Florence (YardRagman)

-204-

(i) Coal heated in air

(ii) Coal heated in nitrogen
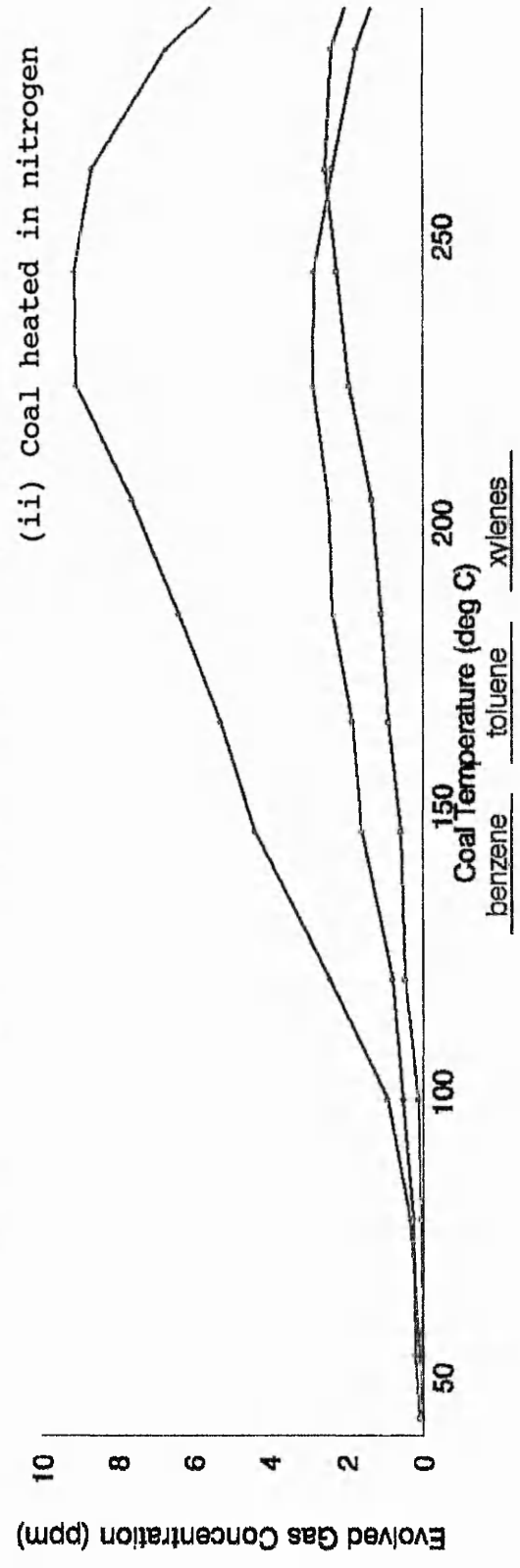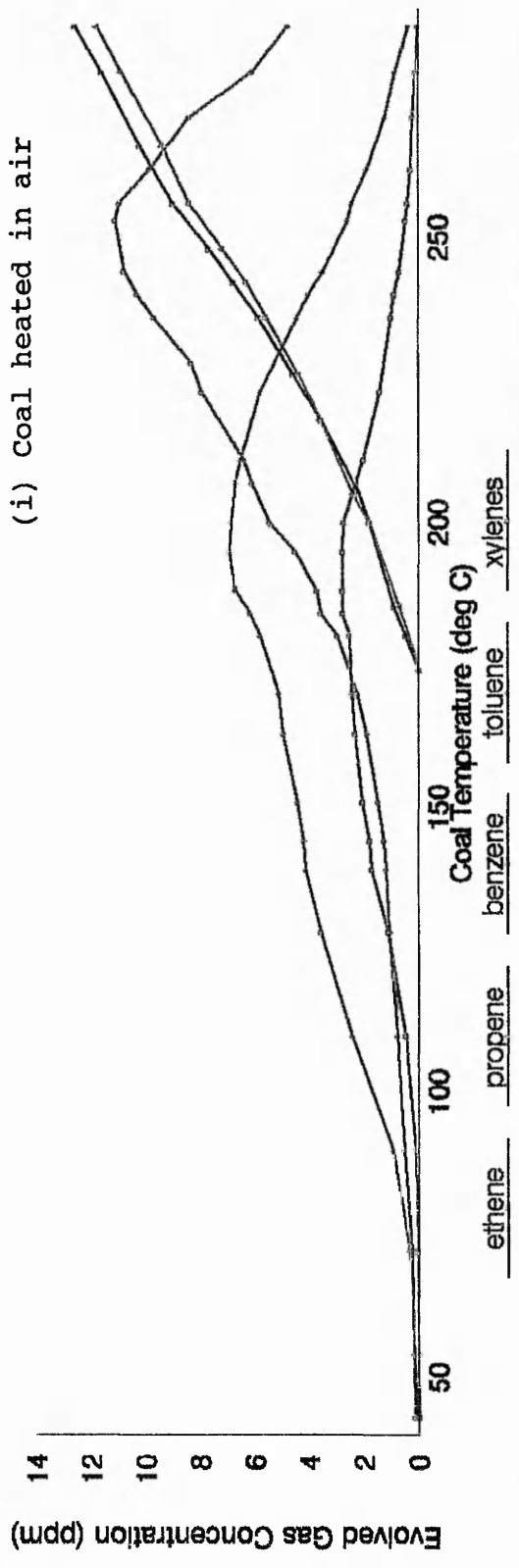
Figure 50.2 Gas Evolution Profiles from Heated Coal - Florence (YardRaqman)
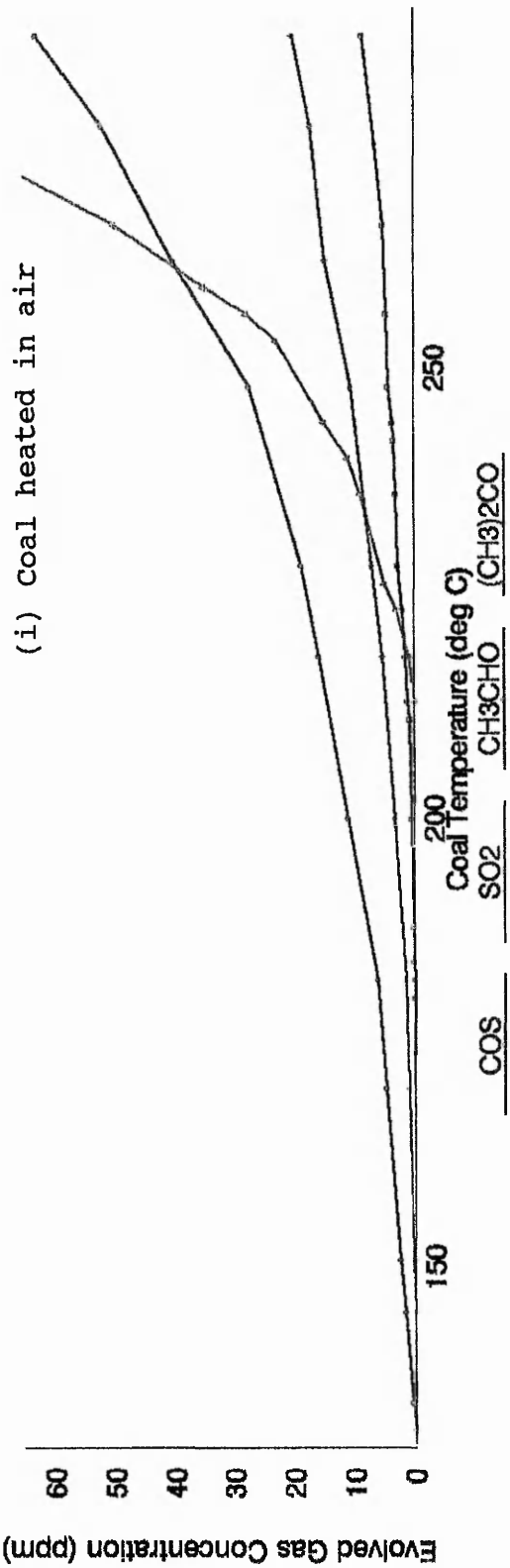
Figure 50.3 Gas Evolution Profiles from Heated Coal - Florence (YardRagman)

(i) Coal heated in air

(ii) Coal heated in nitrogen
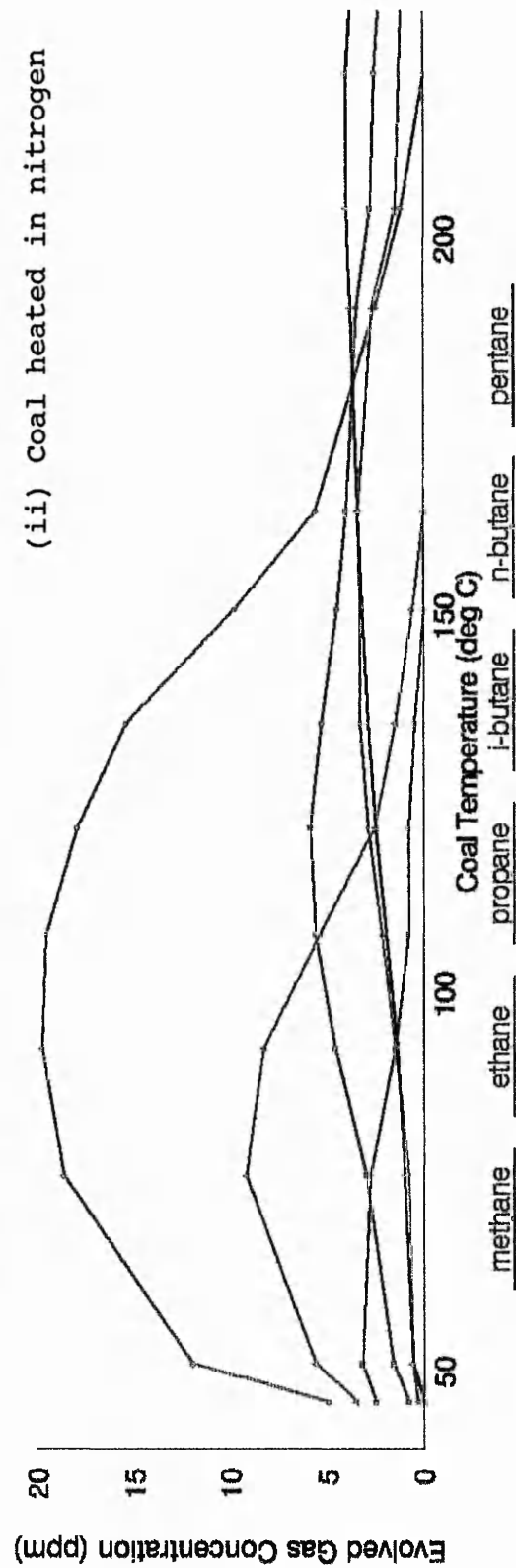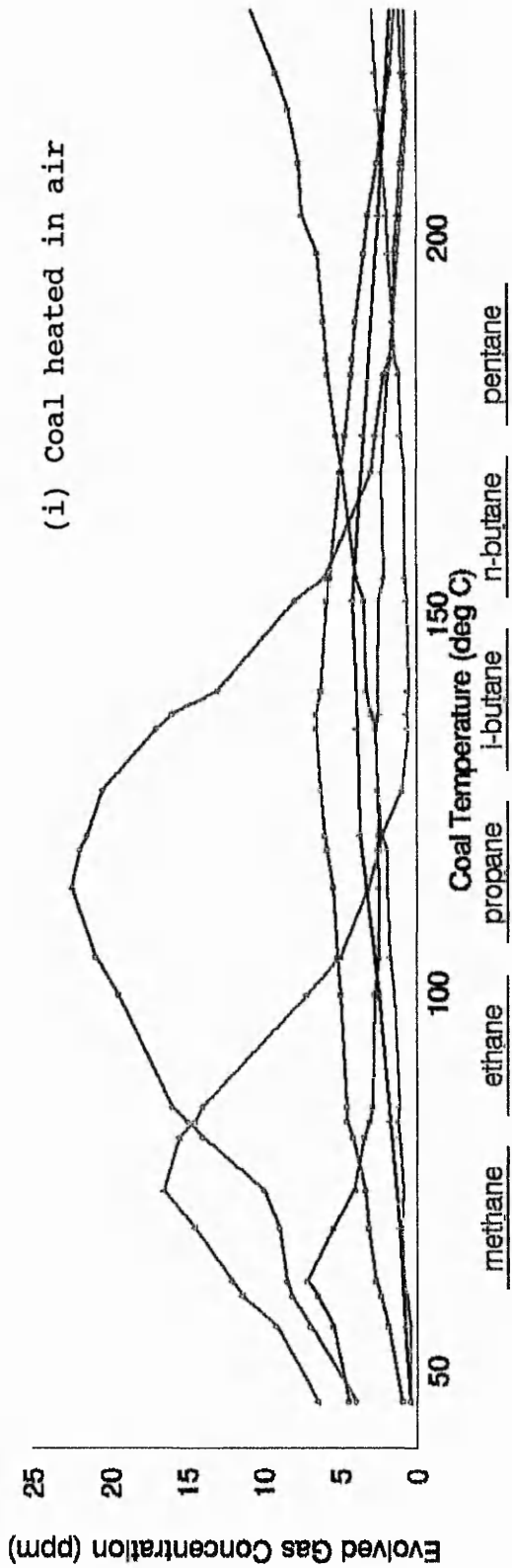
Figure 51.1 Gas Evolution Profiles from Heated Coal - Rossington (Barnsley)

(i) Coal heated in air

(ii) Coal heated in nitrogen

ethene   propene   benzene   toluene   m-/p-xylene   o-xylene
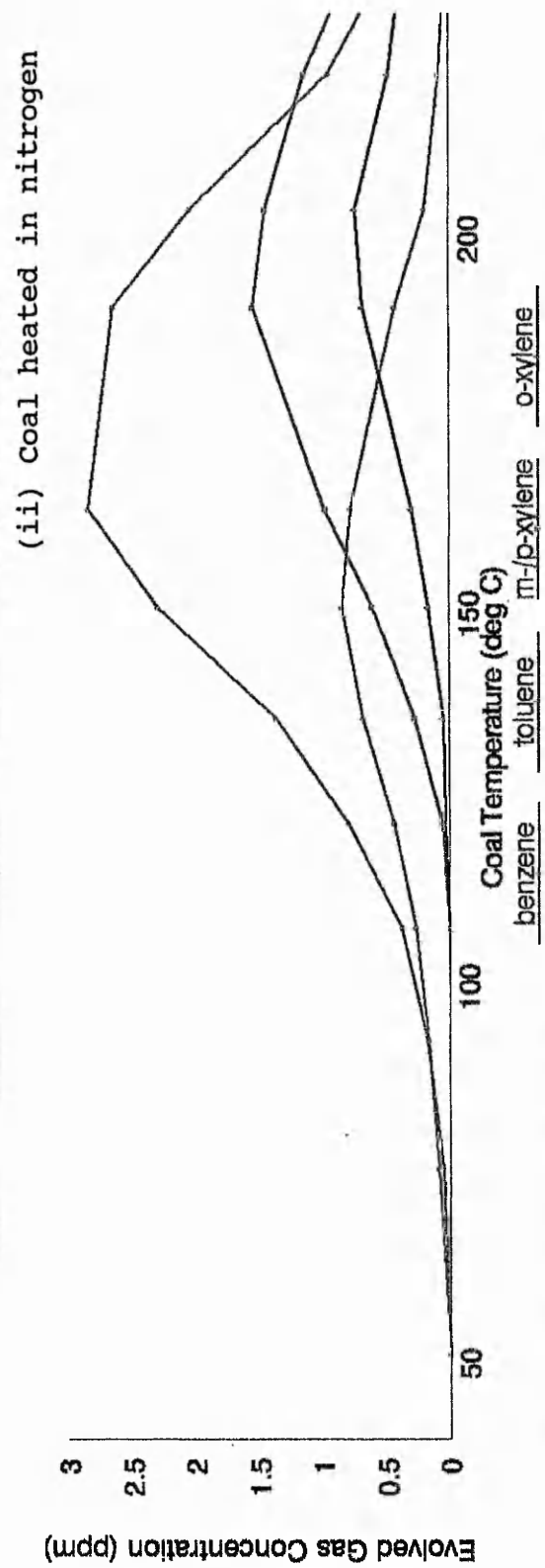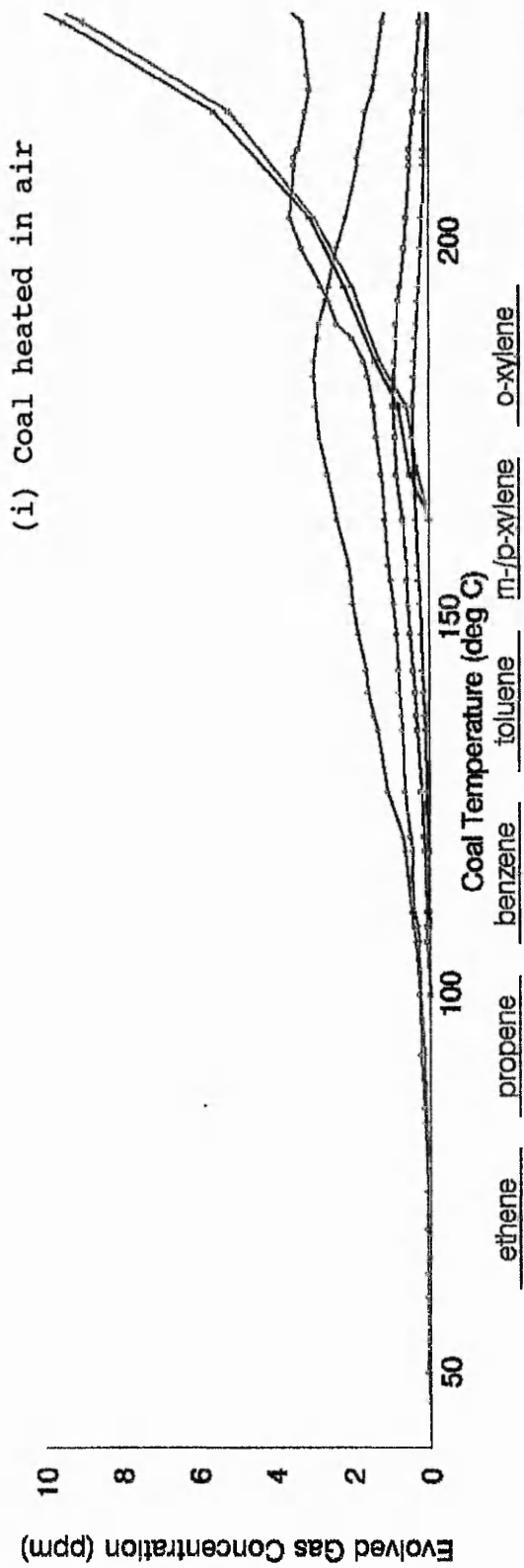
Figure 51.2   Gas Evolution Profiles from Heated Coal - Rossington (Barnsley)

(i) Coal heated in air

Coal Temperature (deg C)

COS   SO2   CH3CHO   (CH3)2CO

Evolved Gas Concentration (ppm)
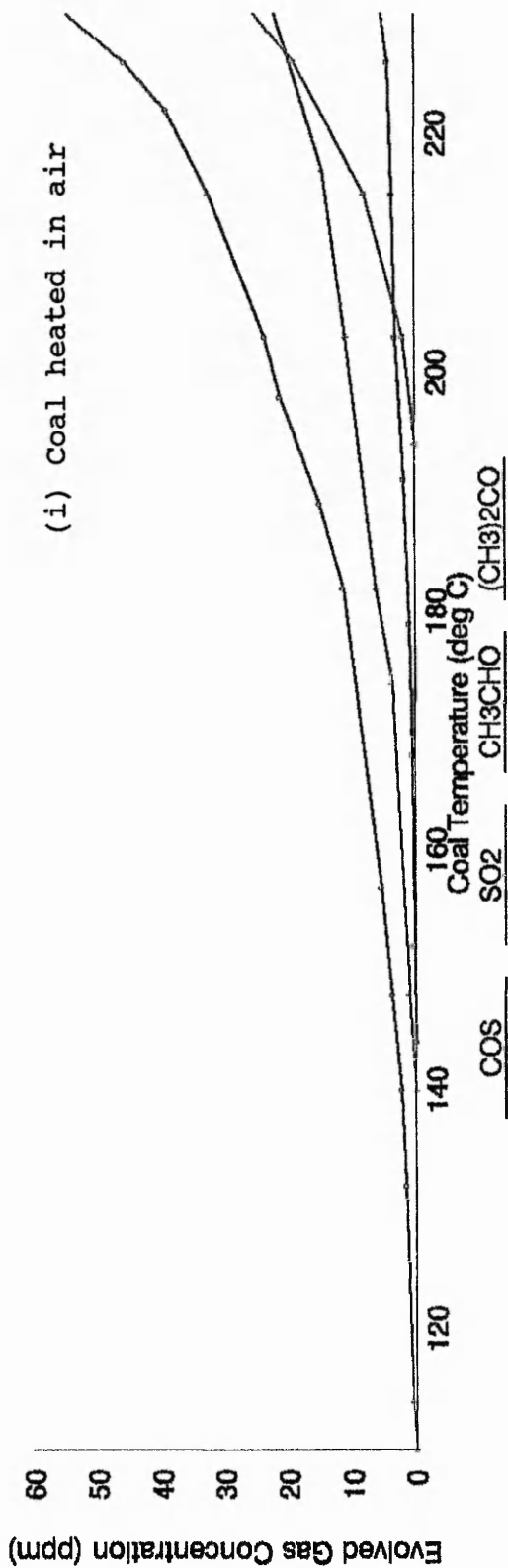
Figure 51.3 Gas Evolution Profiles from Heated Coal - Rossington (Barnsley)
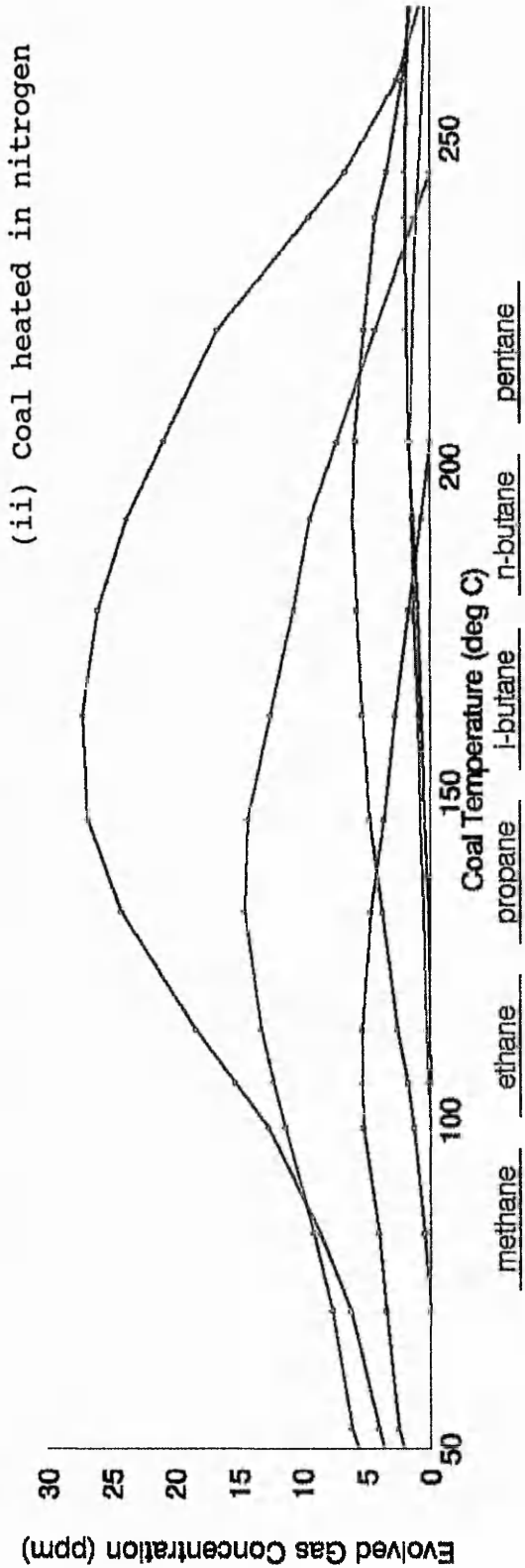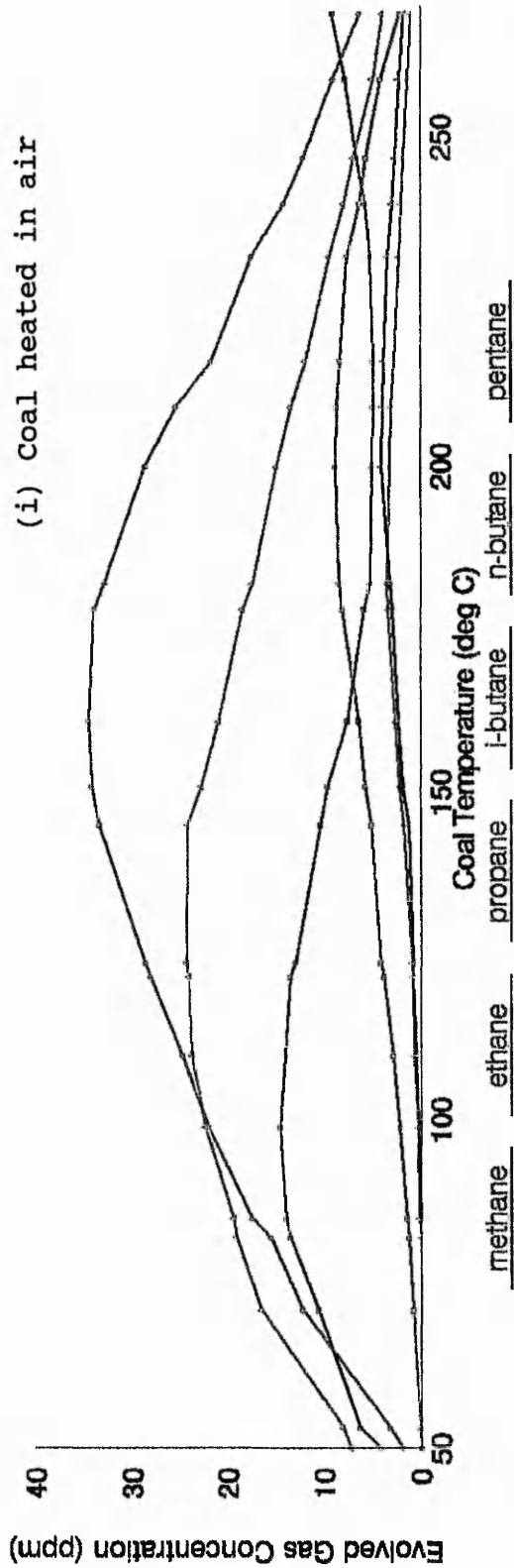
Figure 52.1 Gas Evolution Profiles from Heated Coal – Whitemoor (Barnsley)

(i) Coal heated in air

(ii) Coal heated in nitrogen
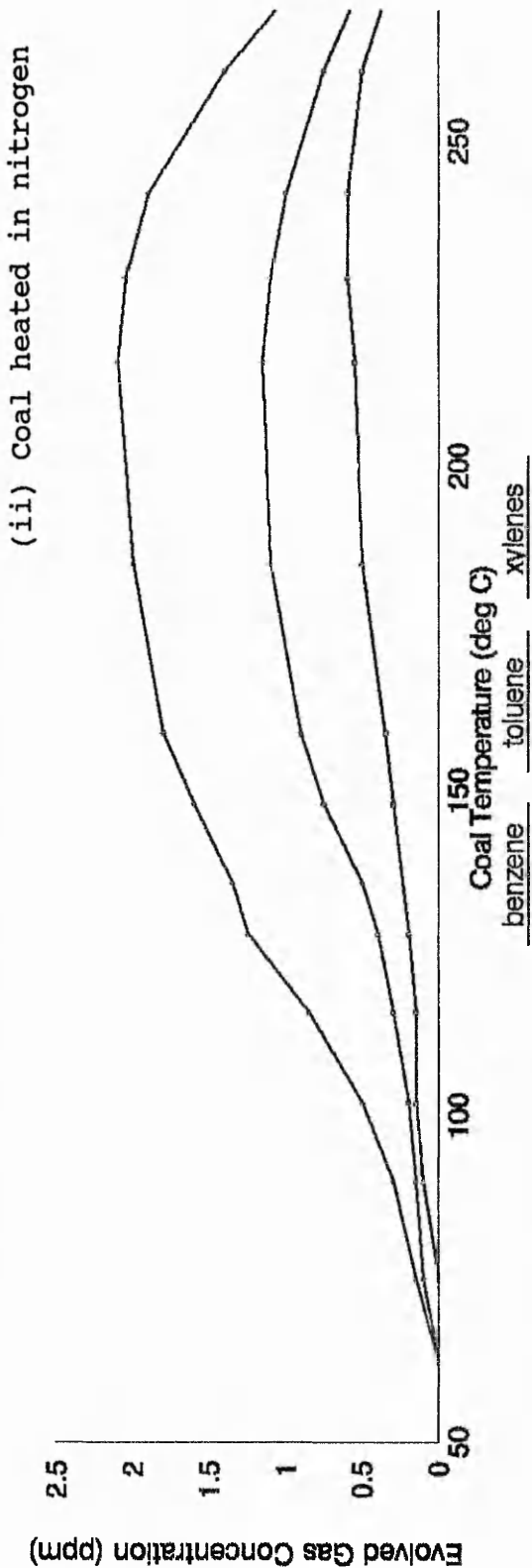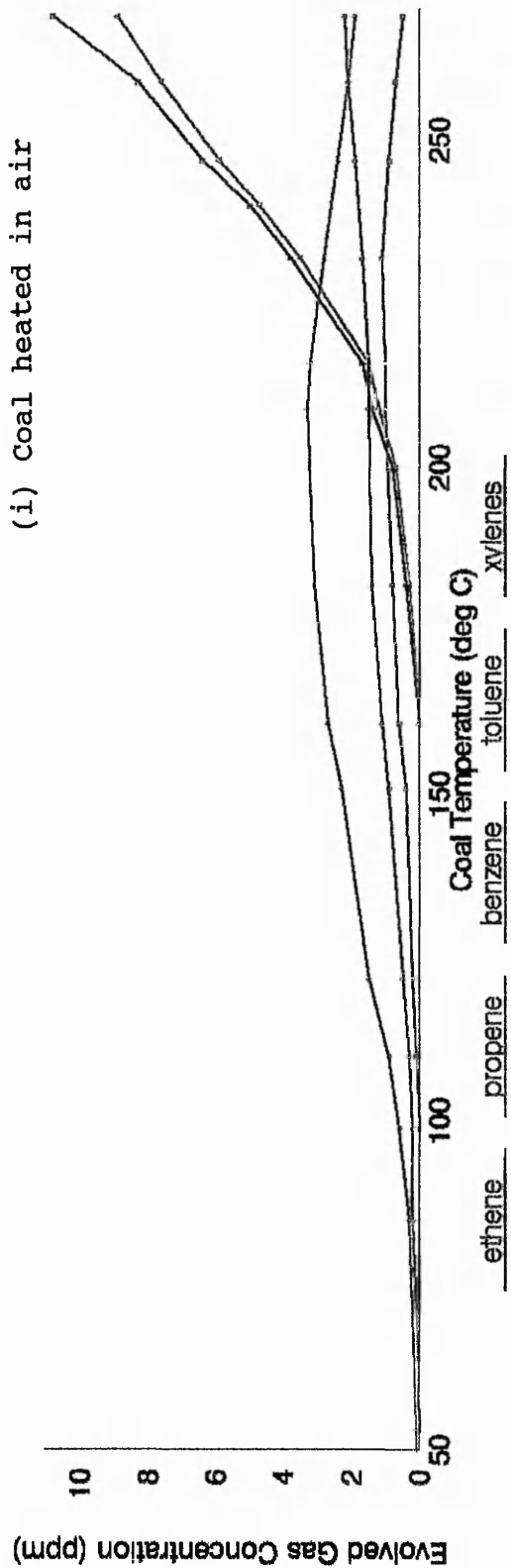
Figure 52.2   Gas Evolution Profiles from Heated Coal - Whitemoor (Barnsley)

-211-

(i) Coal heated in air

(ii) Coal heated in nitrogen
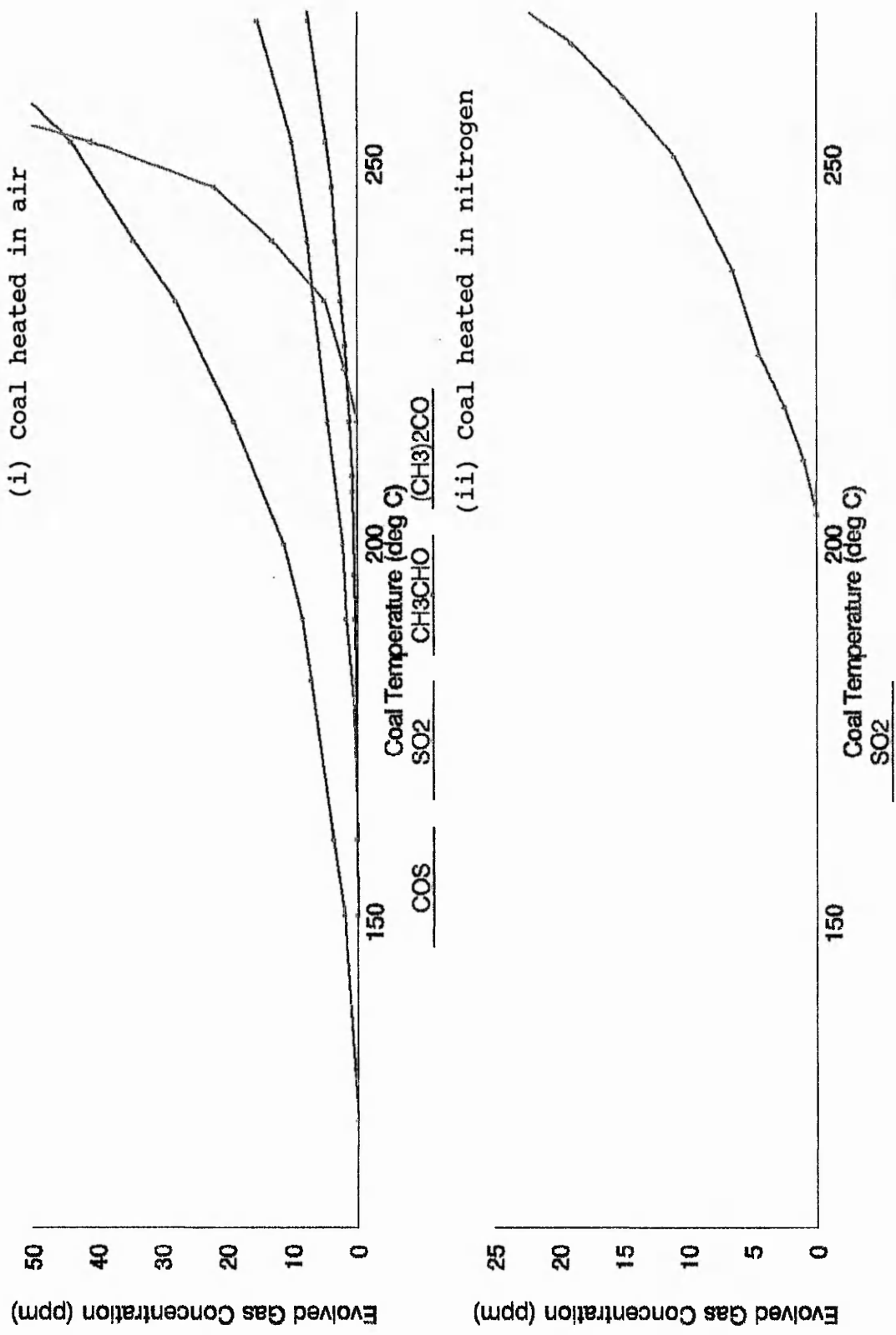
Figure 52.3 Gas Evolution Profiles from Heated Coal - Whitemoor (Barnsley)

(i) Coal heated in air
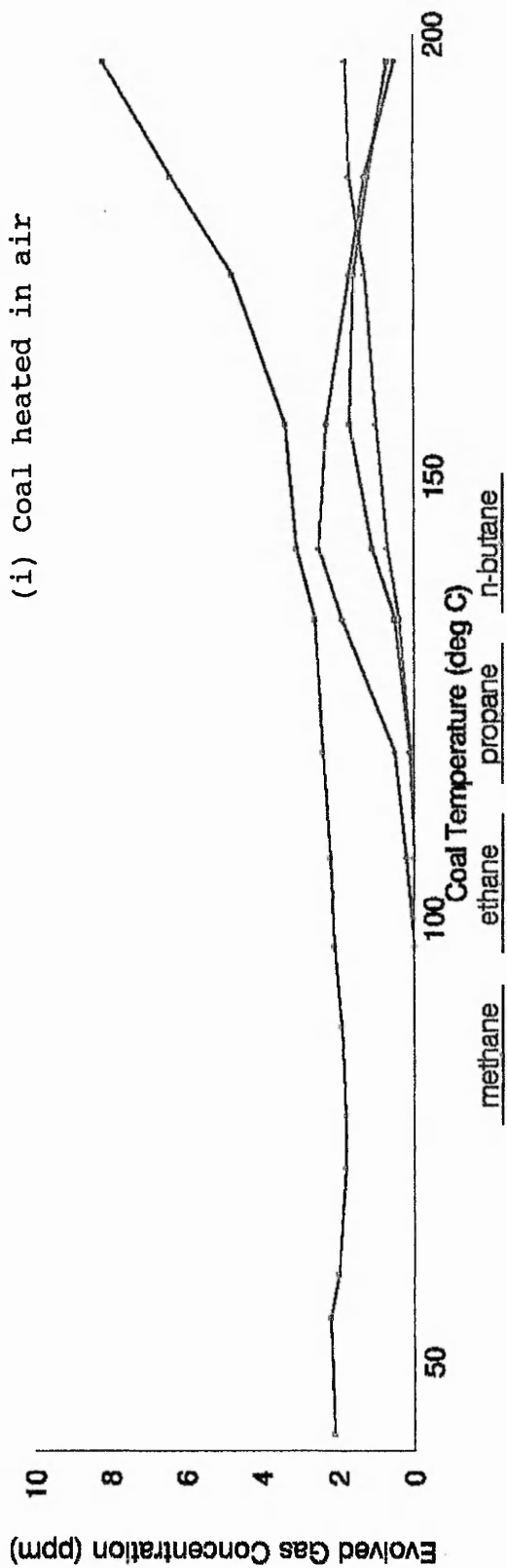
Figure 53.1 Gas Evolution Profiles from Heated Coal - Asfordby (Parkgate)

-213-

(i) Coal heated in air

(ii) Coal heated in nitrogen

ethene   propene   benzene   toluene   xylenes
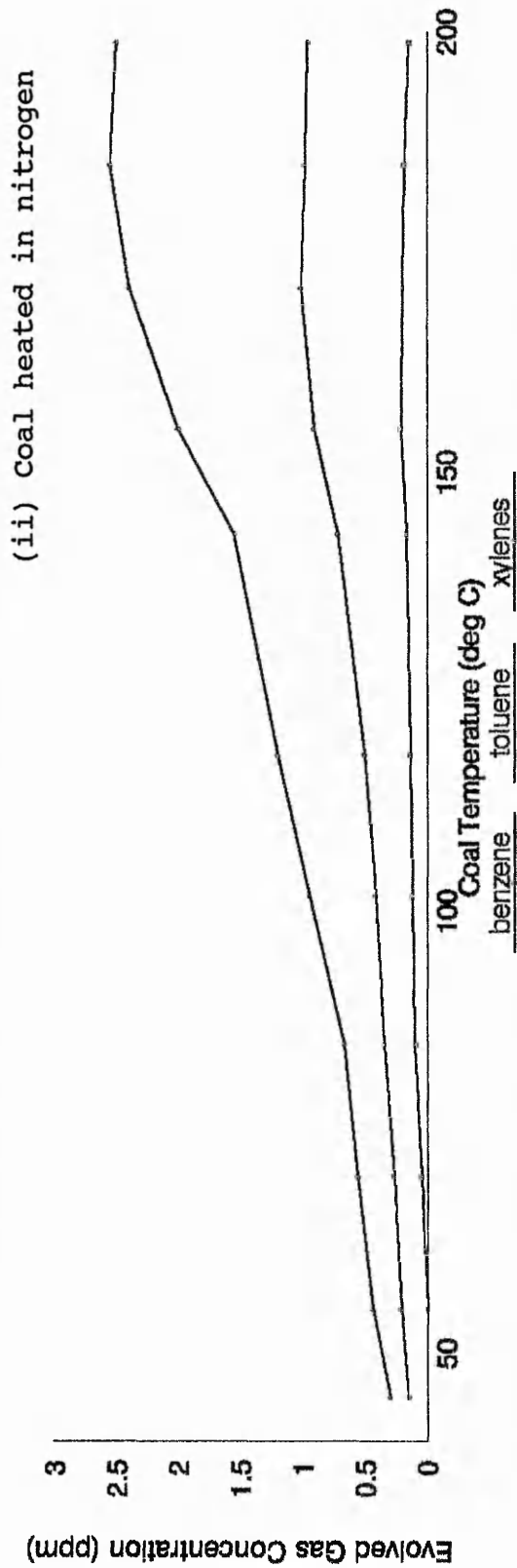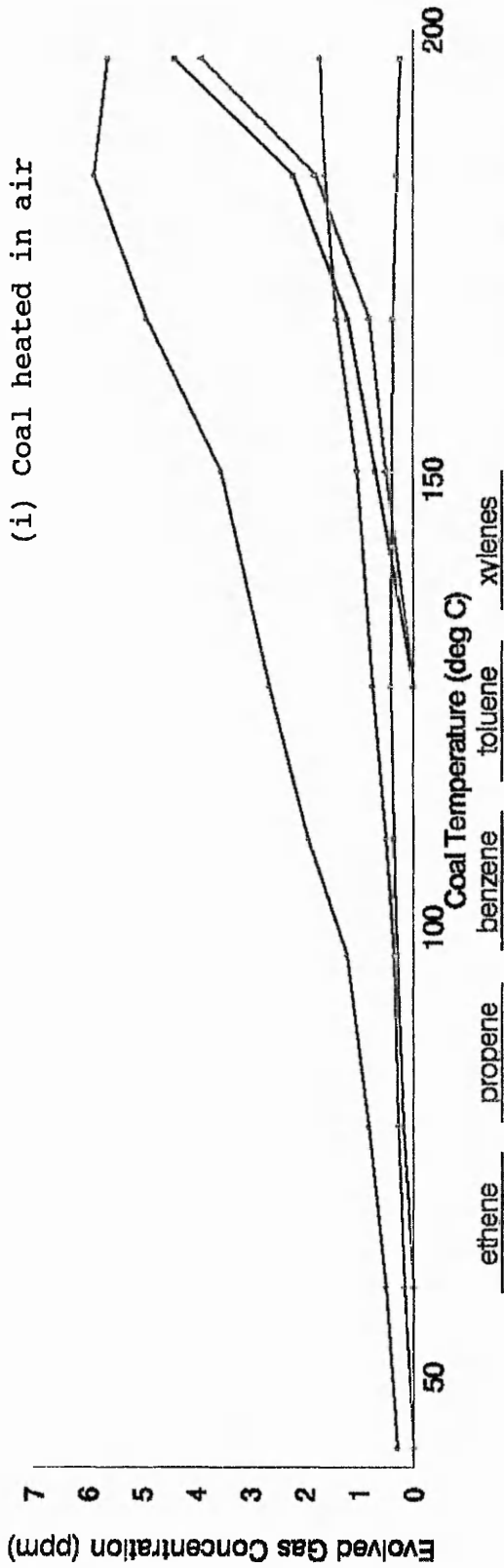
Figure 53.2 Gas Evolution Profiles from Heated Coal - Asfordby (Parkgate)

-214-

(i) Coal heated in air

(ii) Coal heated in nitrogen

CH3CHO   (CH3)2CO

COS

SO2
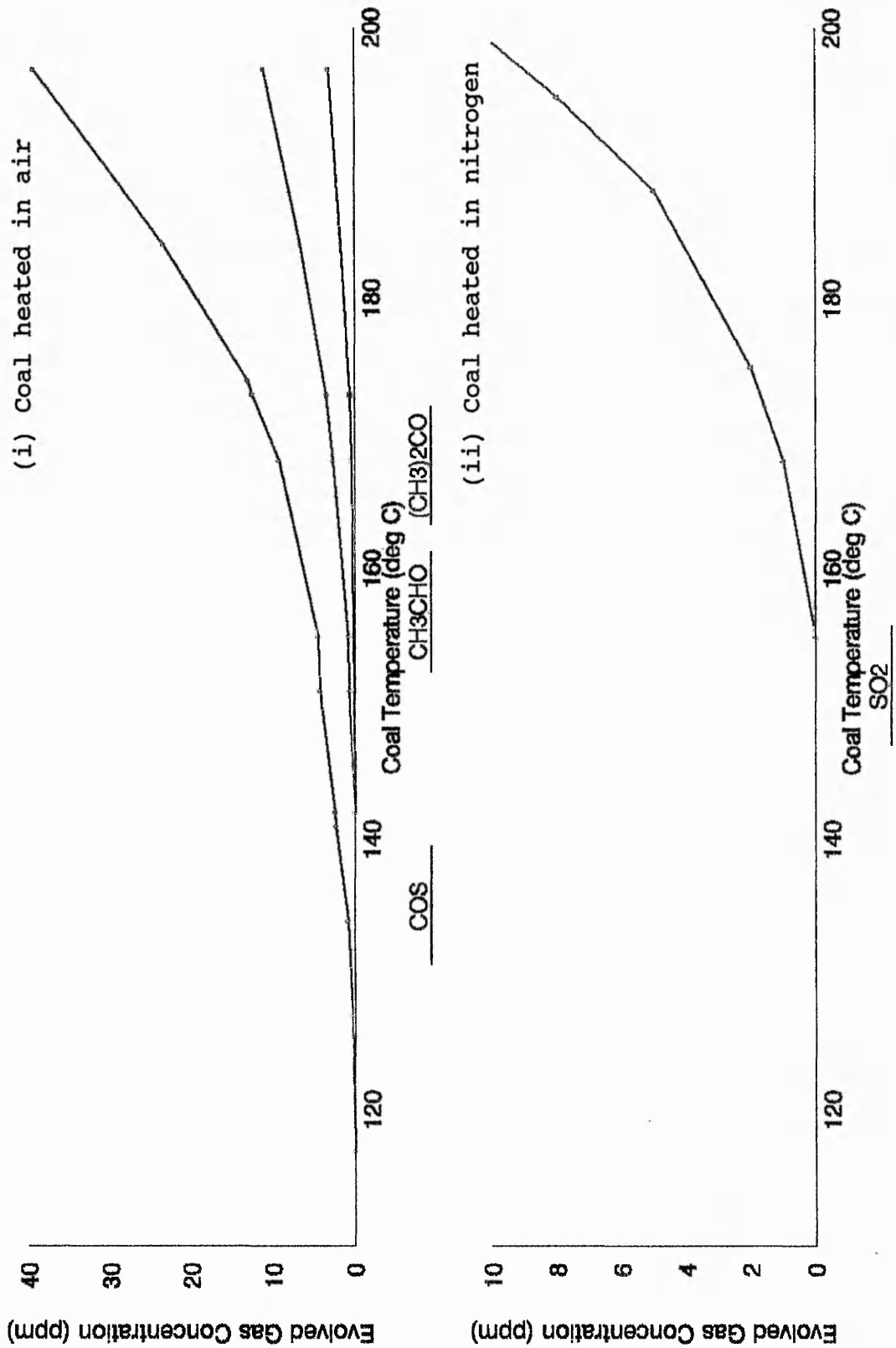
Figure 53.3 Gas Evolution Profiles from Heated Coal — Asfordby (Parkgate)

CHAPTER 6

STUDIES OF ISOTHERMAL COAL OXIDATION PROCESSES

6.1 Introduction

The usefulness of a number of gases as indicators of spontaneous combustion has been demonstrated in chapter 5. Calculation of the kinetic parameters of the formation of these gases was of interest in helping to understand the coal oxidation process. The activation energies for analyte formation reactions may be determined by using the Arrhenius equation (9). By taking natural logarithms as in equation 10, a plot of $\ln(k)$ versus $1/T$ produces a linear graph of slope $-E_A/R$.

$$k = A.e^{-E_A/R.T} \quad ....(9)$$

$$\ln(k) = \ln(A) - E_A/R.T \quad ....(10)$$

k, rate constant; A, pre-exponential factor;

E_A, activation energy; R, gas constant; T, temperature.

This technique requires a method of determining the rate of formation of the analyte gases, which may be obtained by measuring gas concentrations produced during the coal oxidation process. It is important that the evolved gas production has attained a steady state in order to apply the Arrhenius equation.

A number of workers have determined coal oxidation kinetic constants and this work has been reviewed. Historically few results have been reported and values of

-216-

the activation energy of coal oxidation product formation have shown a wide range of 50-400kJ/mol [171]. It is considered that these discrepancies may have resulted from different temperature ranges studied and difficulties in measurements. More recently coal oxidation activation energy values of 68-78kJ/mol, 75-77kJ/mol, 63-84kJ/mol and 51-54kJ/mol have been determined [59,47,172,173,174,175]. These recent results are clearly of the same magnitude, and show a good correlation between modern workers. The activation energies refer to different processes such as the sorption of oxygen and carbonic gas formation.

Several workers have studied the order of evolved gas formation reactions with respect to oxygen during coal oxidation. These values have varied across the ranges 0.54-0.67, 0.5-1.0 and 0.50 [176,177,173]. Although these variations have not been explained in the literature, it is concluded that they may be due to the dissimilar experimental conditions employed.

Petarca et al noted that there are two methods of treating raw kinetic data [46]. One is to assume a set of 'elementary' reactions and combine them. The other approach is to adopt a semi-empirical method by fitting the raw data to the simplest nth order. The latter technique is the more correct since coal oxidation is a group of competing reactions, due to the complexity of coal. It is likely that the heterogeneity of coal is the major reason for the ranges of kinetic constant values that have been calculated in modern times.

6.2   Equipment

Equipment as described in chapters 2, 3, 4 and 5.

Wosthoff gas mixing pump (2-channel).

6.3   Chemicals and Reagents

Gas standards as described in chapters 2 and 3 were employed for the calibration of gas analysers and GC equipment.

6.4   Experimental

6.4.1   Study of Equilibrium Period of Formation of Coal Oxidation Products

The ACCG/EGA system developed in chapter 4 was used to isothermally oxidise selected coal samples. This involved increasing the coal temperature to a constant level and studying the oxidation products formed. The reaction conditions utilised, other than the coal temperature, were the same as those described in table 16, chapter 4 (p.176). It was necessary to determine the time required for the oxidation reaction to equilibrate. A Rossington coal sample was therefore isothermally oxidised at several coal temperatures, using air as the combustion gas. The oxidation reaction was followed by monitoring the formation of carbon monoxide.

6.4.2   Effect of Coal Temperature on Product Formation Rate

The rates of formation of oxidation products were studied by varying the isothermal temperature of coal

samples placed in the ACCG/EGA system. The same reaction conditions were used as described in section 6.4.1. The experiment involved placing a coal sample in the ACCG/EGA system, raising the temperature to the required value, and awaiting equilibration of the coal oxidation reaction. After equilibration had been achieved a gas-tight syringe was used to extract a sample of the effluent gas which was then analysed by GC. The temperatures studied were 100, 125, 150, 160, 170, 180, 190 and 200°C, employing air as the combustion gas.

This process was used to analyse coal samples from Bickershaw, Hem Heath, Florence, Rossington, Whitemoor and Asfordby. CO was produced at sufficiently high concentrations to be readily measured across the temperature range studied. However, with a carrier gas flow rate of 500mls/min the remaining oxidation products were formed at concentrations too low to be measured at the lower temperatures studied. The experiment was therefore repeated using an air combustion gas flow rate of 100mls/min for the Hem Heath coal sample.

6.4.3 Effect of Oxygen Concentration on Product Formation Rate

In order to study the effect that the oxygen concentration of the carrier gas had upon product formation a 2-channel Wosthoff pump was connected to the carrier gas inlet. This was used to mix pure oxygen and nitrogen to vary the oxygen concentration of the carrier gas. The oxygen concentrations employed were 1, 5, 10, 21, 30 and

50% (v/v). The isothermal temperatures studied were 100, 125, 150, 160, 170, 180, 190, 200, 210 and 220°C. Coal samples were placed in the ACCG/EGA system and isothermally heated until equilibration of product formation had been achieved.

A coal sample from Whitemoor colliery was oxidised using this method. After equilibration of product formation had been achieved gas samples were extracted using a syringe and analysed by GC.

6.5   Results and Discussions

6.5.1   Determination of Equilibrium Period of Formation of Coal Oxidation Products

It was necessary to determine appropriate units for studying the rate of formation of products during the coal oxidation process. The gases produced were measured during the experiment as ppm (v/v) concentrations, but this was clearly not a measure of their formation rate. The formation rate units adopted in this work were μmol/g.min. This represents 'μmol of the product formed, per gram of coal used, per minute of the reaction'. The following calculation demonstrates how formation rates were determined by monitoring the production of gas concentrations as units of ppm :

Reaction conditions use carrier gas flow of 500 mls/min.

ie. 0.5 litres of carrier gas in 1 minute.

Now, in 0.5l of carrier gas, 1ppm(v/v) of an analyte occupies a volume of, $(0.5.10^{-6})l = 5.10^{-7}l$.

-220-

At 20.0°C (293.0°K), 1 mole of gas occupies 24.04 litres. Thus, in 0.51 of carrier gas, 1ppm of an analyte represents

$(5.10^{-7})/24.04$ moles analyte = $2.080.10^{-8}$ moles analyte.

Since 5g of coal sample is used,

1ppm of analyte represents $(2.080.10^{-8})/5$ mol/g analyte.

$$= 4.160.10^{-9} \text{mol/g analyte.}$$

$$= 4.160.10^{-3} \mu\text{mol/g analyte.}$$

Since flow rate of 0.51/min employed,

1ppm analyte corresponds to $4.160.10^{-3}\mu$mol/g.min .

This method of measuring the rate of CO formed from a Rossington coal sample was used to monitor the time taken for the formation reaction to equilibrate. Concentrations of CO produced at a number of different isothermal temperatures were used to calculate the formation rate of CO as described. These values have been plotted in figure 54. This clearly demonstrates that a time interval of 20 minutes is sufficient to allow the formation reaction to reach a steady state. Hence this time period may used to allow equilibration of the system at each different temperature studied.

6.5.2 Determination of Kinetic Constants of Formation Reaction of Oxidation Products

The application of the Arrhenius equation as described in section 6.1 was used to determine the activation energy of CO formation for each of the coals studied. This was determined by plotting the natural logarithm of CO formation rate versus the inverse of the coal temperature,

-221-

Figure 54   Formation Rates of CO During Isothermal Coal Oxidation
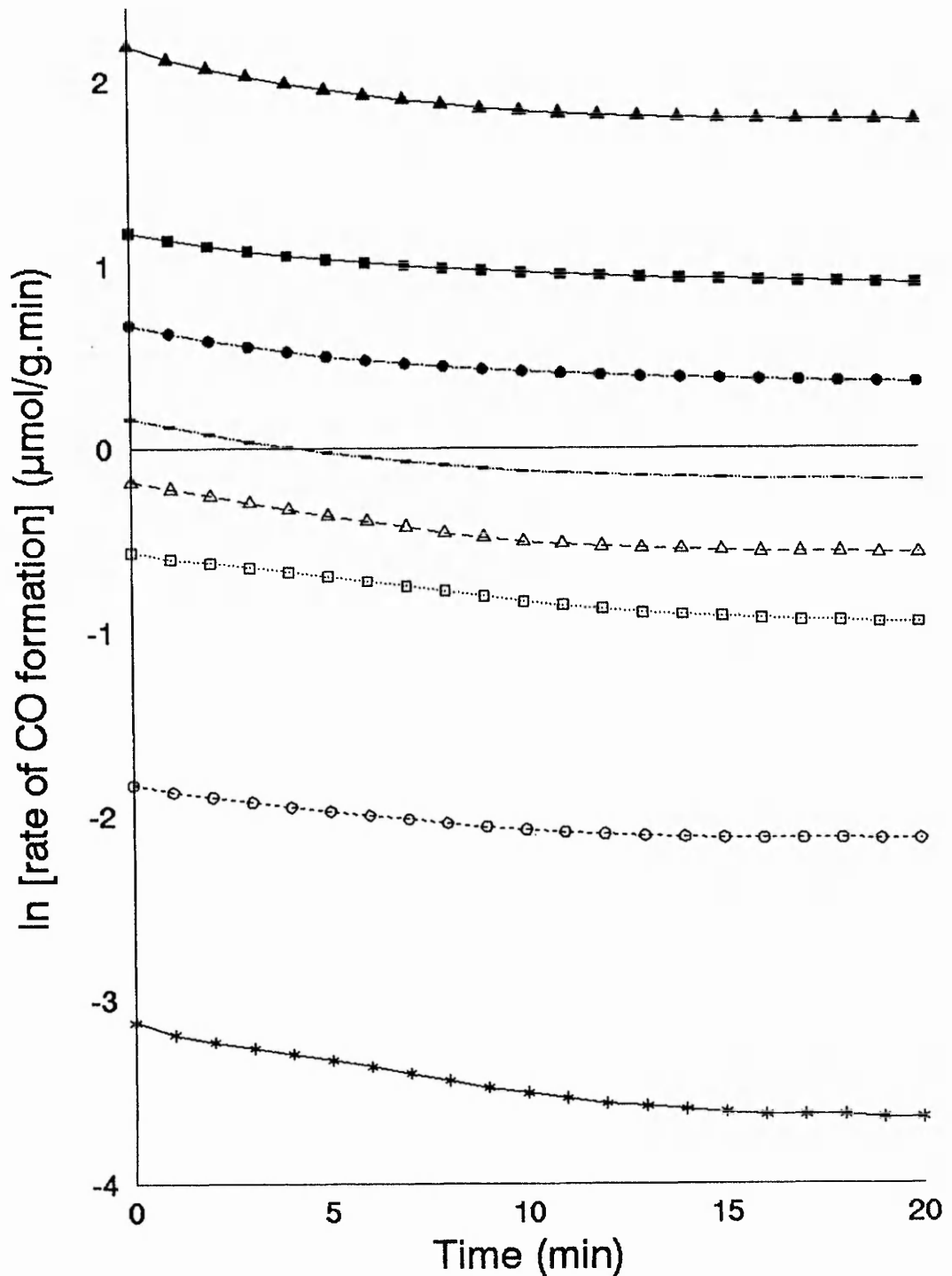
Coal temperature (deg C)

| 98.8 | 126.7 | 150.8 | 161.1 | 172.4 | 181.5 | 192.5 | 203.8 |

as illustrated by the typical plots in figure 55. The slope of this graph was determined by the least squares method, which provided a measure of the activation energy.

Values of the activation energy of CO formation for each of the coals studied have been determined by this method and listed in table 21. The crossing-point temperatures of these coals have also been listed in table 21 in order to relate the coal reactivity to the activation energy of CO formation.

Table 21   Activation Energies of CO Formation Reactions

Colliery Coal Sample	Activation Energy (kJ/mol)	Crossing-Point Temperature (°C)
Bickershaw	76.5	158
Hem Heath	76.5	183
Florence	75.5	172
Rossington	72.5	144
Whitemoor	78.9	185
Asfordby	72.6	151
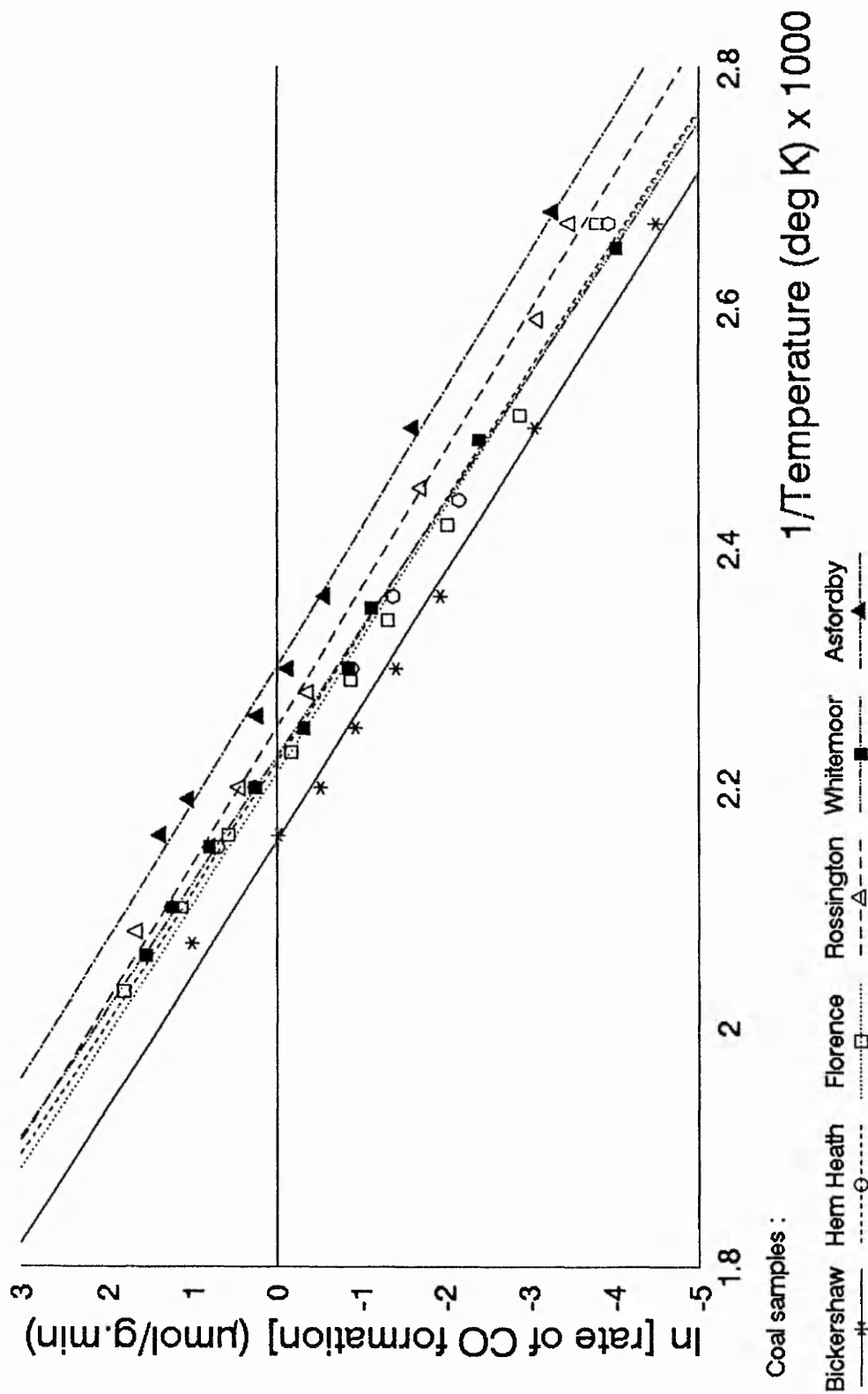
Figure 55   Arrhenius Plots of CO Formation During Coal Oxidation

Coal samples :

Bickershaw   Hem Heath   Florence   Rossington   Whitemoor   Asfordby

It is interesting that the more reactive Asfordby and Rossington coal samples have lower activation energies than the remaining coals implying that the formation of CO requires less energy than for the less reactive coals. Generally however, the activation energies appear to be approximately the same for all of the coals studied, and independent of the coal reactivity. This conclusion is in agreement with modern workers who have concluded that 'activation energies are approximately the same for all coals studied irrespective of rank' [173].

The results of evolved gas production from the Hem Heath coal sample using an air carrier gas flow rate of 100mls/min were used to calculate activation energies of other coal oxidation products by using the Arrhenius equation in a similar manner to that described for CO. They have been listed in table 22.

Table 22   Activation Energies of Evolved Gas
Formation Reactions

EVOLVED GAS	ACTIVATION ENERGY (kJ/mol)
Carbon monoxide	77.1
Carbon dioxide	76.7
Acetaldehyde	64.2
Acetone	68.1
Carbonyl sulphide	87.2
Ethene	86.9
Propene	80.9

6.5.3 Determination of Reaction Order of Formation of Oxidation Products

Consider the coal oxidation reaction in terms of the formation of the evolved gas products :-

Coal + O_2 ————> Products
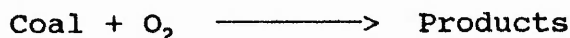
Reaction rate = $k.P^n$...........................(11)

k, constant; P, partial pressure of oxygen,

n, order of reaction.

ln (reaction rate) = ln(k) + n.ln(P)............(12)

The rate of the reaction may be calculated in terms of the rate of formation of evolved gas. Therefore using equation 12, a plot of ln(evolved gas formation rate) versus ln(oxygen partial pressure) produces a linear graph, the slope of which represents the order of the reaction.

This method was used to calculate reaction orders using data from the experiments in which evolved gas concentrations were measured using different oxygen carrier gas concentrations. These measurements were made at a variety of different temperatures allowing the effect that the coal temperature has upon the reaction order to be studied. There was a difficulty in reproducing exactly the same coal temperature for the range of experiments which employed different oxygen concentrations. The evolved gas concentrations that were produced using a variety of coal tmeperatures were therefore measured for each different oxygen concentration. Then, evolved gas concentration versus coal temperature values were solved for each oxygen concentration by using the least squares method. A typical example of this calculation has been illustrated in table

23. This produced values of the slope and y-intercept of the graph which allowed evolved gas concentrations to be calculated at any temperature within the range studied, as illustrated in table 24.

The natural logarithm of analyte concentrations produced using different oxygen concentrations were plotted against the natural logarithm of the oxygen partial pressure. This produced a linear graph, whose slope represents the reaction order of the analyte formation reaction. A typical plot of this graph has been illustrated for CO formation at a variety of temperatures in figure 56. The reaction order was measured in this manner for the temperatures 100, 125, 150, 160, 170, 180, 190, 200, 210 and 220°C. This approach was also adopted to determine the reaction order of analyte formation with respect to oxygen for the oxygenated analytes acetaldehyde, acetone and carbonyl sulphide. These results have been listed in table 25.

Table 23 Least Squares Regression of CO Formation Reactions

Temp. (C)	1/T(K) x1000	Conc. CO (ppm)	ln[CO(ppm)]
100.2	2.679	2.3	0.8329
124.2	2.517	9.2	2.2192
149.2	2.367	29.0	3.3673
158.4	2.318	39.8	3.6839
170.7	2.253	70.5	4.2556
179.9	2.207	101	4.6151
189.6	2.161	153	5.0304
198.2	2.122	219	5.3891
208.5	2.076	323	5.7777
217.5	2.038	460	6.1312

The results in table 23 were solved using the least squares method, producing the results;
slope=-8.1686, y-intercept=22.710, r^2=0.9989.

Table 24 Calculated CO Concentrations

Temp.(C)	CO conc.(ppm)
100	2.2
125	8.9
150	29.9
160	46.7
170	71.5
180	107
190	159
200	231
210	329
220	464
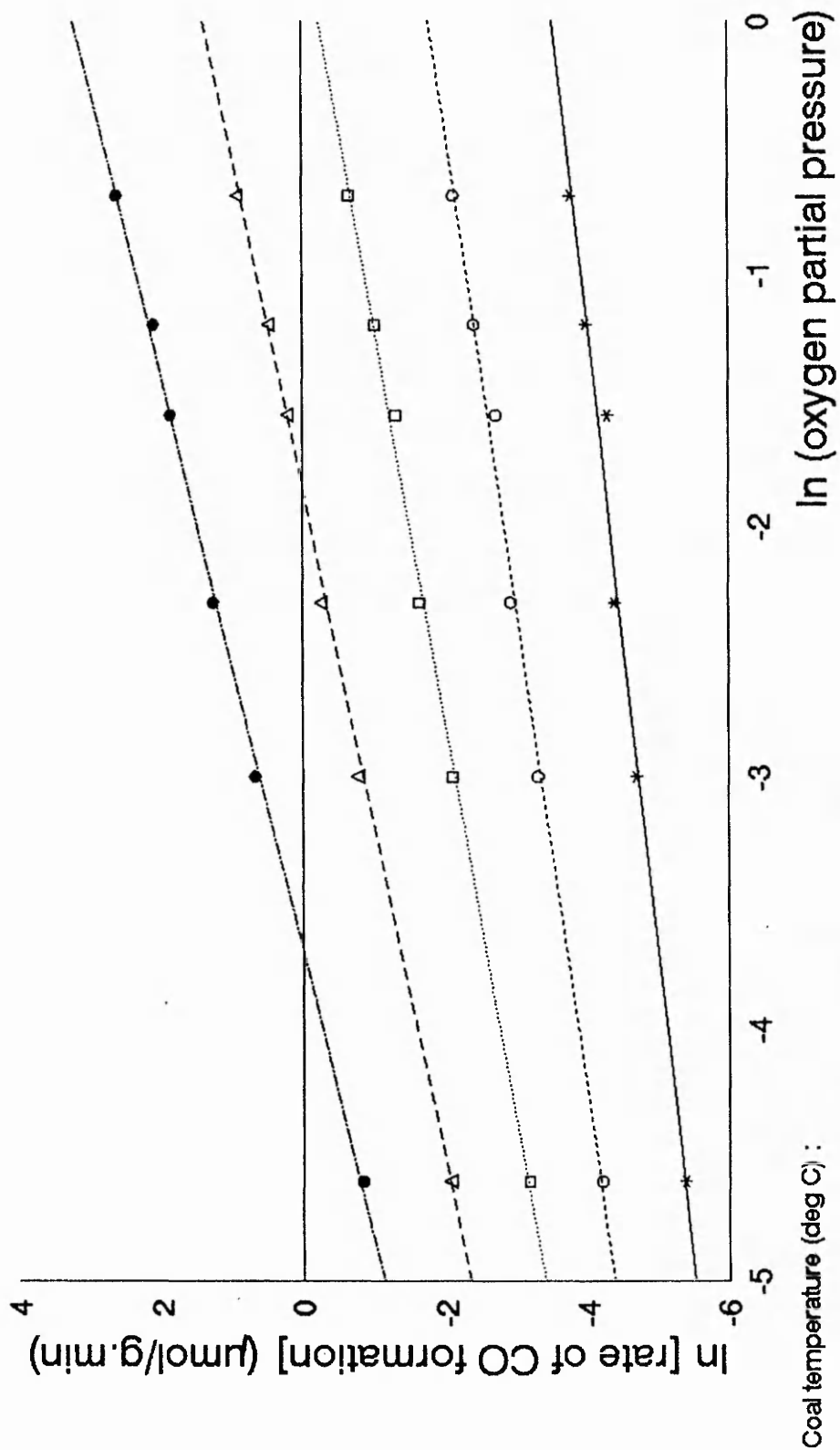
Figure 56 Effect of Oxygen Concentration Upon CO Formation Rate

Table 25 Reaction Orders of Production of Evolved Gases

Temp.(C)	ORDER OF REACTION WITH RESPECT TO OXYGEN			
	Carbon monoxide	Acetaldehyde	Acetone	Carbonyl sulphide
100	0.41	****	****	****
125	0.53	0.59	****	****
150	0.63	0.67	0.59	****
160	0.67	0.70	0.65	0.86
170	0.71	0.73	0.70	0.90
180	0.74	0.75	0.75	0.91
190	0.78	0.78	0.80	0.94
200	0.81	0.81	0.85	0.99
210	0.84	0.84	0.89	1.02
220	0.87	0.86	0.94	1.04

**** indicates that analyte concentrations were below the analytical limits of detection.

The reaction orders of CO formation that have been calculated are in good agreement with those produced by other workers [176,177,173]. Carpenter et al studied the order of oxygen adsorption at 95°C, and calculated values of 0.5 [176]. They suggested that this may be due to dissociative adsorption of oxygen on the coal surface. Since the reaction orders in this work have varied from 0.41 to 0.87 across the temperature range of 100-220°C this would suggest a dissociative adsorption of oxygen giving way to chemisorption of oxygen as the coal temperature increases.

The calculated reaction orders for the formation of the other oxygenated gases in table 25 are of the same order as the values for CO. This implies that the formation mechanism of the oxygenated gases is the same as that for CO. Therefore, since CO is known to represent a useful indicator of spontaneous combustion, this conclusion supports the use of the other oxygenated gases as useful indicators.

6.6 Summary of Conclusions

The activation energies and reaction orders of the formation of a variety of evolved gases have been calculated in this work. These results have shown good general agreement with the limited modern work that has been reported. They have demonstrated marked similarities between data for carbon monoxide and the other indicator gases studied. This suggests that all of these gases are

formed by similar reaction mechanisms. Since carbon monoxide is recognised as a useful indicator of spontaneous combustion this work has validated the use of the other evolved gases as useful indicators.

CHAPTER 7

CONCLUSIONS AND SUGGESTIONS FOR FUTURE WORK

7.1   Conclusions

The purpose of this work was to study the formation and monitoring of gases associated with the spontaneous combustion of coal. The initial step, therefore, was the development of a system capable of analysing the gases evolved from coal undergoing combustion. The most appropriate system was considered to be a gas chromatograph due to the complex sample matrix that existed.

Detailed investigations into the use of different GC columns were carried out by studying separations of gas mixtures. The use of modified alumina as the stationary phase allowed the selectivity of component separations to be suitably controlled. In this manner the separation of components was increased, which could be used to reduce analysis times. A dramatic increase in separation was noted when the physical dimensions of the column were altered. The efficiency increased when the column diameter was reduced. However, maximum column efficiency was obtained when open-tubular columns were employed. The advantages of increased column efficiency achieved with open-tubular columns outweighed the selectivity improvements. It was therefore demonstrated that for component separation in a minimum time, an open-tubular configuration was the optimum. This was illustrated by separating all of the

gases to be studied on only two different open-tubular columns, DB-Wax and PoraPLOT Q.

The response characteristics of a number of detectors were studied with respect to the detection of gases evolved from the combustion of coal. Photoionisation detectors (10.6eV and 10.2eV) demonstrated excellent responses to unsaturated, oxygenated and aromatic gases of interest, with considerably reduced responses relative to saturated hydrocarbons. They therefore represented detection systems capable of monitoring the gases to be studied. Also, their application in monitoring analytes in mine atmospheres which contain saturated hydrocarbons in the matrix is apparent.

The practical application of an 11.7eV photoionisation detector to the analysis of sulphur gases was discounted due to the short lifetime of the detector lamp. However, a flame photometric detector demonstrated suitable responses to the sulphur gases, and this method of detection was employed throughout the work.

An automated coal oxidation system was constructed which was capable of continuously monitoring coal and oven temperatures and specific gas concentrations. The integrity of this system was demonstrated by analysing laboratory coal samples in replicate. This permitted the physical parameters of the coal oxidation conditions to be empirically optimised.

The automated system was used to oxidise a variety of virgin coals freshly sampled from underground locations.

The production of a range of evolved gases was studied by regularly extracting gas samples during the coal oxidaiton process using a gas-tight syringe. This was followed by GC analysis using equipment that had been optimised earlier in the work. The evolution profiles of these gases produced during dynamic coal oxidation allowed their use as indicators of spontaneous combustion to be determined. These results demonstrated that ethene, propene, carbonyl sulphide, acetaldehyde, acetone, carbon monoxide and carbon dioxide represent useful indicators of spontaneous combustion. The results also demonstrated that aliphaitc hydrocarbons, aromatic and other sulphur gases may not be used as indicators of spontaneous combustion since they are coal desorption products.

The formation rate of gases evolved from isothermal coal oxidation allowed kinetic constants to be calculated. Variation of the coal temperature during oxidation produced data which allowed the activation energies of formation of evolved gases to be determined. These were calculated by applying the Arrhenius equation to the experimental data. The values determined for carbon monoxide were of the same order as those calculated by other workers [172-175]. Variation of the oxygen composition of the carrier gas during coal oxidation produced data which allowed the reaction order of formation of the evolved gas to be calculated. The reaction order values determined for carbon monoxide were of the same order as those calculated by other workers [173,177]. The values calculated for acetone,

acetaldehyde and carbonyl sulphide were similar to those determined for carbon monoxide. This implied that the formation mechanisms for all of these gases were similar.

The work previously described demonstrated that other gases evolved from oxidised coal may indicate spontaneous combustion as successfully as carbon monoxide. This was an important observation since carbon monoxide is known to be an excellent indicator from historical evidence. However this work was entirely a laboratory based study involving coal oxidation processes that lead to spontaneous combustion. It was important to validate this work by analysing gas samples taken from collieries during incidents of spontaneous combustion. This was difficult, since such incidents cannot be predicted, and there are problems with the transportation of gas samples due to the reactivity of some of the analytes. However, a number of gas samples were taken during such incidents and they have been listed in Appendix VI. This work clearly validates the use of acetaldehyde, acetone, carbonyl sulphide, ethene and propene as indicators of spontaneous combustion.

7.2   Suggestions for Future Work

A range of gases have been identified which represent useful indicators of the spontaneous combustion of coal. They have been detected in underground colliery locations during incidents of spontaneous combustion, which has validated their use.

Equipment capable of detecting these gases has been

evaluated, and gas chromatographic (GC) methods which employ minimum analysis times have been developed. The use of two different chromatographic columns separated all of the gases studied. Thus the development of a portable GC based on these two columns would provide an excellent method of separating these analytes in a coal mine atmosphere matrix. The detection of these gases could be achieved using a photoionisation detector or multiple parallel photoionisation detectors, which have been demonstrated in this work to provide different responses to the gases studied. In this manner an array of detectors could be arranged, which would be capable of multicomponent analysis by the application of suitable software. This could lead to the development of an expert system based on the proposed GC.

Improvements in the components of the equipment studied in this work could be gained by further investigation. The production of a open-tubular column using a suitably modified alumina stationary phase could combine the separation improvements demonstrated by increasing the selectivity and efficiency. This work would need to focus on technology necessary to coat a column with alumina, and to render the alumina impervious to the effects of trace amounts of water.

Additionally, it would be interesting to investigate the factors that cause different photoionisation detectors to produce dissimilar responses to analytes. This would allow the researcher to develop detectors which respond more

selectively by suitably modifying the PIDs. Factors which are worth studying include the lamp envelope design, filler gas type and pressure, electrode geometry and physical dimensions and the mechanism of lamp excitation. This work would be beneficial towards the development of an array of PIDs which may be capable of the multicomponent analysis described earlier.

REFERENCES

1. Seyler CA, Proc. S. Wales Inst. Eng., 1938, <u>53</u>, 254.

2. van Krevelen DW, 'Coal', Elsevier, 1981.

3. 'The Coal Classification System Used by the NCB', published by NCB, revision of 1964.

4. British Standards Institution, BS 1016, Part 12, "Caking and Swelling Properties of Coal".

5. Neavel RC, in 'Chemistry of Coal Utilization - Second Supplementry Volume', editor Elliott MA, John Wiley & Sons, 1981, 91-158.

6. Given PH, Yarzab RI, in 'Analytical Methods for Coal and Coal Products (Volume 2)', editor Karr C, Academic Press, 1978, 3-41.

7. Maher TP, Schafer HNS, Fuel, 1976, <u>55</u>, 138.

8. Wandless AM, Jnl of Inst of Fuel, 1955, <u>18</u>, 54.

9. Attar A, Dupuis F, in 'Coal Structure', editors Gorbaty ML, Outchi K, Am. Chem. Soc., 1981, 239-256.

10. Berkowitz N, 'The Chemistry of Coal', Elsevier, 1985, 127.

11. Guner D, Hood WC, Trans Ill Acad Sci, 1971, <u>64(2)</u>, 152.

12. Francis W, Wheeler RV, J Chem Soc, 1925, <u>127</u>, 2236.

13. Schultz JL, Kessler T, Friedal RA, Sharkey AG, Fuel, 1972, <u>51</u>, 243.

14. Edgecombe LJ, Fuel, 1955, <u>34</u>, 429.

15. Daybell GN, Pringle WJS, Fuel, 1958, <u>37</u>, 283.

16. Pearce WC, PhD Thesis, Sheffield Polytechnic, CNAA, 1984.

17. Given PH, in 'Coal Science (Volume 3)', editors Gorbaty ML, Larsen JW, Wender I, Academic Press, 1984, 63-252.

18. Stach E, in 'Stach's Textbook of Coal Petrology', editors Stach E, Mackowsky MT, Gebruner Borntraeger, 1982, 87-104.

19. British Standards Institution, BS 6127, Parts 1-5, 'Petrographic Analysis of Bituminous Coal and Anthracite'.

20. International Committee for Coal Petrology, 'International Handbook of Coal Petrography', 2nd edition, Centre National da la Recherche Scientifique, 1963.

21. International Committee for Coal Petrology, 'International Handbook of Coal Petrography', Supplement to 2nd edition, University of Newcastle upon Tyne, 1985, editors Murchison DG, Smith AHV.

22. Gluskoter HJ, Shimp NF, Ruch RR, in 'Chemistry of Coal Utilization - Second Supplementry Volume', editor Elliott MA, John Wiley & Sons, 1981, 369-424.

23. Valkovic V, 'Trace Elements in Coal (Volume 1)', Chemical Rubber Co., 1983, 5.

24. Gorbaty ML, Outchi K, 'Coal Structure', Am Chem Soc, 1981.

25. Wiser WH, in 'Proceedings of the Department of Energy Project Review Meetings', 1978, 4.

26. Dubinin MM, 'Chemistry and Physics of Carbon (Volume 2)', editor Walker PL, Marcel Dekker, 1966, 51.

27. van Krevelen DW, 'Coal', Elsevier, 1981, 127-143.

28. Seewald H, Klein J, Juntgen H, in 'Proc. Intern. Conf. on Coal Science', Sydney Australia, 1985, 861-864.

29. Sharkey AG, McCartney JT, in 'Chemistry of Coal Utilization - Second Supplementary Volume', editor Elliott MA, John Wiley & Sons, 1981, 184-186.

30. Toda Y, Fuel, 1973, _52_, 99.

31. Jenkins RG, Nandi SP, Walker PL, Fuel, 1973, _52_, 288.

32. Cox L, Fuel, 1984, _63(7)_, 1030.

33. Beier E, in 'Proc. of Intern. Conf. on Coal Sci.', Pittsburgh USA, 1983 (code DE8401399), 735.

34. Meuzelaar HLC, Mclennon WH, Cady CC, Metcalf GS, Windig W, Thurgood JR, Hill GR, Am Chem Soc - Division of Fuel Chemistry, 1984 _25(5)_, 167.

35. Fredericks PM, Warbrooke P, Wilson MA, Organic Geochemistry, 1983, _5(3)_, 89.

36. Bend SL, Edwards IAS, Marsh H, Am. Chem. Soc. - Division of Fuel Chemistry, 1989, _34(3)_, 923.

37. Wheeler RV, J Chem Soc, 1918, _113_, 945.

38. Haldane JS, Trans Inst Min Eng, 1916, 53, 194.

39. Sevenster PG, Fuel, 1961, 40, 7.

40. Jones RE, Townend DTA, J Soc Chem Industr, 1949, 68, 197.

41. Chakravorty SL, J Min Met Fuels, 1960, 8, 1.

42. Chamberlain EAC, Barrass G, Thirlaway JT, Fuel, 1976, 55, 217.

43. Cole DA, Herman RG, Simmons GW, Kleir K, in 'Proc. of Intern Conf. on Coal Sci.', Sydney Australia, 1985, 691-694.

44. Dack SW, Hobday MD, Smith TD, Pilbrow JR, Fuel, 1983, 62(12), 1510.

45. Dack SW, Hobday MD, Smith TD, Pilbrow JR, Fuel, 1984, 63(1), 39.

46. Petarca L, Tognotti L, Zanelli S, Bertozzi G, in '21st International Symposium on Combustion', Munich West Germany, 1986, 193-201.

47. Shanina EL, Roginskii VA, Miller VB, Solid Fuel Chemistry (USSR), 1983, 17(4), 49.

48. Polat S, Harris IJ, Fuel, 1984, 63(5), 669.

49. van Krevelen DW, 'Coal', Elsevier, 1981, 239-240.

50. Jones RE, Townend DTA, J Soc Chem Industr, 1949, 68, 197.

51. Jensen EJ, Melnyk N, Wood JC, Berkowitz N, ACS Adv Chem Ser, 1966, 55, 621.

52. Wender I, Heredy LA, Neuworht MB, Dryden IGC, in 'Chemistry of Coal Utilization - Second Supplementary Volume', editor Elliott MA, J Wiley & Sons, 1981, 425-523.

53. Essenhigh RH, in 'Chemistry of Coal Utilization - Second Supplementary Volume', editor Elliott MA, J Wiley & Sons, 1981, 1153-1312.

54. Juntgen H, van Heek KH, Fuel, 1968, 47, 103.

55. Chamberlain EAC, Hall DA, Thirlaway JT, The Min Eng, 1970, 130(121), 1.

56. Tashiro J, Kono M, Takakuwa L, J Min and Met Inst of Japan, 1971, 87, 395.

57. Kim AG, U.S. Bureau of Mine Report 7965, 1974.

58. Street PJ, Smalley J, Cunningham ATS, Jnl of Inst of Fuel, 1975, _48_, 146.

59. Karsner GG, Perlmutter DD, Fuel, 1982, _61(1)_, 29.

60. Karsner GG, Perlmutter DD, Fuel, 1982, _61(1)_, 35.

61. Whiting LF, Langvardt PW, Anal Chem,

62. Herod AA, Smith CA, Fuel, 1985, _64_, 281.

63. Burchill P, Richards DG, Warrington SB, Fuel, 1990, _69_, 950.

64. Gibson S, PhD Thesis, Trent Polytechnic, CNAA, 1988.

65. Carpenter DL, Giddings DS, Fuel, 1964, _43($)_, 247.

66. Banerjee SC, Banerjee BD, Chakravorty RN, Fuel, 1970, _49_, 324.

67. van Krevelen DW, 'Coal', Elsevier, 1981, 242.

68. Banerjee SC, Chakravorty RN, J Mines, Metals & Fuels, 1967, 1.

69. Falcon RMS, Min Sci Eng, 1978, _10_, 28.

70. 'Preventing, Combatting and Stopping Off of Fires Arising from Spontaneous Combustion', Safety and Health Commission for the Mining and Other Extractive Industries, Doc No 6482/13/82e, 1985.

71. Plot R, 'Spontaneous Combustion in Heaps', in 'History of Staffordshire' editor Plot R, 1686.

72. Schmidt LD, Elder JL, Ind & Eng Chem, 1940, 249.

73. Lamplough FES, Hill MA, Trans Inst Min Eng, 1912, _45_, 529.

74. Coward HF, 'Research on Spontaneous Combustion in Mines - A Review', SMRE Research Report No 142, 1952.

75. Coward HF, 'A Review of the Research on Spontaneous Combustion of Coal in Mines', Res Rep Safety in Mines, 1957.

76. Graham JI, Trans Inst Min Eng, 1914, _48_, 521.

77. Scott GS, 'Anthracite Mine Fires : Their Behaviour and Control', U.S. Bureau of Mines Bulletin 455, 1944.

78. Bhattacharya KK, Fuel, 1971, _50(4)_, 367.

79. Mukherjee PH, Lahiri A, Fuel, 1957, 35, 176.

80. Bachelor FW, Majumdar A, Buckmaster HA, Duzmal T, Chakravorty RN, in 'Intern. Conf. on Coal Science', editor Mouljin JA, Elsevier, 1987, 427.

81. Cudmore JF, Sanders RH, 'Spontaneous Combustion of Coal Mine Fires and Interpretation of Mine Gases', 1984, Australian Coal Industry Research Laboratories, Report No 84-10.

82. 'Hazardous Gases Underground', British Coal Corporation, 1990.

83. 'The Tube Bundle Technique for the Continuous Monitoring of Mine Air', NCB Scientific Control Report No 622413, 1977.

84. Herbert MJ, in 'Proc. of 23rd Intern. Conf. on Safety in Mines Research Institutes', US Bureau of Mines, 1989, 200.

85. McCormick G, Jnl of the Operational Research Soc, 1986, 37(6), 591.

86. Hertzburgh M, 'Mine Fire Detection', USBM IC-8768, 1978, 38.

87. Brown N, 'Safety and Legislation : Underground Mine Fires, April 1987 - September 1988', Internal British Coal HQTD Report.

88. 'Ventilation in Coal Mines - A Handbook for Colliery Ventilation Officers', National Coal Board, 1979, 106.

89. Jones K, MSc Thesis, University of Wales, 1970.

90. Pritchard FWP, 'Measurements of Coal Seam Gas Content from Surface Boreholes', NCB Internal Report No 78/19, 1978.

91. Creedy DP, PhD Thesis, University of Wales, 1985.

92. Gedenk R, Forschr Geol Rhainld u Westf, 1963, 11, 205.

93. Dunmore R, 'Proc. Intern. Mine Vent. Congress', Mine Vent Soc of South Africa, 1975, 1117.

94. Braithwaite A, Smith FJ, 'Chromatographic Methods', Chapman and Hall, 1985.

95. Littlewood AB, 'Gas Chromatography', Academic Press, 1970.

96. Snyder LR, 'Principles of Adsorption Chromatography', Marcel Dekker, 1968.

97. Perry JA, 'Introduction to Analytical Gas Chromatography', Marcel Dekker, 1981.

98. Heftmann E, 'Chromatography - Journal of Chromatography Library Volume 22A', Elsevier, 1983.

99. Grob RL, 'Modern Practice of Gas Chromatography', John Wiley & sons, 1985.

100. Jennings W, 'Analytical Gas Chromatography', Academic Press, 1987.

101. Guichon G, Guillemin CL, 'Quantitative Gas Chromatography - Journal of Chromatography Volume 42', Elsevier, 1988.

102. Poole CF, Schuette SA, 'Contemporary Practice of Chromatography', Elsevier, 1984.

103. Dressler M, 'Selective Gas Chromatographic Detectors - Journal of Chromatography Volume 36', Elsevier, 1986.

104. Schoenmakers PJ, 'Optimisation of Chromatographic Selectivity - Journal of Chromatographic Library Volume 35', Elsevier, 1986.

105. Supina WR, Rose LP, Jnl of Chrom Sci, 1970, 8, 214.

106. Rohrshneider L, J Chrom, 1966, 22, 6.

107. McReynoulds W, J Chrom Sci, 1970, 8, 685.

108. Burns S, Hawkes SJ, Jnl of Chrom Sci, 1977, 15, 185.

109. Scott RPW, in 'Advances in Chromatography (Volume 9)', editors Giddings JC, Keller RA, Marcel Dekker, 1970, 193-214.

110. Morgan SL, Deming SN, Jnl of Chrom, 1975, 112, 267.

111. Watson MW, Carr PW, Anal Chem, 1979, 51(11), 1835.

112. Berridge JC, J Chrom, 1982, 244, 1.

113. Hartwick RA, Jnl of Chrom Sci, 1989, 27(4), 161.

114. Sandra P, David F, Proot M, Diricks G, Verstappe M, Verzele M, High Res Chrom & Chrom Commun, 1985, 8, 782.

115. Freeman RR, Kukla D, Jnl of Chrom Sci, 1986, 24, 392.

116. Laub RJ, Purnell JH, J Chrom, 1975, 112, 71.

117. Laub RJ, Purnell JH, Anal Chem, 1976, 48(6), 799.

118. Laub RJ, Purnell JH, Anal Chem, 1976, <u>48(12)</u>, 1720.

119. Price GJ, in 'Advances in Chromatography (Volume 28)', editors Giddings JC, Grushka E, Brown PR, Marcel Dekker, 1989, 113-163.

120. Martin AJP, Synge RLM, J Biochem, 1941, <u>35</u>, 1358.

121. Fritz JS, Scott DM, Jnl of Chrom, 1983, <u>271</u>, 193.

122. Karol PJ, Anal Chem, 1989, <u>61</u>, 1937.

123. van Deemter JJ, Zinderweg FJ, Klinkenberg A, Chem Eng Soc, 1956, <u>5</u>, 271.

124. Giddings JC, Anal Chem, 1965, <u>35</u>, 2215.

125. Mindrup R, Jnl of Chrom Sci, 1978, <u>16</u>, 380.

126. Cowper CJ, DeRose AJ, 'The Analysis of Gases by Chromatography', Pergamon Press, 1983.

127. Dave SB, Jnl of Chrom Sci, 1969, <u>7</u>, 389.

128. Hollis OL, Jnl of Chrom Sci, 1973, <u>11</u>, 335.

129. 'Product Bulletin PB-71-204', Waters Associates Inc, Framingham, Massachusettes, USA.

130. Isabell AF, Sawyer DT, Anal Chem, 1969, <u>41(11)</u>, 1381.

131. Guillemin CL, Dleuil M, Cirendini S, Vermont J, Anal Chem, 1971, <u>43(14)</u>, 2015.

132. Bather Jm, Gray RAC, Jnl of Chrom, 1976, <u>122</u>, 159.

133. Scott CG, Jnl of Inst Petr, 1959, <u>45(424)</u>, 118.

134. Scott CG, in 'Gas Chromatography', editor van Swaay M, Butterworth, 1962, 36-62.

135. Phillips CSG, Scott CG, in 'Progress in Gas Chromatography', editor Purnell JH, Wiley Interscience, 1968, 121-152.

136. Moriguchi S, Naito K, Takei S, Jnl of Chrom, 1977, <u>131</u>, 19.

137. Naito K, Kurita R, MoriguchiS, Takei, Jnl of Chrom, 1982, <u>246</u>, 199.

138. Naito K, Endo M, Moriguchi S, Takei S, Jnl of Chrom, 1982, <u>253</u>, 205.

139. de Souza TLC, Lane DC, Bhatia SP, Anal Chem, 1975, <u>47(3)</u>, 543.

140. Feeney M, deGood J, Warren E, Hewlett-Packard Application Note AN228-25.

141. Supelco GC Bulletin 722J.

142. Geiger E, in 'Applied Headspace Gas Chromatography', editor Kolb B, Heyden & Son, 1980, 73-79.

143. Hild J, in 'Applied Headspace Gas Chromatography', editor Kolb B, Heyden & Son, 1980, 89-94.

144. Mandl B, Wullinger F, Binder W, Piendl A, Brauwissenschaft, 1969, 22, 477.

145. Grant DW, Jnl of Chrom, 1976, 122, 107.

146. Cramers CA, Rijks JA, in 'Advances in Chromatography (Volume 17)', editors Giddings JC, Grushka E, Cazes J, Brown PR, Marcel Dekker, 1979, 101-161.

147. Jennings WG, in 'Advances In Chromatography (Volume 20)', editors Giddings JC, Grushka E, Cazes J, Brown PR, Marcel Dekker, 1982, 197-215.

148. MacZura G, Goodboy KP, Koenig JJ, in 'Kirk-Othmer Encyclopedia of Chemical Technology (Volume 2)', John Wiley & Sons, 1978, 218-244.

149. Golay MJE, in 'Gas Chromatography 1957', editors Coates VJ, Noebls HJ, Fagerson IS, Academic Press, 1958, 1-13.

150. Scott RPW, Hazeldean GSF, in 'Gas Chromatography 1960', editor Scott RPW, Butterworth, 1960, 144.

151. Driscoll JN, Jnl of Chrom Sci, 1985, 23, 488.

152. Langhorst ML, Jnl of Chrom Sci, 1981, 19, 98.

153. Barsky JB, Que Hee SS, Clark CS, Am Ind Hyg Assoc J, 1985, 46(1), 9.

154. Burnett CH, Adams DF, Farwell SD, Jnl of Chrom Sci, 1978, 16, 68.

155. Smith RM, 'Gas and Liquid Chromatography in Analytical Chemistry', John Wiley & Sons, 1988, 106.

156. Leveson RC, Barker NJ, Canadian Patent No. 1158891, 1983.

157. Davenport JN, Adlard ER, Jnl of Chrom, 1984, 290, 13.

158. McMurray J, 'Organic Chemistry', Brooks/Cole, 1984, 176-177.

159. Morgan PA, Robertson SD, Unsworth JF, Fuel, 1986, <u>65</u>, 1546.

160. Morgan PA, Robertson SD, Unsworth JF, Fuel, 1987, <u>66</u>, 210.

161. Wade L, Gouws MJ, Min Sci and Tech, 1989, <u>9</u>, 75.

162. Nandy DK, Banerjee DD, Chakravorty RN, J Min Met & Fuels, 1972, 41.

163. LaCount RB, Anderson RA, Friedman S, Blaustein BD, Fuel, 1987, <u>66</u>, 909.

164. Gorbaty ML, George GN, Keleman SR, Fuel, 1990, <u>69</u>, 1065.

165. Hough DC, Sanyal A, Energy World, 1987, <u>146</u>, 7.

166. Nandi BD, Brown TD, Lee GK, Fuel, 1977, <u>56(4)</u>, 125.

167. Tsai C-Y, Scaroni AW, Energy & Fuels, 1987, <u>1(3)</u>, 263.

168. British Standards Institution, BS 1016, 'Analysis and testing of coal and coke', Parts 1-21.

169. Creedy DP, Min Sci and Tech, 1986, <u>3</u>, 141.

170. British Standards Institution, BS 1017, 'Sampling of coal and coke', Part 1.

171. Essenhigh RH, in 'Chemistry of Coal Utilization - Second Supplementary Volume', editor Elliott MA, J Wiley & Sons, 1981, 1234-1249.

172. Rahman M, Hasan AR, Baria DN, in 'Energy for the 21st Century, 20th Intersociety Energy Conversion Engineering Conference', Society of Automotive Engineers, USA, 1985, 631-642.

173. Kaji R, Hishinuma Y, Nakamura Y, Fuel, 1985, <u>64</u>, 297.

174. Kaji R, Hishinuma Y, Nakamura Y, Fuel, 1987, <u>66</u>, 154.

175. Cronauer DC, Ruberto RG, Silver RS, Jenkins RG, Ismail IMK, Schyler D, Fuel, 1983, <u>62</u>, 1116.

176. Carpenter DL, Giddings DG, Fuel, 1964, <u>43</u>, 375.

177. Young BC, Smith IW, in '1987 Intern Conf on Coal Science', editor Mouljin JA, Elsevier, 1987, 793-796.

APPENDIX I

Glossary of Chromatographic Terms and Mathematical Definitions

AI.1 Definitions of Chromatographic Terms

t_0 column dead-time.

t_R solute retention time from injection.

t_R' corrected solute retention time.

K   distribution ratio.

k   solute partition ratio (also termed capacity factor).

α relative partition ratio (relative capacity factor).

h   height equivalent to a theoretical plate (HETP).

n   number of theoretical plates.

N_{eff} number of effective theoretical plates.

N_{req} number of theoretical plates required to effect a separation between peaks.

l   column length.

u_{lin} average linear carrier gas velocity.

$w_{0.5}$ width of peak at half height.

R_s resolution of two peaks.

A_s peak asymmetry (skew factor).

R   gas constant.

T   temperature.

ΔH_{ads} enthalpy of adsorption.

RI   retention index.

t_{Rn}' corrected retention time of n-alkane eluted immediately before analyte.

t_{Rn+1}' corrected retention time of n-alkane eluted immediately after analyte.

AI.2 Mathematical Formulae for Calculating Chromatography Terms

$$t_R' = t_R - t_0 \quad \dots\dots\dots\dots\dots\dots\dots\dots\dots\dots\dots \quad (1)$$

$$u_{lin} = 1/t_0 \quad \dots\dots\dots\dots\dots\dots\dots\dots\dots\dots\dots\dots \quad (2)$$

$$k = \frac{t_R - t_0}{t_0} = \frac{t_R'}{t_0} \quad \dots\dots\dots\dots\dots\dots\dots\dots \quad (3)$$

$$\alpha = k_1/k_2 \quad \dots\dots\dots\dots\dots\dots\dots\dots\dots\dots\dots \quad (4)$$

$$h = 1/n \quad \dots\dots\dots\dots\dots\dots\dots\dots\dots\dots\dots\dots \quad (5)$$

$$n = 5.54 \left(\frac{t_R}{w_{0.5}} \right)^2 \quad \dots\dots\dots\dots\dots\dots\dots\dots \quad (6)$$

$$N_{eff} = 16 \left(\frac{t_R'}{w_{0.5}} \right)^2 \quad \dots\dots\dots\dots\dots\dots\dots\dots \quad (7)$$

$$N_{req} = 16 \, R_s^2 \left(\frac{\alpha}{\alpha-1} \right)^2 \left(\frac{k+1}{k} \right)^2 \quad \dots\dots\dots\dots\dots \quad (8)$$

$$R_s = \frac{2 \, (t_{R1} - t_{R2})}{(w_1 + w_2)} \quad \dots\dots\dots\dots\dots\dots\dots\dots \quad (9)$$

$$R_s = \frac{N}{4} \frac{(\alpha-1)}{\alpha} \frac{k}{(k+1)} \quad \dots\dots\dots\dots\dots\dots\dots \quad (10)$$

$$\ln(k) = \frac{-(\Delta H_{ads})}{(R \, T)} + c \quad \dots\dots\dots\dots\dots\dots\dots\dots \quad (11)$$

$$RI = (n \, 100) + \frac{\log\left(t_R'\right) - \log\left(t_{Rn}'\right)}{\log\left(t_{Rn+1}'\right) - \log\left(t_{Rn}'\right)} \quad \dots\dots\dots\dots\dots \quad (12)$$

AI.3   Measurements Used to Calculate Chromatography Terms

$$A_s = b/a$$

$$n = 5.54 \cdot \left(\frac{t_R}{w_{0.5}} \right)^2$$

$$R_s = \frac{2 \ (t_{R1} - t_{R2})}{(w_1 + w_2)}$$
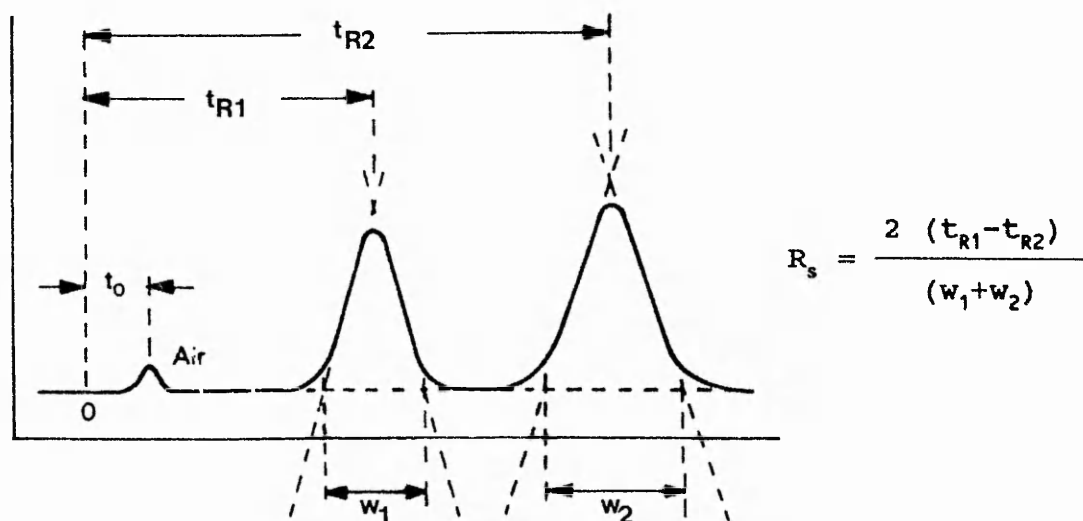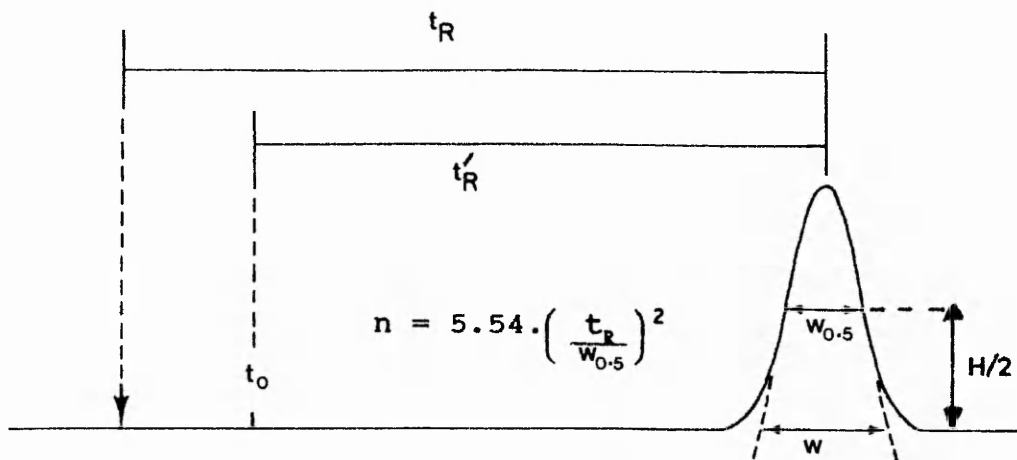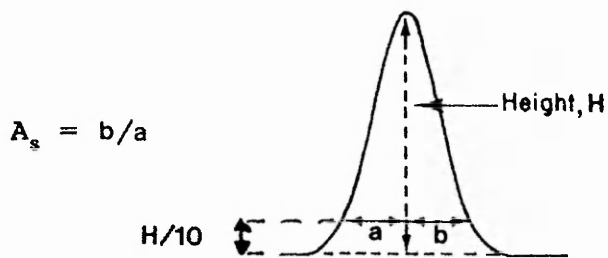
APPENDIX II

A Novel and Rapid Method for the Estimation of Dead-Time

AII.1   Introduction

The novel rapid method developed for the estimation of dead-time herein referred to as the 'carbon number method' is based on the linearity of corrected retention times of a homologous series of alkanes.

In order to evaluate a range of chromatographic columns for their suitability in specific separations a knowledge of the column dead-time (t_0) is necessary. This allows a number of chromatographic functions to be accurately determined including the partition ratio (k) of a component, Kovats retention indices and the mean linear carrier gas velocity (u_{lin}). Historically, several different approaches have been applied to calculate the column dead-time and these may be classified as described below.

Graphical methods involve manually plotting the carbon number of a homologous series versus the logarithm of its' adjusted retention time (t_R'). Empirical variation of the dead-time which therefore causes t_R' to fluctuate is carried out to linearise the plot. This method was first introduced by Evans and Smith but since it is relatively inaccurate and time consuming it cannot be considered practical [A1].

Direct methods utilise a solute to which the GC detector responds and which is assumed to be completely unretained by the GC column. Initially air was considered to be such a solute, but its use is limited due to lack of response by most common GC detectors [A2]. Methane was considered an

adequate substitute, and many workers have used this gas to calculate the dead-time [A3-A5]. More recently the accuracy of the column dead-time calculated by utilising either air or methane has been disputed. Several authors have reported that inaccurate column dead-times calculated by these methods have been due to the retention of the air and methane on the chromatographic column employed [A6,A7]. It is generally accepted that if gas-solid chromatography, low temperatures or high pressures are employed the methane would be retained to a greater degree [A8]. The use of a range of inert gases has been reported by a number of authors [A9,A10]. Several of these found neon to possess the least retention, with nitrogen, hydrogen and argon being slightly more retarded. Although neon apparently represents an accurate method for calculating the column dead-time it has the disadvantage of requiring the relatively sophisticated technique of GC-MS for detection.

Classical methods require simple equations to be solved for a small series of homologues. In the technique of Peterson and Hirsch three evenly spaced homologues were related to an arbitrary reference origin (x_0) [A11]. The distances were measured from x_0 on the chromatogram and the true dead-time (t_0) calculated using equation (13).

$$ d = \frac{(t_{n+1})^2 - (t_n . t_{n+2})}{t_{n+2} + t_n - 2t_{n+1}} \dots \dots \dots \dots \dots \dots \quad (13) $$

where t_n, t_{n+1}, t_{n+2} are the retention times of 3 homologues, and $t_0 = x_0 + d$.

The column dead-time was determined by measuring the

-252-

distance (d) from the arbitrary origin (x_0). Several workers have sought to improve the original method of Peterson and Hirsch [A12-A16]. The most significant of these was by Toth and Zala whose method gave similar results to a statistical method of Grobler and Balizs [A16,A17]. Another method requiring 3 homologues to determine the dead-time termed the "approximate series method" was described by Dominguez et al [A6]. This technique required a more complicated series of calculations but produced no improvement on those classical methods previously discussed.

Statisitical methods are more complex than those previously discussed and require the use of microprocessor based systems. Grobler and Balizs developed a procedure which required the solution to two simultaneous linear regressions [A17]. Initially linear regression of equation (14) yields b as the slope of a graph of $\ln(t_{RZ+1} - t_{RZ})$ versus z, and a second linear regression of equation (15) yields t_0 by plotting $\ln(t_{RZ})$ versus z.

$$\ln(t_{RZ+1}) - (t_{RZ}) = \ln(A) + bz \dots\dots\dots\dots\dots (14)$$
$$\ln(t_{RZ}) = \ln(t_0) + z\ln(cb) \dots\dots\dots\dots (15)$$

where t_{RZ} and t_{RZ+1} are retention times of successive homologues.

This method was extended by van Tulder et al to use equidistant carbon numbers rather than consecutive homologues [A18].

The use of iterative methods was studied by Guardino et al, who described a method which starts with an estimate of the column dead-time allowing the adjusted retention times

to be calculated [A19]. A linear regression of equation (16) was carried out allowing b and c to be calculated thereby producing retention indices for the solutes (calculated as in Appendix I, equation 12).

$$\ln(t_R - t_0) = bz + c \dots\dots\dots\dots\dots\dots\dots\dots\dots\dots (16)$$

The values of retention indices are then subtracted from known values to give a sum of differences. These are compared to preset limits and the value of t_0 incremented or decremented such that the differences are minimised. A disadvantage of this method is that the initial estimate of the dead-time must be less than that of the true mathematical dead-time. Bellas produced a FORTRAN program based on a technique similar to this method, whilst Dominguez et al described an "exact calculator method" which uses the retention times of solutes whose Kovats retention indices are known (eg. n-alkanes) [A20,A6]. A linear regression of the retention times is achieved to determine a new retention time of the least retained compound. A correction factor representing the difference between the two retention times is calculated, and subtracted from all of the retention times of the solutes to produce a new set of retention data. A further linear regression is performed using the new data and the above procedure repeated. After a sufficient number of cycles a final set of adjusted retention times is obtained.

The use of numerical minimisation in the simultaneous non-linear least-squares estimation of dead-time by Nelder and Mead is often termed simplex optimisation [A21]. A

-254-

critical point is that it is necessary to carefully define the objective function that is to be minimised. The method is very complex to program, it may converge on a local rather than global minimum (producing erroneous results), and has a prolonged execution time.

Recently Smith et al showed that the three methods listed below gave identical values of the mathematical dead-time [A8]:

(i) Guardino et al [A19].

(ii) Toth and Zala [A16].

(iii) Flexible simplex method [A21].

Smith et al also showed that these methods gave the most accurate values of dead-time and the method of Guardino et al was the fastest to execute.

AII.2   The Carbon Number Method

The approach adopted in this work for the determination of dead-time is based on a plot of the logarithm of the corrected retention time (t_R') versus the number of carbon atoms, which produces a linear graph for a homologous series of alkanes. This phenomenom can be used to accurately determine the column dead-time (t_0) as described below.

AII.2a   Mathematical Model

The retention times (t_{Rn}) of a homologous series of n-alkanes are accurately recorded on a gas chromatograph. An arbitrary value of the column dead-time (eg. methane

retention time) is then used to determine the corrected retention times (t_R) of the n-alkane series. A plot of the logarithm of these values versus the number of carbon atoms may then be produced. If the column dead-time is varied different corrected retention times are obtained, and it is apparent that the points which produce the line of best fit will be calculated from the most accurate dead-time value. Since the correlation coefficient (r) represents the line of best fit an iterative procedure based on optimising this value by varying the column dead-time allows an accurate measurement of dead-time to be determined. A correlation coefficient of exactly 1 indicates its optimum value.

It is apparent from the theory that the use of low molecular weight alkanes is preferred, since higher carbon numbers require a greater extrapolation and this produces a larger error.

AII.2b   Calculation Procedure Using Spreadsheet

A spreadsheet has been produced which rapidly calculates the column dead-time by the 'carbon number method' described above, and a typical screen display is shown in figure 57. The dead-time calculation is achieved by running a number of consecutive macros, which are listed in the full spreadsheet display illustrated in figure 58. The correlation coefficient as defined by Massart et al is calculated as shown in equation (18) [A22].

$$r_{(x,y)} = \frac{[\Sigma_{i=1}^{n}(x_i - x)(y_i - y)]/(n-1)}{[\Sigma_{i=1}^{n}(x_i - x)^2 \cdot \Sigma_{i=1}^{n}(y_i - y)^2]/(n-1)^2} \quad \ldots\ldots\ldots\ldots (18)$$

-256-

ALKANES	No. C's	Ret Time	tR'	log(tR')
METHANE	1	10.9	1.251	.0972573
ETHANE	2	17.1	7.451	.8722146
PROPANE	3	53.16	43.511	1.638599
BUTANE	4	271.68	262.031	2.418353
PENTANE	5	1548	1538.351	3.187055
mean	3			1.642696

No. of alkanes = 5

Column dead time(secs) = 9.649

Coefficeint of variation = .99999737189   R2= .9999947

To determine column dead time ..... Alt Z

Figure 57   Screen Display of Column Dead-Time Spreadsheet

Spreadsheet columns: A :: B ::C:: D ::E:: F ::G:: H ::I:: J ::K:: L :: M :: N :: O :: P :: Q :: R :: S :: T ::

ALKANES	No. C's	Ret Time	tR'	log(tR')	x-[x]	y-[y]	D & E	(x-[x])^2	(y-[y])^2
METHANE	1	10.9	1.251	.0972573	-2	-1.54544	3.090877	4	2.388380
ETHANE	2	17.1	7.451	.8722146	-1	-.770481	.7704812	1	.5936414
PROPANE	3	53.16	43.511	1.638599	0	-.004097	0	0	.0000168
BUTANE	4	271.68	262.031	2.418353	1	.7756569	.7756569	1	.6016436
PENTANE	5	1548	1538.351	3.187055	2	1.544360	3.088719	4	2.385047
mean	3			1.642696			7.725734	10	5.968729

No. of alkanes = 5

Column dead time(secs) = 9.649   Coeff var(previous)
                                                       .9999974
Coefficient of variation = .99999737189   R2= .9999947   0

To determine column dead time ..... Alt Z

```
(LET F14, F14-0.01)                    (LET F14, F14-0.1)                        (LET F14, F14-1)                         (LET F14, F14-0.001)
(CALC)                                 (CALC)                                    (CALC)                                  (CALC)
(LET L14, F16)                         (LET L14, F16)                            (LET L14, F16)                          (LET L14, F16)
(LET F14, F14-0.01)                    (LET F14, F14-0.1)                        (LET F14, F14-1)                         (LET F14, F14-0.001)
(CALC)                                 (CALC)                                    (CALC)                                  (CALC)
(IF (1-F16)<(1-L14) ) (BRANCH B30)     (IF (1-F16)<(1-L14)) (BRANCH H30)         (IF (1-F16)<(1-L14)) (BRANCH M30)        (IF (1-F16)<(1-L14)) (BRANCH Q30)

(LET F14, F14-0.01)                    (LET F14, F14-0.1)                        (LET F14, F14-1)                         (LET F14, F14-0.001)
(LET L14, F16)                         (LET L14, F16)                            (LET L14, F16)                          (LET L14,F16)
(CALC)                                 (CALC)                                    (CALC)                                  (CALC)
(IF (1-F16)<(1-L14)) (BRANCH B30)      (IF (1-F16)<(1-L14)) (BRANCH H30)         (IF (1-F16)<(1-L14)) (BRANCH M30)        (IF (1-F16)<(1-L14)) (BRANCH Q30)
(IF L14>F16 ) (LET F14, F14+0.02)      (IF L14>F16 ) (LET F14, F14+0.2)          (IF L14>F16 ) (LET F14, F14+2)           (IF L14>F16) (LET F14, F14+0.001)
(IF L14>F16 ) (BRANCH D22)             (IF L14>F16 ) (BRANCH B22)                (IF L14>F16 ) (BRANCH H22)               (CALC)
```

Figure 58   Complete Listing of Column Dead-Time Spreadsheet Including Macros

AII.3   Comparison to Other Methods

Retention data (±0.001second) obtained from the literature for a number of homologous C5-C10 alkanes were used to calculate the column dead-time by the 'carbon number method' [A23]. The resultant dead-time values were compared to similar values calculated by the flexible simplex method as shown in table 26. Statistical analyses of the differences between the calculated dead-times for the two methods was carried out by applying the students t test for 95% confidence limits. The carbon number versus the flexible simplex method yields a mean difference of -0.001±0.019 seconds. These results indicate good agreement between the carbon number and simplex methods, validating the carbon number method for the calculation of an accurate dead-time value for the higher alkanes (C5-C10).

Retention data produced by Smith et al has also been utilised to calculate the column dead-time by the carbon number method [A23]. These results agree with the techniques of Guardino et al, Toth and Zala and the flexible simplex method as described by Smith. The time necessary for calculation by each of these techniques is:

    Guardino et al .... 2.04 mins.

    Toth and Zala .... 6.00 mins.

    Simplex method .... 20.14 mins.

    Carbon number method .... 0.21 mins.

It may therefore be concluded that the carbon number method described in this work is an accurate and rapid technique of determining the column dead-time.

Table 26   Comparison of Methods of Calculating
Column Dead-Time

REPLICATE ANALYSIS NUMBER	CALCULATION OF COLUMN DEAD-TIME (secs)		
	Flexible Simplex	Carbon Number	Difference
1	53.769	53.626	0.143
2	55.067	55.015	0.052
3	54.478	54.510	-0.032
4	55.007	54.973	0.034
5	54.625	54.607	0.018
6	54.255	54.312	-0.057
7	53.812	53.692	0.120
8	53.932	53.908	0.024
9	54.180	54.256	-0.076
10	54.250	54.240	0.010
11	53.968	54.046	-0.078
12	53.670	53.605	0.065
13	53.835	53.873	-0.038
14	53.402	53.267	0.135
15	53.903	53.955	-0.052
16	53.546	53.590	-0.044
17	53.833	53.856	-0.023
18	53.871	53.870	0.001
Mean	**54.078**	**54.067**	
19	62.070	62.054	0.016
20	62.070	61.983	0.087
21	62.033	62.046	-0.013
22	61.151	61.131	0.020
23	60.833	60.834	-0.001
24	61.089	61.123	-0.034
25	61.642	61.723	-0.081
26	61.606	61.644	-0.038
27	60.870	60.844	0.026
28	61.063	61.073	-0.010
29	60.553	60.543	0.010
30	60.768	60.750	0.018
31	59.943	59.853	0.090
32	59.651	59.587	0.064
Mean	**61.096**	**61.085**	
33	77.489	77.482	0.007
34	76.440	76.336	0.104
35	76.415	76.373	0.042
36	75.474	75.510	-0.036
37	75.530	75.509	0.021
38	75.828	75.937	-0.109
39	75.986	76.096	-0.110
40	75.511	75.504	0.007
41	75.486	75.495	-0.009
42	75.053	75.009	0.044
43	75.384	75.491	-0.107
44	74.421	74.483	-0.062
45	75.077	75.185	-0.108
46	73.965	74.030	-0.065
Mean	**75.576**	**75.603**	

AII.4   Linearity of the Plot of Logarithm of Corrected Retention Time Versus Carbon Number

The work in this section confirms the linearity of a plot of logarithm of corrected retention time versus carbon number. A number of workers have described an apparent non-linearity of this plot, specifically for the lower alkanes (C1-C4) [A7,A8,A25]. In this work such a plot produced a linear graph for the C1-C5 alkanes as demonstrated in figure 59. This linearity is substantiated by values of the square of the correlation coefficient (r^2) which varied from 0.999996 to 0.999991 for the experimental data achieved on the five homologous n-alkanes. Such a linear plot is not surprising since the rapid method used in this work is based on optimising the linearity.

It was therefore necesary to test the linearity of the plot of logarithm of corrected retention time versus carbon number and investigate the minimum number of alkanes required. Therefore a gas mixture containing C1-C4 n-alkanes was analysed utilising a packed column (2m long, alumina/NaCl 2%w/w) and photoionisation detector (10.2eV HNU PID). This gave a negative response for methane and ethane, but a retention time for these two solutes was readily obtained. Furthermore, introduction of the sample produced an injection peak at the detector which corresponded to the column dead-time value as illustrated in figure 60. Hence the experimental measurement of column dead-time could be compared to the rapid calculation of column dead-time described in this work, as illustrated in table 27. If detailed consideration of the injection peak
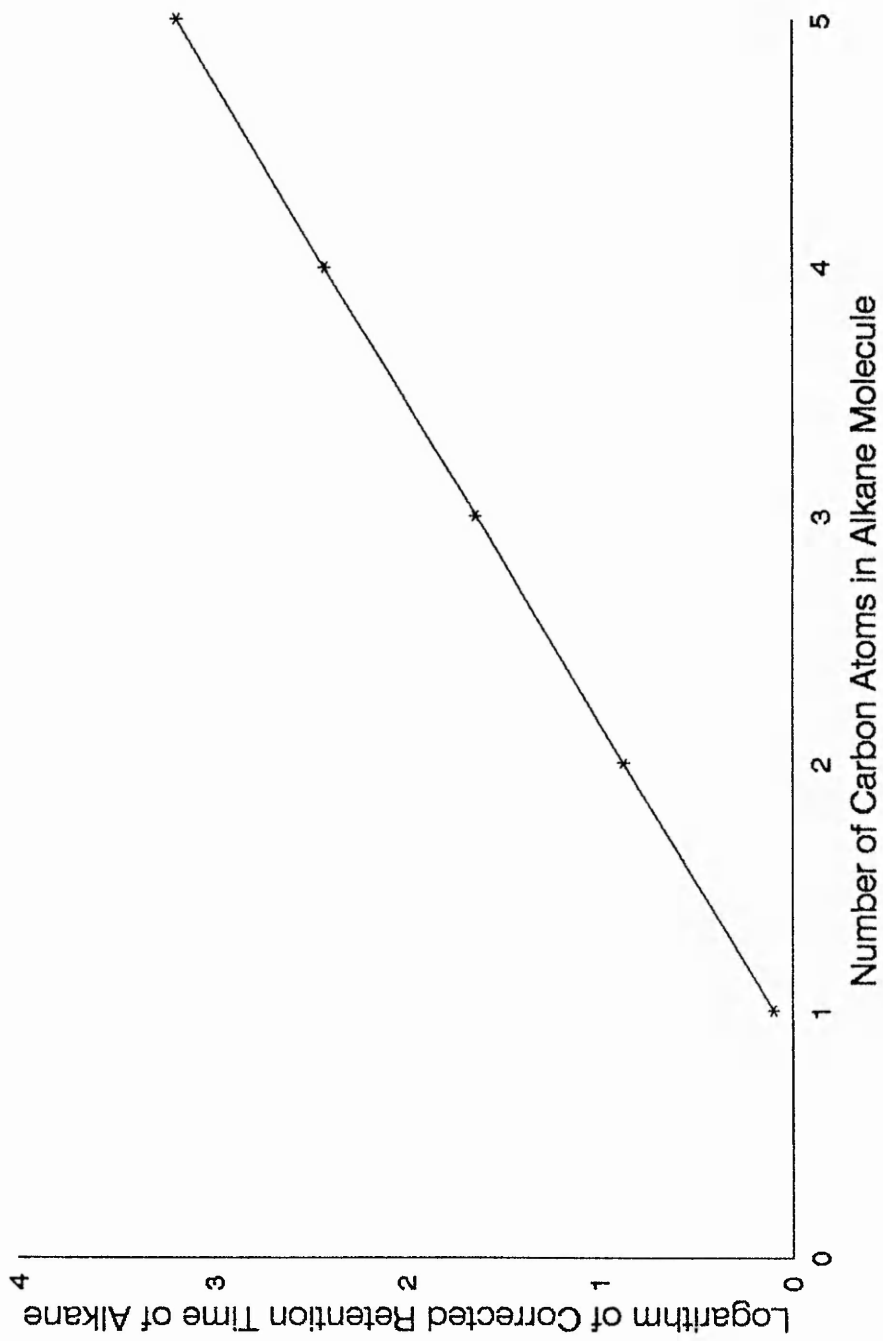
Figure 59   Plot of Logarithm of Corrected Retention Time Versus Carbon Number

-262-
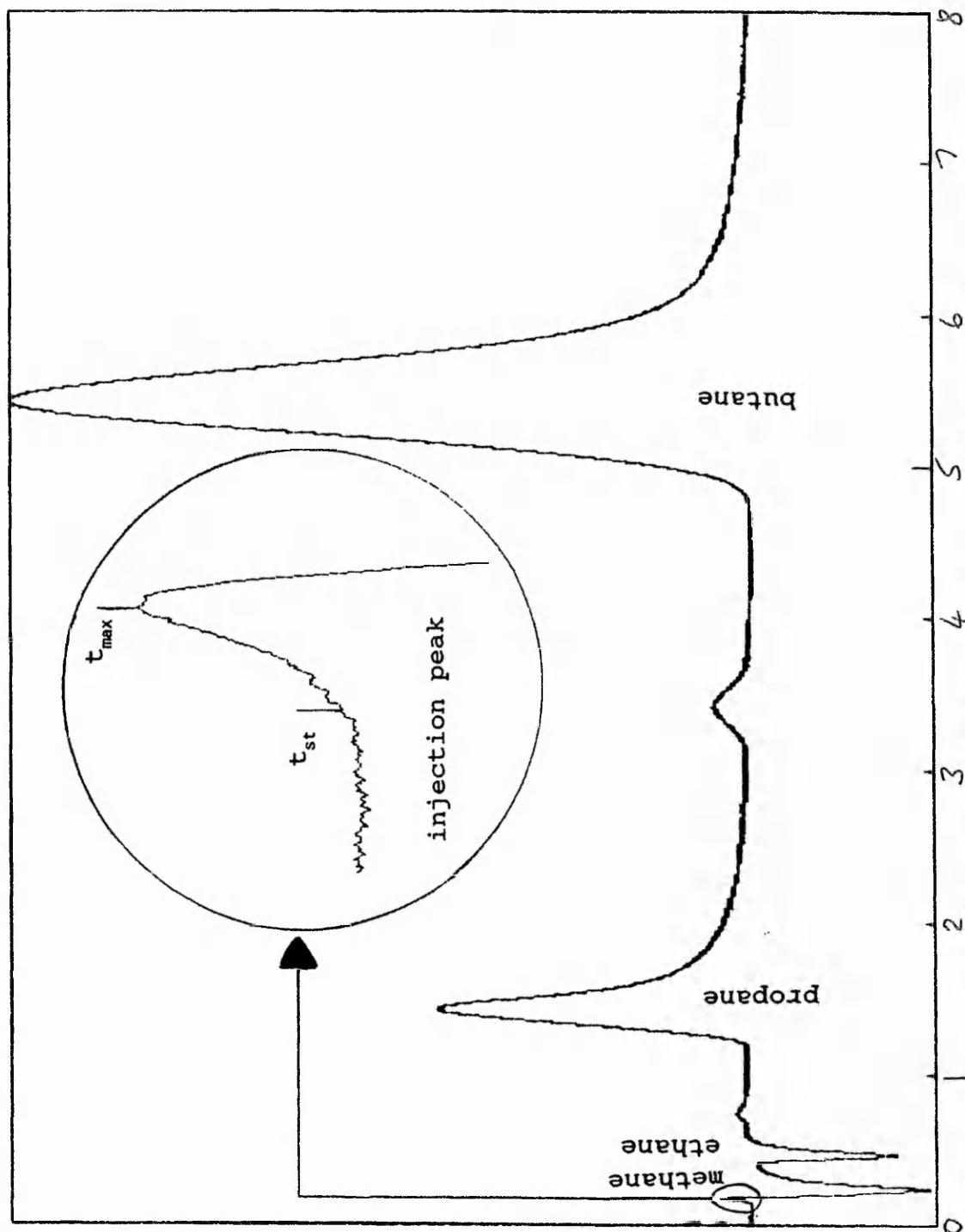
Figure 60   Chromatogram Illustrating 10.2eV PID Response to Alkanes

RETENTION
TIME (MINS)

is made, accurate measurement of the column dead-time is clearly given by the 'leading edge' of this peak. This work therefore substantiates the validity of the rapid dead-time calculation method utilising the lower hydrocarbons (C1-C4). A correlation coefficient squared value of 0.999998 was obtained for the carbon number plot using this data demonstrating a linear relationship of $\log(t_R')$ versus carbon number.

Table 27   Comparison of Column Dead Times of n-Alkanes

Retention Times (seconds)				Dead Time	Inject peak maximum t_{max}	Inject peak start t_{st}
C1	C2	C3	C4			
15.36	28.80	86.10	326.10	11.18	11.94	11.20
15.42	28.98	86.34	323.94	11.15	12.00	11.15

AII.5   Conclusions

A comparison of the carbon number method with the flexible simplex method that is known to be accurate [A24] revealed a dead-time range of -0.020 to 0.018 seconds at 95% confidence limits. Therefore this method of calculating the column dead-time from the retention data of higher alkanes (C5-C10) has produced results within an acceptable degree of accuracy with reference to the simplex method. It has also been shown that a minimum of 4 n-alkanes are required for the calculation of an accurate dead-time value. Furthermore, this method requires considerably less time to calculate the column dead-time than other techniques in order to produce data of the same accuracy.

An apparent non-linearity of the plot of logarithm of adjusted retention times versus carbon number for alkanes lower than pentane has been described in the literature [A7,A8,A22]. Work carried out in section 4 of this Appendix indicated that such a plot including methane is linear since the correlation coefficient squared values for the lower alkanes approached unity. Since accurate retention data (±0.01secs) and good peak shapes were obtained the continuation of linearity down to methane is expected, contrary to data used by other workers.

APPENDIX III

Software Listings of C Programs Controlling Valve
Sampling Systems

Each of the valve sampling systems was controlled by a
C program, the source code of which has been listed below.
In order to achieve the necessary timing control, each C
program was linked to the 't_counts.c' program. After the
files had been linked together to produce an object file,
this was compiled into an executable file (ie. *.exe) by
using a Lattice C complier.

```
/*  t_counts.c -- return current tick from clock  */

#include "\lc\header\dos.h"
#define INT_TIME 0x1A

long t_counts()
{
 union REGS rin, rout;
 long tc;

 rin.h.ah = 0;
 int86(INT_TIME, &rin, &rout);
 tc = ( (long) rout.x.cx ) << 16;
 tc += rout.x.dx;
 return tc;
}
```

```c
/*   valvmk1.c -- Mark 1 Valve Sampling Control Software   */

#include "\lc\header\dos.h"
#include "\lc\header\stdio.h"
#include "\lc\header\string.h"
#include "\lc\header\fcntl.h"

int ba=784,pa=784,pb=785,pc=786,cr=787,dr=788,x,y;
long i,t_counts();
main()
{
 long stim,ftim;
 outp(cr,128);
 outp(dr,8);
 stim=t_counts();
 printf("Sample injected      ");
 relon(0);

 for (i=0;i<100000;i++)
 {
  ftim=t_counts();
  if ((ftim-stim)/18.2 > 2.95 && (ftim-stim)/18.2 < 3.05 )

  {
   reloff(0);
   i=100001;
  }
 }
 printf("End sample loop flush\n");
}

relon(x)
{
 y=(x*2)+1;
 outp(pa,48+y);
 outp(pc,1);
 outp(pc,5);
 outp(pc,1);
 outp(pa,48+y);
 outp(pc,1);
 outp(pc,5);
 outp(pc,1);
}

reloff(x)
{
 y=(x*2);
 outp(pa,48+y);
 outp(pc,1);
 outp(pc,5);
 outp(pc,1);
 outp(pa,48+y);
 outp(pc,1);
 outp(pc,5);
 outp(pc,1);
}
```

```c
/*   valvmk2.c -- Mark 2 Valve Sampling Control Software
*/

#include "\lc\header\dos.h"
#include "\lc\header\stdio.h"
#include "\lc\header\string.h"
#include "\lc\header\fcntl.h"

int ba=784,pa=784,pb=785,pc=786,cr=787,dr=788,x,y;
long i,t_counts();

main()
{
 long stim,ftim;

 outp(cr,128);
 outp(dr,8);

 stim=t_counts();

 printf("Sample injected\n");
 relon(0);
 relon(1);                            /* STEP 2 ... sample
injection  */

 for (i=0;i<10000000;i++)
 {
  ftim=t_counts();
  if ((ftim-stim)/18.2 > 5.95 && (ftim-stim)/18.2 < 6.05 )
  {
   reloff(1);                         /* STEP 3 ... sample loop
flushed  */
   printf("Sample loop flushed \n");
  }
  if ((ftim-stim)/18.2  > 179.95 && (ftim-stim)/18.2 <
180.05 )
  {
   reloff(0);                    /* STEP 4  */
   i=10000001;
  }

 }
 printf("End of valve switching.\n");
}
```

```
/*    valvmk2.c --- continued    */
relon(x)
{
 y=(x*2)+1;
 outp(pa,48+y);
 outp(pc,1);
 outp(pc,5);
 outp(pc,1);
 outp(pa,48+y);
 outp(pc,1);
 outp(pc,5);
 outp(pc,1);
}



reloff(x)
{
 y=(x*2);
 outp(pa,48+y);
 outp(pc,1);
 outp(pc,5);
 outp(pc,1);
 outp(pa,48+y);
 outp(pc,1);
 outp(pc,5);
 outp(pc,1);
}
```

```c
/*  valvmk3.c -- Mark 3 Valve Sampling Control Software  */

#include "\lc\header\dos.h"
#include "\lc\header\stdio.h"
#include "\lc\header\string.h"
#include "\lc\header\fcntl.h"

int ba=784,pa=784,pb=785,pc=786,cr=787,dr=788,x,y;

long i,t_counts();
main()
{
 long stim,ftim;

 outp(cr,128);
 outp(dr,8);

 stim=t_counts();

 printf("Sample injected\n");

 relon(0);  /*  controls valves 1, 2 */
 relon(1);  /*  controls valve 3. STEP 2...sample injection
*/

 for (i=0;i<10000000;i++)
 {
  ftim=t_counts();
  if ((ftim-stim)/18.2 > 5.95 && (ftim-stim)/18.2 < 6.05 )
  {
   reloff(0); /*  controls valves 1, 2 */
reloff(1);  /*   controls valve 3. STEP 3...sample loop
flushed */ printf("Sample loop flushed\n");
  }
  if ((ftim-stim)/18.2 > 24.95 && (ftim-stim)/18.2 < 25.05
)
  {
relon(0); /* controls valve 1,2 */
relon(3); /* controls valves 3,4,5. STEP 4...pre-column
back-flushed */ printf("Pre-column back-flushed\n");
  }
  if  ((ftim-stim)/18.2  >  179.95  &&  (ftim-stim)/18.2  <
180.05 )
  {
reloff(0); /* controls valve 1,2 */
reloff(3);  /*  controls  valves  3,4,5.  STEP  5...end  of
analysis */ i=10000001;
  }

 }
 printf("End of valve switching.\n");
}
```

```
/*   valvmk3.c --- continued        */
relon(x)
{
 y=(x*2)+1;
 outp(pa,48+y);
 outp(pc,1);
 outp(pc,5);
 outp(pc,1);
 outp(pa,48+y);
 outp(pc,1);
 outp(pc,5);
 outp(pc,1);
}


reloff(x)
{
 y=(x*2);
 outp(pa,48+y);
 outp(pc,1);
 outp(pc,5);
 outp(pc,1);
 outp(pa,48+y);
 outp(pc,1);
 outp(pc,5);
 outp(pc,1);
}
```

Calculation of Vapour Concentration by Headspace Technique

A method of preparing vapour mixtures of known concentration was developed in order to calibrate GC analytical equipment. A static method was utilised since this uses readily available laboratory apparatus.

AIV.1   Technique

Approximately 1ml of the liquid analyte was placed in a 5ml sample vial and sealed with an air-tight septum seal. A blank needle was inserted through the septum just into the air space at the top of the vial, as in figure 61. This maintained a uniform pressure in the vial during the withdrawal of vapour by allowing the ingress of air. The required volume of analyte vapour was withdrawn into a gas-tight syringe by inserting the syringe through the septum of the vial, figure 61. This gas sample was then injected into a Tedlar bag containing a measured volume of the diluent gas (typically nitrogen or air). Variation of the syringe and Tedlar bag volumes allowed the required gas concentration to be achieved by a spreadsheet calculation described in section AIV.2.

An accurate measurement of the room temperature at which the headspace vapour sample was taken was obtained. This was necessary since the vapour phase analyte concentration which is determined by the vapour-liquid equilibrium is dependent on temperature (equation 19, p.274).

Needle allowing slight ventilation

100μl gas-tight syringe

Thermometer

septum

liquid sample

1 litre gas-tight syringe

5 litre tedlar bag
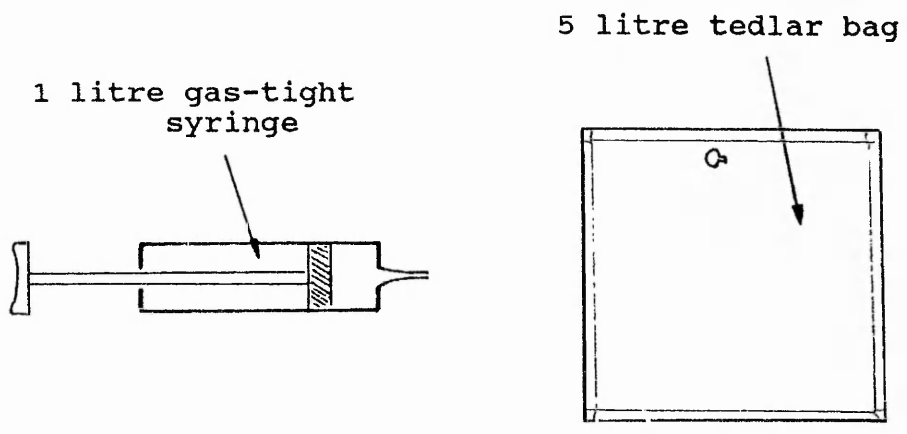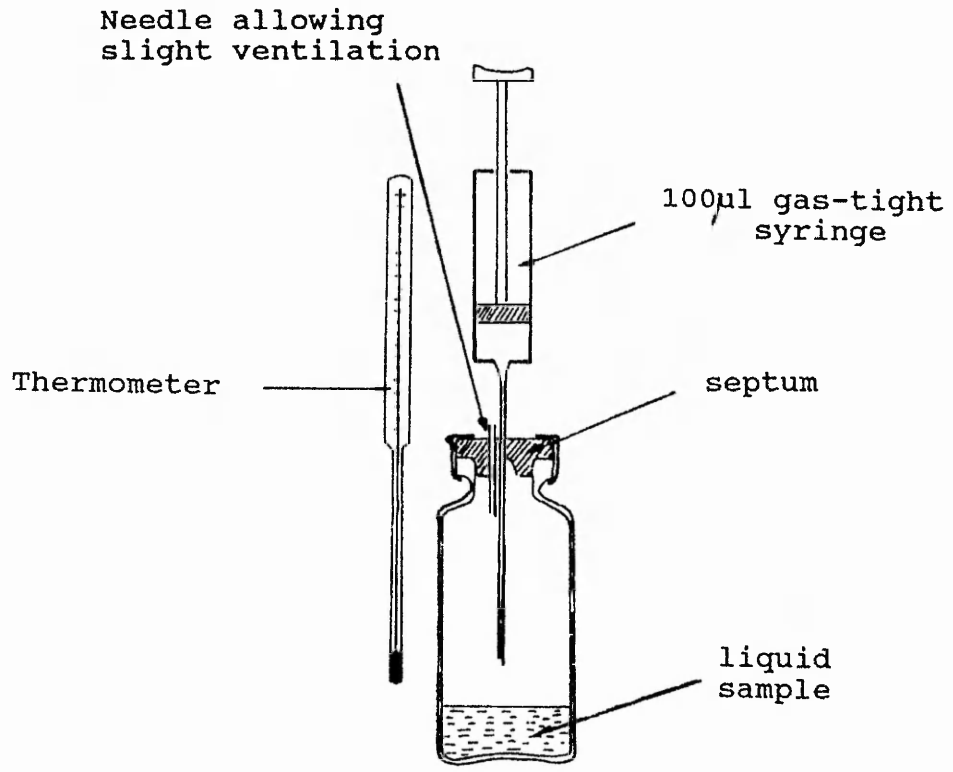
AIV.2 Spreadsheet Calculation of Vapour Concentration

The spreadsheet was developed to calculate vapour pressure at the temperature it was taken. This allowed the analyte vapour concentration in the mixture to be calculated.

The vapour pressure of each analyte compound at a measured temperature was calculated by applying the Antoine equation, as illustrated in equation (19).

$$\log_{10} P = A - [B/(t+C)] \dots\dots\dots\dots\dots\dots (19)$$

P, vapour pressure (mm Hg); t, temperature (°C);
A, B, C, constants obtained from literature [25].

The volume occupied by the analyte vapour at the measured temperature could then be calculated by equation (20) (Boyles law) using the vapour pressure determined from equation (19).

$$V_1 = (P_2/P_1).V_2 \dots\dots\dots\dots\dots\dots\dots (20)$$

$$c = (V_1)/(V_{vess}) \dots\dots\dots\dots\dots\dots\dots (21)$$

$$c = (P_2/P_1).(V_2/V_{vess}) \dots\dots\dots\dots\dots (22)$$

V_1 , volume of analyte at atmospheric pressure (μl);
V_2 , volume of headspace (μl);
P_2 , vapour pressure of headspace sample (mm Hg);
P_1 , atmospheric pressure (760mm Hg).
c , concentration (ppm);
V_{vess}, volume of vessel (l).

The concentration (c) of an analyte in the vapour mixture was therefore calculated from equation (21). Alternatively the concentration may be obtained by the sustitution of equation (20) into (21) to form equation (22).

These equations were incorporated into a spreadsheet as illustrated in figure 62. This allowed the concentration of a vapour to be determined by entering the temperature, gas

-275-

	A	B	C	D	E	F	G	H	I	J	K	L
1												
2				HEADSPACE CALIBRATION CALCUATIONS								
3						Solute			Antoine equation constants			Temperatur
4			Room	Vapour	Solute	Headspace	Vessel					Range (
5			Temp	Press	Conc	Volume	Volume		A	B	C	Applicable
6			(deg C)	(mm Hg)	(ppm)	(microL)	(Litres)					
7												
8	ACETALDEHYDE		24.5	(10^(I8-(J8/(C8+K8))))	(D8/760)*(F8/G8)	100	5		8.0634	1637.083	295.467	-0.20 to 3
9												
10												
11	ACETONE		24.5	(10^(I11-(J11/(C11+K11))))	(D11/760)*(F11/G11)	100	5		7.29958	1312.253	240.705	-13.99 to 2
12												
13	METHANOL		24.5	(10^(I13-(J13/(C13+K13))))	(D13/760)*(F13/G13)	100	5		8.07919	1581.341	239.65	14.90 to 8
14												
15	ETHANOL		24.5	(10^(I15-(J15/(C15+K15))))	(D15/760)*(F15/G15)	100	5		8.24739	1670.409	232.959	0.00 to 7
16												
17	BENZENE		24.5	(10^(I17-(J17/(C17+K17))))	(D17/760)*(F17/G17)	100	5		6.89326	1203.828	219.921	14.55 to 8
18												
19	TOLUENE		24.5	(10^(I19-(J19/(C19+K19))))	(D19/760)*(F19/G19)	100	5		7.11189	1426.448	227.193	-0.02 to 24
20												
21	O-XYLENE		24.5	(10^(I21-(J21/(C21+K21))))	(D21/760)*(F21/G21)	100	5		7.81265	1901.373	246.882	0 to 50.
22												
23	M-XYLENE		24.5	(10^(I23-(J23/(C23+K23))))	(D23/760)*(F23/G23)	100	5		7.96709	1998.545	256.378	0 to 60.
24												
25	P-XYLENE		24.5	(10^(I25-(J25/(C25+K25))))	(D25/760)*(F25/G25)	100	5		7.32399	1644.214	232.921	25.00 to 60.
26												
27	PENTANE		24.5	(10^(I27-(J27/(C27+K27))))	(D27/760)*(F27/G27)	100	5		6.8643	1070.617	232.696	-4.40 to 46
28												
29	HEXANE		24.5	(10^(I29-(J29/(C29+K29))))	(D29/760)*(F29/G29)	100	5		6.33114	1044.038	219.257	-95.45 to -
30												
31	HEPTANE		24.5	(10^(I31-(J31/(C31+K31))))	(D31/760)*(F31/G31)	100	5		7.69313	1635.409	245.812	-87.86 to 2
32												
33	OCTANE		24.5	(10^(I33-(J33/(C33+K33))))	(D33/760)*(F33/G33)	100	5		8.0763	1936.281	253.007	-56.56 to 2
34												
35	NONANE		24.5	(10^(I35-(J35/(C35+K35))))	(D35/760)*(F35/G35)	100	5		6.69999	1492.928	217.255	-53.50 to 3
36												
37	DECANE		24.5	(10^(I37-(J37/(C37+K37))))	(D37/760)*(F37/G37)	100	5		3.08531	440.616	116.254	-29.66 to 3
38												

Figure 62   Spreadsheet Calculation of Vapour Concentration by Headspace Method (Formulae Printout)

headspace volume and volume of the Tedlar vessel.

AIV.3   Validation of Method

The method of preparing vapours of known concentration described in this Appendix required validation. In order to achieve this a number of hydrocarbon vapours were prepared by this method and analysed by a GC which had been calibrated with a BOC standard. A comparison of the two sets of results is shown in table 28. This demonstrates good agreement between the vapour concentrations measured by GC and calculated by the spreadsheet. This validates the method of preparing vapours of known concentration described in this Appendix.

Table 28   Comparison of Vapour Concentrations

ANALYTE	ANALYTE CONCENTRATION (ppm)	
	CALCULATED BY SPREADSHEET	MEASURED BY GC
pentane	121	126
pentane	64.4	61
hexane	35.2	37.0
hexane	37.6	37.3
heptane	12.0	11.1
heptane	12.9	12.2

Software Listing of Program Controlling
Automated Coal Combustion System

The source code of the C program which controlled the
automated coal combustion evolved gas analyser system
described in Chapter 4 is listed below. This consists of
two functions, main() and templ(), written in one file,
comban1.c. This was linked to produce an object file, and
then compiled into an executable file (comban1.exe) by
using a Lattice C compiler.

```c
/* comban1.c  -  Combustion Generation
            Evolved Gas Analyser System */

#include "\lc\header\time.h"
#include "\lc\header\stdio.h"
#include "\lc\header\math.h"
#define delay(q) for(lp2=0;lp2<q;lp2++)

main()
{
 FILE *fp,*ff,*fg;
 long t=0,x=0,y=0,i,i2,lp2,lb,hb;
 int d=0,dd=0,ddd=0,ch,ht;
 int mn=1,co,s,s1,tk=0,x4,y4,key,xx,yy,yyy;
 float co1,co2,ch4,o2;
 long float a,b,r,val;
 float y1,y2,y3,xx1;
 char *chr;

 int pa=784,pb=785,pc=786,cr=787,dr=788;
 int camux=32,ca=16;

 fp=fopen("prn","r+");
 ff=fopen("tst01.tpt","a");
 fg=fopen("tst01.gas","a");

 setnbf(fp);
 setnbf(ff);
 setnbf(fg);

 y1=178;
 y2=178;
 y3=140;
 xx1=30;

 outp(cr,144);
```

```c
         outp(dr,9);
         outp(pc,1);

         templ();
         time(&t);
         x=t;
         y=t;

         fprintf(fp,"     %s\n",ctime(&t));
         fprintf(ff,"     %s\n",ctime(&t));
         fprintf(fg,"     %s\n",ctime(&t));

         for (i=0;i<30000000;i++)
         {
          time(&t);

          if (t>x)
          {
           d=t-y;
           /*DO THIS ACTION EVERY SECOND    */
           tk++;
           x=t;
           i2=i;
           ht=kbhit();
           if (ht==1)
           {
            scanf("%s",chr);
            if (chr == "q" || "Q")
            { goto lab; }
            if (chr != "q" || "Q")
            { goto lub; }
           }
          }

lub:     dd=d-ddd;
          if (dd/60==1.000)
          {
           /*     DO THIS ACTION EVERY MINUTE     */
            tk=0;
            for(ch=0;ch<8;ch++)
            {
             outp(pb,camux+8+ch);
             outp(pc,1);
             outp(pc,3);
             outp(pc,1);
             outp(pb,ca+1);
             co=inp(pa);
             outp(pb,ca);
             label:   s=inp(784+4);
             s1=s & 1;
             if (s1!=0)
             { goto label; }
             outp(pb,ca+2);
             delay(5000);
             lb=inp(pa);
             outp(pb,ca+4);
```

```c
        delay(5000);
        hb=inp(pa);
        hb=hb & 15;
        val=256*hb+lb;
        if (ch==0)
          {
           fprintf(fp,"MINUTES=%d ",mn);
           fprintf(ff,"MINUTES=%d ",mn);
           fprintf(fg,"MINUTES=%d ",mn);
           r=(0.087782*val)+8.28;
           fprintf(ff,"t%d=%.1fC(%.0f) ",ch,r,val);
          }
        if (ch==1)
          {
           r=(0.097537*val)+13.21;
           fprintf(ff,"t%d=%.2fC(%.0f) ",ch,r,val);
           yy=abs(179-(r*0.56));
           xx=abs(xx1);
           if (yy<10)
{ yy=10; }
           dot (xx,yy,2);
          }
        if (ch==2)
          {
           r=(0.087310*val)+2.98;
           fprintf(ff,"t%d=%.2fC(%.0f) ",ch,r,val);
           mn++;
           yyy=abs(179-(r*0.56));
           if (yyy<10)
{ yyy=10; }
           dot (xx,yyy,3);
          }
        if(ch==3)
          {
           r=(0.088970*val)+7.12;
           fprintf(ff,"t%d=%.2fC(%.0f)\n",ch,r,val);
           ddd=60+ddd;
           yyy=abs(179-(r*0.56));
           if (yyy<10)
{ yyy=10; }
           dot(xx,yyy,1);
           xx1=xx1+0.90;
          }
        if(ch==4)
          {
           co1=(73.0/(3059-132))*(val-132);
           fprintf(fp," CO=%.1fppm(%.0f)",co1,val);
           fprintf(fg," CO=%.1fppm(%.0f)",co1,val);
          }
        if(ch==5)
          {
           ch4=(1.01/(1650-285))*(val-285);
           fprintf(fp," CH4=%.2f%(%.0f)",ch4,val);
           fprintf(fg," CH4=%.2f%(%.0f)",ch4,val);
          }
        if(ch==6)
```

```
          {
            co2=(0.99/(1529-323))*(val-323);
            fprintf(fp," CO2=%.2f%(%.0f)",co2,val);
            fprintf(fg," CO2=%.2f%(%.0f)",co2,val);
          }
        if(ch==7)
          {
            o2=(20.89/(3472-979))*(val-979);
            fprintf(fp," O2=%.2f%(%.0f)\n",o2,val);
            fprintf(fg," O2=%.2f%(%.0f)\n",o2,val);
          }
      }
    }
  }

lab:    gcurloc(10,5);
        gcurmove(0,&x4,&y4,&key);
}


templ()
{
 int val[6],c,h,ch,lf,hsize,vsize;

 easyinit();
 initgraf(4,0,0);

 gactplot(30,10,300,179);

 glabinit();
 val[0]=50;
 val[1]=100;
 val[2]=150;
 val[3]=200;

 val[4]=250;
 val[5]=300;

 fontld(0,"IBMROM");
 fontinfo(0,&c,&h,&ch,&lf,&vsize,&hsize);
 fontchg(0,0,h-4,ch-2,lf-8);

 gsetlab(0,0,0,0,"Temperature(y) Versus Time(x)"
 ,1,0,0,NULL,0,0,100,0);

 gsetlab(0,0,3,1,"",1,6,1,&val[0],10,0,300,1);

gsetlab(0,0,2,0,"",1,6,8,&val[0],10,0,300,1);

 glabel();

}
```

APPENDIX VI

Studies of Gases Evolved During Non-Routine Colliery Incidents

A limited amount of work was carried out analysing gas samples taken from collieries during heating incidents. This field work was done in an attempt to validate the experimental results obtained in the laboratory. It was restricted by problems with transporting the samples due to the adsorptive properties of the vapours studied. The routine method of taking samples in pressurised capsules during such incidents was replaced by sampling in Tedlar bags. These samples were then transported to the laboratory for analysis. Mine atmosphere samples were taken from general body locations and from pack pipes located in the goaf, as illustrated in figure 63. These samples were taken from a number of collieries on different occasions. The gases and vapours studied in this work were resticted to those that had been identified in the laboratory work, that is, ethene, propene, carbonyl sulphide, acetaldehyde and acetone.

AVI.1   Studies of Ethene and Propene

The concentrations of ethene and propene were monitored during three heating incidents at different collieries. The results and Graham ratio (Chapter 1, p.32) have been listed in tables 29, 30 and 31. Clearly the concentration changes of ethene and propene corresponded to changes in the concentration of CO. This was particularly notable for pack pipe samples, where gas concentrations were greater.

Roof
supports

Pack pipes

Roadway arches
(typical size,
3m tall, 3m wide)

VIRGIN STRATA

General body
samples are
taken from
this area

RETURN

Goaf

Air doors
(to control
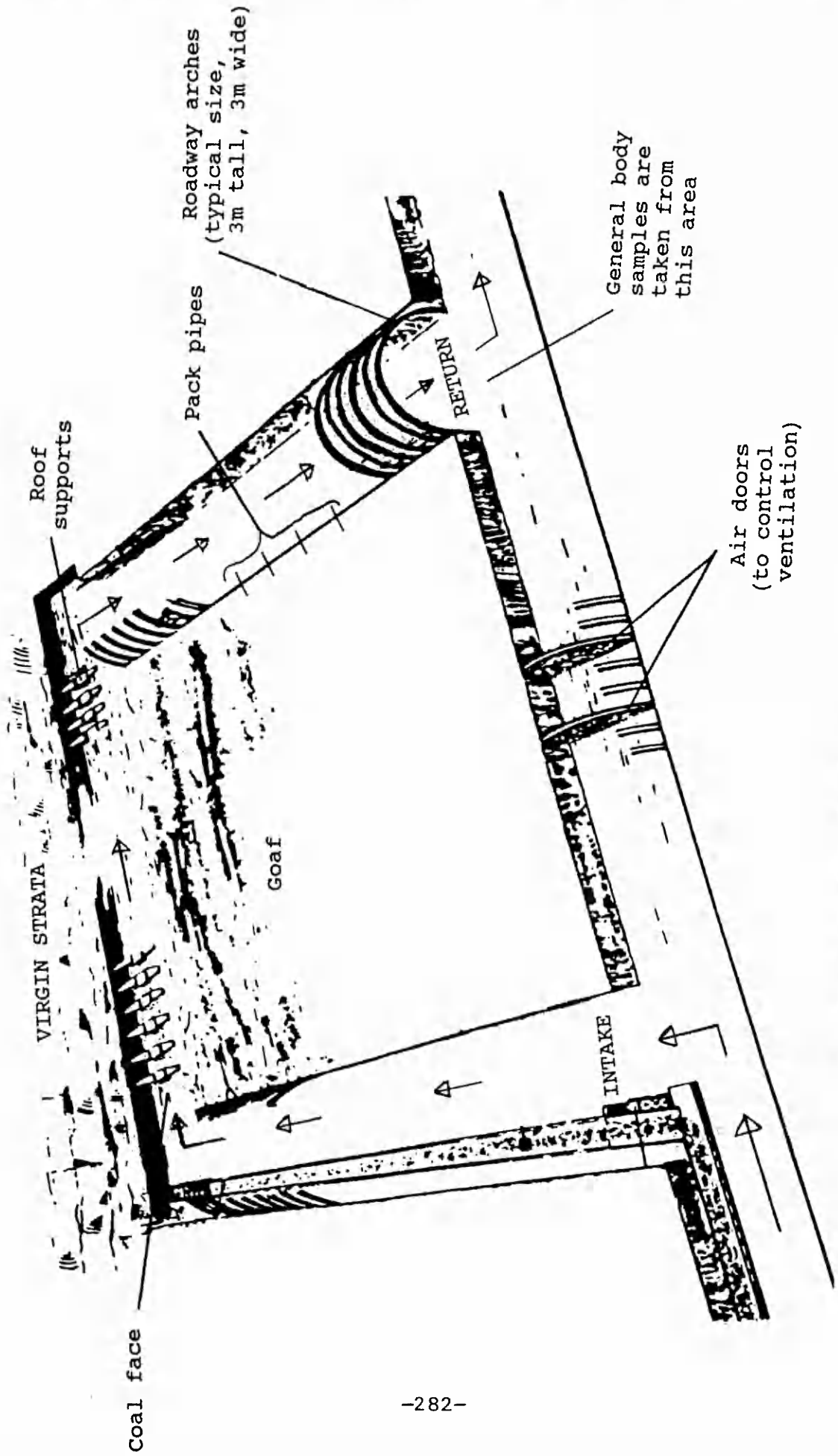ventilation)

Coal face

INTAKE

Figure 63   Illustration of Underground Sampling Positions

Table 29   Incident Located at Colliery A

Sample Location	CO (ppm)	Graham Ratio	Ethene (ppm)	Propene (ppm)
General Body	41	0.42	< 1	< 0.5
	47	0.58	< 1	< 0.5
Pack Pipe	1700	1.99	85	24
	1870	2.44	96	30

Table 30   Incident Located at Colliery B

Sample Location	CO (ppm)	Graham Ratio	Propene (ppm)
Pack	16500	14.73	64
Pipes	17000	14.46	68
	7500	4.96	35
	8800	7.40	45

Table 31   Incident Located at Colliery C

Sample Location	CO (ppm)	Graham Ratio	Ethene (ppm)
General Body	41	0.53	< 1
Various	620	0.45	5
Pack	1200	1.27	10
Pipes	1300	1.28	12
...	570	0.41	5
...	1300	1.13	11
...	1250	1.06	10
...	1100	0.97	9
...	980	0.89	8

It is interesting to note that no specific relationship between CO and ethene or propene existed, the relative proportions of each varied according to the sample location. Typically concentrations of 150ppm CO corresponded to levels of 1ppm ethene or propene. General body samples contained such low levels of ethene and propene, due to dilution by the ventilating air, that these gases could not be detected during the heating incidents.

Thus ethene and propene are useful for monitoring heating situations in the goaf, but their concentrations in the general body were lower than the detection limits of the GC equipment used in this work.

AVI.2   Study of Carbonyl Sulphide

The concentration of carbonyl sulphide was monitored during heating incidents at two different collieries. The results have been listed in tables 32 and 33.

During both heating incidents increasing concentrations of CO were matched by increasing carbonyl sulphide concentrations, demonstrating the potential use of carbonyl sulphide as an indicator of a heating situation. Also the relationship between the concentrations of these two gases remained approximately the same at each colliery. The presence of 200ppm CO corresponded to 0.2ppm carbonyl sulphide. General body samples contained such low levels of carbonyl sulphide, due to dilution by the ventilating air, that it could not be detected during the heating incidents.

-284-

Table 32   Incident Located at Colliery D

Sampling Period	CO (ppm)	Graham Ratio	Carbonyl Sulphide (ppm)
During Heating	140	0.59	0.20
	145	0.69	0.20
	140	0.59	0.20
After Heating	8	0.16	< 0.10

Table 33   Incident Located at Colliery A

Sample Location	CO (ppm)	Graham Ratio	Carbonyl Sulphide (ppm)
General Body	41	0.42	< 0.10
	47	0.58	< 0.10
Pack	1700	1.99	1.35
Pipe	1870	2.44	1.60

AVI.3   Studies of Acetaldehyde and Acetone

The concentrations of acetaldehyde and acetone were monitored during heating incidents at two collieries and they have been listed in tables 34 and 35. They were determined at low levels in general body samples. The presence of 40ppm CO typically corresponded to 1ppm acetaldehyde and 0.3ppm acetone. This gives some validation to the use of these gases as indicators for monitoring heating situations. However, the analysis of samples taken from the goaf showed an absence of acetaldehyde and acetone. It is suggested that these reactive gases are perhaps adsorbed in the high concentrations of moisture present in the goaf. Thus acetaldehyde and acetone are useful for monitoring heating situations in the general body, but not for samples taken from the goaf.

Table 34   Incident Located at Colliery A

Sample Location	CO (ppm)	Graham Ratio	Acetaldehyde (ppm)	Acetone (ppm)
General Body	41	0.42	1	0.2
	47	0.58	1	0.2
Pack Pipe	1700	1.99	< 0.5	< 0.1
	1870	2.44	< 0.5	< 0.1

Table 35   Incident Located at Colliery B

Sample Location	CO (ppm)	Graham Ratio	Acetaldehyde (ppm)	Acetone (ppm)
Pack Pipes	17000	14.46	< 0.5	< 0.1
	7500	4.96	< 0.5	< 0.1

-286-

AVI.4   Conclusions

The results of field work described in this Appendix have validated the use of indicator gases proposed by the laboratory work in this thesis. However, acetaldehyde and acetone could not be used to monitor heatings in the goaf due to the effect of high ambient moisture on these analytes. Additionally ethene, propene and carbonyl sulphide could not be used to monitor heatings in the general body since their concentrations were below the detection limits of the equipment used. Clearly the monitoring of spontaneous combustion requires a careful selection of the analyte to be used as the indicator gas.

Appendix References

A1. Evans MB, Smith JF, Jnl of Chrom, 1962, 9, 147.

A2. James AT, Martin AJP, Biochem J, 1952, 50, 679.

A3. McReynolds WO, Jnl of Chrom Sci, 1970, 8, 685.

A4. Guberska J, Chem Anal, 1973, 18, 1059.

A5. Parcher JF, Johnson DM, Jnl of Chrom Sci, 1980, 18, 267.

A6. Garcia Domiguez JA, Munoz JG, Sanchez EF, Molera MJ, Jnl of Chrom Sci, 1977, 15, 520.

A7. Wainwright MS, Haken JK, Srisukh D, Jnl of Chrom, 1979, 179, 160.

A8. Smith RJ, Haken JK, Wainwright MS, Jnl of Chrom, 1985, 334, 95.

A9. Parcher JF, Johnson DM, Jnl of Chrom Sci, 1980, 18, 267.

A10. Riedo F, Fritz D, Tarjan G, Kovats E, Jnl of Chrom, 1976, 126, 63.

A11. Peterson ML, Hirsch J, J Lipid Res, 1959, 1, 132.

A12. Gold HJ, Anal Chem, 1962, 34, 174.

A13. Hansen HL, Andresen K, Jnl of Chrom, 1968, 34, 246.

A14. Kaiser RE, Chromatographia, 1974, 7, 251.

A15. Al-Thamir WK, Purnell JH, Wellington CA, Laub RJ, Jnl of Chrom, 1979, 173, 388.

A16. Toth A, Zala E, Jnl of Chrom, 1984, 298, 381.

A17. Grobler A, Balizs G, Jnl of Chrom Sci, 1974, 12, 57.

A18. van Tulder PJM, Franke JP, de Zeeuw RA, 7th International Symposium on Column Liquid Chromatography at Baden-Baden, 3-6 May 1983.

A19. Guardino X, Albainges J, Firpo G, Rodriguez-Vinals R, Gassiot M, Jnl of Chrom, 1976, 118, 13.

A20. Bellas TE, Chromatographia, 1975, 8, 38.

A21. Nelder JA, Mead R, J Comput, 1965, 7, 308.

A22. Massart DL, Vandeginste BGM, Deming SN, Michotto Y, Kaufman L, 'Chemometrics: A Textbook', Elsevier, 1988.

A23. Smith RJ, Haken JK, Wainwright MS, Jnl of Chrom, 1978, <u>147</u>, 65.

A24. Heeg FJ, Zinburg R, Neu HJ, Ballschmiter K, Chromatographia, 1979, <u>12</u>, 451.

A25. Ohe S, 'Computer Aided Data Book of Vapour Pressures', Data Publishing Co., Tokyo, Japan, 1976.

MEETINGS OF THE ROYAL SOCIETY OF CHEMISTRY

i   Microcomputer and Microprocessor Group, 16-3-88, 'Software Design, Validation and Portablility', Imperial College, London.

ii Chromatography and Electrophoresis Group, 17-5-89, 'Genetic Fingerprinting', by Prof A Jeffreys (Leicester University), Trent Polytechnic.

iii Thermal Methods Group, 15-11-89, 'Applications of Evolved Gas Analysis', Scientific Societies Lecture Theatre, London.

iv Endowed Theophilus Redwood Lecture, 25-1-90, 'Serially Linked Chromatographic Columns - A Neglected Art', by Prof JH Purnell (Swansea University), Warwick University.

LECTURES AND ASSOCIATED STUDIES

i   Chrompack Seminar, 4-6-87, 'Packed to Wide-bore Columns', by Dr DW Grant, Indescon Court, London.

ii   Hewlett-Packard 1988 Analytical Symposium, 14-9-88, 'Gas Chromatography', Anugraha Hotel, Egham, Surrey.

iii Photovac Seminar, 19-10-88, 'Photovac Photoionisation Users Meeting', by Dr M Collins, Aston Science Park.

iv   HNU Seminar, 27-1-89, 'Application of Photoionisation Detectors for Environmental Monitoring', by Dr M Duffy, Lymm Hotel, Warrington.

v   Perkin-Elmer 1989 Chromatography Symposium, 19-4-89, 'Chromatography for the Modern Analyst', Hotel Russell, Russell Square, London.

PRESENTATIONS

Automatic Methods Group, 12/13-12-90, 'Analysis of the Environment - Earth, Fire, Air and Water', London.

Two posters presented:

'Monitoring Coal Mine Atmospheres - 1. Evolution of Gases'.

'Monitoring Coal Mine Atmospheres - 2. Detection of Gases'.

Royal Society of Chemistry and Commission of the European Communities, 9/13-09-91, 'Clean Air at Work Conference', Luxembourg.

One poster presented:

'A Study of Coal Mine Atmospheres and the Spontaneous Combustion of Coal'.